Research on the Effects of Varying Water Quality on the Corrosion of Different Pipe Materials in the PWVS/Klerksdorp Areas

C Ringas • FJ Strauss • J Gnoinski • BG Callaghan

Report to the Water Research Commission
by
Division of Materials Science
and Technology
CSIR

WRC Report No 254/1/99

Disclaimer

This report emanates from a project financed by the Water Research Commission (WRC) and is approved for publication. Approval does not signify that the contents necessarily reflect the views and policies of the WRC or the members of the project steering committee, nor does mention of trade names or commercial products constitute endorsement or recommendation for use.

Vrywaring

Hierdie verslag spruit voort uit 'n navorsingsprojek wat deur die Waternavorsingskommissie (WNK) gefinansier is en goedgekeur is vir publikasie. Goedkeuring beteken nie noodwendig dat die inhoud die siening en beleid van die WNK of die lede van die projek-loodskomitee weerspieël nie, of dat melding van handelsname of -ware deur die WNK vir gebruik goedgekeur of aanbeveel word nie.

RESEARCH ON THE EFFECTS OF VARYING WATER QUALITY ON THE CORROSION OF DIFFERENT PIPE MATERIALS IN THE PWVS/KLERKSDORP AREAS

by

C Ringas, FJ Strauss, J Gnoinski
and BG Callaghan

Report to the Water Research Commission

by the

CSIR
Mattek
Private Bag X28
AUCKLAND PARK

WRC report no 254/1/99
ISBN 1 86845 482 7

ACKNOWLEDGEMENT

The research in this report emanated from a project funded by the Water Research Commission and was carried out by the Mine Hoisting, Metallurgical and Corrosion Services programme of the Division of Materials Science and Technology of the CSIR.

The title of the project was:
Research on effects of varying water quality on the corrosion of different pipe materials in the PWVS/Klerksdorp area.

The following people comprised the Steering Committee for this project.

Mr H C Chapman	Water Research Commission
Mr D van der Merwe	Water Research Commission
Mr D J M Huyser	Water Research Commission
Mr S van der Merwe	Rand Water Board
Mr J Geldenhuys	Rand Water Board
Mr C Lüdik	Department of Water Affairs
Mr D Nel	Johannesburg City Council
Mrs M J F Krüger	Western Transvaal Regional Water Company
Mr A J Dippenaar	OFS Gold Fields

CONTENTS

EXECUTIVE SUMMARY

The effects of mining operations and the rapid industrialisation and urbanisation of the Pretoria-Witwatersrand-Vereeniging-Sasolburg (PWVS) and Klerksdorp has inevitably led to an increase in the mineral pollution of the Vaal River, from which the PWV complex, the Klerksdorp area, OFS Gold Fields and Kimberley draw the bulk of their water supply. The introduction of water from the Tugela River and the recent agreement to implement the Lesotho Highlands Water Scheme could also have an influence on the quality of water in the PWV and Klerksdorp areas and thus on the performance of existing pipework and on the selection of materials for future pipework.

It would therefore be most important to fully characterise the corrosive effect of the present water supply to the PWV/Klerksdorp areas since the changing mineral content of water due to stream pollution and the introduction of waters from other sources could adversely affect existing pipework. This could lead to corrosion problems, heavy scaling (due to the higher mineral content) and pitting rather than general corrosion of pipes.

The objectives of the project were the following:

(a) To evaluate the corrosion characteristics of water introduced from sources other than the Vaal, as well as blends of these waters with Vaal River water, on the performance of pipes in the PWVS and Klerksdorp areas.

(b) To evaluate the effect of increasing mineralisation on the service performance of various pipe materials in the PWVS/Klerksdorp areas.

(c) To correlate water chemistry (and related indices) to actual corrosion studies in South Africa.

(d) Using the information generated in the PWVS/Klerksdorp areas to provide enabling technology for predicting the likely performance of pipe materials in other water systems in South Africa.

(e) To evaluate the need for dezincification-resistant fittings for various water types in order to

determine whether present restrictive practices are relevant and necessary.

There were three main phases to the project which were carried out in parallel, namely: (1) Electrochemical studies and corrosion monitoring; (2) Correlation of corrosion results with water chemistry; and (3) Long term in-situ exposure programme.

The conclusions from this investigation were as follows:
The water composition affects the corrosion behaviour of alloys, but since there are so many variables in describing water, it is virtually impossible to draw up a simple expression which can be used as a corrosivity indicator.

No correlation could be found between the Langelier Index and the corrosion rate of any alloy at any of the sites. Similarly, none of the other prediction indices showed any correlation to the corrosion rate.

The presence of micro-organisms was detected on all samples at all sites. In particular the presence of sulphate-reducing bacteria complicated the analysis of the corrosivity of the waters towards the alloys. However, conclusive proof was obtained which showed that the SRB were involved in the corrosion of the mild steel coupons in particular, resulting in high corrosion rates and perforation of mild steel coupons in less than 18 months.

Mild steel showed the highest corrosion rate at all the sites generally, but the lowest corrosion rate was detected at Klerksdorp.

On-line corrosion monitoring using mild steel probes showed that fluctuations in the corrosion rate were detectable.

Where possible, accelerated electrochemical corrosion tests should be carried out in-situ as tests performed in a laboratory at a later stage may give erroneous results.

Increasing mineralisation of water supplies could probably lead to increased corrosion rates of carbon steel piping due to an increase in SRB activity.

Blending of Vaal Dam water with Lesotho Highlands and/or Sterkfontein Dam water will tend to decrease the corrosion rate of mild steel. The latter two waters are relatively pure and contain low levels of chloride and sulphate ions and would thus have a diluting effect on the Vaal Dam water.

Electrochemical techniques were more sensitive to change in water composition than the mass loss coupons.

Pitting corrosion of copper samples was detected at Klerksdorp from 9 months onwards. This was in contrast to the low general corrosion rates recorded for the alloy at this site. Once again, this illustrates the importance of monitoring corrosion on-line using appropriate equipment which can detect localised corrosion. However the pits were very small and could only be resolved under high magnification in a scanning electron microscope.

The non-DZR brass used in these tests initially showed high corrosion rates and dezincification at all the sites both in hot and cold water after 3 months. There is thus still a need to use dezincification-resistant fittings in the PWVS/Klerksdorp geographic area.

The corrosion rate of hot dipped galvanised samples was always higher than the galvanised steel samples.

The following recommendations for further study were made:
A thorough analysis of the succession patterns of bacterial colonization of pipe surfaces needs to be made. It is recommended that a programme be set up to determine how soon after colonization SRB initiate corrosion in conjunction with a corrosion monitoring system which would detect the onset of such corrosion. This is prudent in view of the expected increase in sulphate levels in future.

A similar study could be extended to coastal areas which use "soft" waters in order to determine whether similar corrosion mechanisms are operative in those areas.

1. INTRODUCTION

The Division of Materials Science and Technology, through it's Mine Hoisting, Metallurgical and Corrosion Services programme was sponsored by the Water Research Commission to undertake a research project investigating the effect of varying water quality on the corrosion of different pipe materials in the PWVS/Klerksdorp areas. The objectives of the project were as follows:

(a) To evaluate the corrosion characteristics of water introduced from sources other than the Vaal, as well as blends of these waters with the Vaal river water, on the performance of pipes in the PWVS and Klerksdorp areas.

(b) To evaluate the effect of increasing mineralisation on the service performance of various pipe materials in the PWVS/Klerksdorp areas.

(c) To correlate the water chemistry (and the related corrosion prediction indices and diagrams) to actual corrosion studies in South Africa.

(d) Using the information generated in the PWVS/Klerksdorp areas to provide the enabling technology for predicting the likely performance of pipe materials in other water systems in South Africa.

(e) To evaluate the need for dezincification resistant fittings for various water types.

There were three main phases to the project which were carried out in parallel namely: (1) Electrochemical Studies and Corrosion Monitoring; (2) Correlation of corrosion studies with Water Chemistry, and (3) Long term in-situ exposure programme.

2. BACKGROUND

The effects of mining operations and the rapid industrialisation and urbanisation of the Pretoria-Witwatersrand-Vereeniging-Sasolburg (PWVS) and Klerksdorp areas has inevitably led to an increase in the mineral pollution of the Vaal River, from which the PWV complex, the Klerksdorp area, OFS Gold Fields and Kimberley draw the bulk of their water supply. In recent years there has been much concern regarding the pollution impact on the Eastern Transvaal Highveld as a result of power generation, Secunda, chemical plants and other industrial complexes in that area, including the pollution of surface waters and agricultural land.

Over the past 30 years the mineral content of the water in the Vaal River increased to such an extent that the Water Research Commission initiated an investigation into the sources and extent of this mineral build-up and its possible effects on the most industrialized regions of South Africa. The introduction of water from the Tugela River and the recent agreement to implement the Lesotho Highlands Water Scheme could also have an influence on the quality of water in the PWV and Klerksdorp areas and thus on the performance of existing pipework and on the selection of materials for future pipework.

It would therefore be most important to fully characterize the effect of the present water supply to the PWV/Klerksdorp area. The changing mineral content of water due to stream pollution and the introduction of waters from other sources could have serious effects on existing pipework. It could lead to:

(i) Costly corrosion problems with attendant water loss, repair and maintenance of pipes and possibly the need for elaborate water pre-treatment and/or a choice of alternative pipe materials.

(ii A higher mineral content of the water could cause heavy scaling or even blockage of pipes. This effect could vary, in the same water, dependent on pipe material

itself.

(iii) Alternatively, it may promote pitting rather than general corrosion of pipes. Pitting corrosion is often more disastrous than general corrosion because, due to its localized nature, pitting can cause penetration of the pipes in a very short period. The introduction of relatively soft waters could modify the corrosion process to such an extent that pipework, at present performing satisfactorily, could become vulnerable to corrosion in a short period of time. Thus the effect of changing mineralization and the diluting effect of some water sources may mean that great care will be needed in the selection of materials for pipework, dependent on the type of corrosion that will be encountered. This research is to provide the 'know how' at the time it is needed.

The present systems of water conditioning, softening, stabilization and corrosion prediction are all based on the equilibrium of the carbonic species in water, based on careful water analyses. From these analyses various indices are derived such as the Langelier and Ryznar indices, also various equilibrium diagrams (such as the Modified Caldwell Lawrence diagrams linking pH, alkalinity, acidity, carbonate species) have been developed. These are used to predict whether a metal will corrode or scale. Whilst these can be used as an initial guideline, our practical experience indicates that these predictions are often misleading. The reason for this poor correlation between water chemistry and corrosion is simple. By definition, corrosion is the reaction of a metal to its environment and the process almost invariably occurs via an electrochemical mechanism. All the indices and equilibrium diagrams consider the equilibrium of the water, i.e. the environment - not one of these consider the metal reaction, the type of metal involved and its inherent corrosion/electrochemical tendencies. It is assumed that water chemistry and hence water saturation characteristics will prevail, but the reaction of the metal itself changes the immediate micro-environment at the metal's surface.

Our field experience with various metals has confirmed this discrepancy between the metal's actual performance and that predicted from water chemistry. It is essential to have an adequate understanding of metals and their corrosion processes and to combine this with corrosion testing. A full understanding of the metallurgical conditions of the metal and metal coatings and their electrochemical characteristics is necessary, as well as the characteristics of polymeric coatings where used. If this is then combined with water chemistry, a better understanding will be achieved since water chemistry alone is inadequate.

As already indicated in above, all corrosion prediction indices for waters are based on the equilibrium characteristics of waters and do not take into consideration the metal concerned. Because of the difficulties of carrying out 'in situ' electrochemical work within pipe systems at pressure and elevated temperatures, most work is carried out in electrochemical cells with waters removed from the pipe system. The changes that can occur in a water removed from a tap (for example changing oxygen and carbon dioxide levels) could lead to erroneous results. Thus there are limitations to corrosion studies that are based on water chemistry alone, or on electrochemical tests on waters that have changed due to their release from a pressurised pipe system.

The present study takes cognizance of these limitations and will take the electrochemical cell to the pipeline and carry out measurements under conditions of pressure, temperature and water movement within a typical domestic pipeline. This work will be correlated to coupons exposed under the same environmental conditions and furthermore, water specimens removed from pipes and from the raw water supplies will also be evaluated to compare 'in line' electrochemical work with 'removed' laboratory type studies. Regular monitoring of water chemistry with electrochemical measurements, backed by coupons and pipe sections exposed in the water will help to fill in any gaps in our knowledge of the corrosion system.

Numerous benefits will accrue from such a study, including:

i) Correlation between predictions based on water chemistry with that based on electrochemical studies of different metals in the same water, providing guidelines based on South African conditions.

ii) An assessment of the likely impact of mineralization and of varying water quality on existing water pipes.

iii) Provide guidelines for the selection of the most suitable pipe materials for future water schemes

iv) This project could be extrapolated, or possibly extended in the future, to other areas of the country. This will facilitate the decisions of planners and developers in the development of new housing schemes, including low-cost schemes, to ensure the correct selection of materials to provide a cost effective approach to water reticulation.

v) Provide information on the likely performance of heating elements, geysers, fasteners, taps and other fittings.

vi) Besides the huge economic implications of corrosion prevention the results of the project could help to reduce unnecessary wastage of water, materials and the attendant costs involved due to in service failures.

vii) Questions on the necessity for providing dezincification resistant fittings will also be studied to determine whether present restrictive practices are relevant and necessary.

3. LITERATURE SURVEY

A brief summary of pertinent information will be presented in order to allow an evaluation of the results to be made.

3.1 Composition of waters

3.1.1 Dissolved salts

The main constituent ions in natural waters are positively charged cations, such as calcium (Ca^{2+}), magnesium (Mg^{2+}), sodium (Na^{+}), and negatively charged anions such as chloride (Cl^{-}), sulphate (SO_4^{2-}), bicarbonate (HCO_3^{-}), carbonate (CO_3^{2-}) and hydroxide (OH^{-})

3.1.2 Total dissolved solids

The total dissolved solids can either be determined directly by evaporating to dryness or estimated fairly accurately from the electrical conductivity of the water. The total dissolved solids, in ppm, is close to one-fifteenth of the conductivity, in reciprocal ohms. Generally speaking, the higher the TDS, the higher the corrosion rate. There may be cases where high TDS values result in the formation of protective scales.

3.1.3 Chlorides and sulphates

These ions make up the bulk of the corrosive salts present in most waters. In general, the amount of dissolved chloride is greater than the amount of sulphate and only in certain highly-mineralised waters is the sulphate predominant (1).

Chloride is often taken as an index of the corrosive potential of the water. Furthermore, high levels of chlorides can cause localised corrosion of alloys relying on a passive film for protection such as stainless steels.

3.1.4 Carbonate and bicarbonate

These constitute the bulk of the dissolved salts in natural waters. They are closely linked with the carbon dioxide and calcium content of the water and will be discussed in detail later.

3.1.5 Minor inorganic constituents

Among the minor inorganic constituents present, there is silica and traces of certain heavy metals which are indicative of the corrosive nature of the water or its toxicity. Silica is often present in waters usually as metasilicic acid $(H_2SiO_3)_n$. Silicates have certain inhibitive properties and are added to soft waters to reduce corrosion. However, silica is undesirable in high-pressure steam raising equipment since even at small concentrations it forms hard encrustations.

Iron present in waters (from corrosion of steel piping) causes "red water" problems and may render water unsuitable for domestic use. When present in tap water, copper is usually derived from copper pipes. Very small amounts are capable of stimulating attack on aluminium, to a lesser extent on zinc and to some degree on iron.

Zinc is sometimes present in waters due to the corrosion of galvanised steel piping.

3.1.6 Dissolved gases

The most important dissolved gases from a corrosion point of view are oxygen and carbon dioxide. Most public supplies of water are well oxygenated with an oxygen content of 2 to 8 ppm at ordinary temperatures (1). The solubility decreases with a rise in temperature and is virtually zero at the boiling point. Deoxygenation often occurs in "dead ends" and segment areas of distribution

schemes.

The amount of free carbon dioxide in natural waters is seldom greater than 10 ppm and a part of this is closely associated with the carbonate equilibria.

3.1.7 Organic matter

The organic matter present in water consists of living organisms and the products of their metabolism or decay. Microscopic organisms such as bacteria, fungi and algae produce significant changes in the composition of the water in their immediate vicinity as a result of their metabolism. For example, hydrogen sulphide may be produced by sulphate reducing bacteria. Failure to take cognisance of the microbial content of waters may lead to unexpected corrosion failures.

3.1.8 Bicarbonate equilibria

Carbon dioxide dissolves freely in water with a solubility depending on the partial pressure. Most of the dissolved carbon dioxide is present in solution in the molecular state. A small amount reacts with the water to form carbonic acid, thus:

$$CO_2 + H_2O = H_2CO_3$$

with $$\frac{(H_2CO_3)}{(CO_2)} = 0{,}003$$

The carbonic acid dissociates in two stages, first to form bicarbonate ions (HCO_3^-), and subsequently carbonate ions (CO_3^{2-}), according to the following equations:

$$H_2CO_3 = H^+ + HCO_3^-$$
$$HCO_3^- = H^+ + CO_3^{2-}$$

From the above equations, the first and second dissociation constants can be calculated. From this data, the variation in the ratios of the various components may be calculated by equations for any given value of pH. Natural waters have pH values in the range 6,0 to 9,5, thus we are generally concerned with the free carbon dioxide - bicarbonate equilibria.

3.1.9 Alkalinity and hardness

The amount of hydroxide, carbonate and bicarbonate present in water is referred to as the alkalinity.

$$\text{i.e. Alkalinity} = [H_2CO_3]+[HCO_3^-]+[CO_3^{2-}]+[OH^-]$$

Calcium and magnesium are the constituents producing hardness in the water and are able to destroy the detergent properties of soaps, for example. The total hardness is often determined by direct estimation of the calcium and magnesium contents. Carbonate hardness is generally the same as the total alkalinity. The difference between the carbonate hardness and the total hardness, estimated from the calcium and magnesium, is called non-carbonate hardness.

3.1.10 Langelier Index

The solubilities of the principal carbonates in water (expressed as ppm calcium carbonate) are: calcium carbonate 13; magnesium carbonate 75; sodium carbonate 289 000. The amount of carbonate present in water is controlled by the solubility of calcium carbonate i.e. the solubility product K_s.

$$K_s = [Ca^{2+}][CO_3^{2-}]$$

By combining the above equation, and the equation for the first dissociation equation for carbonic acid to bicarbonate ions, and by knowing the dissociation

constant of water, an equation relating the concentration of participating ions at equilibrium can be derived.

By taking logarithms and rearranging, an equation can be derived which will allow the pH of a solution saturated with calcium carbonate to be obtained. This value is known as the saturation pH and is denoted as pH_s. Hence, if the calcium hardness, the total alkalinity, the pH and temperature of water are known, the saturation pH may be calculated from the equation mentioned above or from curves constructed from it. The difference between this and the actual pH i.e pH-pH_s is known as the Langelier index for the water at a given temperature. If this is positive, deposition of calcium carbonate from the water will occur while if it is negative, the water will be capable of dissolving any calcium carbonate with which it comes into contact until it is saturated.

3.1.11 Temperature

Increases in temperature affect the chemical composition and physical properties of waters, the nature and properties of deposits and the actual behaviour of the metal itself. The water composition is affected by changes in the stability and solubility of the dissolved solids. The solubility and diffusion rate of dissolved gases also vary appreciably with temperature and of particular interest is the behaviour of oxygen. Although temperature can have a dramatic effect on solubility, given the relatively narrow range of temperatures which are likely to be encountered in the bulk piping of water, this factor, too, is of minor importance (2).

3.1.12 pH

The pH value of a solution is the negative value of the logarithm of the hydrogen ion concentration. The pH value influences the corrosion rate in a varied manner depending on whether a metal is noble or whether its oxide is soluble in acid or both acid and alkali. Noble metals such as platinum and gold are stable

in both acid and alkaline solutions and their corrosion behaviour is independent of pH. Zinc and aluminium are amphoteric metals and are soluble in both acid and alkaline solutions. These metals have a characteristic pH value at which the corrosion rate is a minimum.

3.2 Effect of material condition on corrosion

Rothwell (3) stated that a greater understanding of the interaction of water chemistry and corrosion processes was necessary. Van der Kooij et al (4) in a study of the corrosion in the water distribution system of The Netherlands concluded that the materials used for constructing water distribution systems may adversely affect drinking water quality in a number of ways, such as, promotion of bacterial growth, and the release of organic and inorganic compounds influencing taste, odour, colour or toxicity of drinking water. Furthermore, both the water composition and the nature of the construction materials are involved with these processes and hence, water quality deterioration may be prevented or reduced either by adjusting water quality, or by using properly-selected materials.

Borgioli et al (5), in a study of the influence of materials on the water quality degradation in distribution systems and noting the chemical and microbiological effects on corrosion, concluded that an ad-hoc study of each material to be used in a particular application had to be made. Ahmad et al (6) found that the metallurgical condition of steel i.e. heat treatment state was important in material stability in flowing potable water.

3.3 Prediction of water corrosivity by indices

Kennett (7) found that of the six combined parameters which give an indication of pitting propensity of a water, lack of correlation has been found in practice. Neff et al (8) conducted a study to investigate the interrelationships between corrosion rate, metal concentrations and water quality occurring within galvanised

steel and copper plumbing systems. They found that statistical analysis of the water quality and corrosion data failed to identify any meaningful relationships because of the variation in quality. This was as a result of the large number of factors and interrelationships affecting corrosion than can be taken into account by statistical models. The authors also recommended that a procedure be developed to produce instantaneous measurement of corrosion rates and to detect short-term variations in the corrosivity of public water supplies.

Pisigan and Singley (9) showed that $CaCO_3$ precipitated regardless of the saturation index of the water. The authors concluded that the Langelier Index should only be used with caution in corrosion control and that the prediction of a water's corrosivity should also consider the influence of other water quality parameters. This is because the Langelier Index is only a thermodynamic measure of the tendency of a water to deposit or dissolve calcium carbonate and is not a corrosivity indicator.

3.4. Factors influencing the future quality of water in the PWV

In 1974 the Water Research Commission initiated an investigation into the mineral pollution of the Vaal River with the main emphasis on a stretch of the River which serves the Pretoria, Witwatersrand, Vereeniging and Sasolburg areas (10). The investigation revealed that the TDS values of the present water supply were in the region of 300mg/l and if unrestrained, would be expected to rise to 800 mg/l towards the end of the century. The increased TDS values could be expected to influence the RWB (due to increased algal growths), local authorities (due to corrosion of steel water mains) and industrial undertakings.

An investigation into the contribution of mine dumps to the mineral pollution load in the Vaal Barrage undertaken by Jones et al (11) for the Water Research Commission found that mine deposits in the catchment of the Vaal Barrage discharged approximately 50 000 tons of salts into the near surface environment

in 1985, but it was not known what proportion of this was eventually transported by surface streams or ground water to the Vaal Barrage.

Rimmer (12) showed that the levels of chloride, sulphate and TDS of treated water piped to Johannesburg were increasing and causing a deterioration in the quality of the water. The sulphate levels were in excess of the maximum recommended by the U.K. Water Research Centre. A strong correlation between the number of repairs to mains (which were carried out in Johannesburg) to the sulphate concentration could be found.

4. EXPERIMENTAL PROCEDURE

4.1 Flow loop system

Water was fed through a Feenix (1 bar) pressure regulator and then through a manifold and into tanks containing the immersion specimens. The flow rate was regulated by a 3 mm orifice on the outlet side of the tanks resulting in a flow rate of 1,47 cm/min. Electrochemical probes based on a three-electrode system were situated in the manifold. The probes were used to determine the corrosion rate by electrochemical means using the linear polarisation resistance technique (LPR). Furthermore, a corrosion cell (constructed in perspex) containing a 304, 3CR12, galvanised steel and mild steel electrode was incorporated in the system. This allowed the determination of corrosion rates using a standard calomel electrode. The electrodes were replaced at intervals depending on their surface condition. Thus, corrosion rates were determined by three methods, namely, electrochemical probe, electrochemical cell and immersion coupons.

The weight losses obtained from the immersion coupons were the mean values of five specimens. All the specimens were immersed at the start of the programme and periodically removed at three-monthly intervals. In addition, the

mass loss of mild steel was determined on a monthly basis. The mild steel specimens were removed at monthly intervals and new specimens immersed at the same time. This was over and above the mild steel specimens immersed at the start of the programme and removed at three monthly intervals. The results of the monthly mass losses were used to determine the reproducibility of coupon testing and to detect any water variations.

The corrosivity of sampled water was compared to that of 'in situ' water using accelerated electrochemical techniques. This was performed in order to determine whether the corrosivity of water decreased once it was stored for a number of days in a container. The procedure was as follows. The 'sampled' water was stored in a container for eight days. It was then placed in the electrochemical cell in the laboratory and air was bubbled through for two minutes. After two minutes, the air supply was diverted so that only the headspace of the cell was aerated. A linear polarisation resistance scan was then performed and repeated ten times so that a meaningful average could be obtained.

4.2 Alloys

Table 1 lists the chemical composition of all the alloys used in this investigation. Galvanised steel was originally used and this was supplied in sheet form. However, it was decided by the Steering Committee to incorporate samples prepared by hot dip galvanizing and this was carried out. Three grades of cast iron were used, namely, grey cast iron, malleable cast iron and spheroidal graphite cast iron. These alloys were immersed on 11/12/89 at the CSIR and on 18/12/89, 2/1/90 and 3/1/90 at Klerksdorp, Vereeniging and Vaal Dam respectively. The cast iron specimens were prepared in two ways. Firstly, coupons were cut from plate material and the edges were painted. Secondly, samples were machined so that all edges were smooth.

A corrator on-line corrosion monitor was used to determine the corrosion rate on a daily basis at the Klerksdorp and CSIR sites. The instrument was connected to the electrochemical cell at each of the sites and daily readings of the corrosion rate were taken.

A limited number of tests were carried out on various blends of Lesotho Highlands Water, Sterkfontein Dam Water and Vaal Dam water. The blends were made according to the following ratios:
Vaaldam 50% - Sterkfontein 50%; Vaaldam 75% - Sterkfontein 25%; Vaaldam 25% - Sterkfontein 75% and Vaaldam 90% - Sterkfontein 10%. Similar blends were made between the Vaaldam and the Lesotho Highlands Water.

4.3 Test Sites

Four test sites were used in this project situated at the CSIR site in Pretoria, Rand Water Board at Vereeniging, Western Transvaal Regional Water Company at Klerksdorp and the Vaal Dam wall. The localities of the sites are shown in Figure 1 and a typical experimental set up in Figure 2.

4.4 Epoxy coating

At the recommendation of the steering committee, it
was decided to coat a limited number of specimens with an epoxy coating. Thus, 62 mild steel and 16 3CR12 panels were coated with 'Copon' (Plascon Evans Paints (Tvl) Ltd -Copon EP.2300). This is a polyamide cured epoxy containing synthetic iron oxide pigment and is applied directly to abrasive-blasted steel. The epoxy coating cures to a semi-gloss finish and is used extensively as a multicoat lining on pipelines (internal or external) and for valves, gates and pumps.

In the past, many costly experiments evaluating the performance of coatings have been invalidated due to poor panel preparation. For this reason, it was decided to have the panels prepared by a reputable consultant and consequently Mr G Stead of Nardini and Bird Inc. prepared the panels. The mild steel panels were abrasive blast cleaned using 'Angrit' to a profile of 50-90 µm and a cleanliness of Sa 3 (Plascon data sheet E-13-D specifies a Grade Sa 2,5 min. and 30-50 µm profile) and stored in an anhydrous environment prior to coating. The 3CR12 panels were pickled and passivated (as recommended by Middelburg Steel and Alloys (Pty) Ltd) by Duva Chemicals.

The coating was mixed in the ratio of 3:1:0,5 base, curing agent and coupon thinners (CTH 520) and left for a minimum of 30 minutes prior to coating. The coating was brush applied and successive coats of red oxide (JYA) and paler oxide (JYA2) were applied to distinguish between coats. The interval between coats varied from 24 to 48 hours depending on the temperature.

The dry film thicknesses recorded in microns, were as follows:

Minimum	:	242 and 395
Maximum	:	292 and 738
Mean	:	270 and 467
Standard Deviation	:	10,5 and 193,7

4.5 X-Ray Diffraction

Twenty eight coupons from the various sites were analysed to determine the composition of the corrosion products on the surface. The analysis was confined to brass, copper, mild steel and galvanised steel. The X-ray diffractograms were recorded on a Philips diffractometer using Cu Kα radiation generated at 50 kV and 30 mA. The 2θ range was 15-80°, step size 0,05° and recording time 2s per step. The data was captured and analysed using Philips APD software on a DEC Micro-PDP11 computer.

4.6 Water Analysis

The water chemistry was monitored on a monthly basis at the CSIR and on a weekly basis at Vereeniging, Klerksdorp and Vaal Dam. The water analysis at the CSIR was performed by the Water Technology Division, the water analysis at Vereeniging was supplied by the Rand Water Board, that at Klerksdorp by the Western Transvaal Regional Water Company and the analysis at the Vaal Dam was supplied by the Department of Water Affairs.

4.7 Statistical Analysis

In order to determine whether there was any correlation between the corrosion rate and the Langelier index and the water quality parameters, a thorough and extensive statistical analysis of the results was undertaken. Since the original budget did not cater for this work, it was decided to restrict the analysis to the results obtained at the CSIR and attempts were made to derive twelve models. Six of the relationships sought were between water quality variables and monthly corrosion rate. The remaining six were between the Langelier index and corrosion rate.

4.8 Microbiological Testing

It was noticed that microbial activity was evident on some of the coupons, especially the mild steel. In order to gain an appreciation as to whether any significant amounts of microbes were present, a limited amount of microbiological tests were carried out. This portion of the work was considered important and since no provision had been made in the original contract, the investigation was funded by the CSIR. The results are presented in Appendix 7.

TABLE 1: Composition of alloys

Element	304	3CR12	En3B	GC	MC	SG	Brass
Carbon	0.042	0.035	0.04	2.79	2.26	3.69	
Manganese	1.44	1.06	0.36	0.72	0.47	0.39	
Sulphur	<0.005	<0.005	0.011	0.05	0.025	0.021	
Phos.	0.027	0.085	0.006	0.044	0.029	0.024	
Silicon	0.52	0.4	<0.01	1.78	1.45	2.28	
Chromium	18.05	11.32	<0.01	0.1	0.06	0.04	
Molybdenu.	<0.01	<0.01	0.02	0.04	0.02	<0.01	
Nickel	8.63	0.58	<0.01	0.03	0.04	<0.01	0.05
Copper	0.12	0.15	<0.01	0.05	<0.01	<0.01	61.3
Aluminium	0.009	0.027	0.008	0.012	0.007	0.017	0.07
Vanadium	0.11	0.04	<0.005	0.011	0.018	0.015	
Niobium	<0.01	0.01	<0.005	<0.005	0.01		
Titanium	0.03	0.3	<0.005				
Magnesium			<0.005				
Zinc							36.7
Lead							1.94
Tin							0.03

Compositions in weight percent.
GC= Grey iron.
MC= Malleable iron.
SC= Spheroidal graphite iron.

5. RESULTS

5.1 Vaal Dam Site

Figure 1 in Appendix 1 shows the monthly mass loss of mild steel versus the Langelier index. If the low corrosion rate in the fifth month is excluded then it can be seen that the corrosion rate of the mild steel fluctuates within a narrow range. Figures 2 and 3 in Appendix 1 show the corrosion rate (calculated on a monthly basis) versus the Langelier index using the electrode and probe respectively. The corrosion rate obtained with the electrode (Figure 2) shows a large scatter and does not seem to correlate with the Langelier index. Figure 3 also shows that there was no correlation between the Langelier index and the corrosion rate. It is clear that the lowest corrosion rate was obtained by the mass loss method whereas the results obtained using the probe and the electrochemical cell tended to overestimate the corrosion rate.

Figure 4(a) shows the three monthly mass loss of brass versus the Langelier index and Figure 4(b) shows the monthly corrosion rate (measured by the probe) versus the Langelier index. It is apparent from both figures that no correlation was evident between the Langelier index and the corrosion rate of brass. The three monthly mass loss results show a general decrease in the corrosion rate whereas the probe results show a significant increase between twelve and thirteen months and a sharp decrease thereafter. Furthermore, the corrosion rate obtained by the mass loss coupons and the brass probe are similar.

The results for copper are shown in Figures 5(a) and 5(b) and are similar to those presented for brass. The three monthly mass loss results also showed a decrease in the corrosion - see Figure 5(a). The monthly probe results (shown in Figure 5(b)) also showed a sharp increase in corrosion rate at thirteen months. The results for galvanised steel are summarised in Figures 6(a) and (b) and Figure 7(a).

The graphs of the Langelier index versus corrosion rate obtained by mass loss, electrode and probe for 3CR12 are shown in Figures 7(a), 8 and 9 respectively. There was no apparent correlation between the corrosion rate and the Langelier index in all three cases. Furthermore, it can be seen that the corrosion rates were generally low except for those obtained with the probe.

Similarly, the graphs of the Langelier index versus the corrosion rate obtained by mass loss, electrode and probe for 304 are shown in Figures 10, 11 and 12 respectively. Once again the corrosion rates were lower generally except for those obtained with the probe. Furthermore, no correlation between the Langelier index and the corrosion rate was apparent.

5.2 Klerksdorp Site

The results for this site are presented in a series of graphs in Appendix 2. Figure 13 compares the Langelier index for mild steel in cold water versus the monthly corrosion rate. No correlation was evident between the Langelier index and the corrosion rate. Figures 14 and 15 compare the Langelier index with the corrosion rate of mild steel obtained with the electrode and the probe in cold water respectively. The corrosion rate was similar for both techniques and no correlation between the Langelier index and the corrosion rate was apparent.

Figures 16, 17, 18 compare the Langelier index with the corrosion rate obtained by mass loss, electrode and probe for mild steel in hot water respectively. The mass loss obtained with the coupons was half that measured in cold water, whereas corrosion rate measured with the electrode was twice that measured in cold water. The mass loss obtained with the probe was much higher than that obtained with the other two techniques and there was a large variation in the corrosion rate between these three techniques. In contrast, Figure 19 compares the corrosion rate of 4 mild steel measured by the three methods in cold water and clearly shows that the results were similar.

Figures 20 and 21 show the Langelier index and the corrosion rate measured by mass loss and probe in cold water respectively. Similarly, the corrosion rate measured by three monthly mass loss and probe versus the Langelier index in hot water is shown in Figures 22 and 23.

The graphs for copper are presented in Figures 24 to 29. Figure 28 shows the corrosion of copper calculated by different means and it is clear that the corrosion rate with the probe is higher than that obtained by mass loss. In contrast however, the results for copper in hot water (besides the increase at nine months for the probe results) show that the corrosion rate obtained with both techniques was similar.

The corrosion rates for 3CR12 in Klerksdorp water are presented in Figures 30 to 35. The corrosion rates for 3CR12 were generally lower than those obtained for the other alloys. Corrosion rates obtained with the probe (see Figures 31 and 34) were much higher than those obtained by mass loss on the electrochemical cell.

Similarly, the corrosion results for 304 are summarised in Figures 36 to 41 and the probe corrosion rates were also higher than those obtained with the other two techniques.

5.3 Vereeniging site

The graphs for this site are presented in Appendix 3. A comparison between the Langelier index and the corrosion rate determined by monthly mass loss, electrode and probe in cold water for mild steel is shown in Figures 42, 43 and 44 respectively. No correlation between the Langelier index and the corrosion rate was evident. The probe tended to show the highest corrosion rate and the electrode the lowest. The results obtained in hot water are shown in Figures 45 to 47. The corrosion rate measured with the probe and electrode was higher in hot water than in cold water. However, the corrosion rate determined with the

monthly mass loss coupons was lower in hot water than in cold water.

A small increase in the three-monthly mass loss results of galvanised steel in cold water was noticed and is shown in Figure 48. Once again, there appears to be no correlation between the Langelier index and the corrosion rate. This is also evident in the corrosion rates determined with the electrode and the probe shown in Figures 49 and 50 respectively. The lowest corrosion rate for galvanised steel in cold water in Vereeniging was determined with the electrode.

There was a definite increase in the corrosion rate of galvanised steel in hot water at Vereeniging and is clearly shown in Figures 51 to 53. As shown in Figure 51, the three-monthly mass loss results decreased with time, whereas the corrosion rate determined with the electrode showed an increase with time. The corrosion rate determined with the probe in hot water showed a fluctuation between high and low corrosion rates - see Figure 53.

Figures 54 and 55 summarise the corrosion rate of brass in cold water in Vereeniging determined by three-monthly mass loss and the probe respectively. The mass los results show a general decrease in the corrosion rate whereas the probe results were relatively constant with occasional increases in corrosion. The corrosion of brass in hot water at Vereeniging is shown in Figures 56 and 57. There was a steady decrease in the corrosion rate of the three-monthly mass loss coupons as shown in Figure 56. The probe results (see Figure 57) showed an increase in corrosion rate to very high values after the eighth month and a sharp decrease was noted at the twelfth month.

The corrosion rate of copper in cold water at Vereeniging is summarised in Figures 58 and 59. The three-monthly mass loss results showed a decrease with time as did the probe results. The corrosion rate measured with the probe was higher than that measured by mass loss. Higher corrosion rates were measured for copper in hot water in Vereeniging than those obtained in cold water as shown in Figures 60 and 61. No correlation was evident between the corrosion rate and

the Langelier index as was evident in Figures 58 to 61.

The corrosion rate of 3CR12 in hot and cold water at Vereeniging is presented in Figures 63 to 67. The corrosion rate in hot water was slightly higher than that obtained in cold water. Once again, no correlation was evident between the corrosion rate and the Langelier index.

Similar results were obtained for 304 and are shown in Figures 68 to 74. Generally speaking, the corrosion rate of 304 (in both hot and cold water) was lower than all the other alloys. Figure 71 compares the corrosion rate of 304 in cold water obtained with mass loss coupons and probe and it is apparent that up to the twelfth month the corrosion rates were similar. However, an increase in the corrosion rate for the probe was noted after twelve months and since then the corrosion rate measured by the probe was higher than that obtained with the mass loss coupons.

5.4 CSIR Site

The results for the CSIR site are summarised in Appendix 4. Figure 75 shows the monthly corrosion rate for mild steel in cold water at the CSIR. There was no clear trend and the corrosion rate varied from month to month. Figures 76, 77, 78 and 79 compare the Langelier index with the corrosion rate of mild steel in cold water calculated by monthly mass loss three-monthly mass loss, electrode and probe respectively. The mass loss results were lower than those obtained with the probe and the electrode. It was also evident that there was no correlation between the Langelier index and the corrosion rate. The corrosion results calculated with the different techniques are compared in Figure 80. There was some scatter in the results originally but at sixteen months the corrosion rates were very similar and continued to be similar for months 17, 18 and 19, although the probe results showed a higher corrosion than the other techniques. The monthly mass loss results are compared to the SO_4^{2-}+$C1^-$/alkalinity ratio in Figure

81. Although there is no clear correlation, there appears to be an increase in the corrosion rate when there is an increase in the ratio.

Figure 82 shows the monthly mass loss of mild steel in hot water at the CSIR site. Generally speaking, the corrosion rate of mild steel in hot water was similar to that in cold water and in fact the corrosion rate was lower than that in cold water for the 19 and 20 month results. In addition, a significant increase in corrosion rate was noted for the results at 10 months. This is similar to the increase observed in cold water at 9 months - see Figure 75. Figures 83, 84 and 85 compare the Langelier index to the corrosion rate of mild steel in hot water calculated by monthly mass loss, electrode and probe respectively. As can be seen, no correlation was evident between the corrosion rate (calculated by three methods) and the Langelier index. The corrosion rates obtained by the different techniques are summarised in Figure 86. The corrosion rates obtained with the probe and the electrode were generally much higher than those obtained by mass loss. A comparison of the SO_4^{2-}+Cl^-/alkalinity ratio with the monthly corrosion rate in hot water presented in Figure 87 showed no clear correlation.

Comparisons of the Langelier index to the corrosion rate of galvanised steel calculated by three-monthly mass loss, electrode and probe are presented in Figures 88, 89 and 90 respectively. From the Figures, it is obvious that there is no correlation between the corrosion rate and the Langelier index. A comparison of the corrosion rates calculated by the three methods is shown in Figure 91. In this case, the corrosion rates of the electrode and the mass loss were similar but once again, the corrosion rates obtained with the probe were much higher. Similarly, comparisons of the Langelier index to the corrosion rate of galvanised steel in hot water at the CSIR are presented in Figures 92, 93 and 94 respectively. There was no obvious correlation between the Langelier index and the corrosion rate.

The comparisons between the Langelier index and the corrosion rate for brass in cold water calculated by three-monthly mass loss and the probe are presented in Figures 95 and 96 respectively. The mass losses show a decrease in the corrosion rate with time whereas the probe results show a significant increase in the corrosion rate after sixteen months. Similar results were obtained in hot water, see Figures 97 and 98.The results for copper are shown in Figures 99 and 100. No correlation was evident between the Langelier index and the corrosion rate. Figure 101 shows that the corrosion rate obtained with the probe was always higher than that obtained with the three-monthly mass losses. The probe results in hot water are shown in Figure 102, while the comparison of the corrosion rates is shown in Figure 103. Once again, the corrosion rate measured with the probe was higher than that measured by mass loss.

The results for 3CR12 in cold water are summarised in Figures 104 to 106. A comparison of the corrosion rates determined by the different techniques in cold water is shown in Figure 107. The lowest corrosion rates were determined with the mass loss coupons, followed by the electrode and the highest with the probe. The corrosion rates in hot water are summarised in Figures 108 to 110 and the corrosion rates compared in Figure 111. It is interesting to note that both electrochemical techniques (electrode and probe) were able to respond to changes in water quality whereas the three-monthly mass loss coupons were unable to do so.Figures 112 to 114 compare the corrosion rate of 304 in cold water to the Langelier index at CSIR, and the corrosion rates are compared in Figure 115. As has been the case with other alloys, the highest corrosion rate was obtained with the probe followed by the electrode and then the three-monthly mass loss results. Similarly, the hot water results are summarised in Figures 116 to 118 and the corrosion rates compared in Figure 119. No correlation was evident between the Langelier index and the corrosion rate and the highest corrosion rate was measured with the probe.

5.5 X-Ray Diffraction

Twenty eight mass loss coupons (four each of brass, copper, mild steel and galvanised steel) from the four locations were examined by X-ray diffraction in order to determine the corrosion products. The diffractograms are presented in Appendix 5.

5.5.1 Copper samples

All the diffractograms showed patterns consistent with cuprite (Cu_20) and copper in varying ratios. The samples from the Vaal Dam (sample D), Klerksdorp in hot water (sample Ks) and Vereeniging in hot water (sample V.) showed relatively higher levels of cuprite - see Figures 120 to 126.

Only the sample from the Vaal Dam showed any other peaks. It was not possible to identify these peaks but they could possibly be due to graphite or some form of mica.

5.5.2 Brass samples

All the brass samples showed peaks consistent with cuprite and copper as well as a brass phase. The samples from Vaal Dam, Vereeniging (cold water) and Vereeniging (hot water) showed relatively higher levels of cuprite. The presence of lead was detected in all the samples. Once again, the sample from the Vaal Dam showed an extra peak at 3,35 Å. The sample from Klerksdorp immersed in hot water showed extra peaks which are probably due to a zinc corrosion product but it was difficult to make a positive identification. The results are shown in Figures 127 to 133.

5.5.3 Mild steel samples

The mild steel samples were examined in two conditions. Initially, they were

examined in the as-received condition which resulted in relatively poor diffractograms. Therefore, the corrosion products were scraped off and ground and then examined.

The samples from cold water in Klerksdorp and both cold and hot water from Vereeniging contained goethite and calcite. The sample from the CSIR in cold water contained goethite and magnetite whereas the sample in hot water at the CSIR showed goethite only. The sample from the Vaal Dam showed goethite and calcite and the sample immersed in hot water in Klerksdorp showed peaks for goethite, calcite and magnetite. Furthermore, both samples showed peaks due to Lepidocrocite (γFe00H). Results are summarised in Figures 134 to 140.

5.5.4 Galvanised steel samples

The sample immersed in cold water at the CSIR was relatively uncorroded and the galvanising showed a distinct "spangled" effect. All the samples with the exception of that from the Vaal Dam showed peaks for zincite (ZnO) as well as a set of peaks tentatively identified as due to an iron-zinc intermetallic. The zincite formation appeared greatest in the samples immersed at Klerksdorp and generally higher in the samples exposed in hot water than cold water. The intermetallic peaks were fairly constant in all samples but the zinc peaks showed distinct signs of varying textures.

The sample from the Vaal Dam, as in the copper and brass samples showed a peak at 3,35 Å, possibly due to mica or graphite, while the sample immersed in hot water in Klerksdorp almost certainly had calcite. The sample immersed in cold water in Klerksdorp and both samples immersed in Vereeniging also showed peaks for calcite and it is significant that these correspond to the mild steel samples which showed calcite.

It should be mentioned that the galvanised samples presented considerable difficulties in interpretation, partly because the diffraction patterns of the iron-

zinc intermetallics are complex and poorly understood. Most of the samples also showed some other peaks which were unidentifiable; there were also some very broad background peaks due either to an amorphous corrosion product or to a crypto-crystalline intermetallic. The diffractograms are shown in Figures 141 to 147.

In general, it was noticeable that all the samples immersed in hot water in Klerksdorp (KH) seemed to indicate a greater degree of corrosion than corresponding samples from other locations, whereas the samples immersed in cold water at the CSIR (LC) seemed in general to show a lower degree of corrosion. Also the possibility of the phase marked "intermetallic iron zinc" in the galvanised steel samples in fact being a zinc corrosion product cannot be ruled out.

In order to aid in the interpretation of the diffractograms, the following table was drawn up.

B	Brass
C	Calcite ($CaCo_3$)
Cu	Copper
F	Ferrite (α-Fe)
G	Goethite (α-FeOOH)
I	Fe-Zn intermetallic
L	Lepidocrocite (γ-FeOOH)
M	Magnetite (Fe_3O_4)
O	Cuprite (Cu_2O)
Pb	Lead
Z	Zincite (ZnO)
Zn	Zinc
?	On its own - unidentified peak
	Combined - identification tentative

5.6 Statistical Analysis

As was stated many times in the previous sections, there appeared to be no correlation between the Langelier index and the corrosion rate of any of the alloys. In order to determine whether it was statistically possible to establish whether a correlation existed, an exhaustive statistical analysis of one set of results was undertaken.

5.6.1 Introduction

Attempts were made to derive twelve models for data collected at the CSIR. Six of the relationships sought were between water quality variables and monthly corrosion rate. The remaining six were between the Langelier index and corrosion rate.

Using various subset regression selection methods, models were sought that contained the smallest number of significant predictors while satisfying various statistical criteria for acceptable model fit.

Models to predict corrosion rate from water quality variables, that satisfied the criteria, could be found in all but one of the six cases. In only one case was a rather poor second order model found to predict corrosion rate from the Langelier index.

5.6.2 Modelling Procedure

The first step is to establish whether the response variable (corrosion rate) needs to be transformed. A transformation may be necessary to ensure the variability is similar over the entire range of the (transformed) response variable, a necessary assumption for deriving a prediction model. For two of "cold water" models transformations were used.

Models, with the smallest number of parameters, were selected such that the residuals, the differences between observed and predicted corrosion rate, are randomly distributed about the zero line. Therefore the residuals do not show any obvious structure as the structure is captured in the model. For the models to be useful for prediction purposes, all predictors in the model must have significantly non-zero regression coefficients.

The process of identifying a model involves selecting predictor variables that best describe the variability inherent in the response variable data (either the corrosion rates as measured or as transformed). A subset of all potential predictors is identified that satisfies the criteria of random residuals and significant regression coefficients.

Therefore each model given below can be used to predict corrosion rate from the water quality variables for the conditions under which the data was collected.

5.6.3 Comment

The relationship between corrosion rate and the water quality variables appears to be rather complex. In general it is not possible, from the components of a derived model, to establish the role of each predictor in describing the rate of corrosion. To establish which variables are responsible for corrosion would, firstly, require a screening experiment to identify the subset of variables that may be important, followed by an experiment specifically designed to establish the contribution of each variable in the subset, independently of the influence of any of the other variables. As the concentrations of none of the water quality variables were controlled in a systematic way it is not possible to establish the contribution of each variable to the observed rate of corrosion.

However, as indicated above, the models found are useful for predicting corrosion rate within the observed range of the prediction variables.

It was not possible to find a statistically significant model to predict corrosion rate in cold water, as measured by the probe method.

Nor was it possible to model, satisfactorily, corrosion rate in terms of the Langelier index. From two dimensional plots it is unlikely that linear or quadratic relationships exist between these two measures. The poor models found for the monthly mass loss data sets confirm this. For hot water the models are highly suspect. Removing one set of 5 coupons, suspected to be outliers, and no statistically significant relationship can be found. For cold water the second order relationship accounts for less than 15% of the inherent variability. This increases to 16% if two possible outliers are removed. None of the remaining data sets could be modelled. It does not appear feasible to use the Langelier index as a predictor for corrosion rate.

5.6.4 Results

Comment

R^2 : coefficient of determination, is given for all models that are statistically significant and that satisfy the criteria of random residuals and significant coefficients. It gives a measurement of how well the model fits the actual data. Should the model be a perfect fit, then $R^2 = 1$. If there is no relationship, then $R^2 = 0$.

Models Fitted

a) Corrosion rate vs Water quality
Monthly Mass Loss
Cold Water

$$(\text{Corrosion Rate})^{-0.5} = 0.207\ 63 - 0.105\ 92 \times \text{Ca-Hardness} - 0.213\ 57 \times (\text{S04+C1})\text{Alkalinity}$$

+0.168 70 x (SO4+C1)/Ca+Mg-Hardness
+0.263 30 x Ca
+0.004 384 5 x Conductivity
-0.558 17 x Conductivity/Total-Hardness
-0.000 750 05 x Alkalinity
+0.099 189 x Conductivity/Alkalinity
-0.000 811 35 x C1

$R^2 = 0.7699$

b) Corrosion Rate vs Water Quality

Monthly Mass Loss

Hot Water

Corrosion = -2 819.10

Rate +30 315.49 x Conductivity/Total-Hardness
-27.140 9 x pH
-80.994 5 x Ca-Hardness
+32.014 7 x Total-Hardness
+0.307 47 x $(Ca\text{-}Hardness)^2$
-18.454 8 x$(Conductivity/Alkalinity)^2$
-44 125.40 x $(Conductivity/Total\text{-}Hardness)^2$
-50.624 x $(SO4+C1/Ca+Mg\text{-}Hardness)^2$
-274.411 x (SO4+C1)/Alkalinity
-33.098 2 x Mg-Hardness

$R^2 = 0.9837$

c) Corrosion Rate vs Water Quality

Electrodes

Cold Water

(Corrosion = 0.053 748

$Rate)^{-1}$ 0.006 777 9 x Mg
-0.199 50 x (SO4+C1)/Alkalinity
+0.146 90 x (SO4+C1)/(Ca+ Mg-Hardness)

-0.001 114 0 x Alkalinity
+0.002 502 2 x Conductivity
-0.240 52 x Conductivity/Total-Hardness
-0.000 497 38 x C1

$R^2 = 0.8736$

d) Corrosion Rate vs Water Quality

Electrodes

Hot Water

Corrosion Rate = 7 104.44
-31.500 4 x Alkalinity
+444.244 x Ca-Hardness
-429.845 x Total-Hardness
+437.257 x Mg-Hardness
-3 785.85 x (Ca+Mg)/(SO4+C1)
-2 392.31 x (SO4+C1)/(Ca+Mg-Hardness)

$R^2 = 0.7899$

e) Corrosion Rate vs Water Quality

Probe

Cold Water

No statistically significant model could be found.

f) Corrosion Rate vs Water Quality

Probe

Hot Water

Corrosion Rate = 5 266.62
-368.866 x Mg-Hardness
-862.682 x Ca
+335.114 x Total-Hardness
-8 698.09 x Conductivity/Total-Hardness

g) Corrosion Rate vs Langelier
Monthly Mass Loss
Hot Water

(i) Corrosion Rate = 81.608 98 +60.712 97 x Langelier +35.632 70 x Langelier^2

$R^2 = 0.0946$

There are 5 possible outliers. If they are removed, none of the predictors are significant and R^2 drops to 0.0253.

(ii) Corrosion Rate = 81.654 52 +19.663 69 x Langelier

$R^2 = 0.0512$

There are also 5 possible outliers. If they are removed, Langelier is not significant predictor and R^2 drops to 0.0000.

h) Corrosion Rate vs Langelier
Monthly Mass Loss
Cold Water
Corrosion Rate = 82.953 50 +15.290 39 Langelier +15.438 15 x Langelier^2

$R^2 = 0.1588$

Two possible outliers were removed to obtain this model.

i) (i) Corrosion Rate vs Langelier
Electrode
Cold Water
No relationship was found between Corrosion Rate and the Langelier

index.

(ii) Corrosion Rate vs Langelier
Electrode
Hot Water
No relationship was found between Corrosion Rate and the Langelier index.

j) Corrosion Rate vs Langelier Probe
Cold Water
No relationship was found between Corrosion Rate and the Langelier index.

k) Corrosion Rate vs Langelier
Probe
Hot Water
No relationship was found between Corrosion Rate and the Langelier index.

5.6.5 Conclusion

Models were found to predict corrosion rate from the water quality variables. In only one case was a poor model found between the Langelier index and corrosion rate.

5.7 Water Composition

The composition of the waters at the various sites (for the first 20 months) is presented in Tables 2 to 5.

5.8 On-line monitoring results

The corrosion rate monitored over a period of 19 days at Klerksdorp is summarised in Table 6. The temperature varied between 30 and 34° C and the

average corrosion rate was 186μm/y.

The corrosion monitoring results at CSIR are shown in Table 7. A larger variation was detected and this may be due to the fact that the water composition is more variable at the CSIR. Since the water is treated at Klerksdorp, it can be expected that it will be less variation there.

TABLE 2

Monthly Water Composition at Vaal Dam

MONTH	1	2	3	4	5	6	7	8	9	10	11	12	13	14	15	16	17	18
pH	7.81	8.02	7.71	7.95	7.74	8.00	7.93	7.93	7.98	7.63	7.82	7.70	7.48	7.54	7.50	8.06	8.14	8.16
Conductivity mS/m	15	17	17	16	16	18	18	18	18	21	21	22	23	21	22	25	28	27
Total Hardness (ppm $CaCO_3$)	67	63	62	62	63	67	65	72	70	74	75	68	70	81	70	75	79	82
Ca (ppm)	35	32.5	32.5	35	32.5	35	35	35	35	40	40	32.5	35	42.5	40	40	40	42.5
Mg (ppm)	7.8	7.3	7.2	7.3	7.4	7.7	7.3	8.3	7.8	8.3	8.5	7.3	7.8	9.4	10	8.4	8.9	8.8
Sulphates (ppm)	14	14	13	14	18	17	17	17	14	19	10	14	14	18	13	14	20	14
Chlorides	12	-	-	-	-	13	-	-	-	-	-	N	-	-	-	-	-	-
Alkalinity (ppm $CaCO_3$)	68	65	64	64	65	63	66	71	69	71	76	74	74	75	70	82	77	82
Total (dissolved salts) (ppm)	108	122,4	122,4	115,2	115,2	129,6	129,6	129,6	129,6	151,2	151,2	158,4	165,6	151,2	158,4	180,0	201,6	194,4
Calcium hardness (ppm $CaCO_3$)	-	-	-	-	-	-	-	-	-	-	-	-	-	-	-	-	-	-
Magnesium hardness ($CaCO_3$ ppm)	-	-	-	-	-	-	-	-	-	-	-	-	-	-	-	-	-	-
Langelier Index	-0,59	-0.45	-0.74	-0.50	-0.71	-0.43	-0.45	-0.45	-0.36	-0.71	-0.49	-0.67	-0.89	-0.73	-0.84	-0.11	-0.18	-0.08

TABLE 3

Monthly Water Composition at Klerksdorp

MONTH	1	2	3	4	5	6	7	8	9	10	11	12	13	14	15	16	17	18
pH	7.83	7.89	8.31	7.98	7.88	7.61	7.58	7.71	7.60	8.06	8.71	8.15	8.10	7.76	7.89	7.56	7.63	7.61
Conductivity mS/m	119	132	125	117	89	87	101	93	71	75	691	492	71	99	115	115	101	93
Total Hardness ($CaCO_3$ ppm)	342	352	348	346	292	302	266	288	262	210	306	250	300	326	390	374	332	304
Ca (ppm)	-	-	-	-	-	-	-	-	60	42	68	-	-	-	-	-	-	-
Mg (ppm)	-	-	-	-	-	-	-	-	27	24	32	-	-	-	-	-	-	-
Sulphates (ppm)	87	104	105	105	135	115	104	95	115	115	125	204	187	-	243	224	225	210
Chlorides	102	122	129	104	93	77	89	85	72	55	78	58	65	88	99	94	88	85
Alkalinity ($CaCO_3$ ppm)	116	88	110	136	135	115	132	122	104	88	106	122	126	108	132	142	152	148
Total (dissolved salts) ppm)	687	730	781	741	627	571	718	608	540	471	554	422	502	613	699	738	641	590
Calcium hardness (ppm)	180	178	190	186	164	172	162	188	150	106	170	142	168	186	174	210	190	184
Magnesium hardness(ppm)	162	174	158	160	128	130	104	100	112	104	136	-	-	-	-	-	-	-
Langelier Index	0.29	0.22	0.74	0.52	0.37	0.07	0.05	0.24	-0.04	0.21	1.13	0.55	0.59	-0.19	0.39	0.17	0.23	0.18

TABLE 4

Monthly Water Composition at Veresenging

MONTH	1	2	3	4	5	6	7	8	9	10	11	12	13	14	15	16
pH	8.04	8.03	8.12	8.13	7.74	7.78	7.80	7.80	7.70	7.90	7.54	8.03	7.98	7.97	8.15	7.84
Conductivity mS/m	55	27	41	28	24	29	41	33	40	27	25	24	27	33	24	26
Total Hardness ($CaCO_3$ ppm)	220	120	120	105	99	115	140	115	145	105	93	97	84	115	66	65
Ca (ppm)	63	38	36	32	31	37	42	35	42	30	25	23-	23	35	18	17
Mg (ppm)	15	62	7.8	6.5	5.2	5.0	8.3	6.3	9.3	7.5	7.4	9.6	6.4	6.3	5.0	5.4
Sulphates (ppm)	115	30	54	29	26	39	65	58	72	22	21	15	17	24	17	16
Chlorides	40	11	23	14	12	18	29	17	14	-	-	11	-	13	-	-
Alkalinity ($CaCO_3$ ppm)	120	110	81	91	75	91	86	81	93	82	83	82	71	105	59	69
Total (dissolved salts) (ppm)	-	-	-	-	-	-	-	-	-	-	-	-	-	-	-	-
Calcium hardness (ppm)	-	-	-	-	-	-	-	-	-	-	-	-	-	-	-	-
Magnesium hardness(ppm)	-	-	-	-	-	-	-	-	-	-	-	-	-	-	-	-
Langelier Index	0.48	0.26	0.18	0.19	-0.21	-0.10	-0.60	-0.08	-0.12	-0.10	-0.42	-0.08	-0.19	0.13	-0.21	-0.46

TABLE 5

Monthly water composition at CSIR

MONTH	1	2	3	4	5	6	7	8	9	10	11	12	13	14	15	16	17	18	19	20
pH	8	-	8	7.8	7.7	7.7	7.6	7.9	8.4	8.1	7.7	7.8	6.5	6.8	7.5	7.6	7.8	8	7.6	7.7
Conductivity mS/m	36	-	36.8	37.6	35.1	33.9	32.7	31.9	28.6	28.4	31.9	34.6	37.7	36.3	31.7	29.2	29.4	35.3	29.1	31.9
Total Hardness ($CaCO_3$ ppm)	114.1	-	173.2	112.4	96.3	100.4	104.3	95.3	70.3	86.9	86.0	107	115.1	115.9	104.3	98.4	100.4	85	95	100
Ca (ppm)	29	-	54	34	29	31	29	27	22	22	23	29	29	33	27	26	31	22	21	27
Mg (ppm)	10	-	12	7	6	6	8	7	4	8	7	7	10	8	9	8	6	7	9	8
Sulphates(ppm)	36	-	63	26	18	34	85	27	72	16	24	31	59	35	27	27	34	26	6	33
Chlorides	20	-	21	17	14	17	102	51	16	18	20	24	34	29	17	17	27	19	16	21
Alkalinity $CaCO_3$ ppm)	100	-	141	107	79	117	95	89	76	92	80	77	88	102	101	94	115	94	16	64
Total (dissolved salts) (ppm)	194.7	-	213.3	209.3	189.3	201.3	189.3	189.3	146.6	138.6	180	186.6	237.3	195	173.3	246.6	181	187	165	212
Calcium hardness (ppm)	72.4	-	134.8	84.9	72.4	77.4	72.4	67.4	54.9	54.9	57.4	72.4	72.4	82.4	67.4	64.92	-	55	52	67
Magnesium hardness(ppm)	41.2	-	49.4	28.8	24.7	24.7	32.9	28.8	16.5	32.9	28.8	28.8	41.2	32.9	37.0	32.93	-	29	37	33
Langelier Index	-0.07	-	0.28	-0.21	-0.31	-0.05	-0.30	-0.03	-0.31	0.21	-0.30	-0.11	-1.48	-1.14	-0.45	-0.36	0.00	0.10	1.26	0.17

TABLE 6: On-line corrosion results at Klerksdorp

DATE	CORROSION RATE µm/y
04-07-90	195
05-07-90	205
06-07-90	207
09-07-90	193
10-07-90	186
11-07-90	180
12-07-90	180
13-07-90	181
16-07-90	184
17-07-90	180
18-07-90	183
19-07-90	182
20-07-90	177
23-07-90	179
24-07-90	181
25-07-90	186
26-07-90	186
27-07-90	189
30-07-90	185

TABLE 7: On-line corrosion results at CSIR

PERIOD EXPOSED DAYS	CORROSION RATE µm/y
1	200
2	168
5	152
6	180
7	146
9	179
12	178
13	196
14	191
20	196
22	189
23	188
27	189
29	173
30	167
34	168
35	172
36	165
37	159
40	158

5.9 Corrosivity of "sampled" versus "in-situ" water

The results of the corrosivity of sampled versus "in-situ" water at Vaal Dam are summarised in Table 8. The average corrosion rate for the "in-situ" tests was 226,7 μ/y and the free corrosion potential (E_{corr}) was -552 mV. In contrast, the average corrosion rate of the "sampled" water performed eight days later was 112,5 μm/y and the free corrosion potential was -651 mV. The variation in the free corrosion potential is not considered to be significant but the corrosion rate is approximately half that of the "in-situ" test.

The results for Klerksdorp are summarised in Table 9. The average corrosion rate for the "in-situ" tests was 89 μ/y and a free corrosion potential of -583 mV while the average for the "sampled" water was a corrosion rate of 219,9 μm/y and a free corrosion potential of -695 mV.

The Vereeniging site showed the highest corrosion rates, i.e. 502,4 μm/y for "in-situ" water versus 249 μm/y for sampled water, see Table 10. Similarly, at the CSIR site the corrosion rate of the "sampled" water (163,7 μm/y) was lower than that of the "in-situ" water (187,2 μm/y) as shown in Table 11.

TABLE 8: Comparison of corrosivity of in-situ versus sampled water from Vaal Dam.

IN-SITU WATER		SAMPLED WATER	
CORROSION RATE µm/y	E_{Corr}	CORROSION RATE µm/y	E_{Corr}
224,3	-543	110,7	-655
229,6	-544	107,9	-652
225,0	-546	111,2	-647
225,0	-549	112,8	-649
224,5	-551	111,2	-651
235,7	-553	110,7	-655
219,2	-555	113,3	-653
222,0	-557	123,4	-652
225,8	-560	115,6	-653
236,0	-562	108,7	-647

TABLE 9: Comparison of corrosivity of in-situ versus sampled water from Klerksdorp

IN-SITU WATER		SAMPLED WATER	
CORROSION RATE µm/y	E_{Corr}	CORROSION RATE µm/y	E_{Corr}
156,2	-572	214,1	-705
81,0	-566	215,1	-700
93,7	-563	220,7	-698
85,1	-589	217,2	-696
68,8	-589	220,7	-693
93,7	-596	224,5	-694
91,7	-592	218,9	-693
115,3	-594	220,2	-693
82,6	-591	220,2	-689
221,0	-579	227,8	-689

TABLE 10: Comparison of corrosivity of in-situ versus sampled water from Vereeniging

IN-SITU WATER		SAMPLED WATER	
CORROSION RATE µm/y	E_{Corr}	CORROSION RATE µm/y	E_{Corr}
495,8	-524	232,2	-707
493,3	-525	240,5	-704
514,1	-525	242,1	-701
500,4	-526	240,0	-702
496,6	-527	240,3	-702
503,2	-528	253,4	-701
503,4	-530	257,3	-700
502,4	-530	260,8	-698
503,2	-531	264,4	-698
511,3	-532	260,3	-699

TABLE 11: Comparison of corrosivity of in-situ versus sampled water from CSIR

IN-SITU WATER		SAMPLED WATER	
CORROSION RATE µm/y	E_{Corr}	CORROSION RATE µm/y	E_{Corr}
225,6	-654	151,6	-628
187,2	-647	177,0	-673
226,1	-663	160,8	-673
184,7	-655	160,0	-672
172,2	-631	162,3	-671
182,9	-628	147,8	-677
185,9	-640	167,6	-675
177,8	-625	168,4	-674
223,8	-651	167,9	-671
212,3	-663	174,0	-663

5.10 Corrosion of blended water

A limited series of corrosion tests were carried out on various blends of Vaal Dam, Sterkfontein Dam and Lesotho Highlands Water. Since the Vaal Dam receives water from the Sterkfontein Dam and is expected to receive water from the Lesotho Highlands development, it was useful to determine what effect water from these two sources would have on the corrosivity of Vaal Dam water.

Consequently, samples of water were received from the Vaal Dam (at the site in the dam wall), Sterkfontein Dam (courtesy of Department of Water Affairs) and from the Sengu River. Corrosion tests were carried out in the undiluted water and then in various blends as indicated in section 4.2. Corrosion rates were determined on mild steel coupons using the linear polarisation technique and the average values of five specimens are reported. It was however pointed out that the composition of the Vaal Dam water was not typical of that at Vereeniging. The tests were therefore repeated using Vaal Dam water taken from point A18 at Vereeniging. The water compositions are shown in Table 12, and the corrosion rates in Table 13.

TABLE 12: Composition of waters used for blending

PARAMETER	VAAL DAM (TEST SITE)	VAAL DAM (POINT A18)	STERKFONTEIN DAM	LESOTHO WATER
pH	7,92	7,3	7,1	7,4
Conductivity	94	17,8	10,5	8,3
mS/m		-1,5	-1,86	-1,18
Langelier Index	260	61	19,2	40,2
Hardness	64	16	6	10
Calcium (Ca)	24	5	1	4
Magnesium (Mg)	195	36	10	7
Sulphate	105	9	<2	2
Chloride	115	73	32	37
Alkalinity		173	24	57,3
Dissolved solids		40	15	25
Ca hardness		21	4,1	16,5
Mg hardness		8,83	8,96	8,58
pHs				

TABLE 13: Corrosion rates of mild steel in blended waters

BLEND	CORROSION RATE µm/yr
Vaal Dam (Test Site)	82,3
Vaal Dam (Point A18)	75,6
Sterkfontein	34,5
Lesotho	33,1
Vaal (Test Site) 25% - Sterkfontein 75%	40,4
Vaal (Test Site) 50% - Sterkfontein 50%	50,3
Vaal (Test Site) 75% - Sterkfontein 51,4	51,4
Vaal (Test Site) 90% - Sterkfontein 10%	54,5
Vaal (Test Site) 25% - Lesotho 75%	59,7
Vaal (Test Site) 50% - Lesotho 50%	51,1
Vaal (Test Site) 75% - Lesotho 25%	56,2
Vaal (Test Site) 90% - Lesotho 10%	59,5
Vaal (Point A18) 25% - Sterkfontein 75%	42,6
Vaal (Point A18) 50% - Sterkfontein 50%	47,3
Vaal (Point A18) 75% - Sterkfontein 25%	52,0
Vaal (Point A18) 90% - Sterkfontein 10%	51,8
Vaal (Point A18) 25% - Lesotho 75%	41,2
Vaal (Point A18) 50% - Lesotho 50%	47,1
Vaal (Point A18) 75% - Lesotho 25%	51,0
Vaal (Point A18) 90% - Lesotho 10%	54,3

6. DISCUSSION

Figure 148 in Appendix 6 summarises the three-monthly mass loss results for mild steel in cold water at the four sites. The highest corrosion rate was recorded at the CSIR site and the lowest at Klerksdorp. With the exception of the 18 month results, the second highest corrosion rate was determined at Vereeniging followed by the Vaal Dam results. The variation in the chloride/sulphate ratio over 20 months at the four sites is shown in Figure 149. It is interesting to note that the lowest ratio after approximately seven months is present at Klerksdorp. Figure 150 shows the hardness and alkalinity variation at the four sites over 20 months. There was no distinguishable trend but the highest ratio was at Klerksdorp for the first 12 months. Figure 151 shows the chloride and sulphate/alkalinity ratio over 20 months at the four sites. The Figure shows that the treated waters showed a larger variation than the Vaal Dam water. Furthermore, the ratio for Vereeniging, CSIR and Vaal Dam ratios was similar whereas the ratio at Klerksdorp was higher than the rest.

The mass loss of mild steel converted to a corrosion rate in hot water at the four sites is shown in Figure 152. A change in the corrosion behaviour was evident and the lowest corrosion rate was obtained at the CSIR site and the highest rate was generally recorded at the Klerksdorp site. This is a reversal to the behaviour in cold water. Chloride and sulphate ions are known to be corrosive towards mild steel whereas high alkalinity values may decrease the corrosion rate. Consequently, the chloride and sulphate/alkalinity ratio may be useful in determining the corrosivity of waters towards mild steel. A high ratio would indicate a corrosive water (i.e. more aggressive ions) whereas a low ratio would indicate a less corrosive water. This aspect is clear in Figure 123 which shows that the highest ratio was at the Klerksdorp site. Generally speaking, the corrosion rate in cold water was generally higher than that obtained in hot water.

A further complicating factor was the presence of sulphate - reducing bacteria (SRB) on the mild steel coupons. These bacteria are known to cause very high corrosion rates. Figure 153 shows a mild steel coupon which was perforated after an immersion period of eighteen months at the CSIR site in cold water. The voluminous scale, consisting of an inner iron sulphide corrosion product and an outer iron oxide layer is indicative of this type of attack. A further characteristic feature of corrosion by SRB is the intergranular morphology of the attack. This is clearly shown in Figures 154 and 155 which show the morphology of attack on mild steel coupons immersed at Klerksdorp and at the Vaal Dam respectively. Furthermore, Figure 156 shows an EDS trace of the corrosion product on the surface of the coupon shown in Figure 155 and the strong signal for sulphur is further proof of the action of SRB. The particular morphology of attack described above has been observed before in laboratory studies using pure cultures of SRB and thus confirms that the bacteria are contributing to the corrosion of the mild steel coupons.

The implication of SRB in the corrosion of mild steel complicates the analysis of the results. This is because it is difficult to differentiate between the contribution of the water chemistry to the corrosion rate and that of the bacteria. Clearly, this is an area requiring further study in order to accurately determine how much of the observed corrosion was due to bacterial action and how much to "chemical" corrosion. This is especially important when one considers that SRB were detected on all mild steel coupons at all the sites - see Appendix 7.
The tuberculation shown in Figure 153 is also apparent at the other sites and this is shown in Figures 157 to 162.

The monthly mass loss results for mild steel in cold water and hot water are summarised in Figures 163 and 164. It is obvious that there was more variation in the monthly mass loss results than the three monthly mass loss results - see Figures 148 and 152. However, the same ranking was observed in both cases i.e. the highest mass loss in cold water was recorded at the CSIR and the lowest at

Klerksdorp. The pH values at CSIR and Klerksdorp were similar, the major difference was that the hardness at the Klerksdorp site was much higher than that at the CSIR. In addition, the sulphate concentration at Klerksdorp was higher than that at the CSIR.

There was a discrepancy between the monthly mass loss results in hot water and the three monthly results. Figure 152 clearly showed that the lowest mass loss was at the CSIR site. In contrast, the monthly mass loss results (especially after 13 months) showed that the corrosion rate at the CSIR was higher than the other two sites. It would thus appear that some protection was afforded to the coupons exposed at the beginning of the test programme by surface deposits. Obviously, such a scale was unable to develop on the coupons exposed for one month at a time. Furthermore, the scale on the surface of the coupons immersed in cold water was more friable than that formed on the coupons immersed in hot water. Consequently, the scale formed on the samples immersed in hot water (and removed at three monthly intervals), would confer a greater degree of protection. The coupons exposed for one month at a time would be unable to form a protective scale.

As was mentioned previously, it was surprising to note that the corrosion rate of mild steel in hot water was generally lower than that measured in cold water. A perusal of Figure 8 in Appendix 7 shows that the total number of bacteria in hot water was much lower than that in cold water. As was shown in Figure 153, the SRB can cause very high corrosion rates. It is felt therefore that the high corrosion caused by the bacteria overshadowed the corrosion caused by the inorganic constituents of the water. This is one of the reasons why higher corrosion rates were obtained in cold water.

A comparison of the corrosion rates of mild steel obtained by the different techniques in cold water is shown in Figure 165. It is clear that the lowest corrosion rate was obtained with the three-monthly mass loss coupons. The corrosion rate of the monthly mass loss coupons and the electrode were similar while the highest corrosion rate was obtained with the probe. However, it is apparent that the more frequent the measurement, the more sensitive the reading and consequently variations in water chemistry can be detected. Similarly, Figure 166 compares the corrosion rates obtained in hot water and similar results were obtained.

An analysis of the X-ray diffraction results yields some interesting information. The mild steel samples immersed at the CSIR contained goethite and magnetite in cold water and goethite only in hot water. In contrast, the samples immersed in Klerksdorp (which showed the lowest corrosion rate) contained goethite and calcite in cold water and goethite, calcite and magnetite in hot water. Clearly, the presence of calcite must have contributed to the greater corrosion resistance displayed by mild steel at Klerksdorp. The Langelier index at Klerksdorp was almost always slightly positive, whereas the Langelier index was almost always negative at the CSIR.

The corrosion rates for the cast iron coupons after immersion in cold water for one year at the various sites are summarised in Figure 167. It is interesting to note that the highest corrosion rate was shown at the CSIR site, followed by Klerksdorp, then Vereeniging and the lowest corrosion rate was obtained at the Vaal Dam. Generally speaking, the specimen preparation had little effect on the corrosion rate. It was noticeable that the malleable cast iron had a lower corrosion rate than the other alloys. There wasn't much of a difference between the corrosion rate of the cast iron specimens and that of mild steel. It was however apparent that the treated waters were more aggressive towards cast iron than the raw Vaal Dam water. This may be due to the fact that in raw water,

carbonaceous corrosion products can become plugged with rust or other insoluble corrosion products thus conferring protection to the base material.

The mass loss results for galvanised steel in cold water at the various sites are summarised in Figure 168. The highest corrosion was measured at the Vaal Dam site, followed by Klerksdorp, then Vereeniging and the lowest rate was obtained at the CSIR site. In fact the corrosion rate at the CSIR site was fairly constant whereas the corrosion rate at Vereeniging and Klerksdorp tended to increase with time. There also appeared to be a gradual reduction in the corrosion rate at the Vaal Dam site. The results in hot water are summarised in Figure 169. Generally speaking, the corrosion rates were higher in hot water than cold water at all the sites. It also appeared that the lowest rate was obtained at the CSIR site.

The corrosion rates of the hot-dipped galvanised samples (HDG) immersed in cold water at the four sites are summarised in Figure 170. The results are similar to those shown in Figure 168 for the galvanised steel samples. The highest corrosion rates were at the Vaal Dam site and the lowest at the CSIR site. However, the corrosion rates of the HDG-samples were higher than the galvanised steel samples. Figure 171 summarises the corrosion rates of the HDG-samples immersed in hot water at three sites. No clear trends were distinguishable but generally speaking the highest corrosion rate was measured at the CSIR site.

Figures 172 to 178 compare the corrosion rates of the HDG samples to the galvanised steel samples at the four sites. With the exception of the hot water results at Vereeniging, the corrosion rate of the HDG samples was higher than that of the galvanised steel samples. Galvanised steel sheet normally contains a thin layer of zinc since there is not sufficient time for extensive reactions between the steel substrate and the molten zinc to take place. However, hot dipped galvanised samples usually spend a longer time in the bath and the zinc coating consists of a number of intermetallic layers and a thin layer of pure zinc

on the outermost surface. It is thus possible to have areas where corrosion of the thin layer of zinc can expose intermetallic compounds which are not as corrosion resistant as the zinc itself.

The three-monthly mass loss results for brass in cold water and in hot water are presented in Figures 179 and 180 respectively. The highest corrosion rate in cold water was at the Vaal Dam with the CSIR being the lowest. In hot water, the highest corrosion rate was at Klerksdorp and the lowest at the CSIR. In cold water, the corrosion rate in the treated waters did not vary significantly whereas a larger variation was noted in hot water. The X-ray diffraction results showed that higher levels of cuprite (Cu_2O) were present on the samples exposed in the Vaal Dam. Furthermore, the X-ray diffractogram of the sample immersed in hot water at Klerksdorp (which showed higher corrosion rates than the other sites) contained a large number of extra peaks which were difficult to identify.

The mass loss results for copper in cold water are summarised in Figure 181. The highest mass loss was recorded at the Vaal Dam and the lowest at the CSIR. Generally speaking however, the corrosion rate at the CSIR and the Vaal Dam decreased with time. Also, the corrosion rates of copper in cold water were lower than those for brass. The corrosion rate of copper at Klerksdorp was low for the first six months and only increased marginally thereafter. From this it can be inferred that the corrosion performance of copper was adequate. An examination of copper coupons in the SEM revealed the presence of pits and these are shown in Figures 182, 183 and 184 which correspond to immersion times of 9,12 and 18 months respectively. It is evident from the Figures that pitting corrosion was established at nine months and the penetration rates increased with increasing length of exposure. It would therefore be erroneous to measure the mass loss and convert that figure to a corrosion rate as this would be an underestimation of the actual corrosion rate. Pitting corrosion would only result in a small mass loss but could penetrate a pipe wall in a relatively short period of time. Pitting corrosion was only detected in copper samples immersed

in cold water at Klerksdorp and at no other site. Chloride ions are notorious for causing localised corrosion such as pitting. The average chloride levels at the four sites over 18 months were 88 ppm for Klerksdorp, 21 for the CSIR site, 18 for Vereeniging and 12 for Vaal Dam. It would thus appear that the higher chloride levels could explain why pitting corrosion occurred at Klerksdorp. In hot water, the corrosion rate of copper was highest at Klerksdorp, followed by Vereeniging and the lowest was at the CSIR - see Figure 185. The corrosion rate at Vereeniging was similar to that at the CSIR.

The X-Ray analysis of the copper coupons (see Figures 120 to 126) detected only the presence of cuprite (Cu_2O) on the surface. The presence of $CaCO_3$ was not detected. Similar results were reported for brass. Calcite was only found on the mild steel and galvanised steel samples. It may therefore be easier for chloride ions to initiate pitting corrosion on copper because no $CaCO_3$ scale was present. Since the calcite scale is fairly thick in most cases, it may act as a physical barrier to the chloride ions.

The corrosion rates for 3CR12 in cold water determined by mass loss are summarised in Figure 186 while those for hot water are summarised in Figure 187. It should be noted that all the corrosion rates were relatively low i.e. below 1,4 µm/yr. However, in cold water the highest corrosion rate was shown at Vaal Dam until 9 months. The corrosion rate of 3CR12 was low at the CSIR initially but by 18 months the CSIR site showed the highest (relatively speaking) corrosion rate. As can be seen in Figure 187, the corrosion rate of 3CR12 in hot water was lower than that in cold water. There was a distinct minimum detected in the corrosion rate at nine months (this was also the case in cold water). From 12 months onwards, the highest corrosion rate was measured at Klerksdorp.

The three monthly mass loss results for 304 in cold water and in hot water are summarised in Figures 188 and 189 respectively. The corrosion rates in both hot and cold water were typically below 0,5 µm/yr. This is to be expected since 304 is corrosion resistant and is passive in potable water. The predominant corrosion mechanism would be pitting corrosion but as was explained previously this would only result in small changes in mass even if the pitting rate was quite high. In cold water, the Vaal Dam water was the most corrosive initially, but after 12 months, the Klerksdorp water showed the highest corrosion rate. The corrosion rate of the treated waters showed a distinct minimum at 9 months in cold water.

The hot water results also showed a minimum at nine months but there was no clear trend as to which site was the most corrosive.

6.1 Mild Steel

The mild steel samples showed the highest corrosion rates at all four sites. With the exception of Klerksdorp, the corrosion rate in hot water was lower than that in cold water. Due to the fact that sulphate-reducing bacteria were present on all the coupons used for the three-monthly mass loss results, it is difficult to simply ascribe the mass loss obtained in this series of tests to the water composition when no cognizance is taken of the biological component of the system. However, as was noted in Appendix 7, it was found in general that bacterial counts were higher in cold water while the fungi predominated in the hot water systems. Furthermore, the mild steel coupons generally supported the most microbial growth (except for the CSIR site). This may be due to the larger amount of corrosion product on the mild steel coupons which can act as a substrate for the microbes. The presence of SRB may explain why the corrosion rate of mild steel was higher at the CSIR and Vereeniging sites than at the Vaal Dam site as shown in Figure 148.

The monthly mass loss coupons could be used to evaluate the changes in water composition since there was probably insufficient time for bacteria to establish themselves. However, it was not possible to correlate the water composition with the monthly mass loss. This can be due to a number of reasons. Firstly, not all the parameters of water are sampled for in a standard water analysis. Secondly, since the water composition varies, sampling at one particular point in time may give a false impression. It is thus preferable to monitor both the corrosion rate and the water composition on a continuous on-line basis.

The corrosion rates of mild steel in the blended waters clearly showed that they were less aggressive than the raw Vaal Dam water. The variation in the water composition is summarised in Figure 190. The Lesotho and Sterkfontein dam waters are pure and have low levels of chlorides and sulphates and very low conductivities. In addition they have negative Langelier indices and low hardness. It is probable therefore that mixing of the Vaal Dam water with Lesotho and/or Sterkfontein Dam water will have a diluting effect on the Vaal Dam water and make it less aggressive towards mild steel.

6.2 Galvanised steel

The corrosion rate of the galvanised steel was higher in hot water than in cold water. The corrosion rates obtained with the probe were similar to those obtained by mass loss. The X-ray diffraction results showed that there was generally more zincite on the coupons exposed in hot water than those exposed in cold water which is in agreement with the corrosion rates.

Surprisingly, the corrosion rate of the hot-dipped galvanised (HDG) samples was always higher than the galvanised steel samples. This is probably due to the different structure of the zinc coating obtained by the two depositional routes. It

is clear however that the raw water was the most aggressive towards the HDG samples at 17,1 µm/yr (compared to 5,38 µm/yr, 8,3 µm/yr and 7,88 µm/yr at the CSIR, Vereeniging and Klerksdorp sites respectively). In cold water the Vaal Dam water was also the most corrosive towards the galvanised steel. The deposition of the surface scales (such as calcium carbonate) in the treated waters is beneficial to the alloys.

6.3 Brass

In cold water, the corrosion rate of brass was highest at the CSIR (15,1 µm/yr) followed by the Vaal Dam (8,94 µm/yr), Vereeniging (5,20 µm/yr) and Klerksdorp (4,86 µm/yr). However, in hot water the highest corrosion rate was at Klerksdorp (13,2 µm/yr) followed by Vereeniging (7,73 µm/yr) and the CSIR (4,82 µm/yr). The corrosion rate of brass was similar to that of galvanised steel and even higher in some cases (Vereeniging in cold water and Klerksdorp in hot water). It should be mentioned that dezincification was detected on all the brass samples at all the sites. The brass used (see composition in Table 1) was not a DZR-resistant grade.

6.4 Copper

The highest corrosion rate for copper in cold water was recorded at the Vaal Dam (8,28 µm/yr) followed by the CSIR (3,18 µm/yr), Vereeniging (3,00 µm/yr) and Klerksdorp (2,50 µm/yr). In hot water, the highest corrosion rate was at Klerksdorp (5,70 µm/yr), followed by Vereeniging (5,02 µm/yr) and CSIR (2,05 µm/yr). This pattern was similar to that reported for brass. It appears that a non-DZR-resistant brass behaves in the same way as copper. The X-ray diffraction results showed that no calcite formed on the copper and brass samples but did form on the mild steel and galvanised steel samples.

Even though the lowest corrosion rate in cold water was recorded at Klerksdorp, SEM examination showed that pitting of the copper coupons occurred. It would thus be beneficial to use a technique which would be sensitive enough to detect the presence of pitting corrosion. Clearly, relying on mass loss results may lead to erroneous conclusions.

6.5 3CR12

The corrosion rates of 3CR12 were low at all sites. In cold water, the highest corrosion rate was recorded at the Vaal Dam (0,74 µm/yr), followed by Klerksdorp (0,41 µm/yr), Vereeniging (0,32 µm/yr) and CSIR (0,15 µm/yr). However, the corrosion rate at all sites was less than 1 µm/yr and can therefore be regarded as negligible. Similarly, in hot water the highest corrosion rate was at Klerksdorp (0,41 µm/yr) followed by Vereeniging (0,36 µm/yr) and CSIR (0,13 µm/yr). No pitting corrosion was detected on the coupons and hence their performance in both hot and cold water was satisfactory.

6.6 AISI 304

The corrosion rates of 304 were generally lower than those measured for 3CR12 with the exception of the hot water at the CSIR site. In fact, the corrosion rates can be regarded as negligible. The specimens were generally free of any surface deposit and in cases some deposits were found, they were easily washed off in running water.

6.7 "Sampled" versus "in-situ" corrosion tests

The results have shown that with the exception of Klerksdorp, the corrosion rates obtained with sampled water were lower than those obtained during "in-situ"

tests. A possible explanation could be that the oxygen concentration decreases when stored and thus the waters are less aggressive after eight days. In neutral and near-neutral waters, the oxygen concentration is important since it governs the rate of the cathodic reaction. Oxygen is an effective cathodic depolariser and increases the corrosion rate of many metals (1). However, as soon as a water sample is removed from a pipe, the equilibrium changes and the concentration of gases such as oxygen and carbon dioxide changes. It is important to note however that the corrosion rate of the "sampled" water was different to the "in-situ" water in all cases. This reinforces the premise at the beginning of this project that where possible accelerated electrochemical tests should be carried out in situ.

6.8 Corrosion Monitoring

The on-line corrosion monitoring results have shown that relatively minor variations in the corrosion rate are observed on a day-to-day basis. The sampling rate of the monitoring equipment can be adjusted to suit the application and could record a corrosion rate reading every ten minutes. It would be extremely beneficial to also monitor the water parameters on a continuous basis and correlate these to the corrosion rate. In this way it would be able to detect an instantaneous change in the corrosion rate which could be related to a change in the water quality.

6.9 General

In cold water, the ranking in terms of corrosion rate was the same at the sites with treated water and was as follows:

Mild Steel > Brass > Galvanised Steel > Copper > 3CR12 > 304.

The ranking at the Vaal Dam was as follows:

Mild Steel > Galvanised Steel > Brass > Copper > 3CR12 > 304.

Individually, the highest corrosion rate measured by three-monthly mass loss in cold water for mild steel was at CSIR (54,5 μm/yr) and the lowest at Klerksdorp (13,5 μm/yr). For galvanised steel, the highest was at the Vaal Dam (10,3 μm/yr) and the lowest at Vereeniging (3,65 μm/yr). The results for brass show the highest corrosion rate at the CSIR (15,1 μm/yr) and the lowest at Klerksdorp (4,86 μm/yr) while for copper the highest corrosion rate was at the Vaal Dam (8,28 μm/yr) and the lowest at Klerksdorp (2,50 μm/yr). 3CR12 showed the highest corrosion rate at the Vaal Dam (0,74 μm/yr) and the lowest at the CSIR (0,15 μm/yr) and similarly 304 showed the highest corrosion rate at the Vaal Dam (0,46 μm/yr) and the lowest at the CSIR (0,13 μm/yr).

From the above results a number of factors emerge. The highest SRB counts were recorded at Klerksdorp. Klerksdorp also has the highest sulphate levels of all the sites. Consequently, since the SRB use sulphate as their principal ion in their metabolism (converting it to sulphide), an increase in sulphate levels may lead to an increase in the population of SRB in pipelines. This is an important consideration from the corrosion point of view as increased mineralisation of water supplies results in an increase in sulphate levels (amongst others). It can therefore be concluded (provided everything else remains equal) that increasing mineralisation of water supplies in the PWVS/Klerksdorp area will probably lead to an increase in corrosion of mild steel piping as a result of increased SRB activity.

The corrosion rate of mild steel at Klerksdorp is lower than the corrosion rate of brass at the CSIR. This illustrates the high corrosion rates which can be expected if non-DZR-resistant fittings are used in potable waters. The raw water at the Vaal Dam appeared to be more corrosive copper and to a lesser extent brass than the other sites. Copper relies for its corrosion protection on a copper oxide scale which builds up in service. However, the Vaal Dam site is situated below the level of the water on surface and oxygen levels may be low in such an area. Consequently, the copper (and brass) is unable to form protective scales on the

surface. The low corrosion rate of galvanised steel at Vereeniging is similar to the corrosion rate of copper at Klerksdorp. It may therefore be possible to use certain alloys in areas where they show lower corrosion rates than other alloys. It may therefore be prudent to use galvanised steel piping in Vereeniging (for cold water) instead of mild steel and brass. At Klerksdorp for instance, copper showed the lowest corrosion rates of all the alloys (except for 3CR12 and 304). It should however be remembered that pitting corrosion of copper was detected at Klerksdorp, although this could only be resolved under high magnification in a scanning electron microscope. Copper also showed the lowest corrosion rate at the CSIR. It must be borne in mind that coupons were used in this investigation which contained no crevices. In practice however, crevices and other fabrication defects will be present in plumbing material which may affect the corrosion rate.

However, in hot water copper showed the lowest corrosion rate at all sites and should therefore be used in hot water piping systems.

7. CONCLUSIONS

A number of conclusions can be drawn from this study and these are listed as follows:

7.1 The water composition affects the corrosion behaviour of alloys, but since there are so many variables in describing water, it is virtually impossible to draw up a simple expression which can be used as a corrosivity indicator.

7.2 No correlation could be found between the Langelier Index and the corrosion rate of any alloy at any of the sites. Similarly, none of the other prediction indices showed any correlation to the corrosion rate.

7.3 The presence of micro-organisms was detected on all samples at all sites. In particular the presence of sulphate-reducing bacteria complicated the analysis of the corrosivity of the waters towards the alloys. However, conclusive proof was obtained which showed that the SRB were involved in the corrosion of the mild steel coupons in particular, resulting in high corrosion rates and perforation of mild steel coupons in less than 18 months.

7.4 Mild steel showed the highest corrosion rate at all the sites generally, but the lowest corrosion rate was detected at Klerksdorp.

7.5 On-line corrosion monitoring using mild steel probes showed that fluctuations in the corrosion rate were detectable.

7.6 Where possible, accelerated electrochemical corrosion tests should be carried out in situ as tests performed in a laboratory at a later stage may give erroneous results.

7.7 Increasing mineralisation of water supplies could probably lead to increased corrosion rates of carbon steel piping due to an increase in SRB activity.

7.8 Blending of Vaal Dam water with Lesotho Highlands and/or Sterkfontein Dam water will tend to decrease the corrosion rate of mild steel. The latter two waters are relatively pure and contain low levels of chloride and sulphate ions and would thus have a diluting effect on the Vaal Dam water.

7.9 Electrochemical techniques were more sensitive to changes in water composition than the mass loss coupons.

7.10 Pitting corrosion of copper samples was detected at Klerksdorp from 9 months onwards, although this was only visible under high magnification in a scanning electron microscope. This was in contrast to the low general corrosion rates

recorded for the alloy at this site. Once again, this illustrates the importance of monitoring corrosion on-line using appropriate equipment which can detect localised corrosion.

7.11 The non-DZR brass used in these tests initially showed high corrosion rates and dezincification at all the sites both in hot and cold water after 3 months. There is thus still a need to use dezincification-resistant fittings in the PWVS/Klerksdorp geographic area, even if Sterkfontein water is mixed with Vaal Dam water.

7.12 The corrosion rate of hot dipped galvanised samples was always higher than the galvanised steel samples.

8. RECOMMENDATIONS FOR FUTURE STUDY.

8.1 A thorough analysis of the succession patterns of bacterial colonization of pipe surfaces needs to be made. It is recommended that a programme be set up to determine how soon after colonization SRB initiate corrosion in conjunction with a corrosion monitoring system which would detect the onset of such corrosion. This is prudent in view of the expected increase in sulphate levels in future.

8.2 A similar study could be extended to coastal areas which use "soft" waters in order to determine whether similar corrosion mechanisms are operative in those areas.

8.3 Similar experiments using actual pipe samples should be undertaken to determine whether corrosion rates between coupons and pipes are similar.

9. RECOMMENDATIONS TO LOCAL AUTHORITIES

9.1 Uncoated mild steel corrodes in potable water, the corrosion rate varies depending on locality. Corrosion products developing on mild steel piping may affect water quality and cause blockage of plumbing components should they break off and be carried by the water. It is thus advisable to use internally coated mild steel for conveying potable water.

9.2 Sulphate-reducing bacteria (SRB) were detected at all sites and were responsible for extensive tuberculation of mild steel coupons. Perforation of 1 mm thick coupons occurred in less than 18 months. Since biocides cannot be used in potable waters and SRB will colonise uncoated mild steel surfaces, it is preferable to coat mild steel piping.

9.3 The brass used in this investigation was not a dezincification-resistant (DZR) grade and started showing signs of corrosion after three months at all the sites. The highest corrosion rate (in cold water) for brass was recorded at the CSIR site and amounted to 15.1 μm/yr. It is thus apparent that DZR-resistant brass should be used in the PWV/Klerksdorp area for both hot and cold water installations.

9.4 The corrosion rate of galvanised steel coupons was higher in hot water than in cold water.

9.5 In terms of commonly used pipe materials, copper showed the lowest corrosion in hot water at all sites and should therefore be used in hot water installations.

9.6 The Langelier Index cannot be used as a corrosivity index.

10. REFERENCES

1. Butler G and Ison H.C.K Corrosion and its prevention in waters. Leonard Hill, London, 1966.

2. Rimmer R. The quality of water as it affects pipeline performance. Symposium, 13 October 1986, Practical problems with pressure pipelines.

3. Rothwell G.P. Corrosion mechanisms applicable to metallic pipes. Pipes and Pipelines International, February 1979.

4. van der Kooij, D, van den Hoven J.J., Schulting F.L. and Van der Zwan J.T. Influence of materials on water quality degradation in distribution systems. The Netherlands Waterworks Testing and Research Institute Kicoa Ltd, P.O. Box 70, 2280 A B Rijswijk, The Netherlands.

5. Borgioli A, Terzano C, De Fulvio S and Olori L. Influence of material on water quality - Degradation in distribution systems. ACEA, Pzzle Ostiense No. 2, 00154, Rome.

6. Ahmad NAI, Ismail MI and Al-Ameeri R.S. Corrosion in fresh water systems: role of metallurgical factors in stability of steel. Anti-Corrosion, December 1987.

7. Kennett C.A. Treatment of water to potable standards with corrosion prevention. Corrosion prevention and control, April 1984.

8. Neff CH, Schock MR and Marden J.I. Relationships between water quality and corrosion of plumbing materials in buildings. United States Environmental Protection Agency, Research and Development, EPA/600/52-87/036, July 1987.

9. Pisigan RA and Singley J.E. Effects of water quality Parameters on the corrosion of galvanised steel. Journal Awwa, November 1985, pg 76.

10. Heynike J.J.C. The economic effects of the mineral content present in the Vaal River Barrage on the community of the PWVS-Complex. Water Research Commission, 1981.

11. Jones G.A., Brierley S.E, Geldenhuis S.J.J. and Howard J.R. Research on the contribution of mine dumps to the mineral pollution load in the Vaal Barrage. WRC Report 136/1/89.

12. Rimmer R. The quality of water as it affects pipeline performance. Symposium on Practical Problems with pressure pipelines, 13/10/86.

Figure 1: Location of test sites.

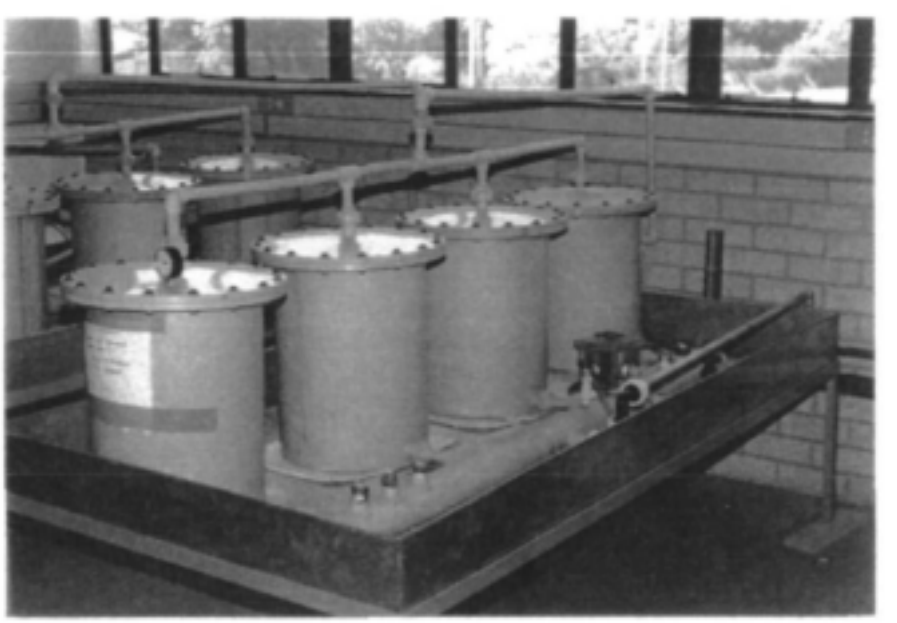

Figure 2: Typical experimental apparatus situated at the CSIR site.

Appendix 1. Results of corrosion testing at Vaal Dam

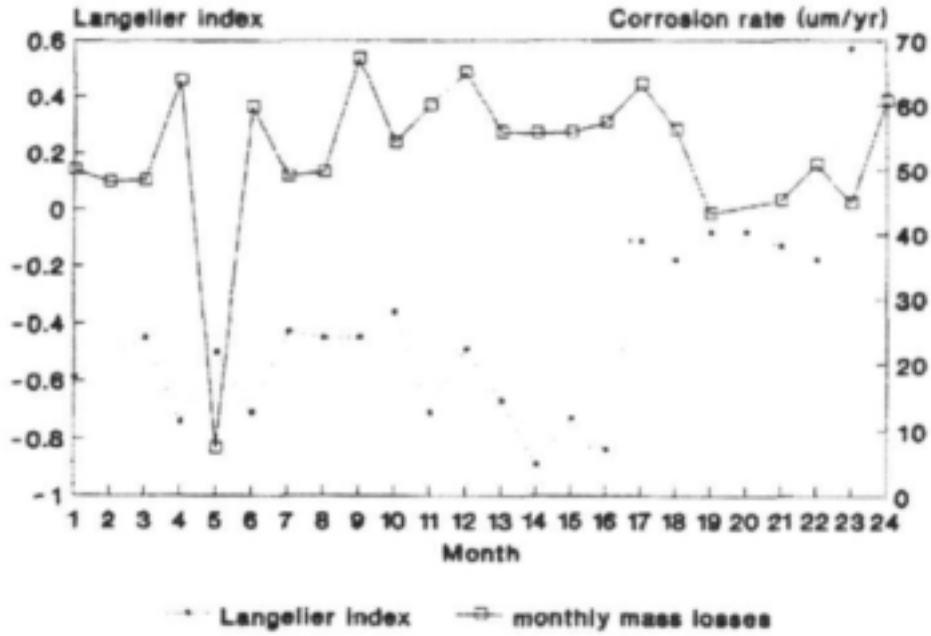

Figure 1: Langelier index versus corrosion rate of mild steel measured by monthly mass loss (Vaal Dam).

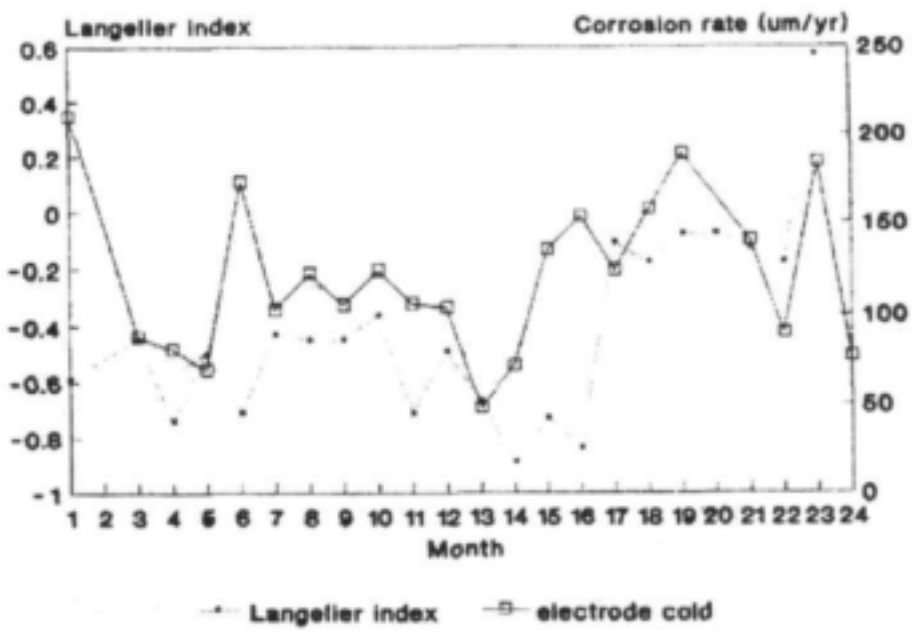

Figure 2: Langelier index versus corrosion rate of mild steel measured by an electrode (Vaal Dam).

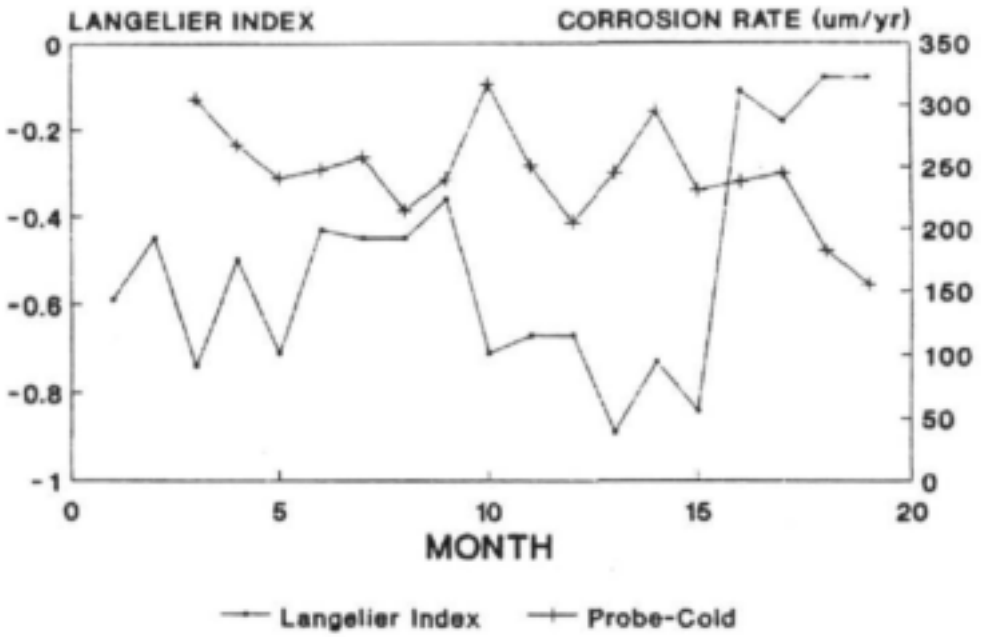

Figure 3: Langelier index versus corrosion rate of mild steel measured by a probe (Vaal Dam).

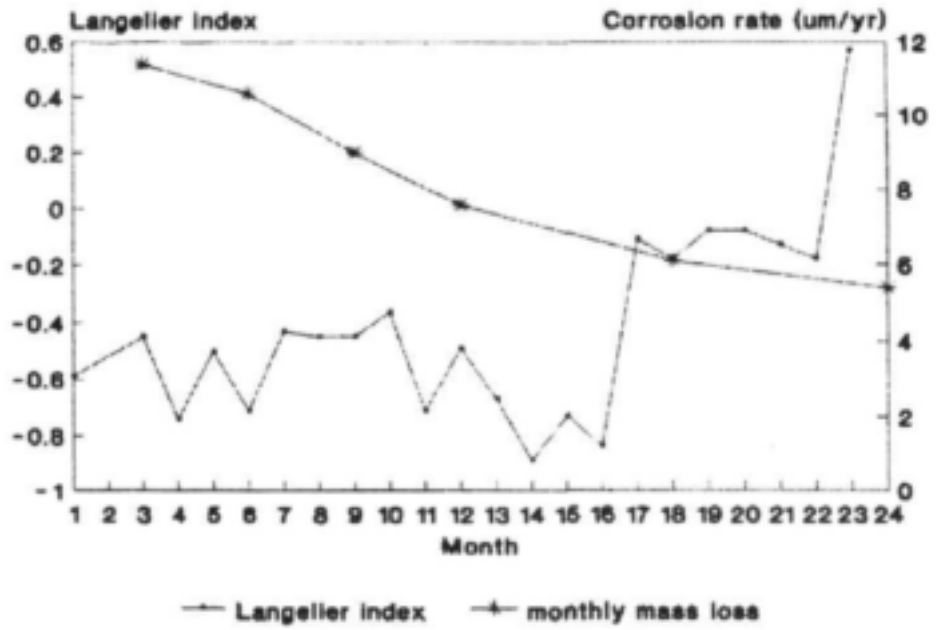

Figure 4a. Langelier index versus corrosion rate of brass measured by 3-monthly mass loss (Vaal Dam).

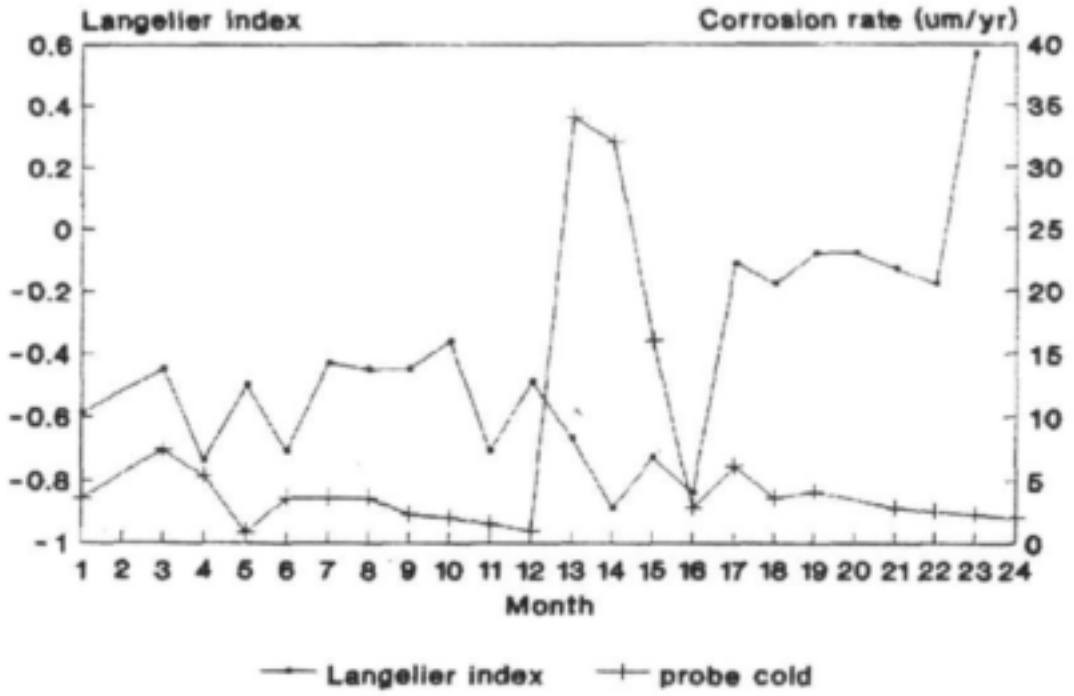

Figure 4b. Langelier index versus corrosion rate of brass measured by a probe (Vaal Dam).

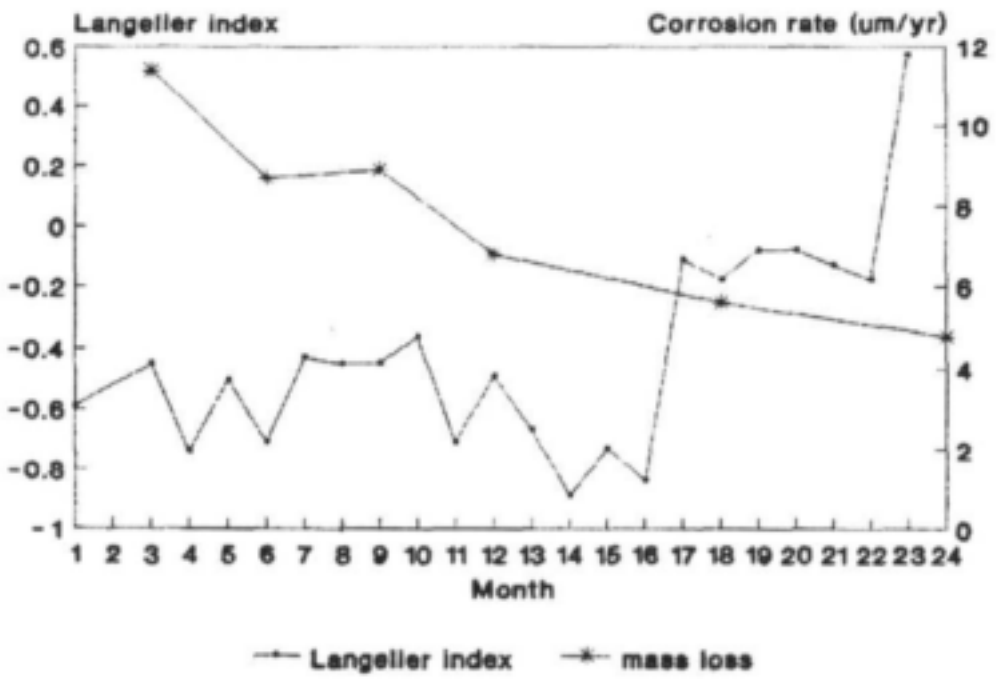

Figure 5a. Langelier index versus corrosion rate of copper measured by 3-monthly mass loss (Vaal Dam).

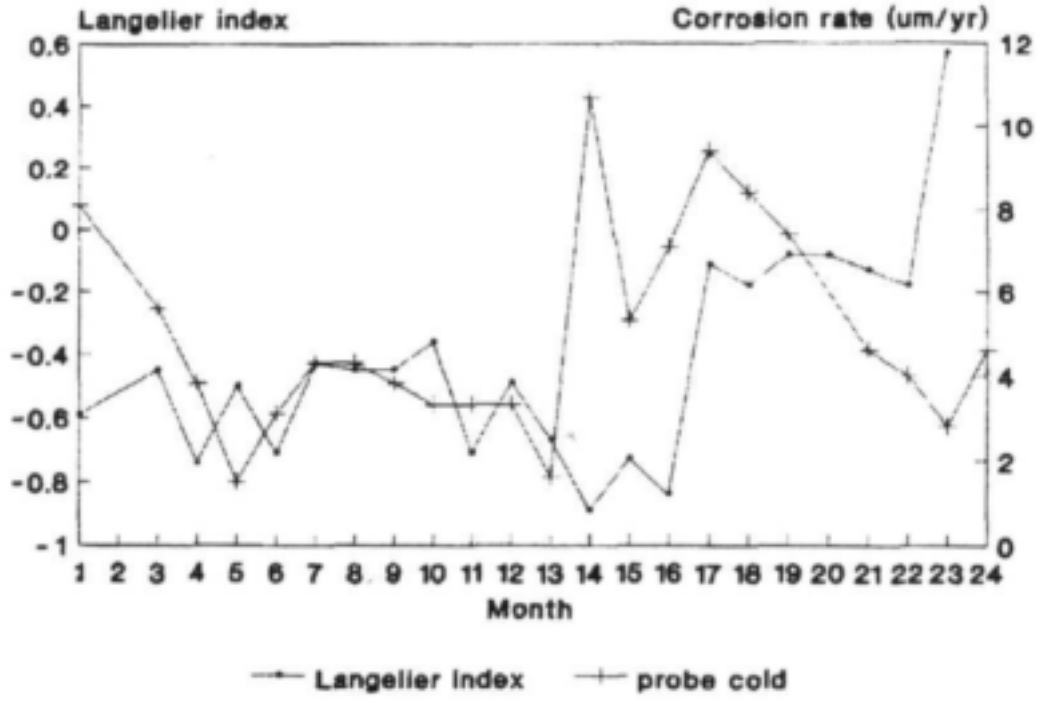

Figure 5b. Langelier index versus corrosion rate of copper measured by a probe (Vaal Dam).

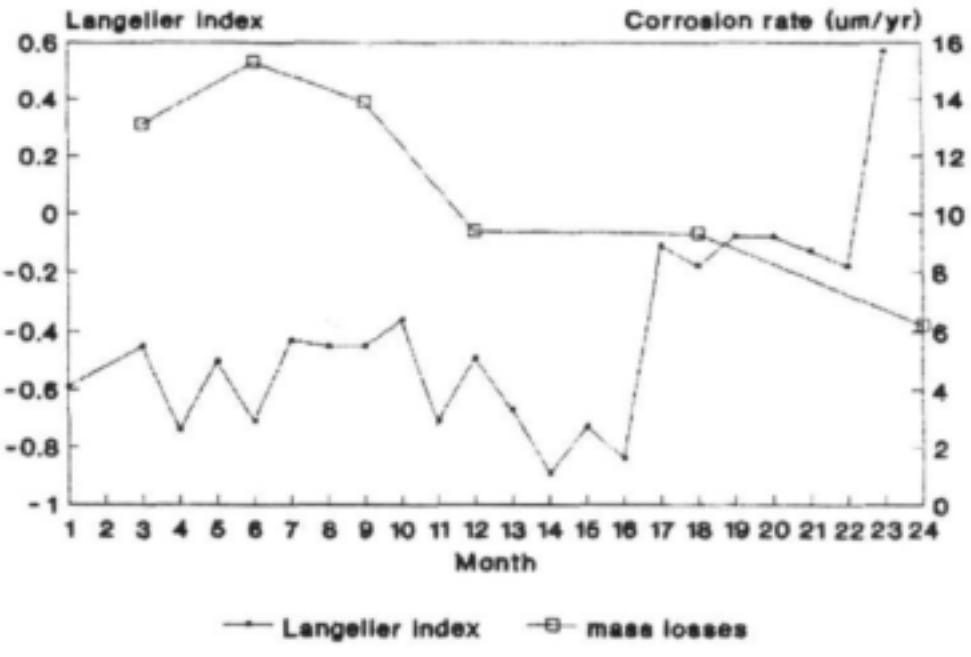

Figure 6a. Langelier index versus corrosion rate of zinc measured by 3-monthly mass loss (Vaal Dam).

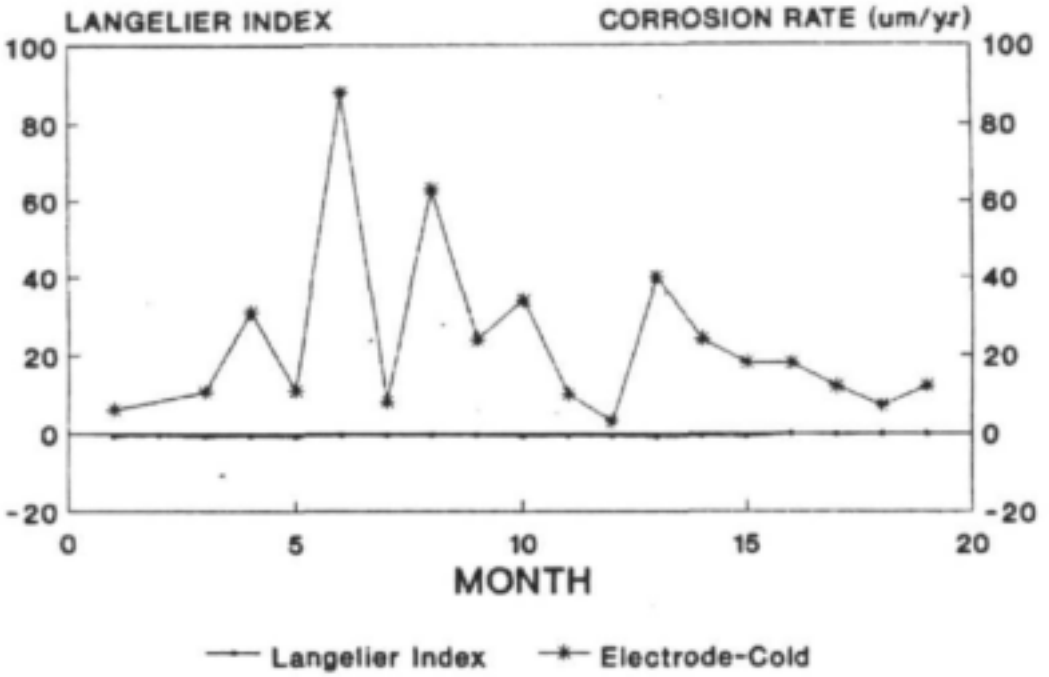

Figure 6b. Langelier index versus corrosion rate of zinc measured by an electrode (Vaal Dam).

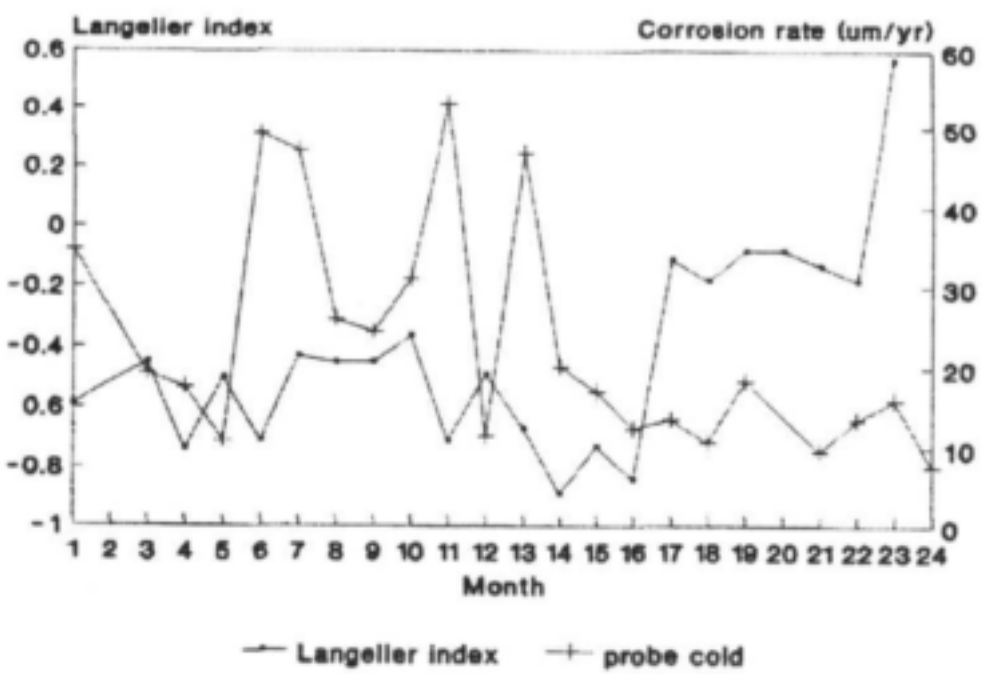

Figure 7a. Langelier index versus corrosion rate of zinc measured by a probe (Vaal Dam).

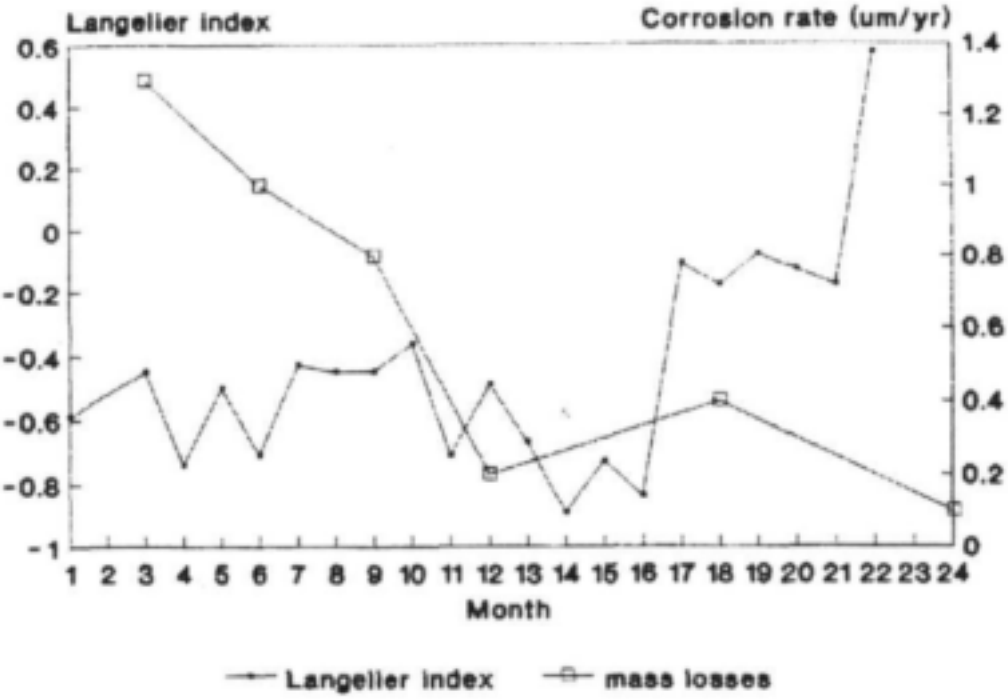

Figure 7b. Langelier index versus corrosion rate of 3CR12 measured by 3-monthly mass loss (Vaal Dam).

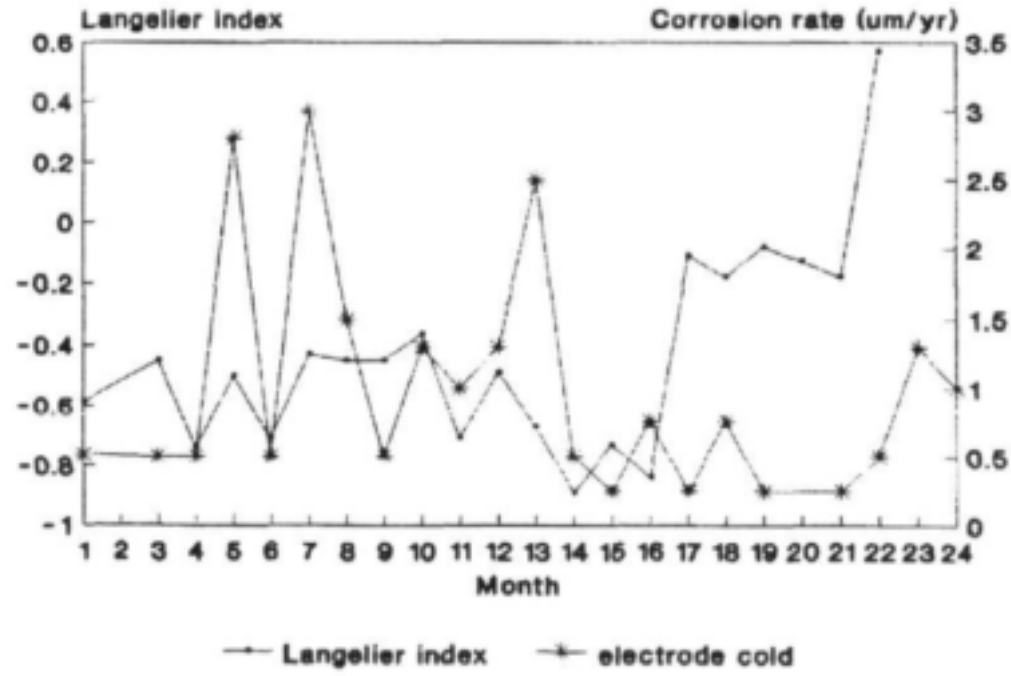

Figure 8. Langelier index versus corrosion rate of 3CR12 measured by an electrode (Vaal Dam).

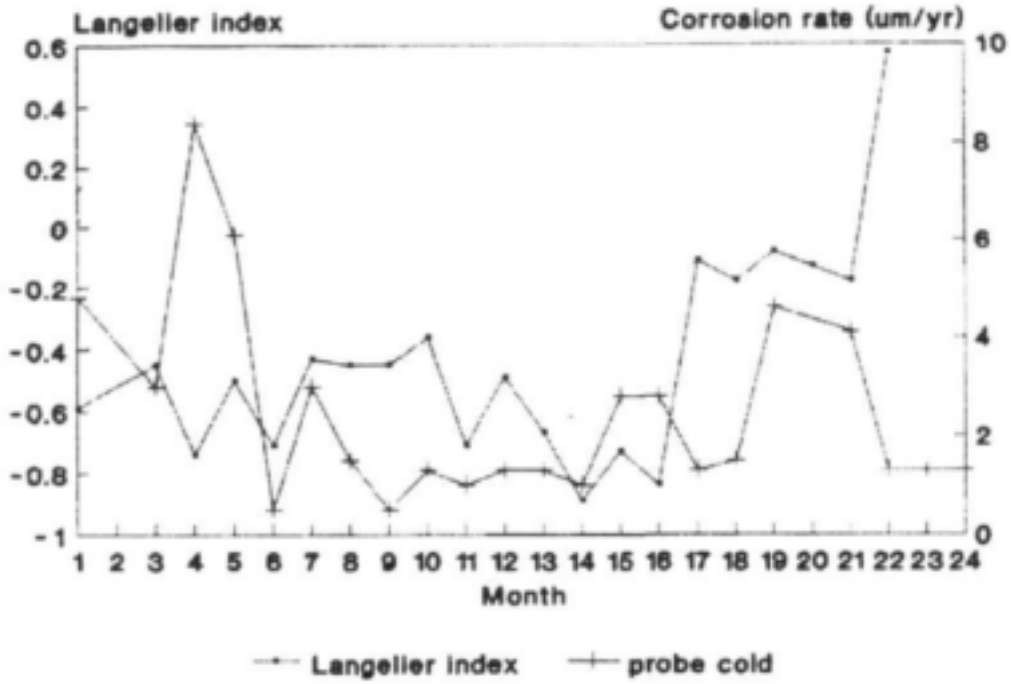

Figure 9. Langelier index versus corrosion rate of 3CR12 measured by a probe (Vaal Dam).

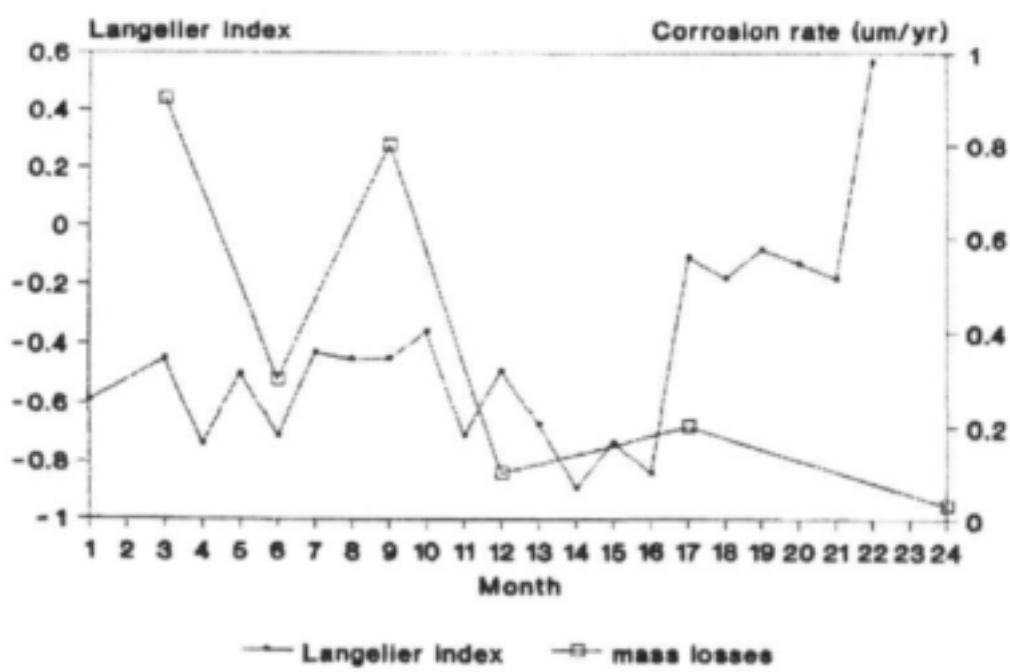

Figure 10. Langelier index versus corrosion rate of 304 measured by 3-monthly mass loss (Vaal Dam).

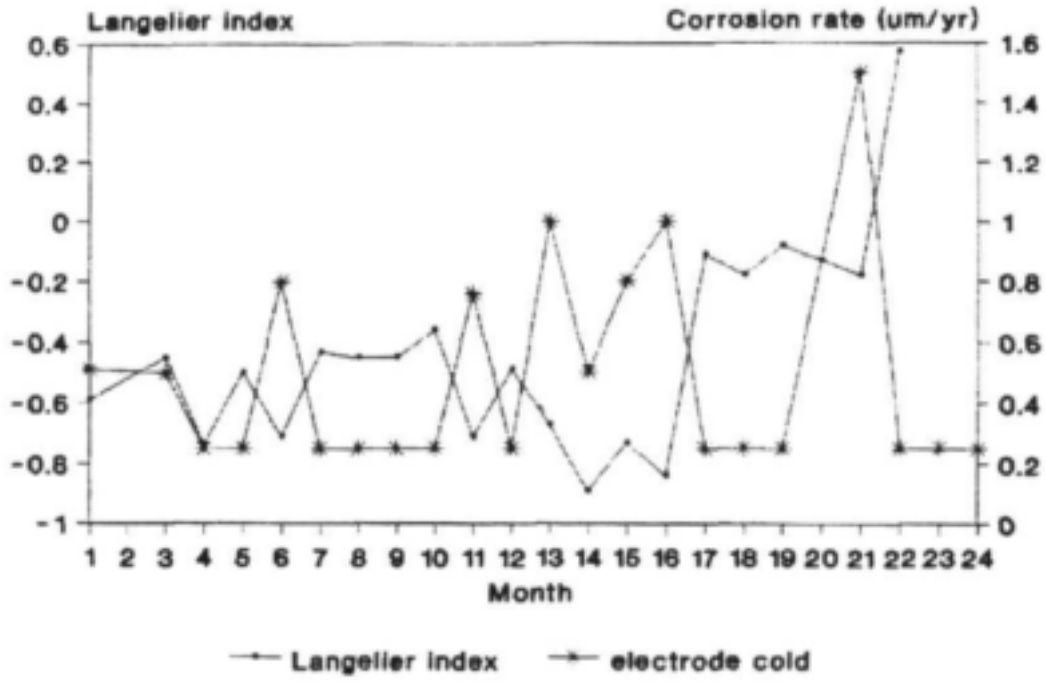

Figure 11. Langelier index versus corrosion rate of 304 measured by an electrode (Vaal Dam).

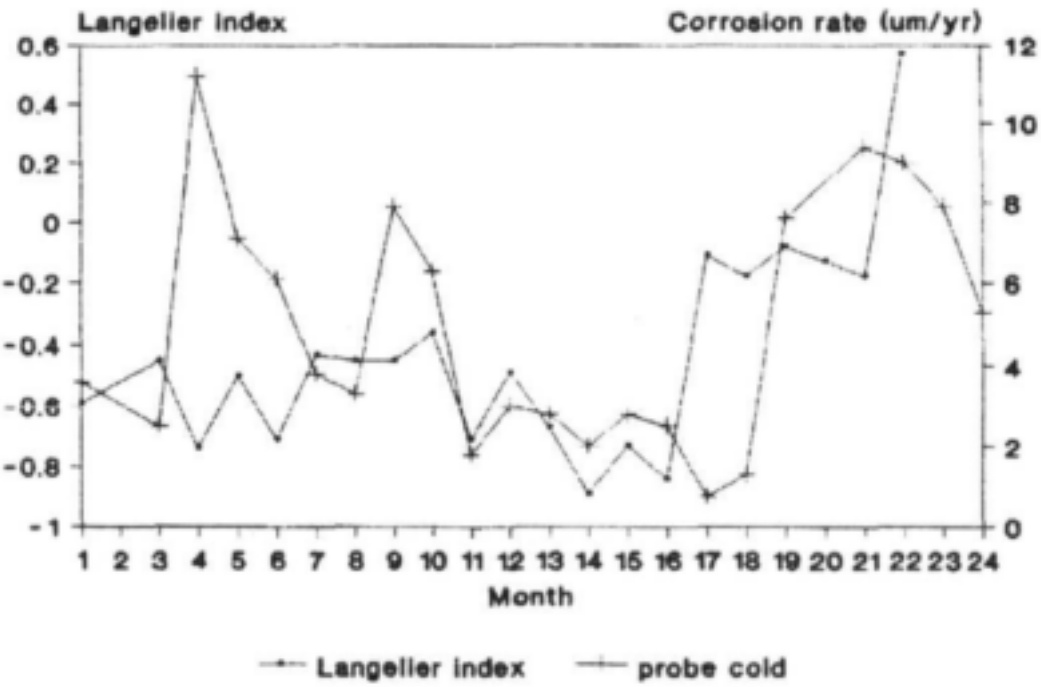

Figure 12. Langelier index versus corrosion rate of 304 measured by a probe (Vaal Dam).

Appendix 2. Results of corrosion testing at Klerksdorp

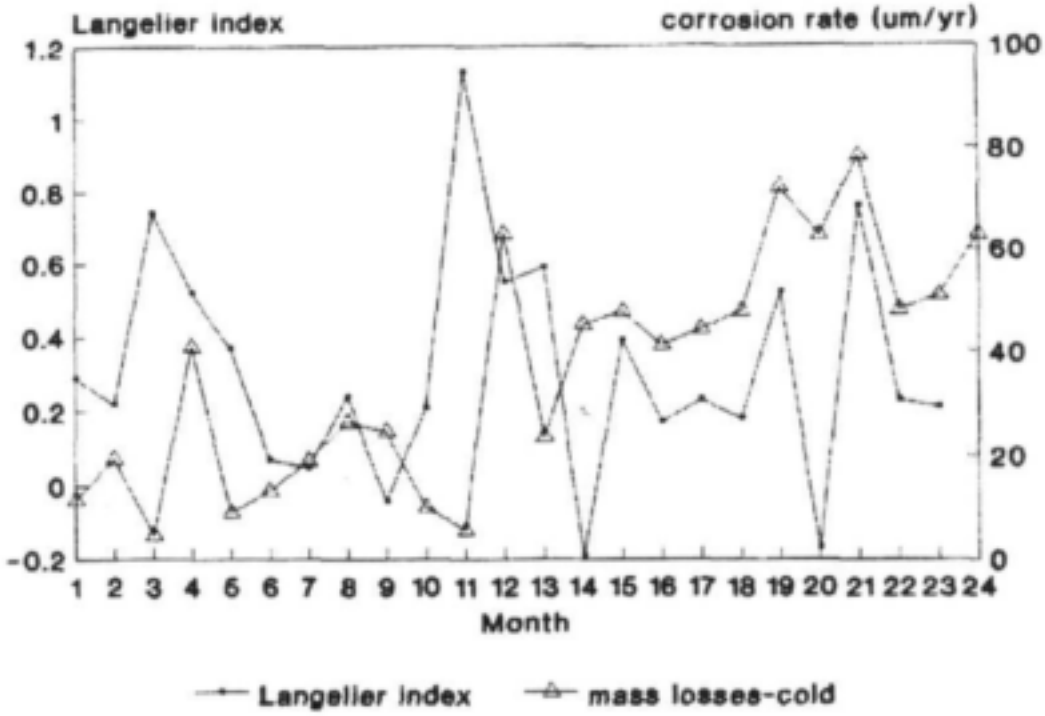

Figure 13. Langelier index versus corrosion rate of mild steel measured by monthly mass loss in cold water (Klerksdorp).

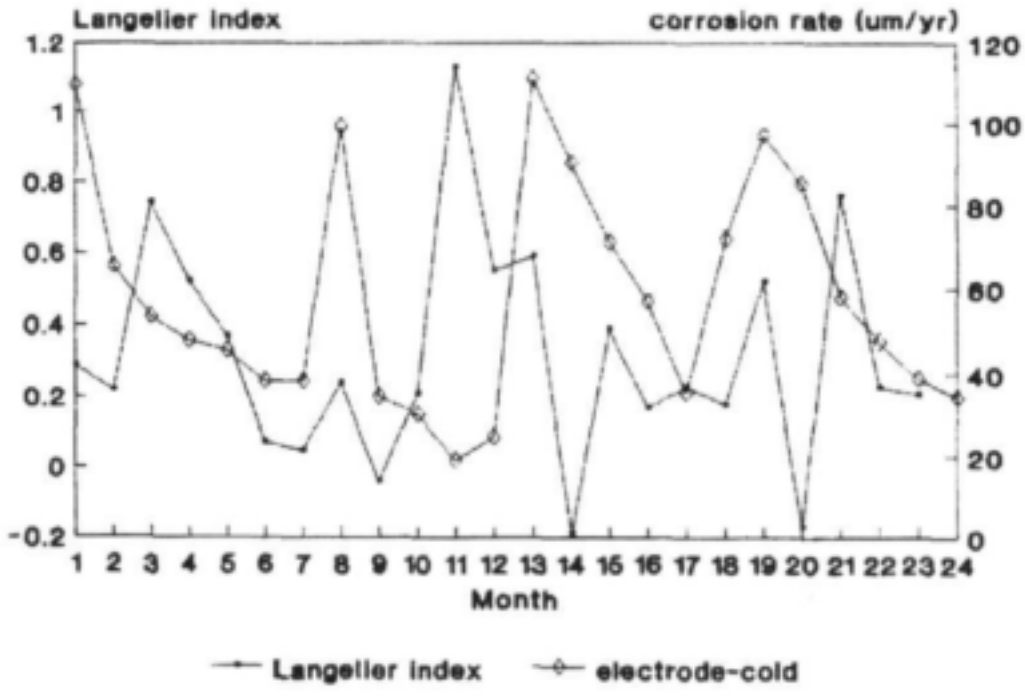

Figure 14. Langelier index versus corrosion rate of mild steel measured by an electrode in cold water (Klerksdorp).

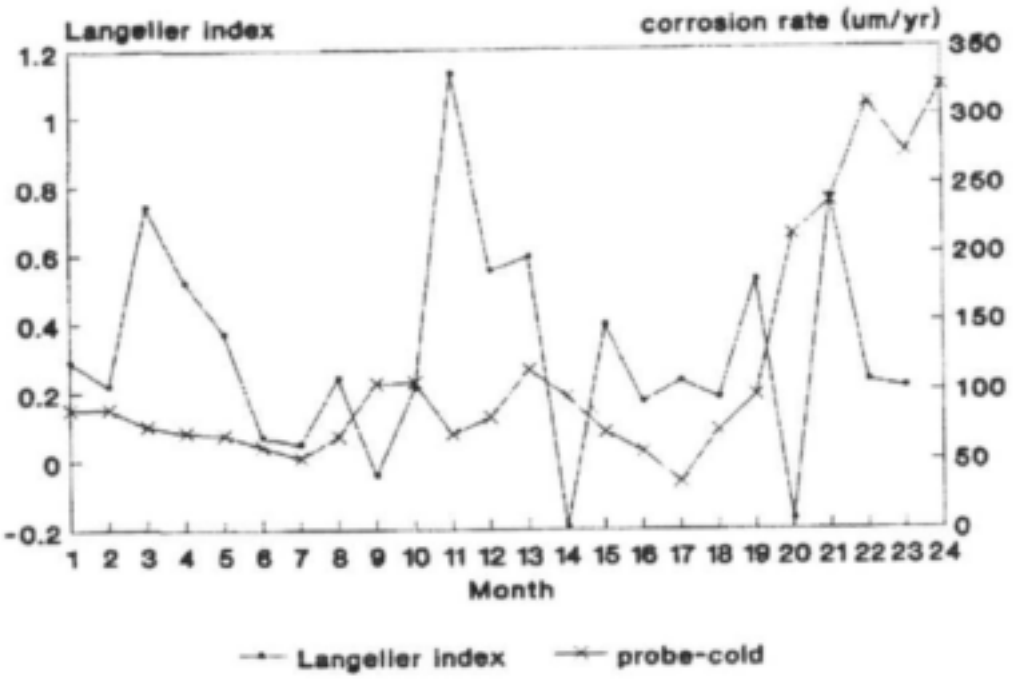

Figure 15. Langelier index versus corrosion rate of mild steel measured by a probe in cold water (Klerksdorp).

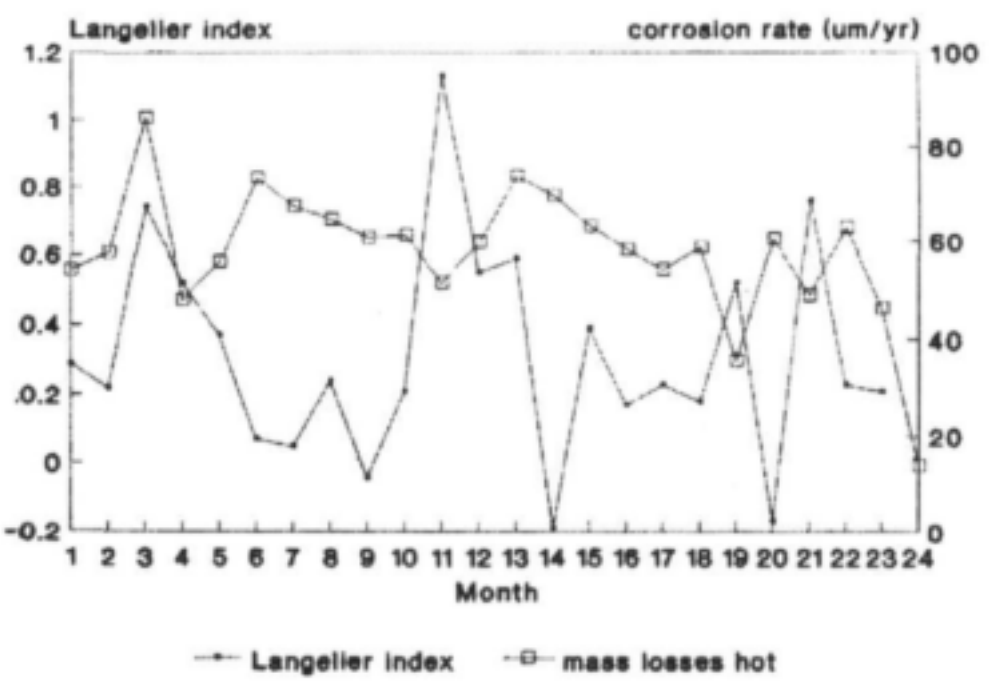

Figure 16. Langelier index versus corrosion rate of mild steel measured by monthly mass loss in hot water (Klerksdorp).

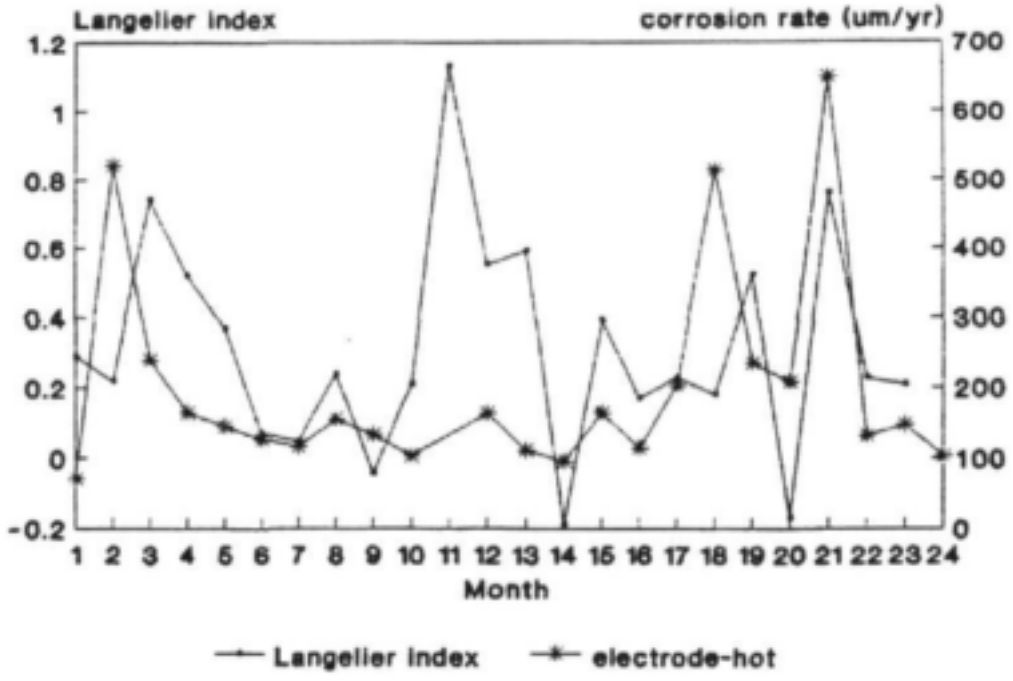

Figure 17. Langelier index versus corrosion rate of mild steel measured by an electrode in hot water (Klerksdorp).

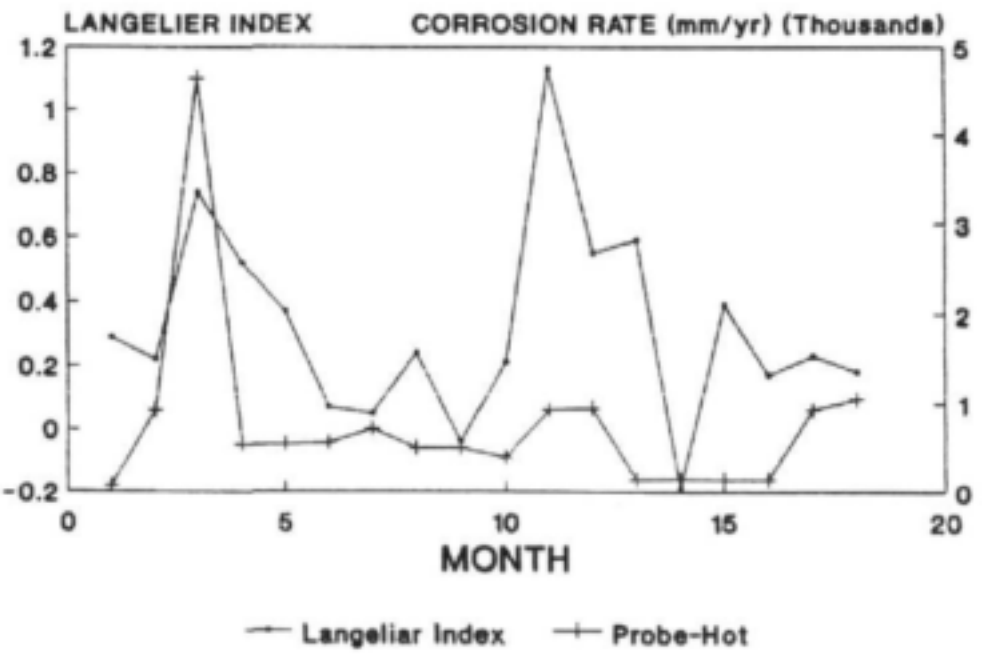

Figure 18. Langelier index versus corrosion rate of mild steel measured by a probe in hot water (Klerksdorp).

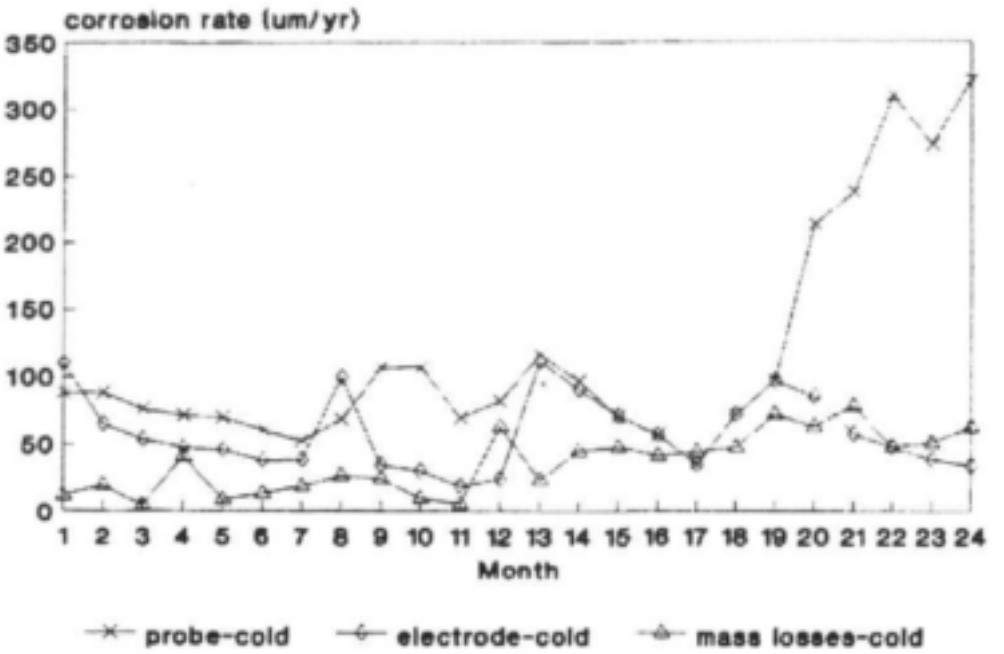

Figure 19. Comparison of corrosion rates of mild steel obtained by different techniques in cold water (Klerksdorp).

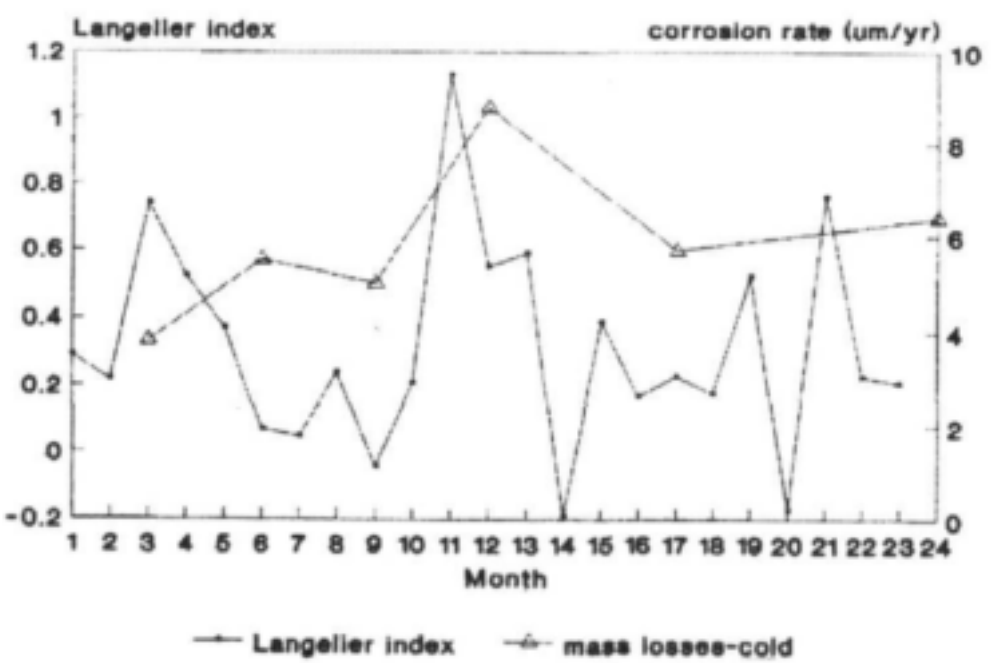

Figure 20a. Langelier index versus corrosion rate of zinc measured by 3-monthly mass loss in cold water (Klerksdorp).

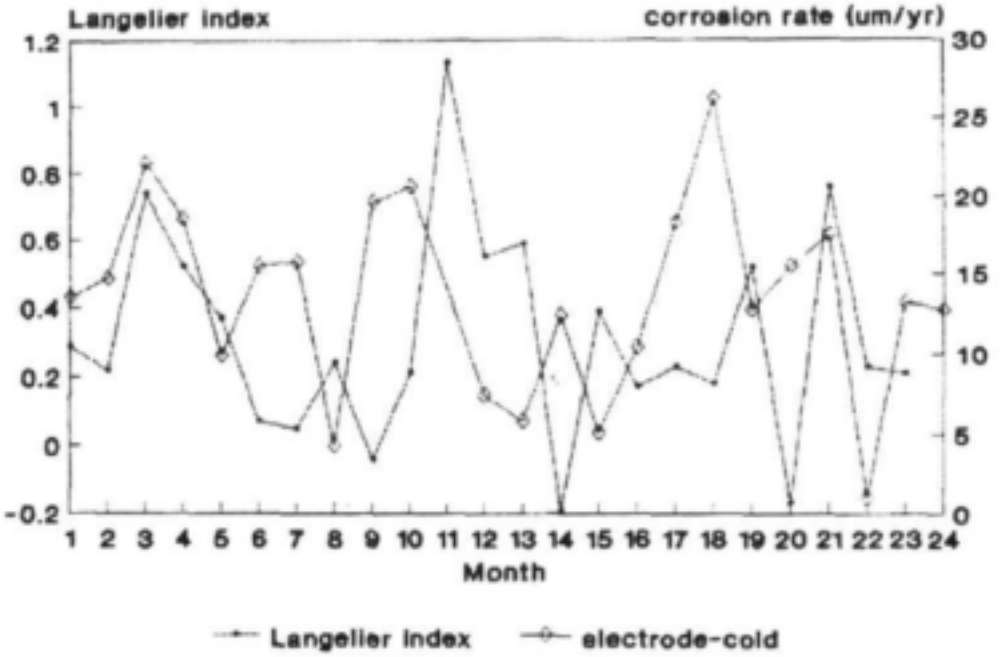

Figure 20b. Langelier index versus corrosion rate of zinc measured by an electrode in cold water (Klerksdorp).

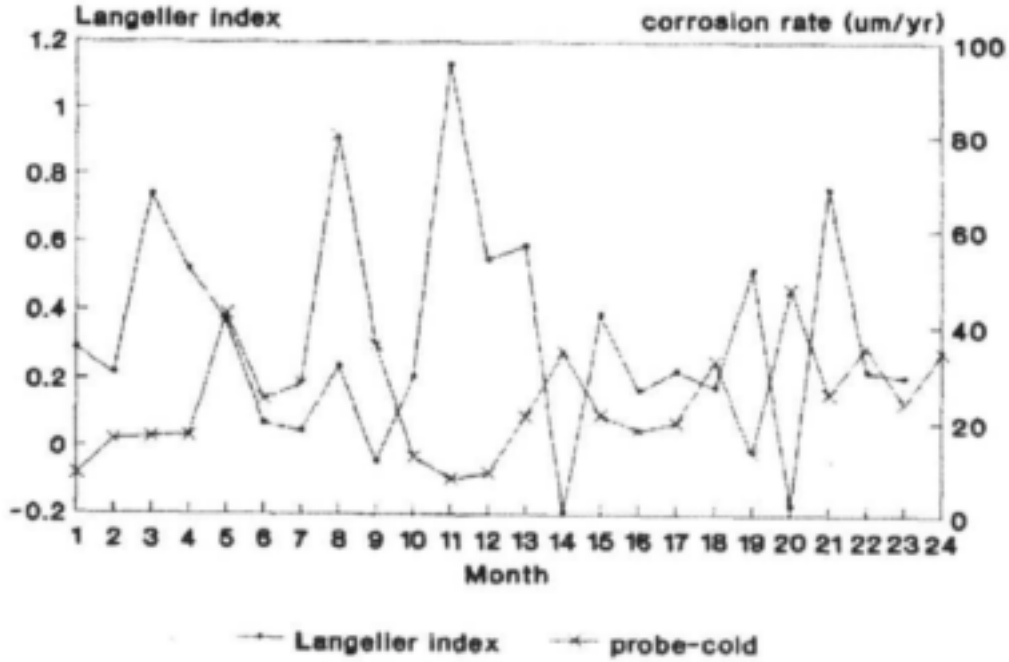

Figure 20c. Langelier index versus corrosion rate of zinc measured by a probe in cold water (Klerksdorp).

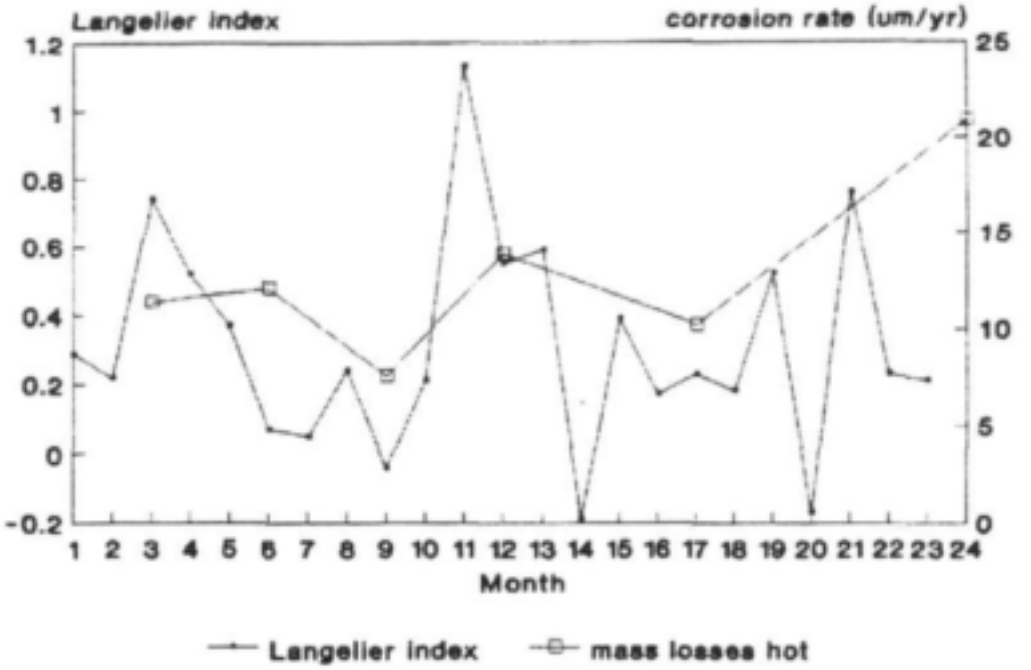

Figure 20d. Langelier index versus corrosion rate of zinc measured by 3-monthly mass loss in cold water (Klerksdorp).

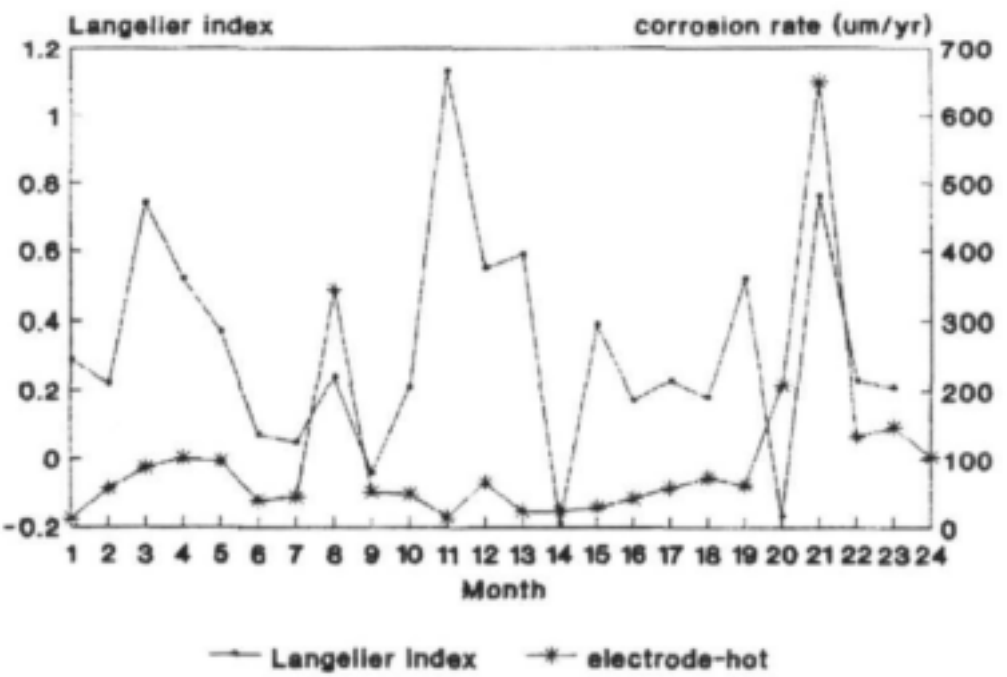

Figure 20e. Langelier index versus corrosion rate of zinc measured by an electrode in hot water (Klerksdorp).

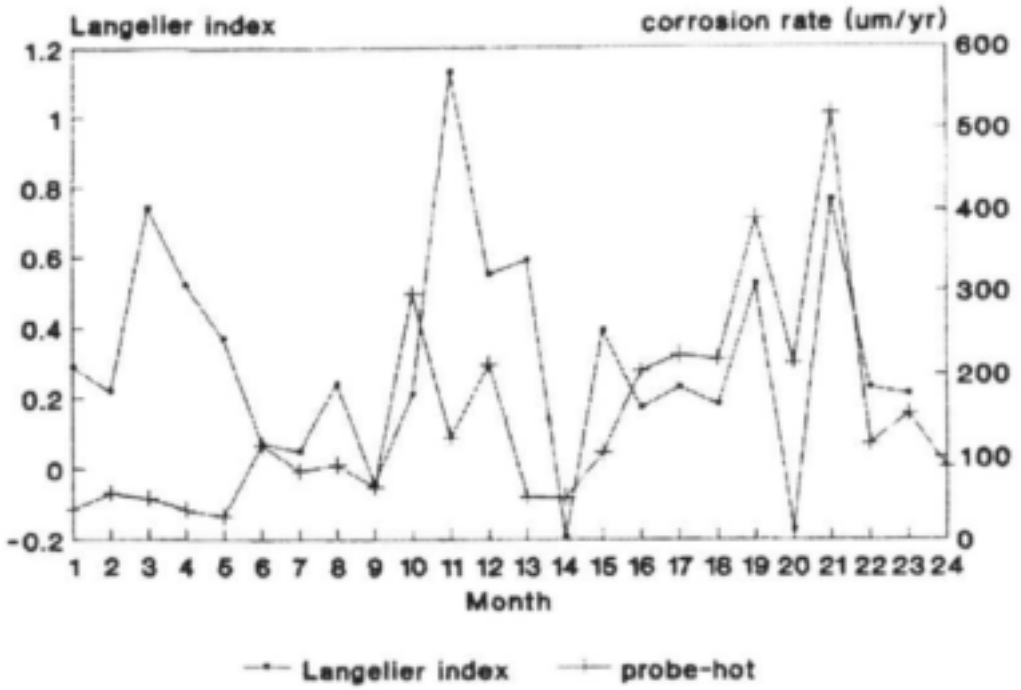

Figure 20f. Langelier index versus corrosion rate of zinc measured by a probe in hot water (Klerksdorp).

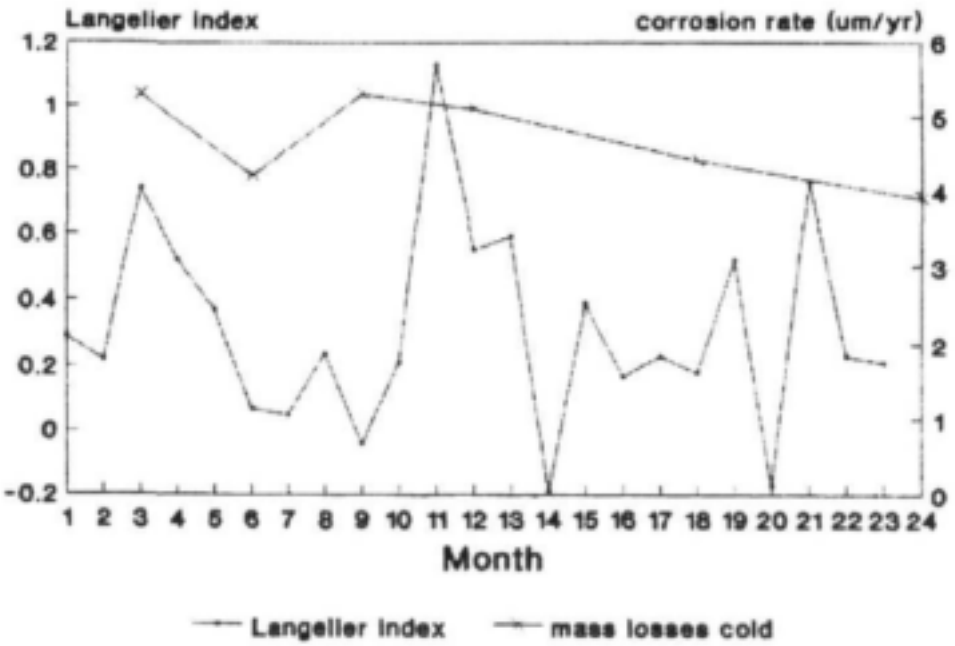

Figure 21a. Langelier index versus corrosion rate of brass measured by 3-monthly mass loss in cold water (Klerksdorp).

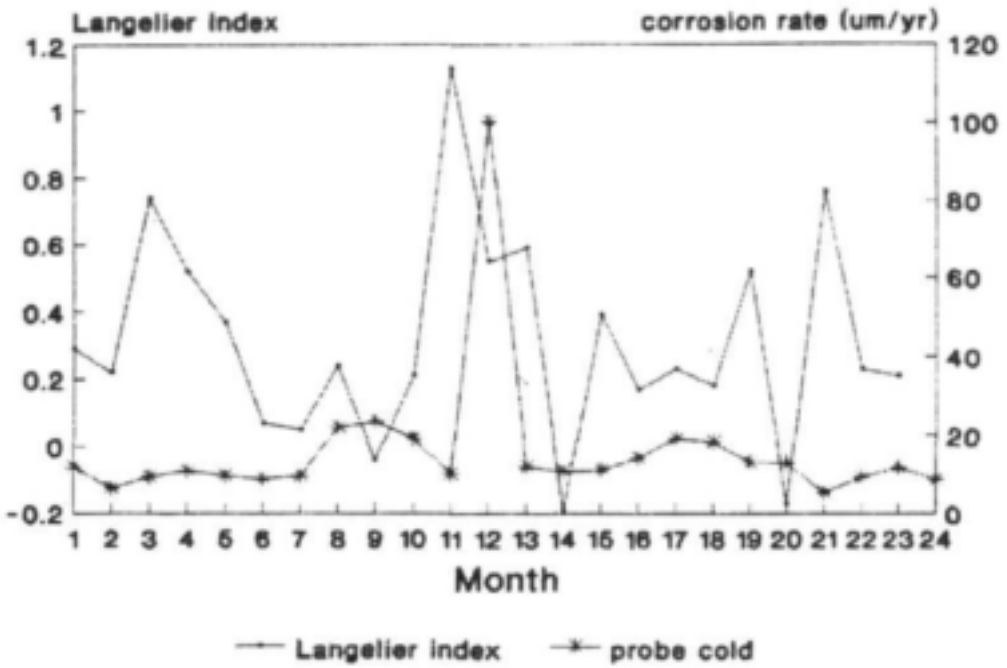

Figure 21b. Langelier index versus corrosion rate of brass measured by probe in cold water (Klerksdorp).

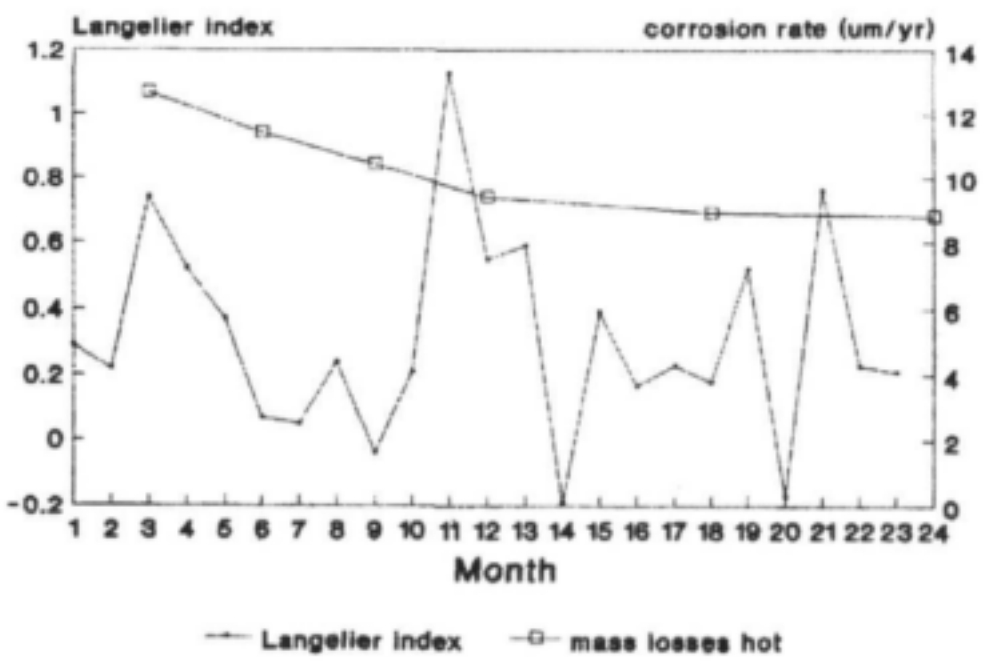

Figure 22. Langelier index versus corrosion rate of brass measured by 3-monthly mass loss in hot water (Klerksdorp).

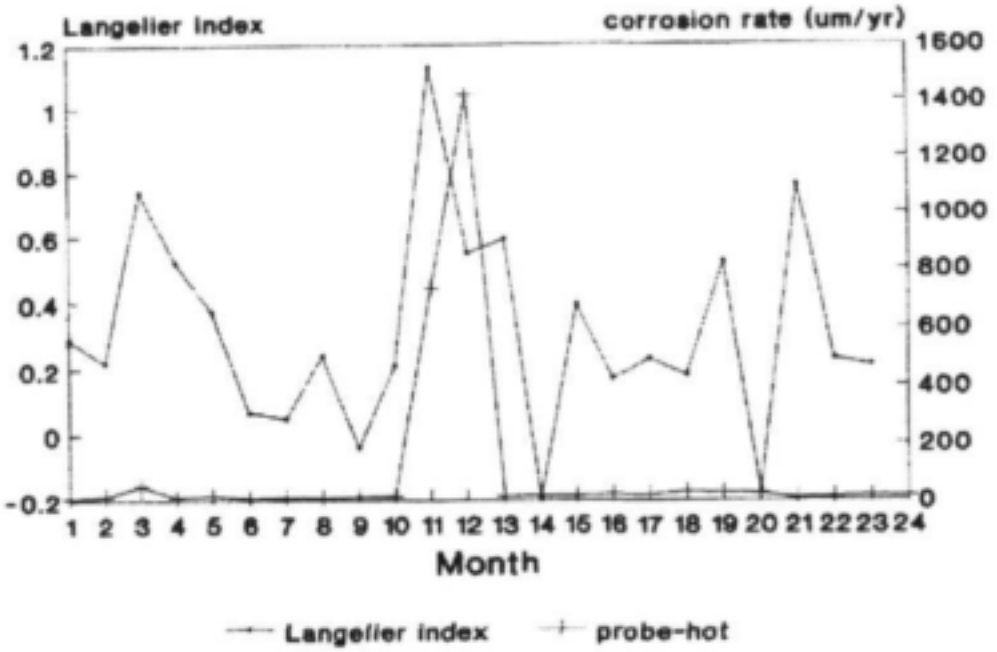

Figure 23. Langelier index versus corrosion rate of brass measured by a probe in hot water (Klerksdorp).

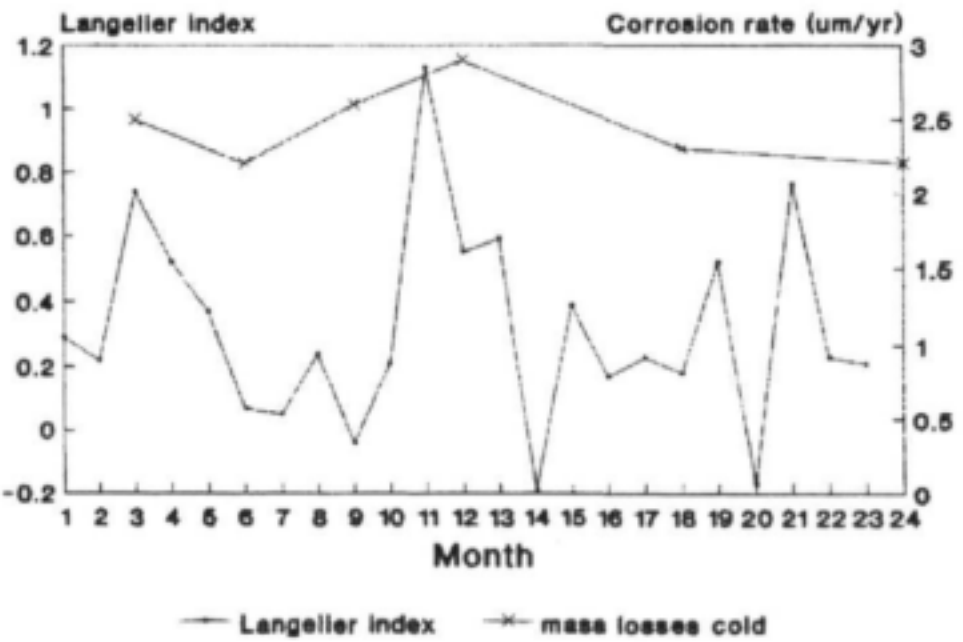

Figure 24. Langelier index versus corrosion rate of copper measured by 3-monthly mass loss in cold water (Klerksdorp).

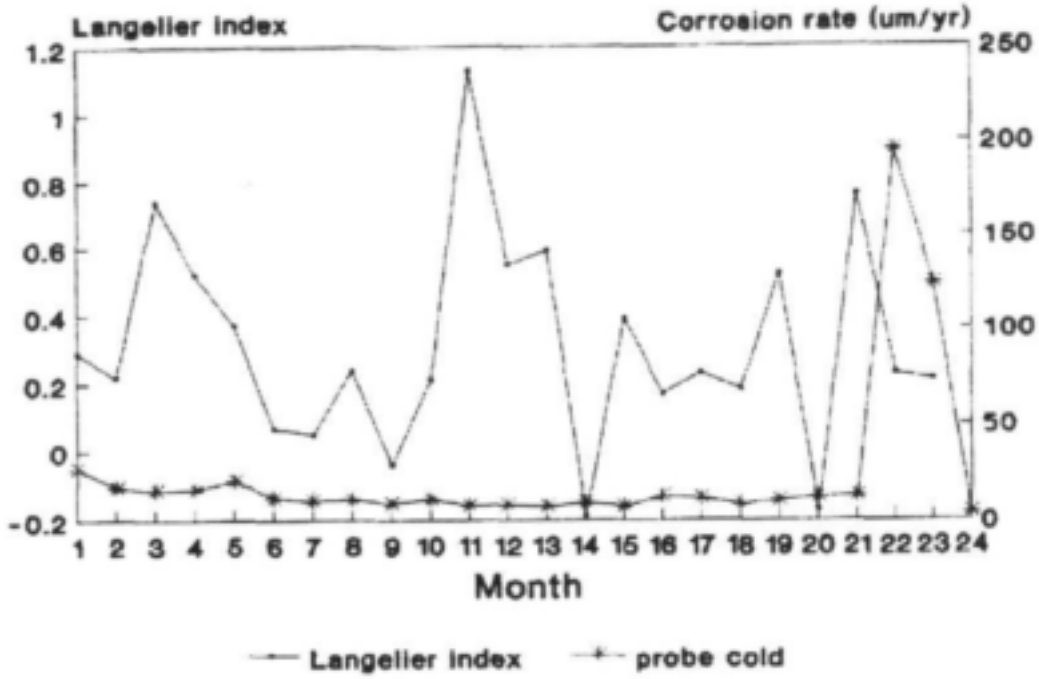

Figure 25. Langelier index versus corrosion rate of copper measured by probe in cold water (Klerksdorp).

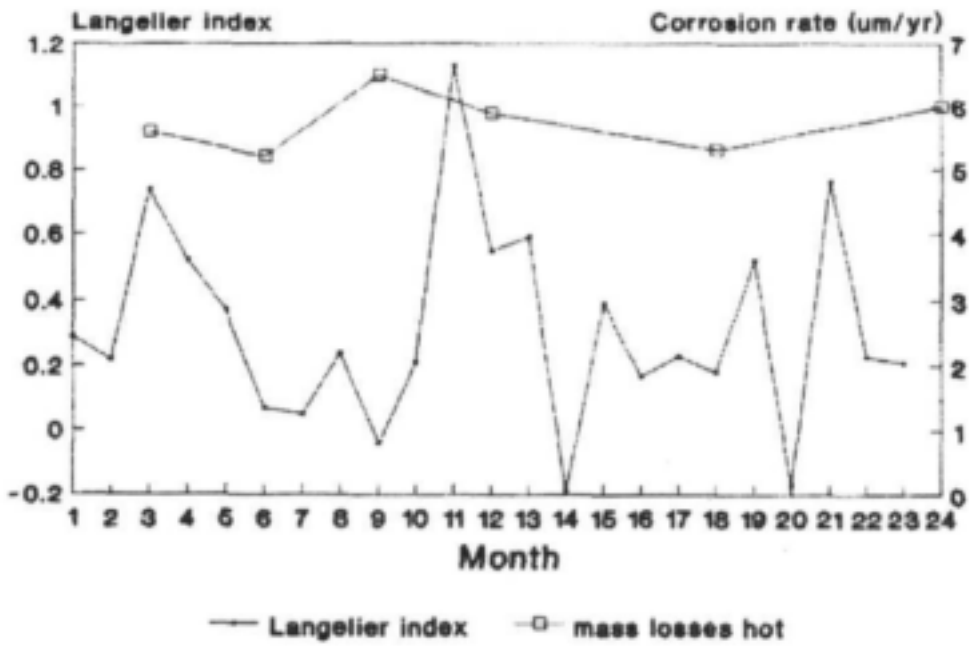

Figure 26. Langelier index versus corrosion rate of copper measured by 3-monthly mass loss in hot water (Klerksdorp).

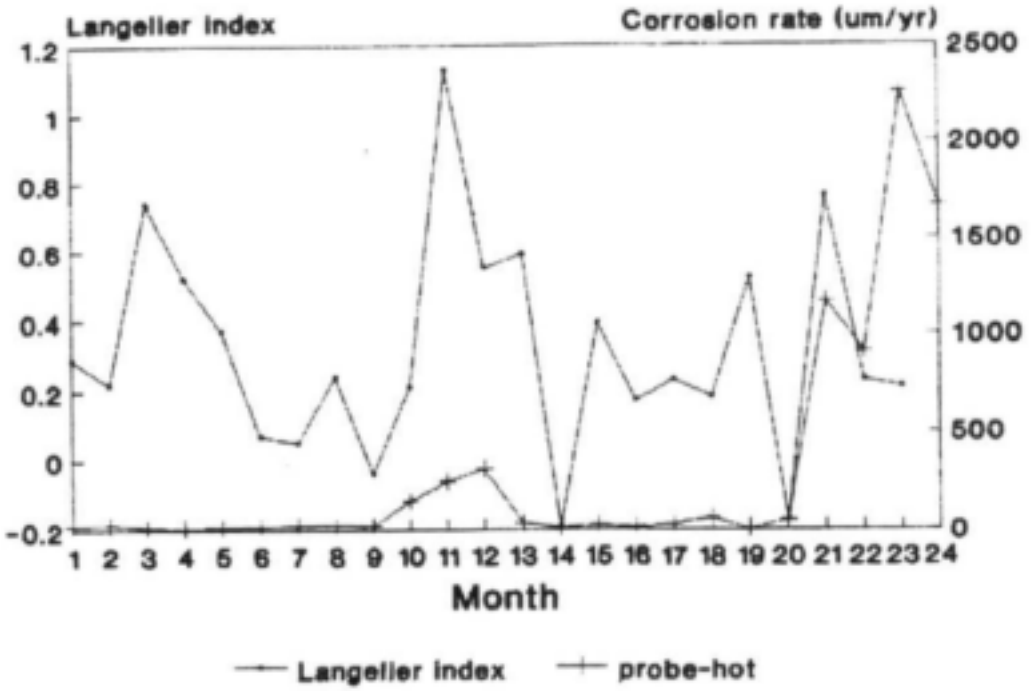

Figure 27. Langelier index versus corrosion rate of copper measured by a probe in hot water (Klerksdorp).

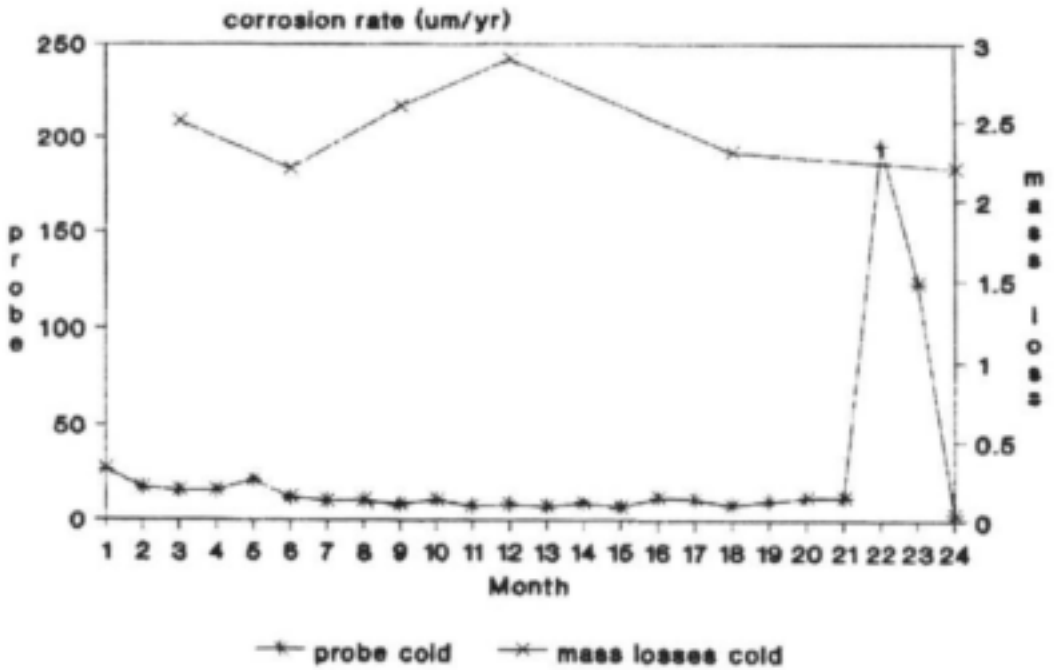

Figure 28. Comparison of corrosion rates of copper obtained by different techniques in cold water (Klerksdorp).

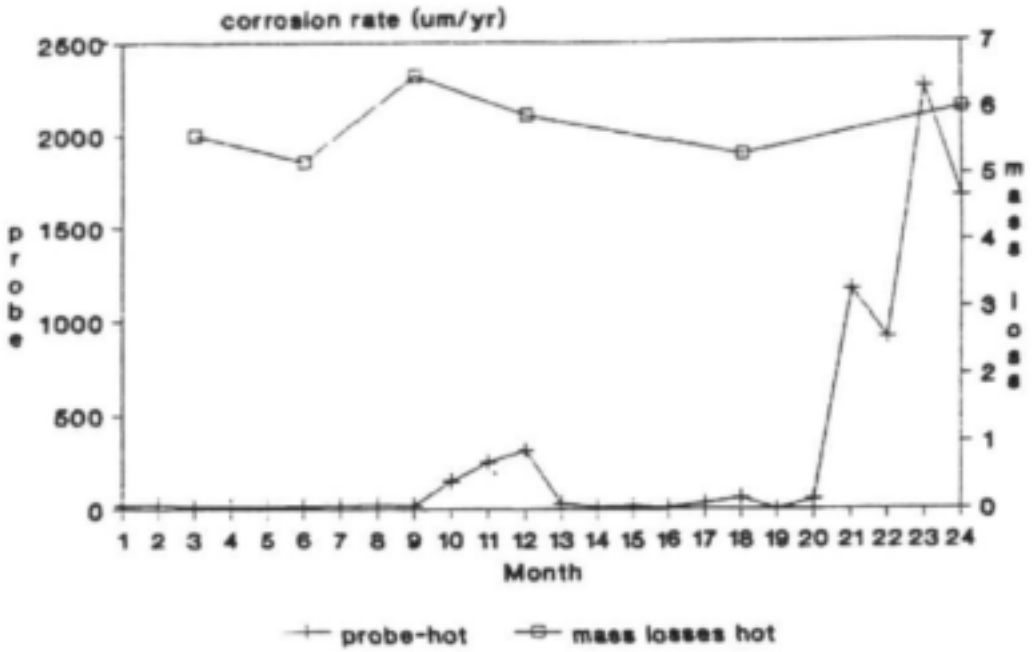

Figure 29. Comparison of corrosion rates of copper obtained by different techniques in hot water (Klerksdorp).

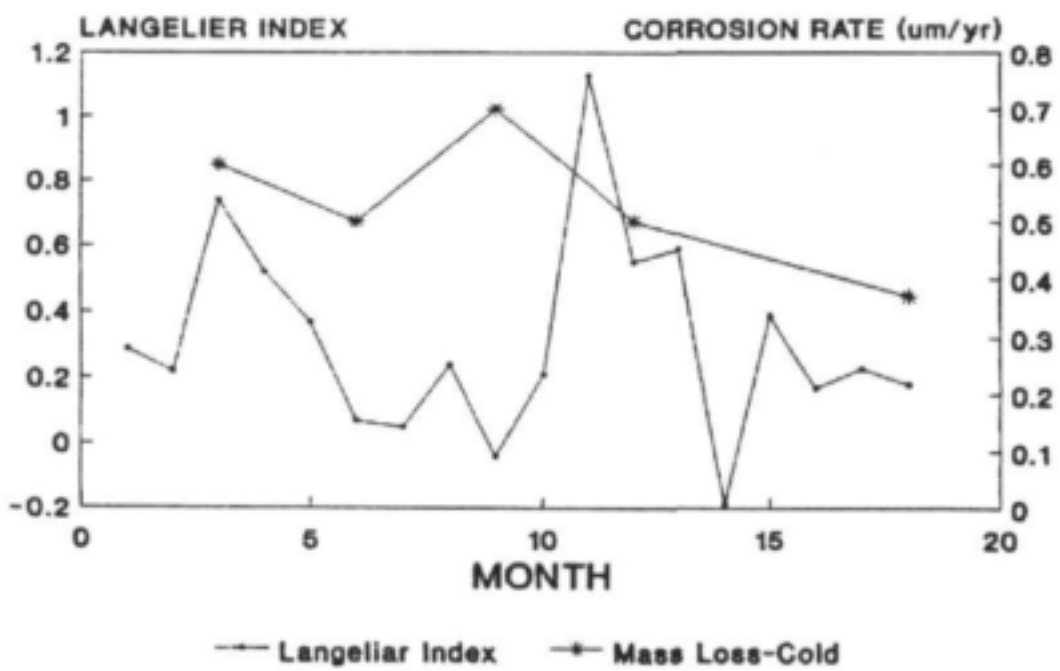

Figure 30. Langelier index versus corrosion rate of 3CR12 measured by 3-monthly mass loss in cold water (Klerksdorp).

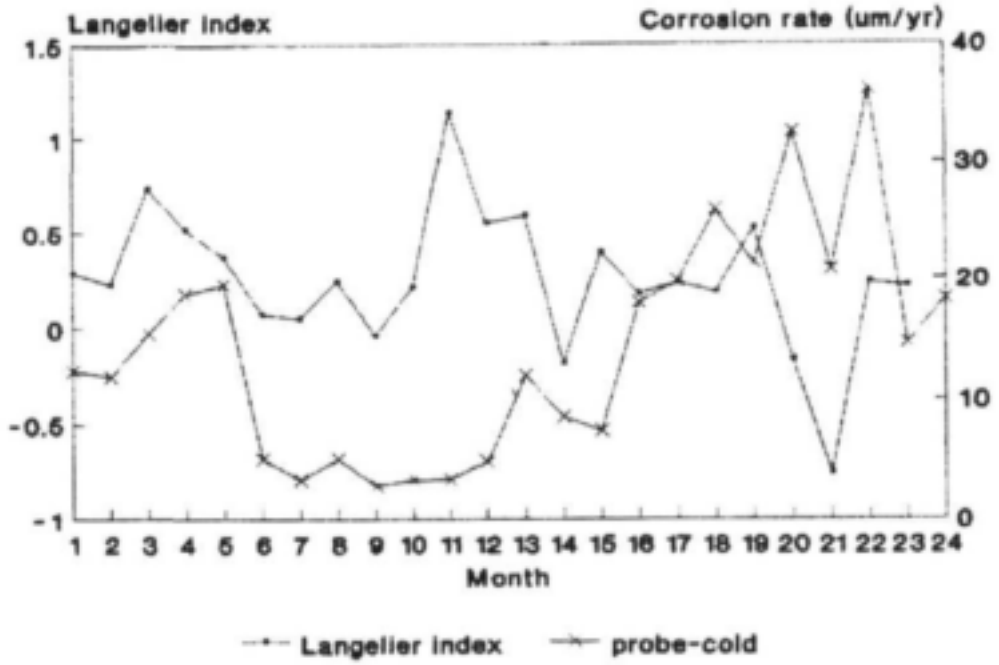

Figure 31. Langelier index versus corrosion rate of 3CR12 measured by a probe in cold water (Klerksdorp).

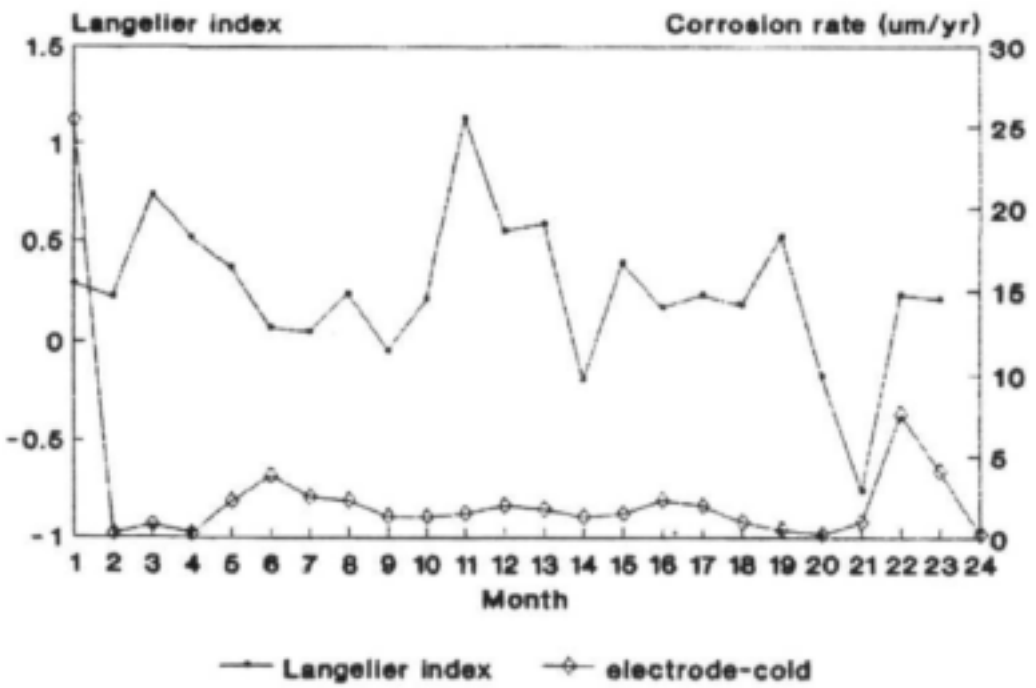

Figure 32. Langelier index versus corrosion rate of 3CR12 measured by an electrode in cold water (Klerksdorp).

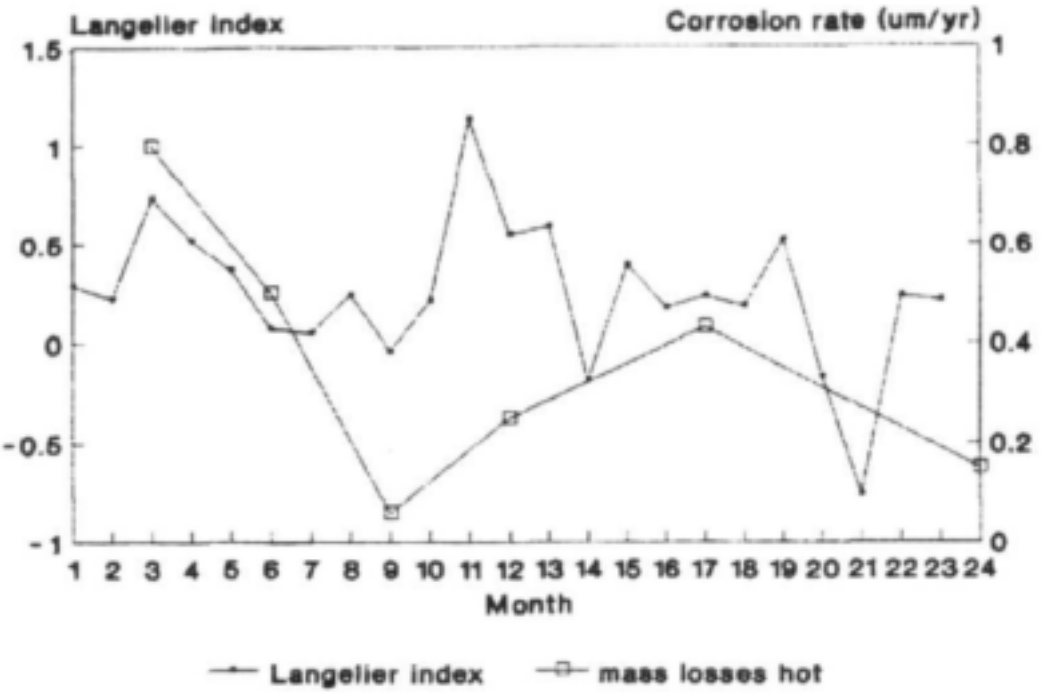

Figure 33. Langelier index versus corrosion rate of 3CR12 measured by 3-monthly mass loss in hot water (Klerksdorp).

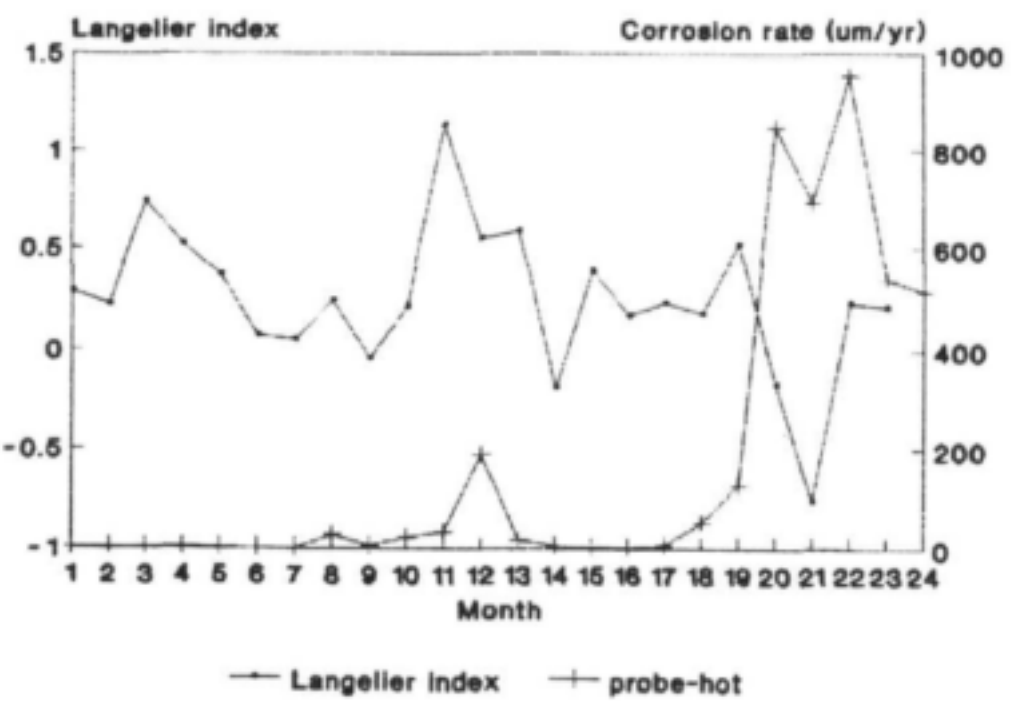

Figure 34. Langelier index versus corrosion rate of 3CR12 measured by a probe in hot water (Klerksdorp).

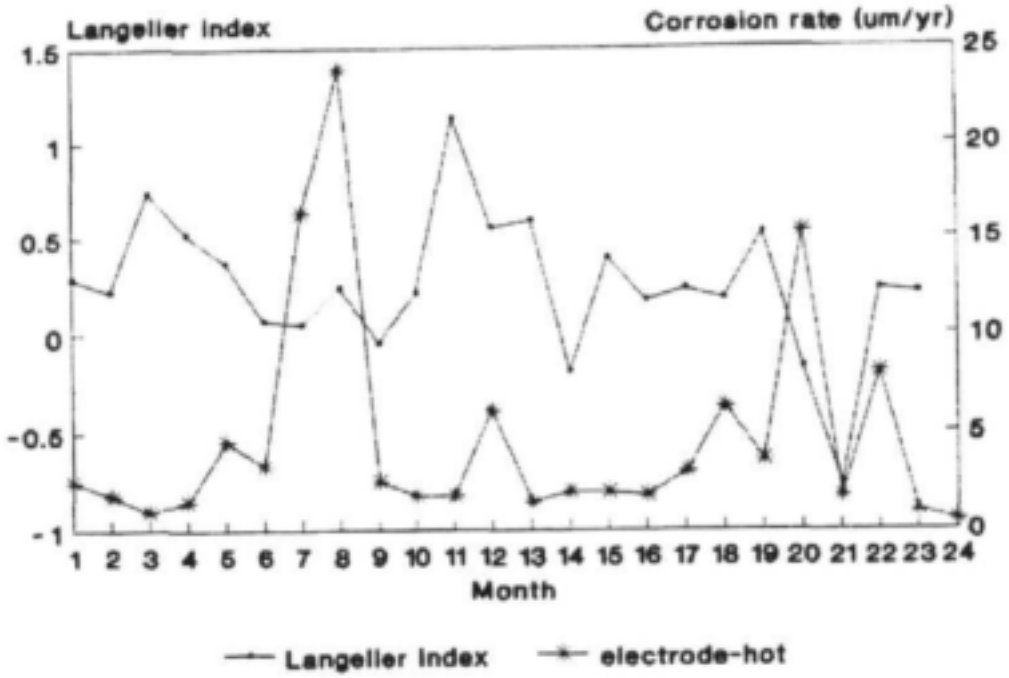

Figure 35. Langelier index versus corrosion rate of 3CR12 measured by an electrode in hot water (Klerksdorp).

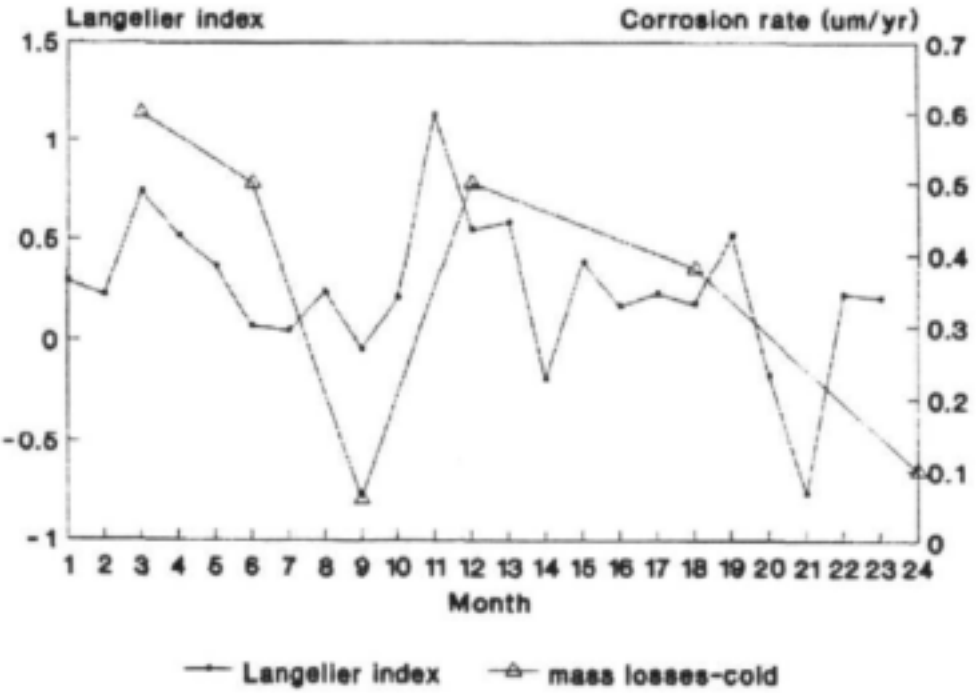

Figure 36. Langelier index versus corrosion rate of 304 measured by 3-monthly mass loss in cold water (Klerksdorp).

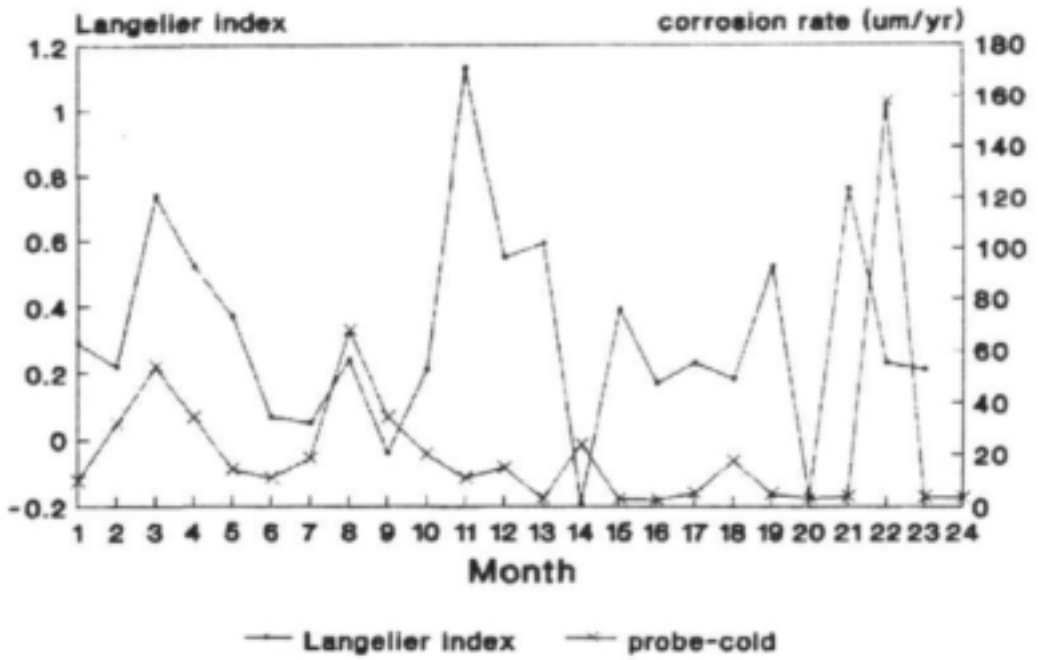

Figure 37. Langelier index versus corrosion rate of 304 measured by a probe in cold water (Klerksdorp).

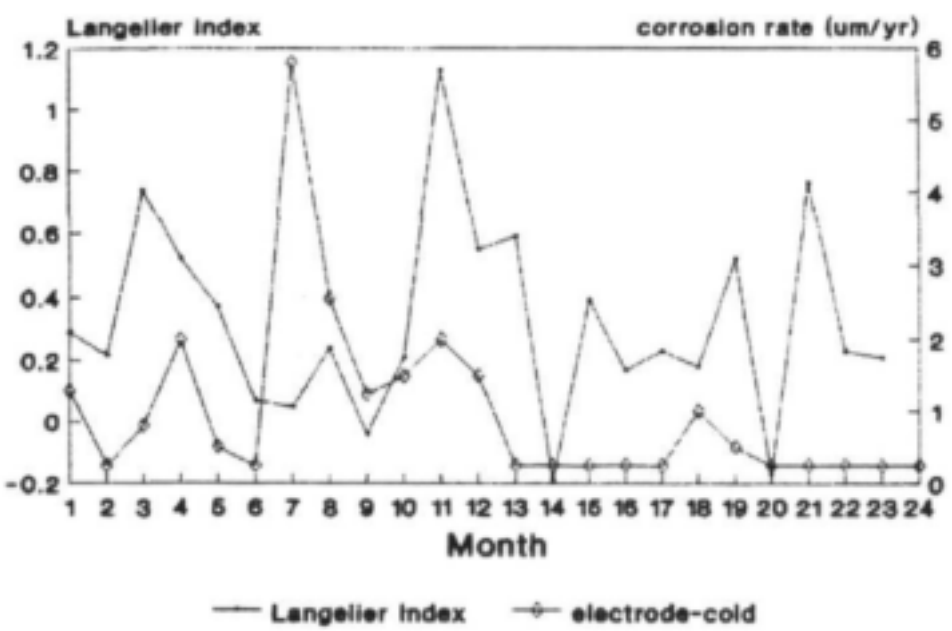

Figure 38. Langelier index versus corrosion rate of 304 measured by an electrode in cold water (Klerksdorp).

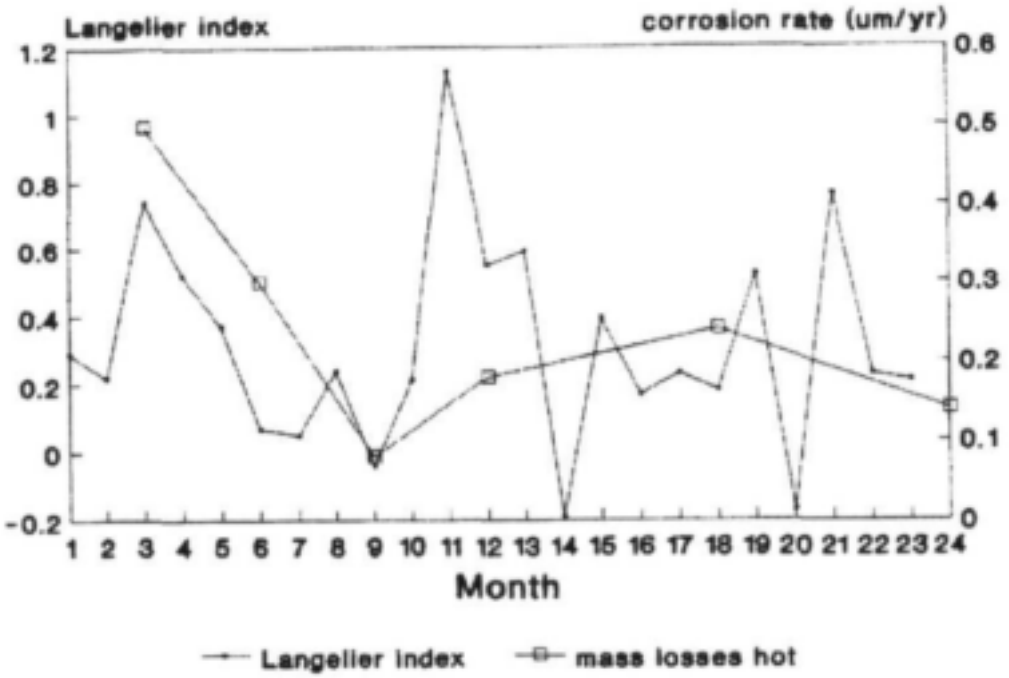

Figure 39. Langelier index versus corrosion rate of 304 measured by 3-monthly mass loss in hot water (Klerksdorp).

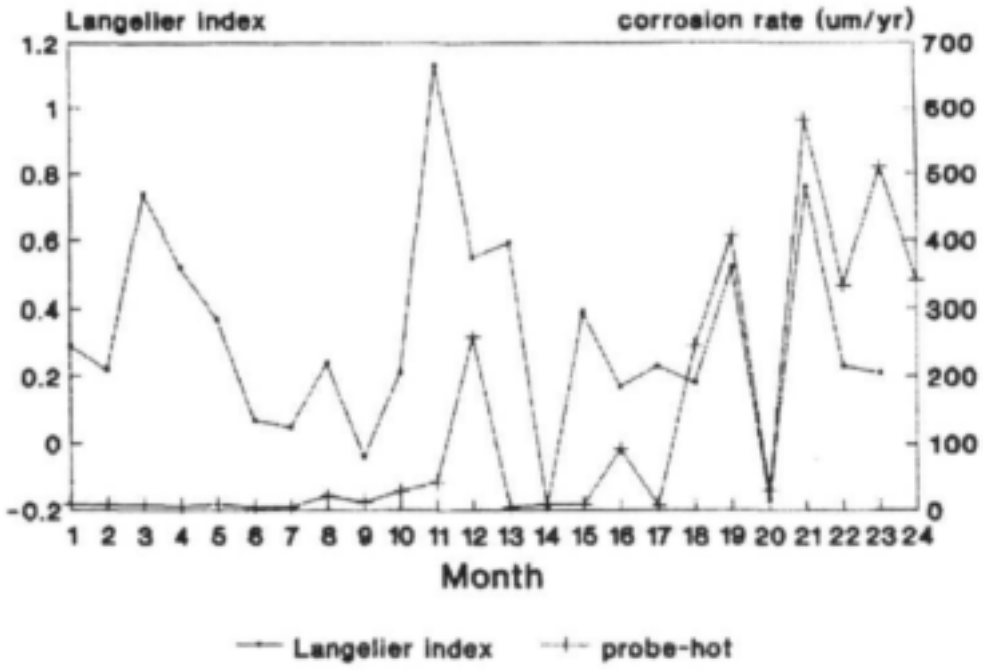

Figure 40. Langelier index versus corrosion rate of 304 measured by a probe in hot water (Klerksdorp).

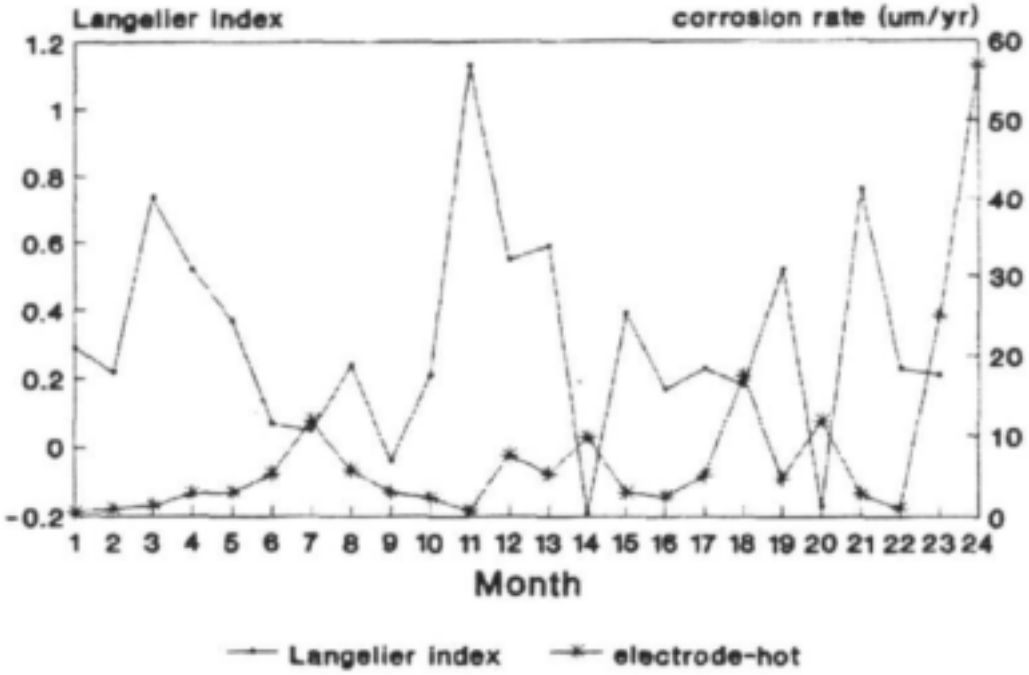

Figure 41. Langelier index versus corrosion rate of 304 measured by an electrode in hot water (Klerksdorp).

Appendix 3. Results of corrosion testing at Vereeniging

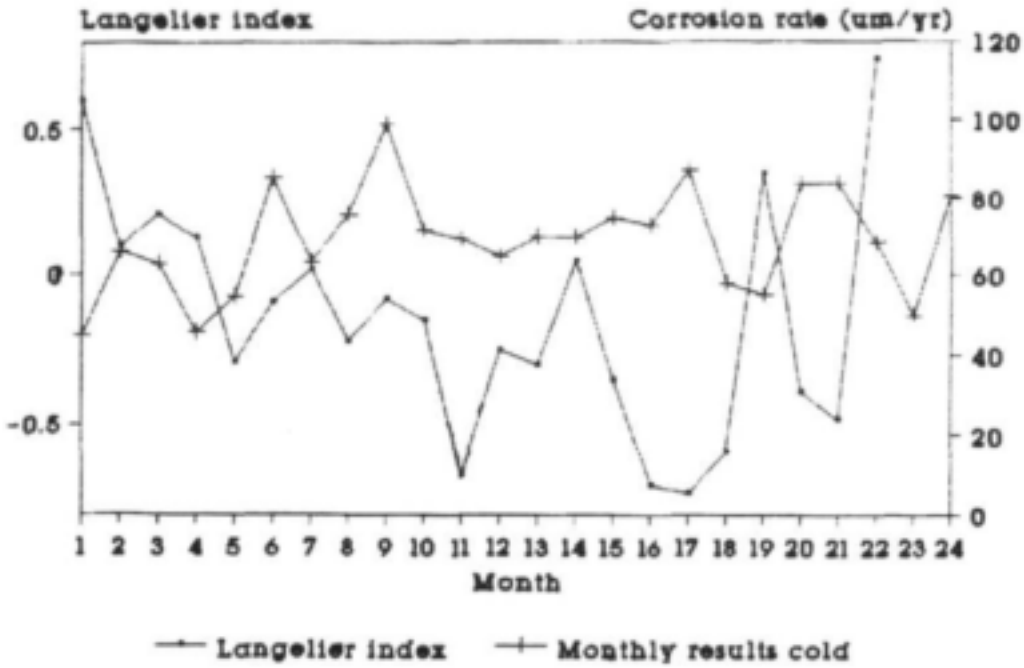

Figure 42. Langelier index versus corrosion rate of mild steel measured by monthly mass loss in cold water (Vereeniging).

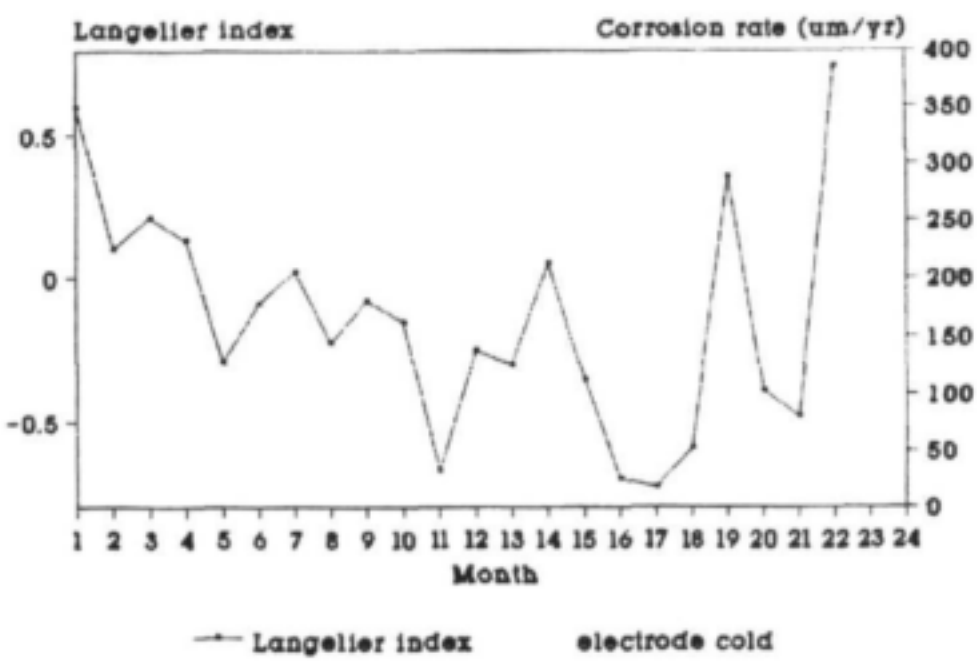

Figure 43. Langelier index versus corrosion rate of mild steel measured by an electrode in cold water (Vereeniging).

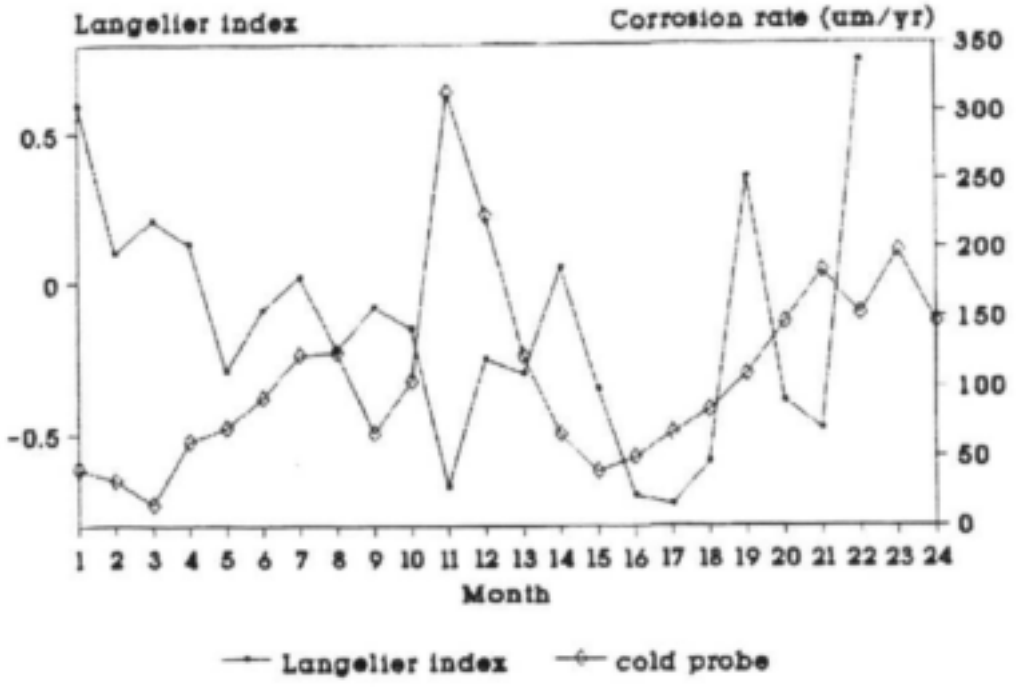

Figure 44. Langelier index versus corrosion rate of mild steel measured by a probe in cold water (Vereeniging).

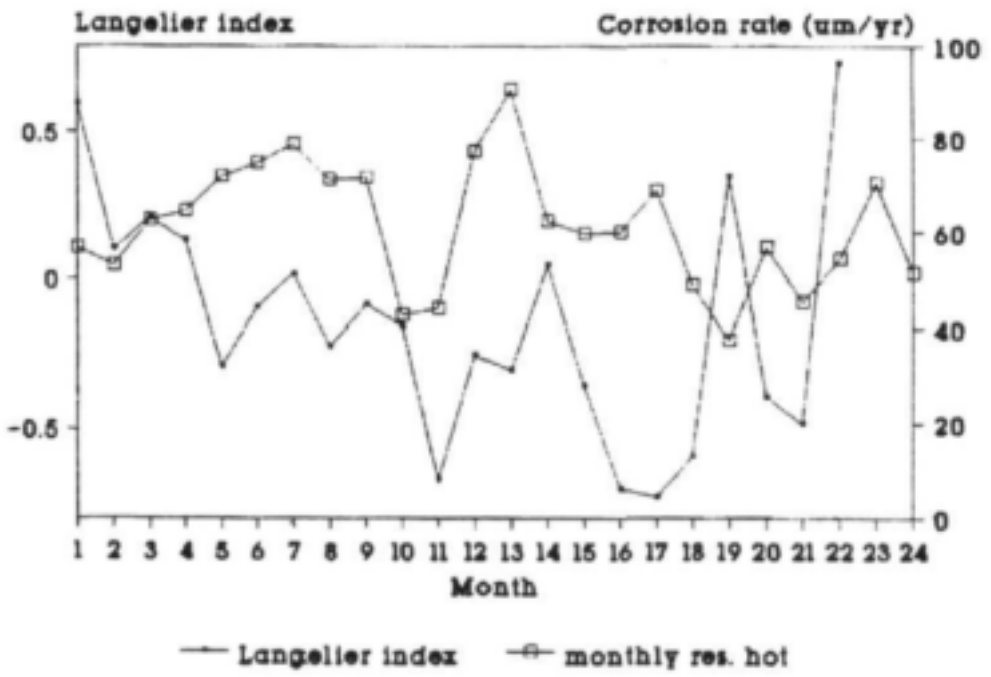

Figure 45. Langelier index versus corrosion rate of mild steel measured by monthly mass loss in hot water (Vereeniging).

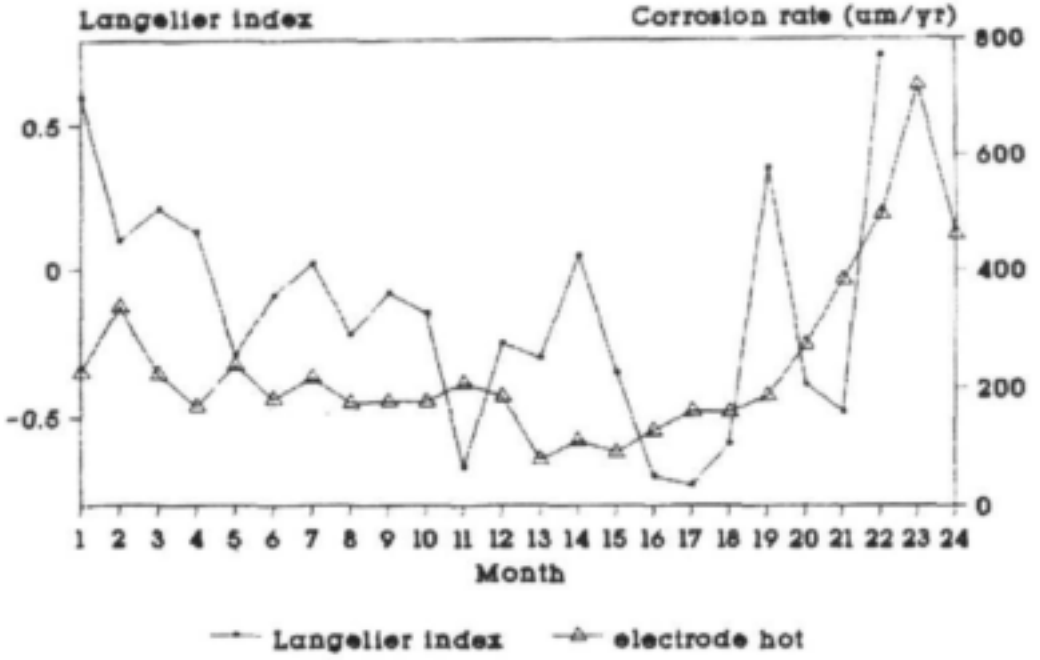

Figure 46. Langelier index versus corrosion rate of mild steel measured by an electrode in hot water (Vereeniging).

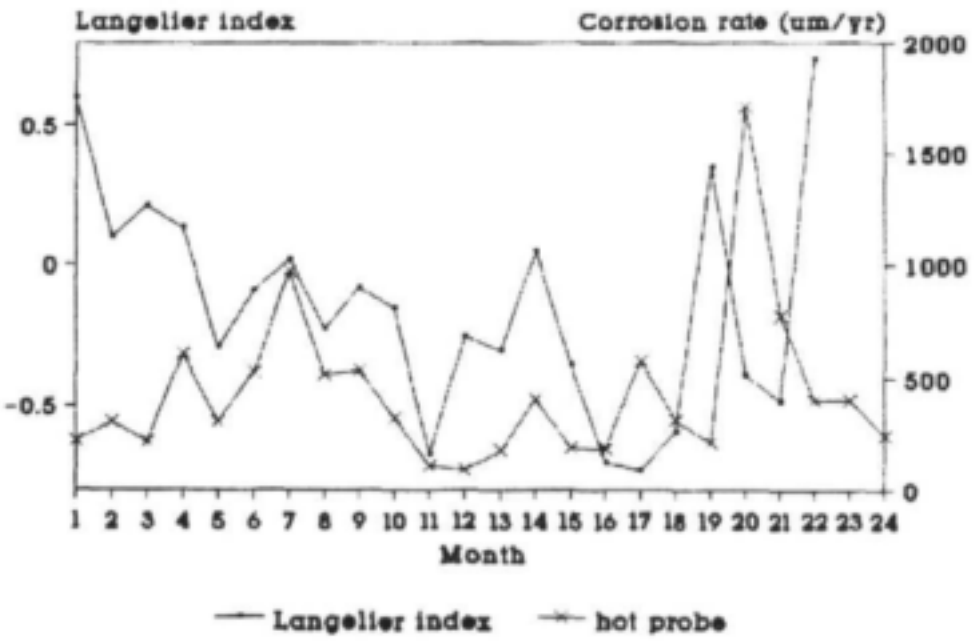

Figure 47. Langelier index versus corrosion rate of mild steel measured by a probe in hot water (Vereeniging).

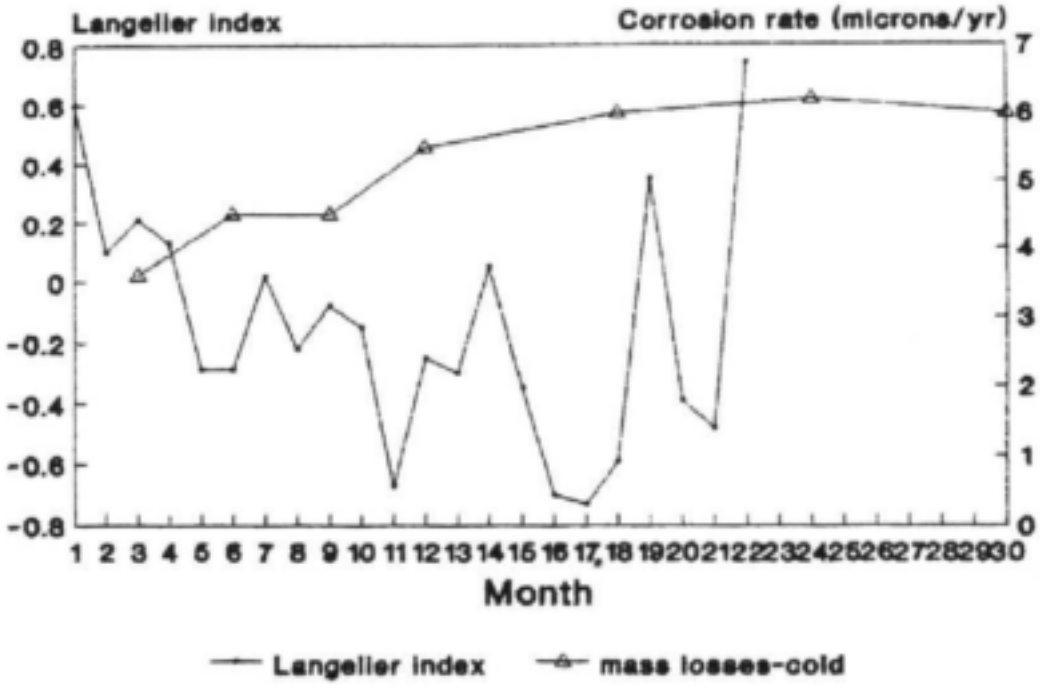

Figure 48. Langelier index versus corrosion rate of zinc measured by 3-monthly mass loss in cold water (Vereeniging).

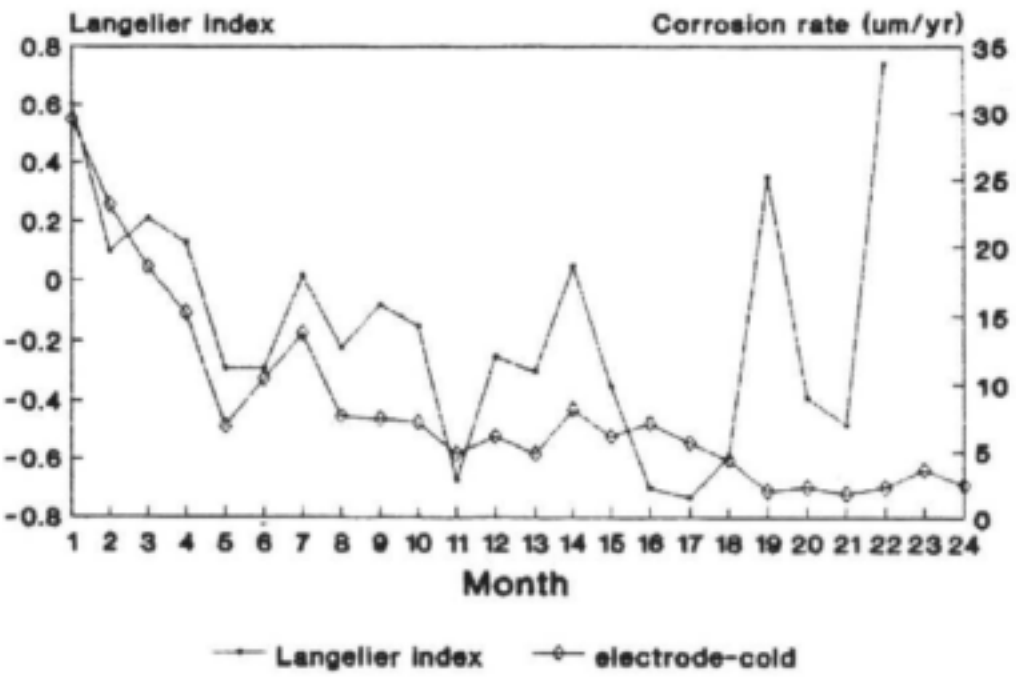

Figure 49. Langelier index versus corrosion rate of zinc measured by an electrode in cold water (Vereeniging).

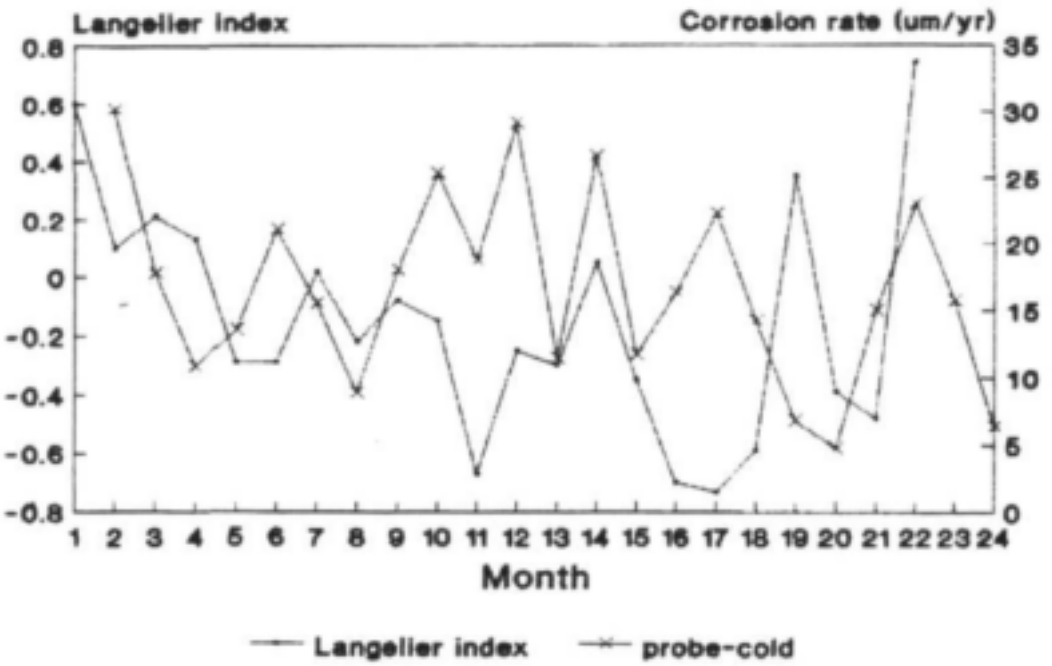

Figure 50. Langelier index versus corrosion rate of zinc measured by a probe in cold water (Vereeniging).

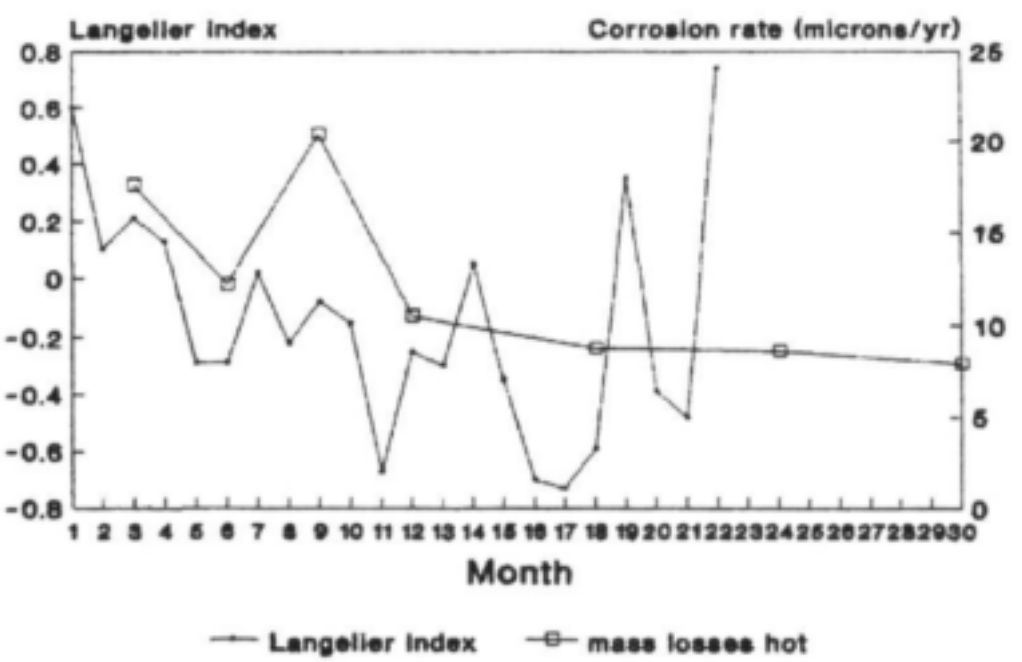

Figure 51. Langelier index versus corrosion rate of zinc measured by 3-monthly mass loss in hot water (Vereeniging).

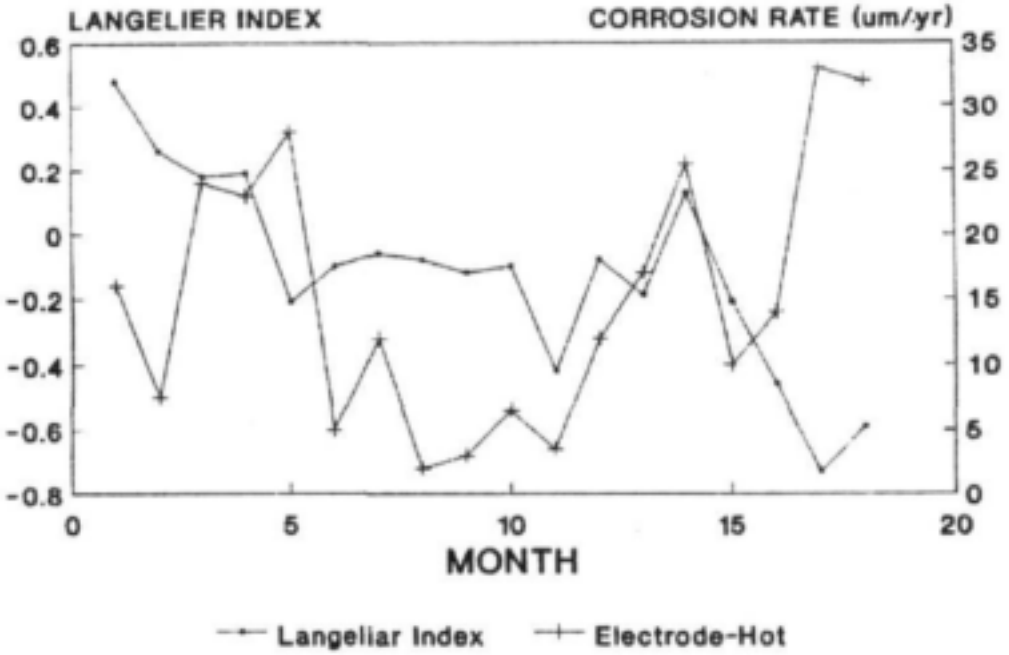

Figure 52. Langelier index versus corrosion rate of zinc measured by an electrode in hot water (Vereeniging).

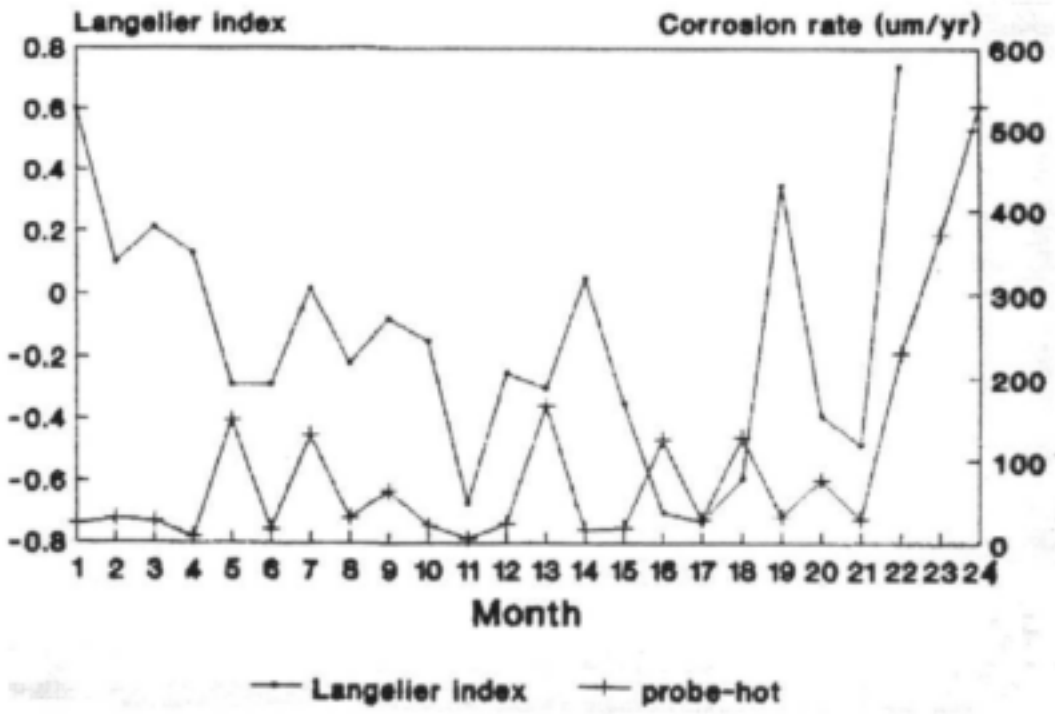

Figure 53. Langelier index versus corrosion rate of zinc measured by a probe in hot water (Vereeniging).

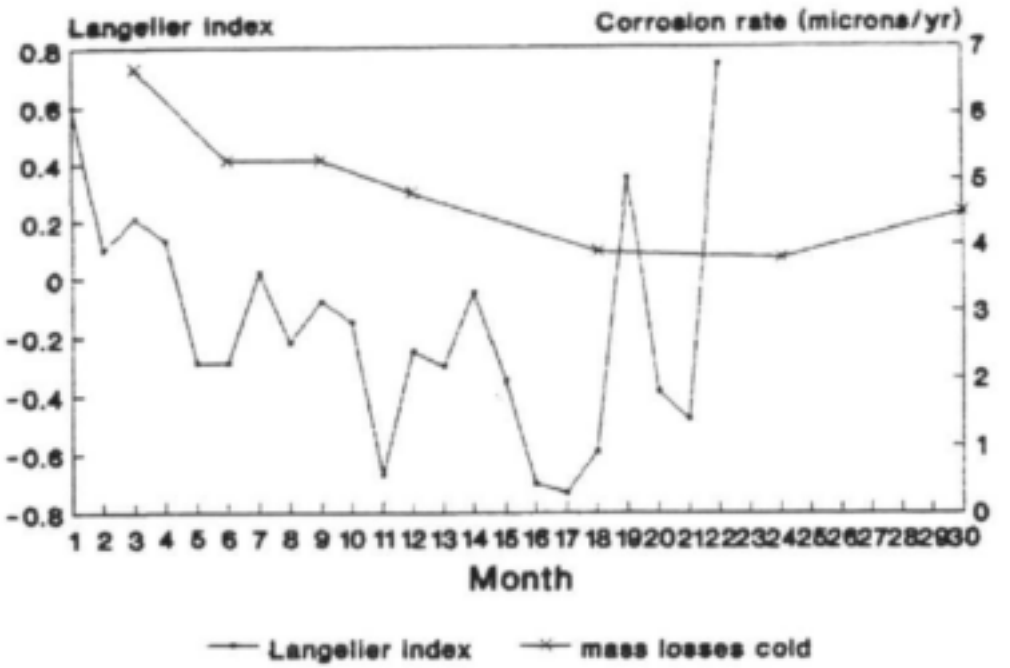

Figure 54. Langelier index versus corrosion rate of brass measured by 3-monthly mass loss in cold water (Vereeniging).

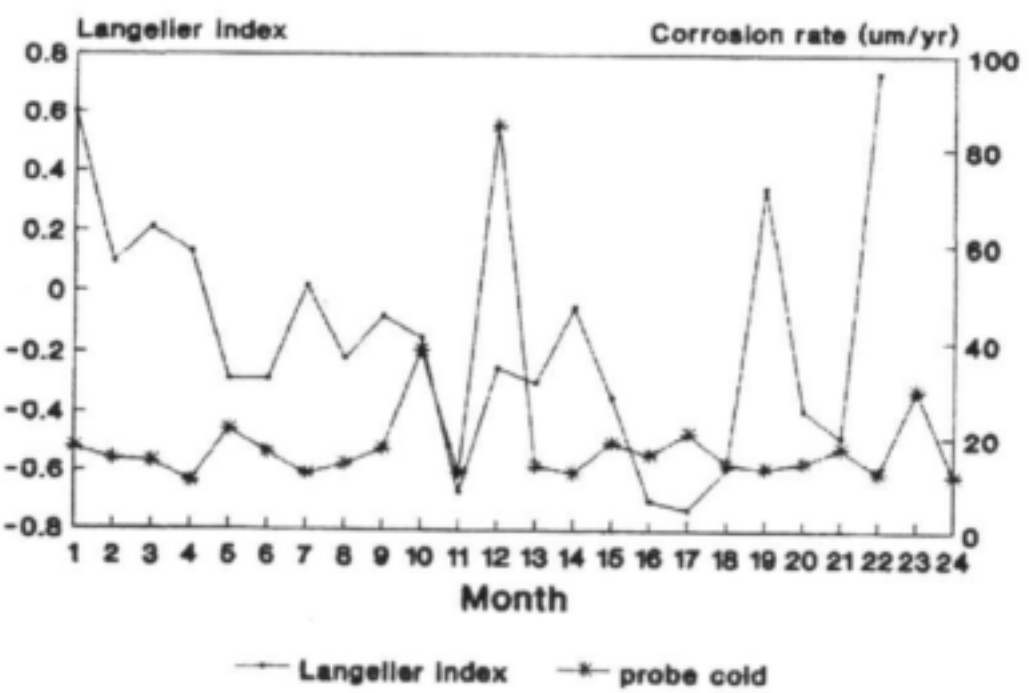

Figure 55. Langelier index versus corrosion rate of brass measured by a probe in cold water (Vereeniging).

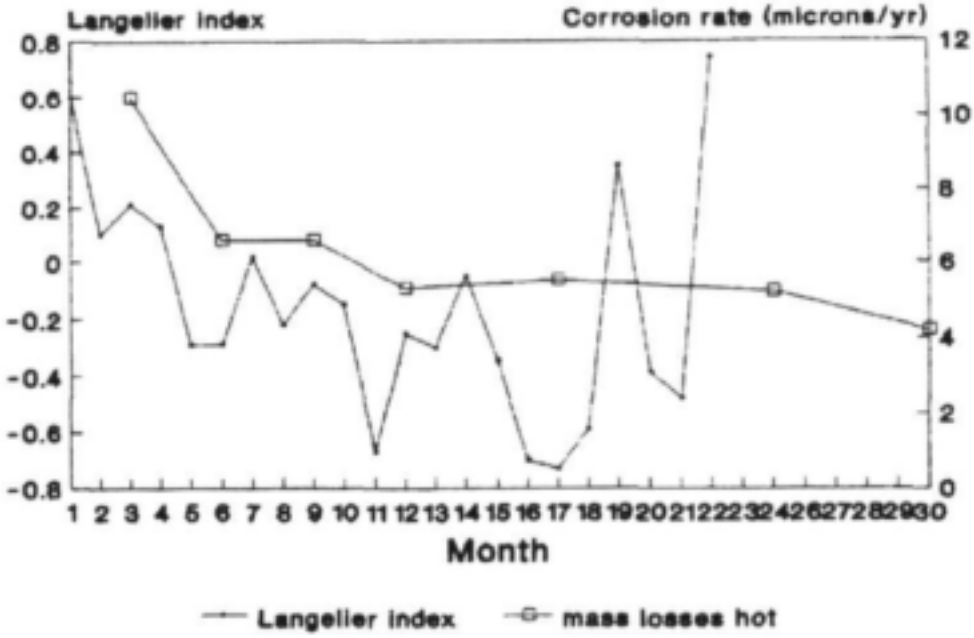

Figure 56. Langelier index versus corrosion rate of brass measured by 3-monthly mass loss in hot water (Vereeniging).

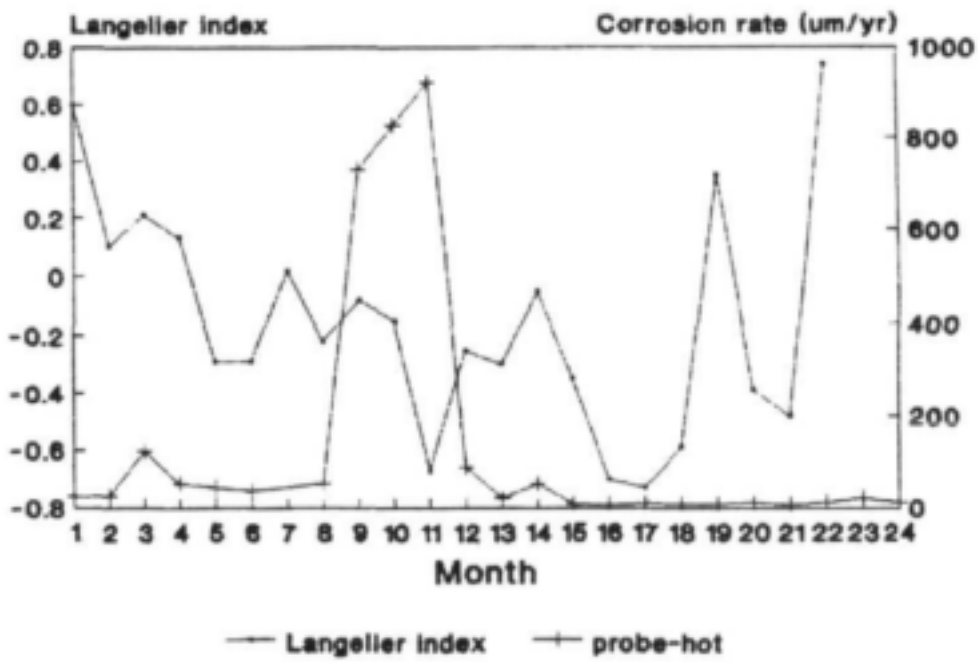

Figure 57. Langelier index versus corrosion rate of brass measured by a probe in hot water (Vereeniging).

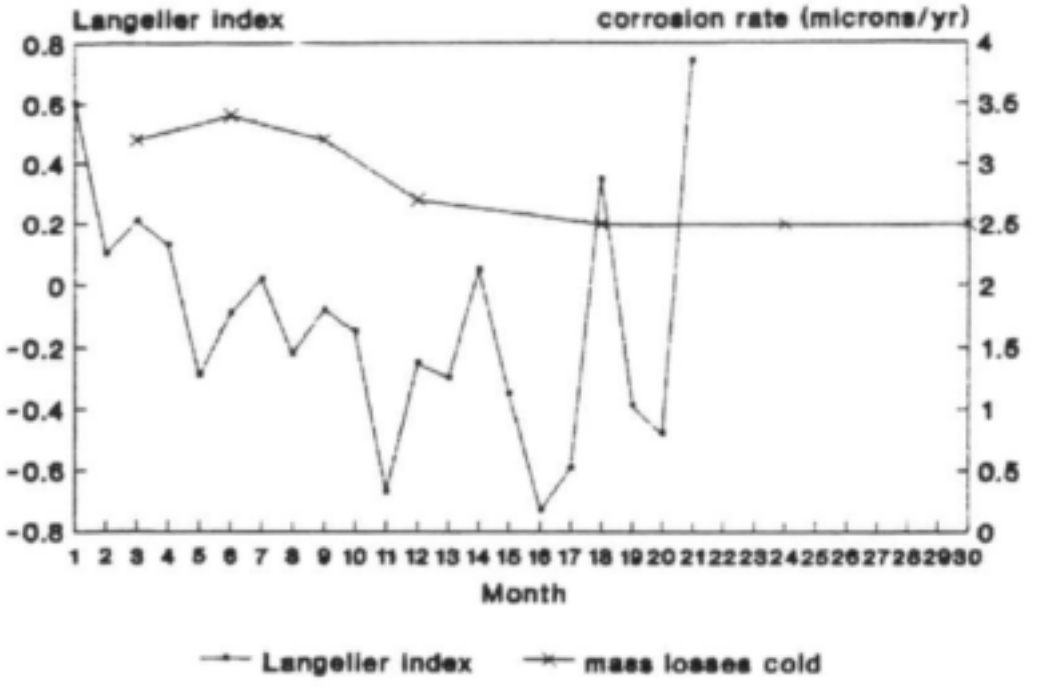

Figure 58. Langelier index versus corrosion rate of copper measured by 3-monthly mass loss in cold water (Vereeniging).

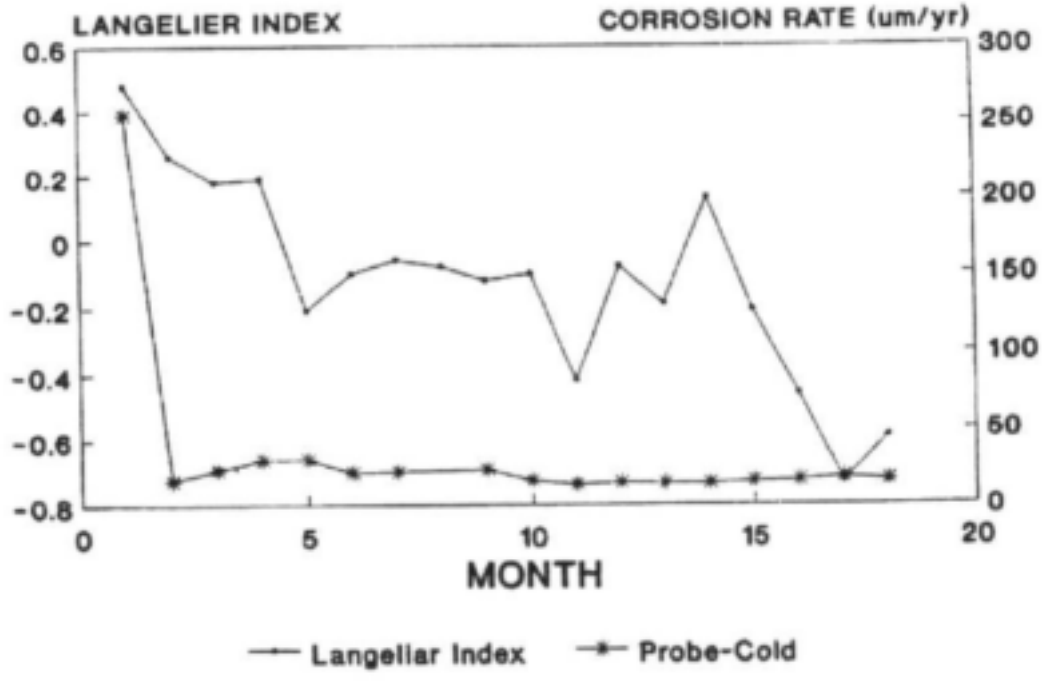

Figure 59. Langelier index versus corrosion rate of copper measured by a probe in cold water (Vereeniging).

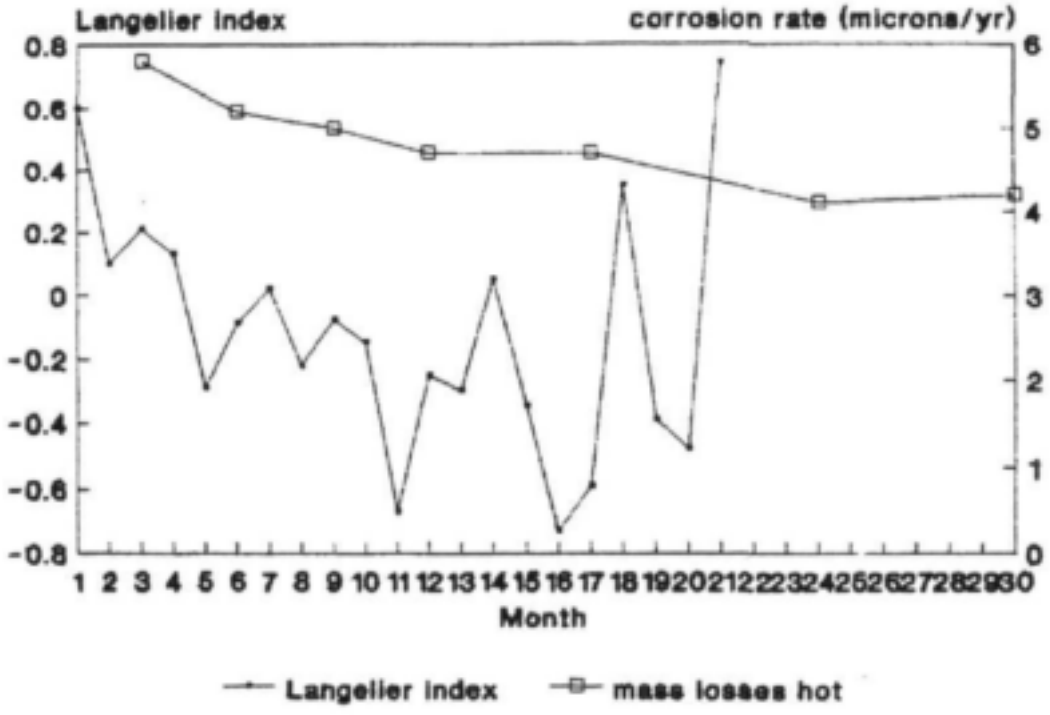

Figure 60. Langelier index versus corrosion rate of copper measured by 3-monthly mass loss in hot water (Vereeniging).

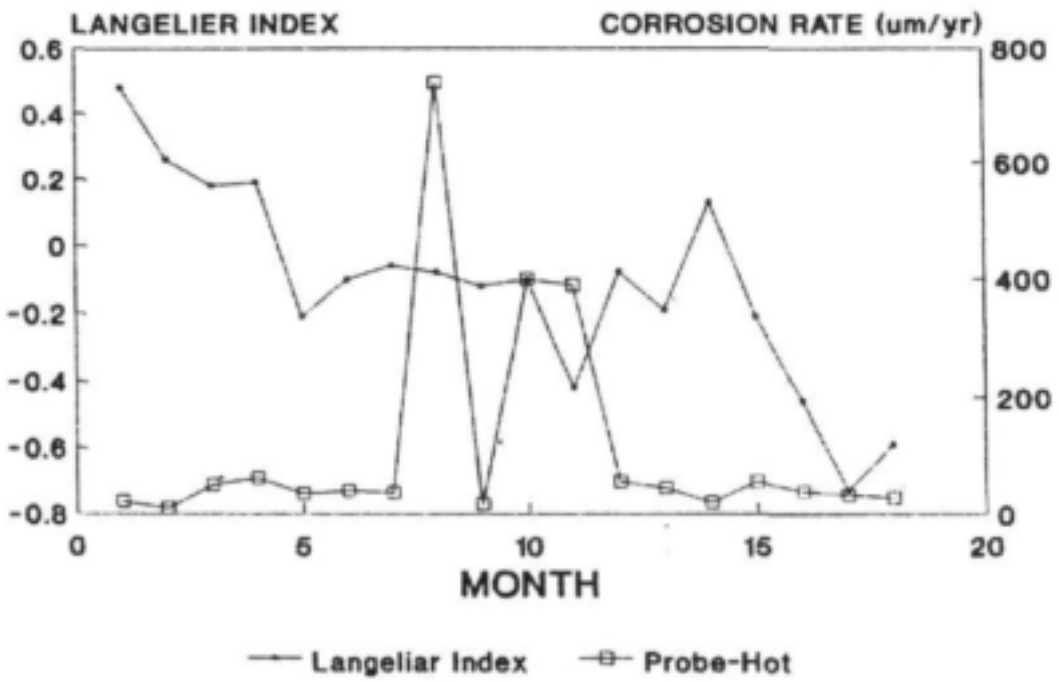

Figure 61. Langelier index versus corrosion rate of copper measured by a probe in hot water (Vereeniging).

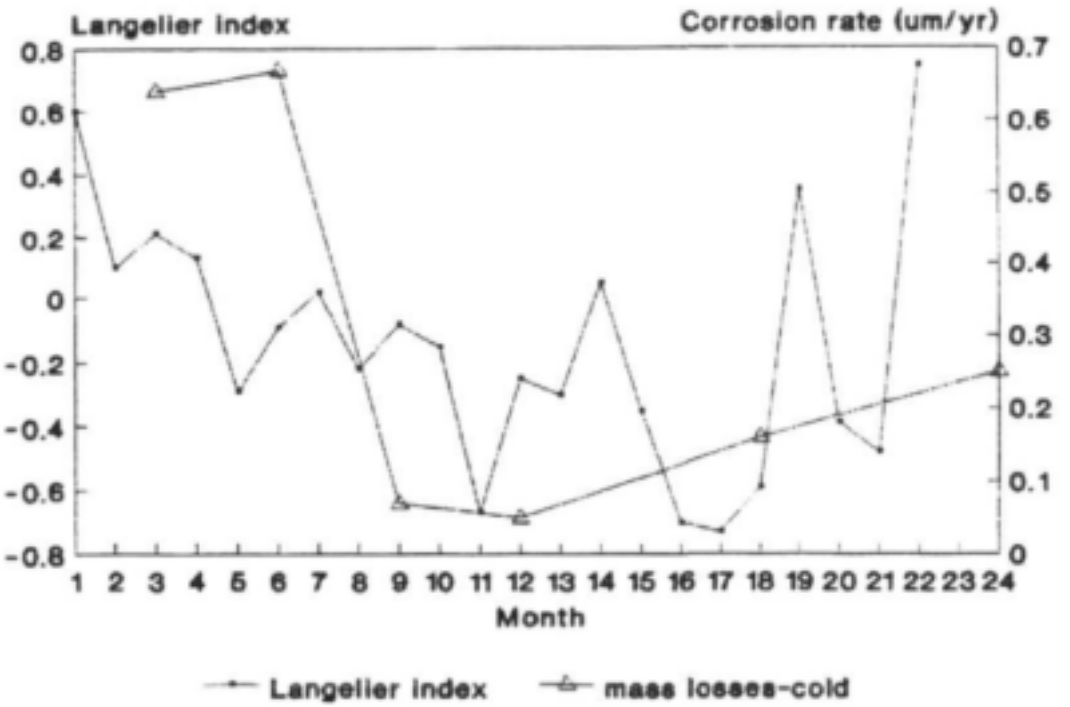

Figure 62. Langelier index versus corrosion rate of 3CR12 measured by 3-monthly mass loss in cold water (Vereeniging).

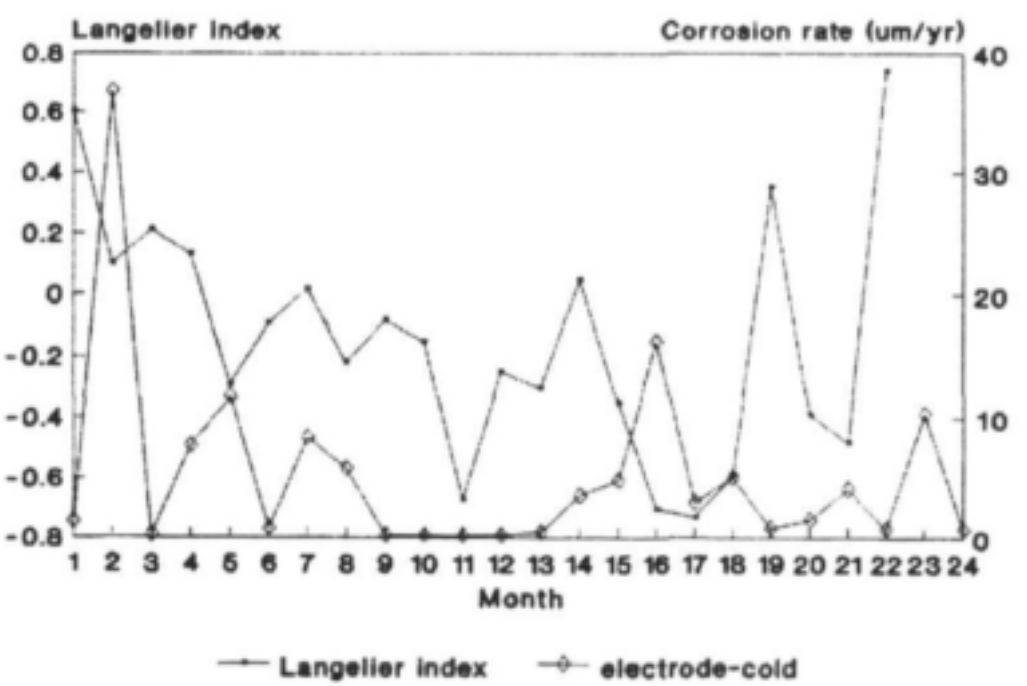

Figure 63. Langelier index versus corrosion rate of 3CR12 measured by electrode in cold water (Vereeniging).

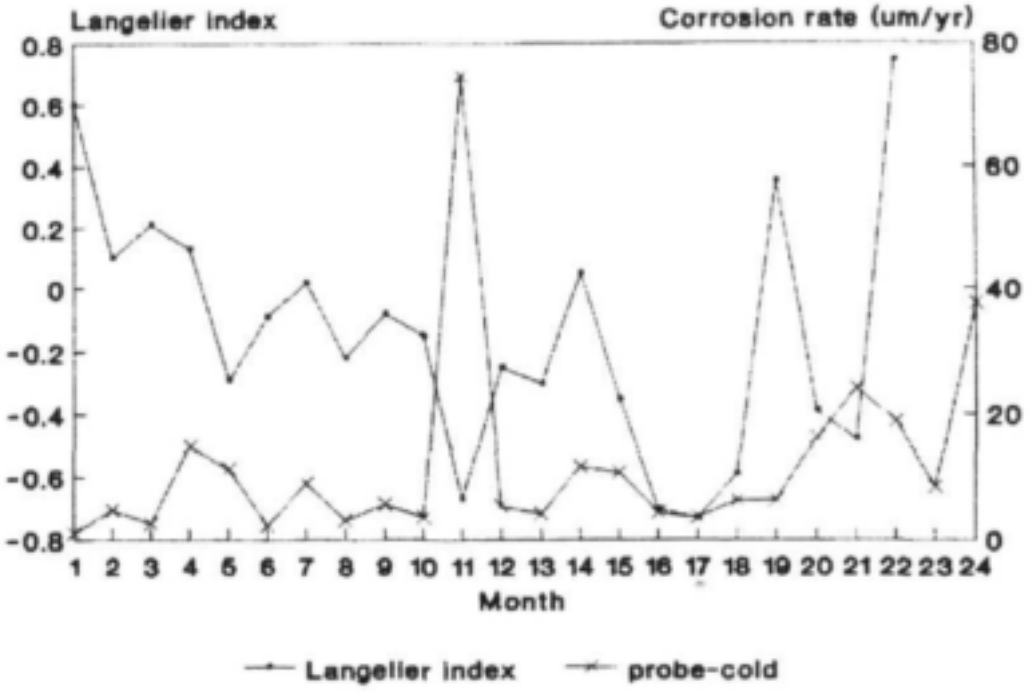

Figure 64. Langelier index versus corrosion rate of 3CR12 measured by a probe in cold water (Vereeniging).

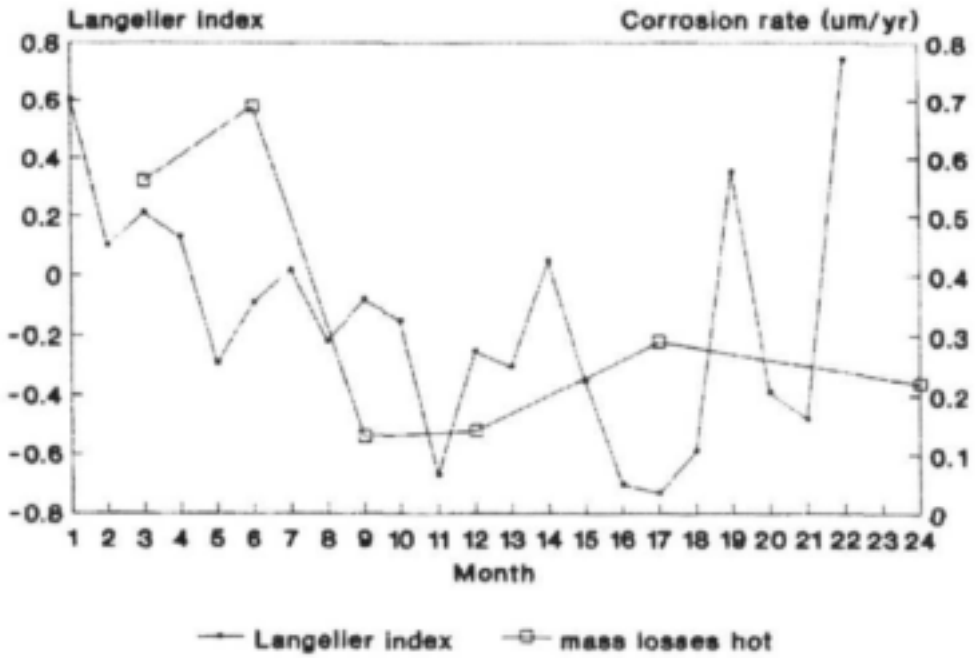

Figure 65. Langelier index versus corrosion rate of 3CR12 measured by 3-monthly mass loss in hot water (Vereeniging).

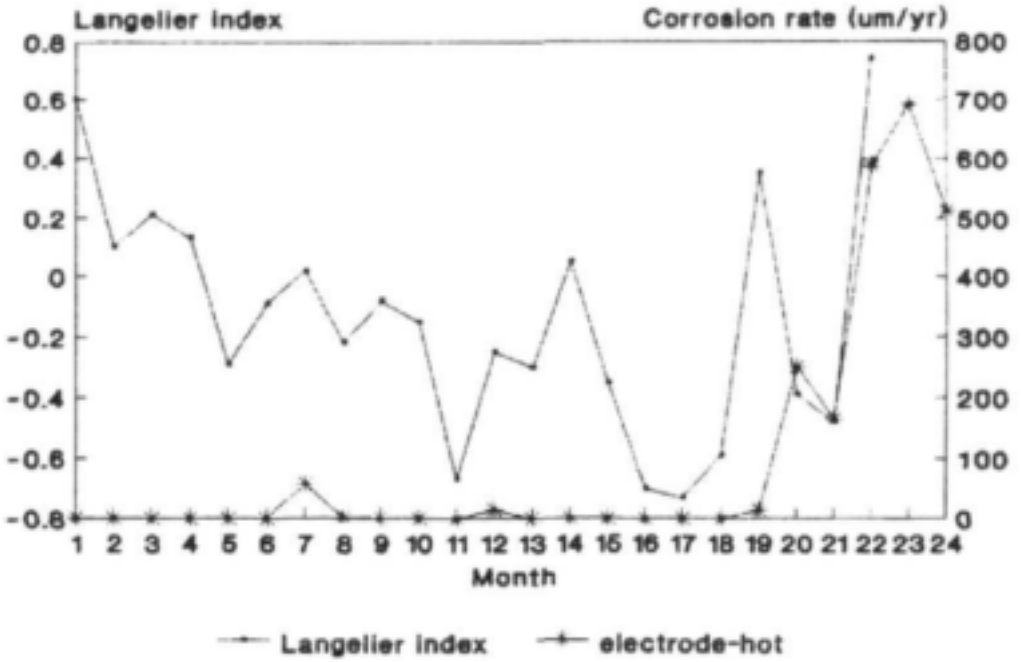

Figure 66. Langelier index versus corrosion rate of 3CR12 measured by an electrode in hot water (Vereeniging).

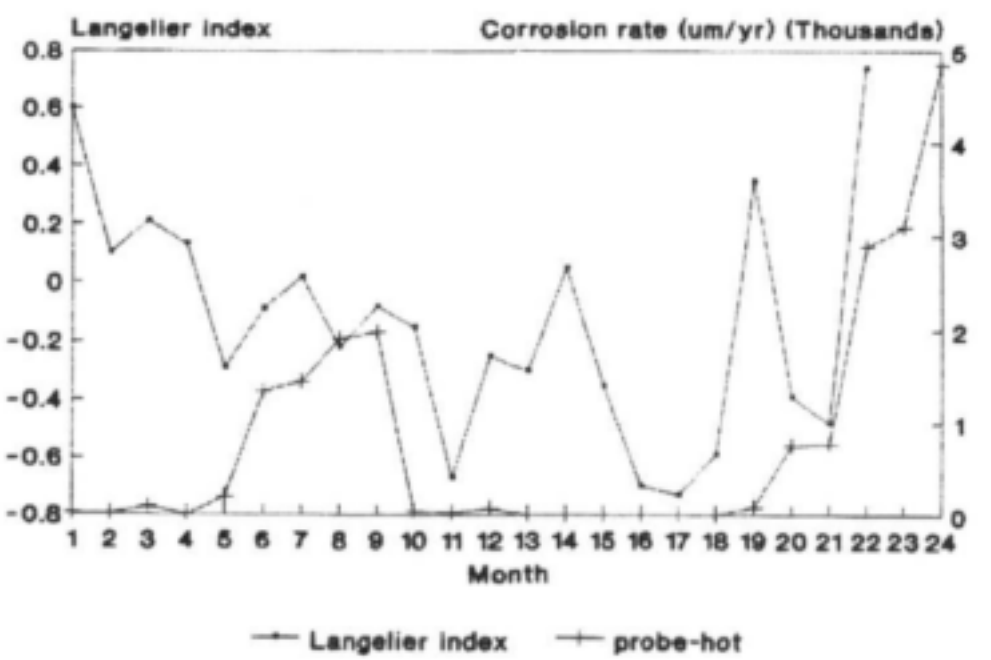

Figure 67. Langelier index versus corrosion rate of 3CR12 measured by a probe in hot water (Vereeniging).

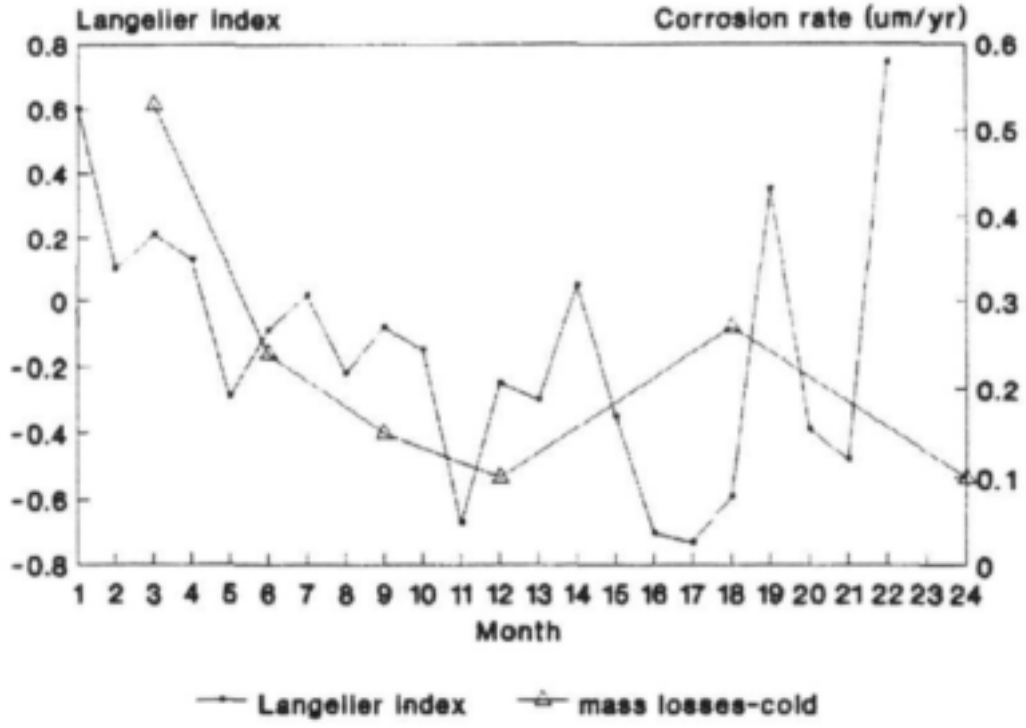

Figure 68. Langelier index versus corrosion rate of 304 measured by 3-monthly mass loss in cold water (Vereeniging).

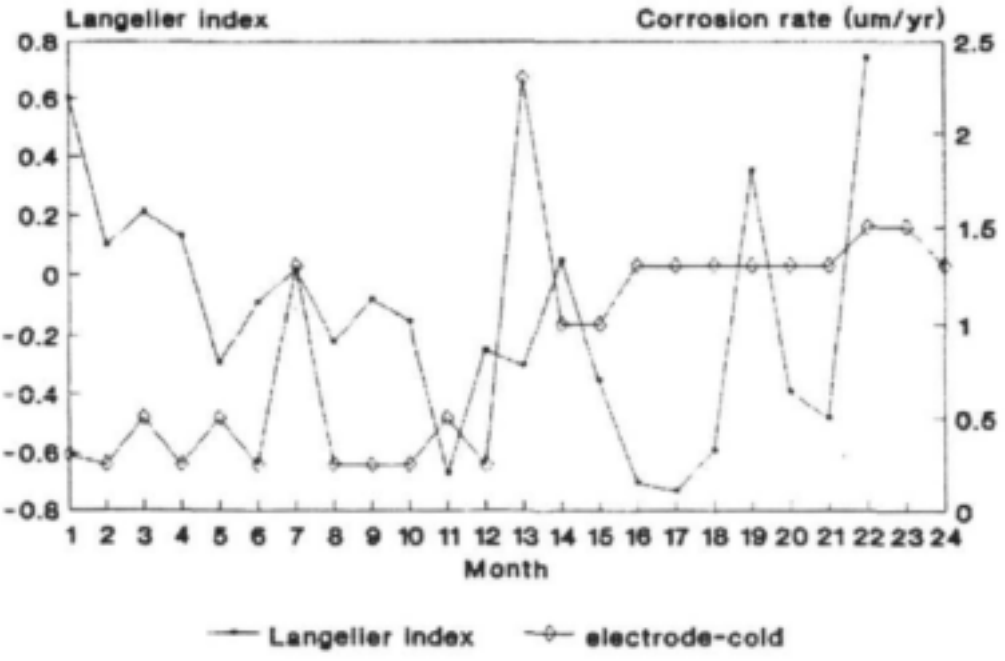

Figure 69. Langelier index versus corrosion rate of 304 measured by electrode in cold water (Vereeniging).

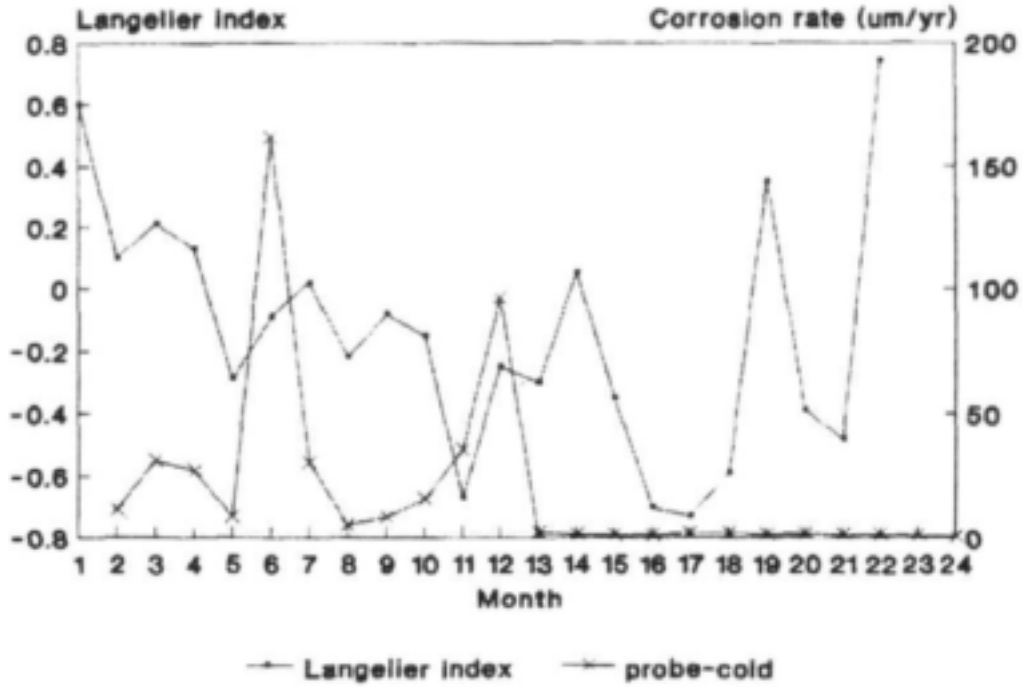

Figure 70. Langelier index versus corrosion rate of 304 measured by a probe in cold water (Vereeniging).

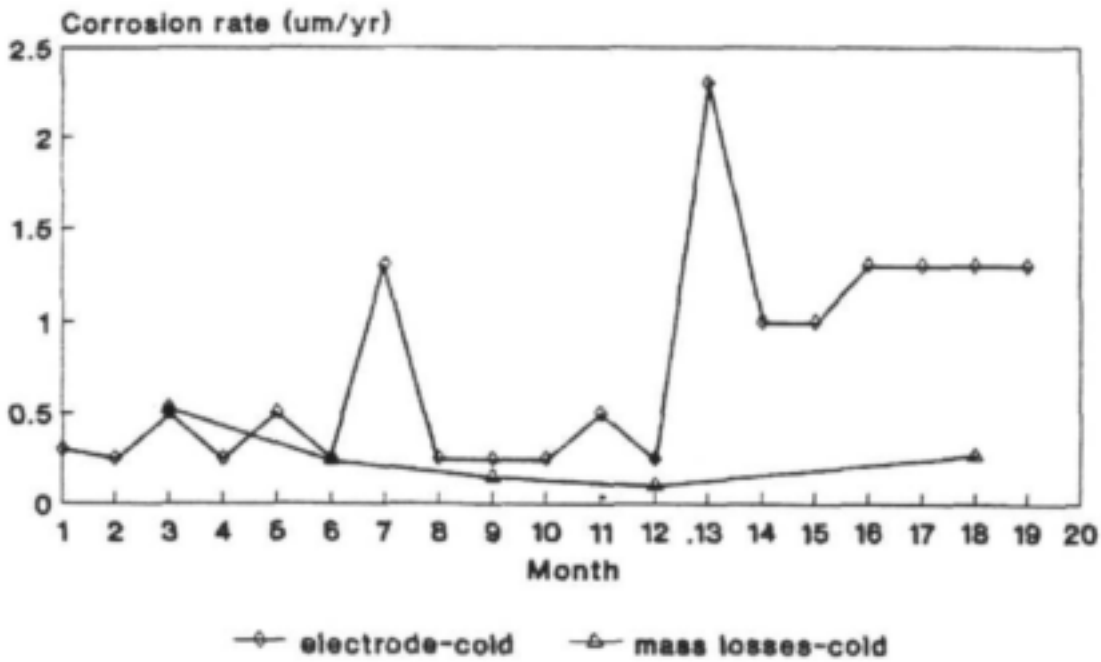

Figure 71. Comparison of corrosion rates of 304 obtained by mass loss and electrode in cold water (Vereeniging).

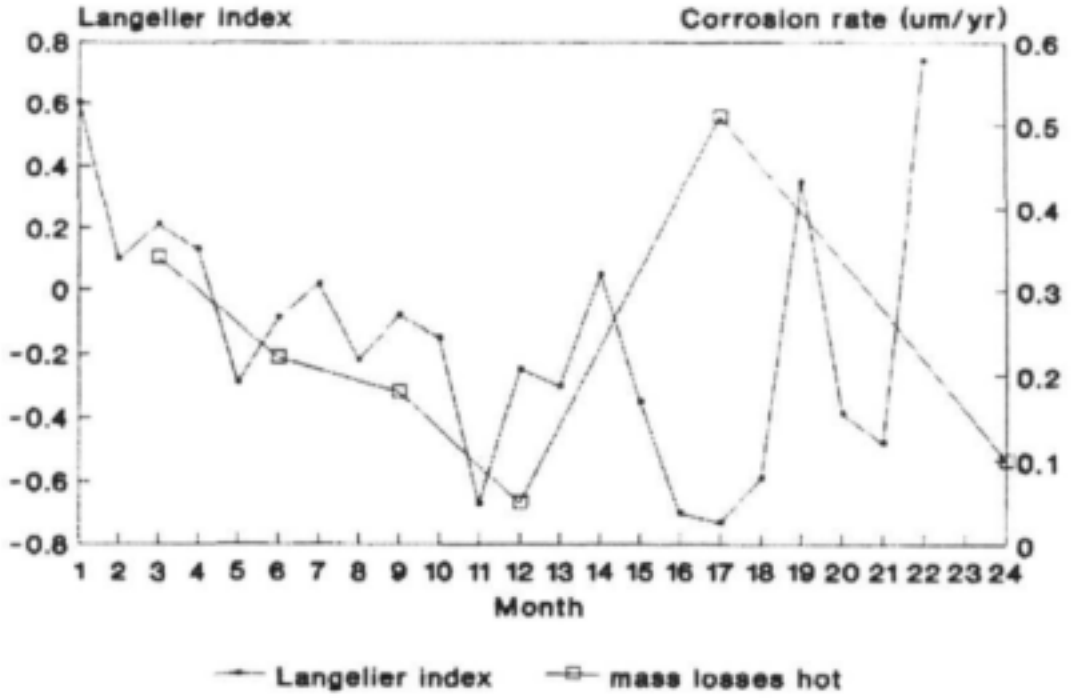

Figure 72. Langelier index versus corrosion rate of 304 measured by 3-monthly mass loss in hot water (Vereeniging).

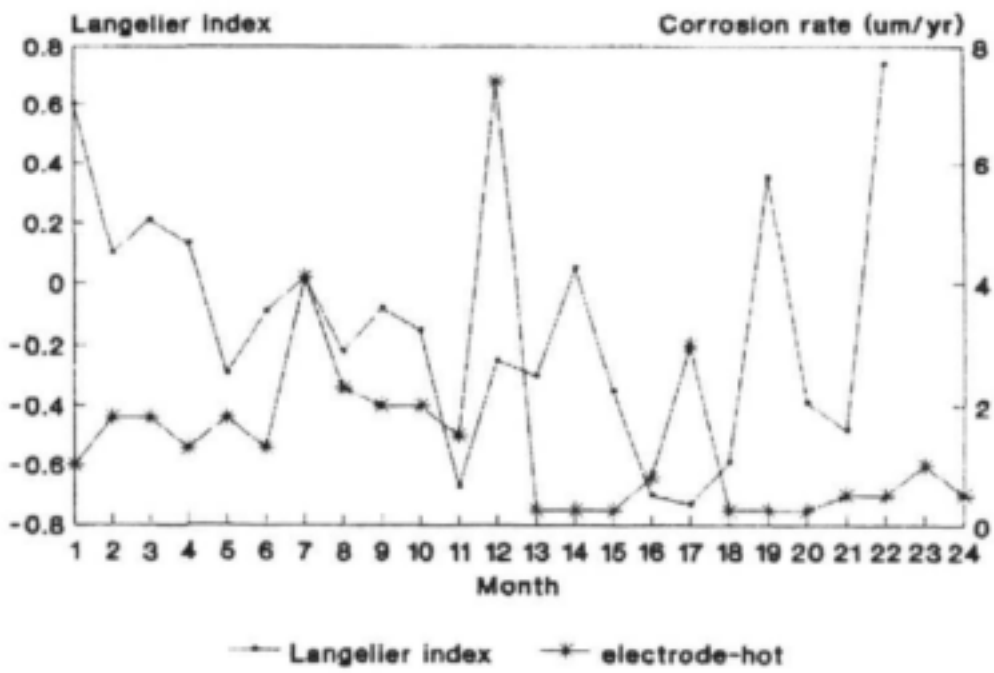

Figure 73. Langelier index versus corrosion rate of 304 measured by an electrode in hot water (Vereeniging).

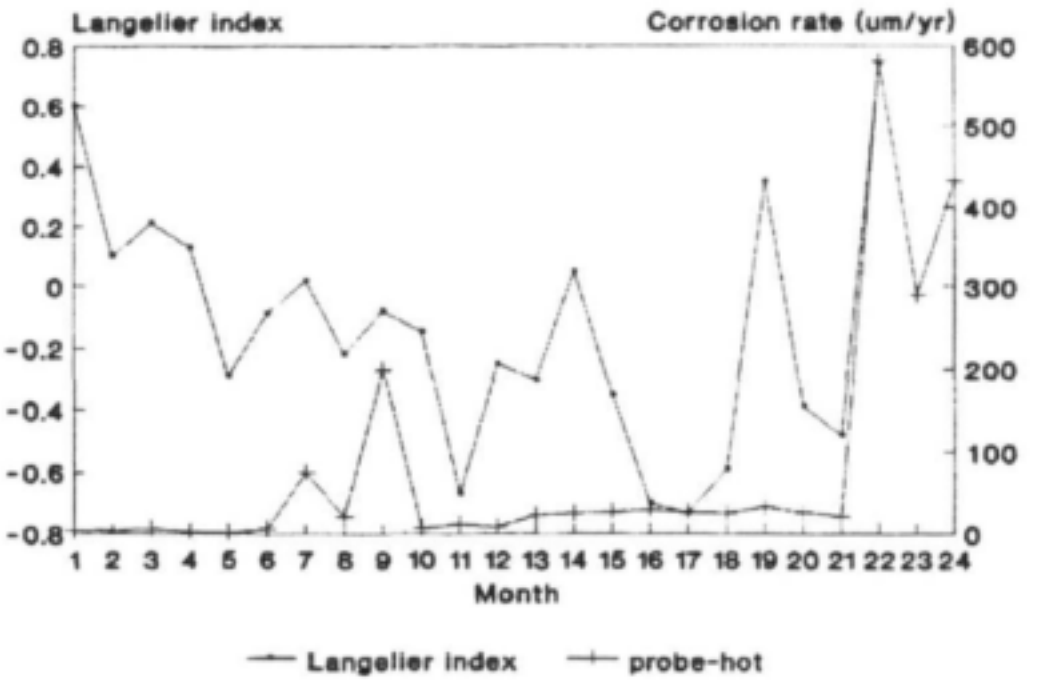

Figure 74. Langelier index versus corrosion rate of 304 measured by a probe in hot water (Vereeniging).

Appendix 4. Results of corrosion testing at CSIR

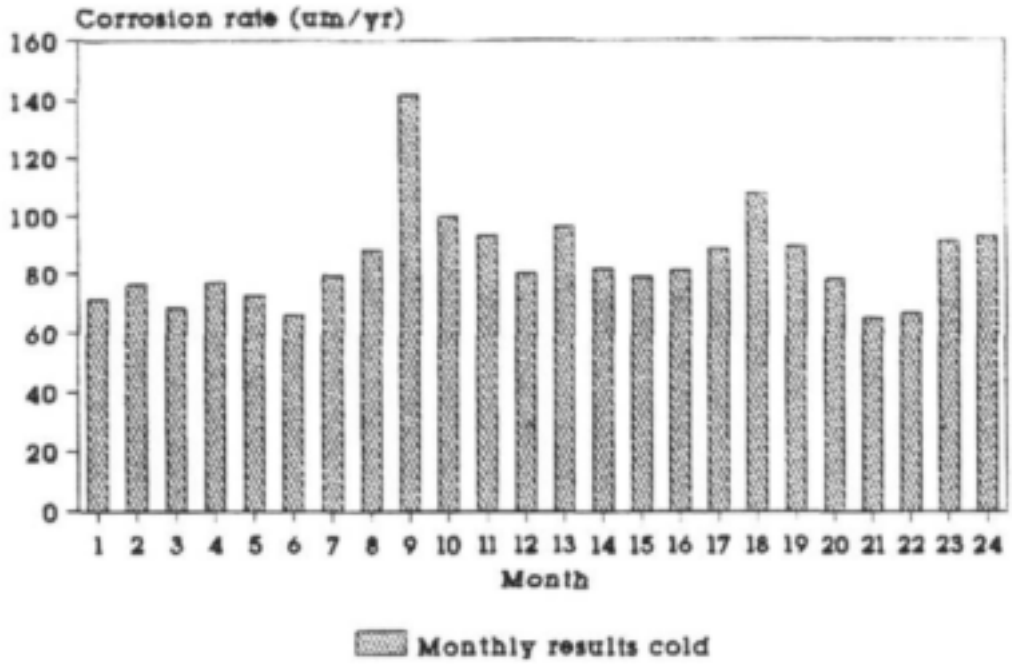

Figure 75. Change in the corrosion rate of mild steel measured by mass loss over 24 months in cold water (CSIR).

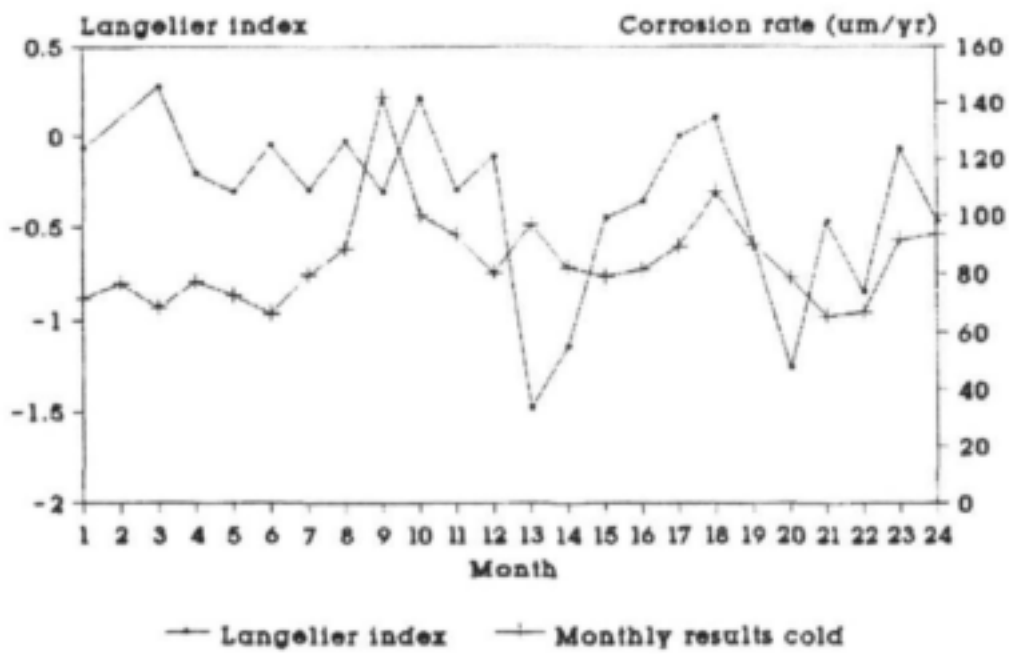

Figure 76. Langelier index versus corrosion rate of mild steel measured by monthly mass loss in cold water (CSIR).

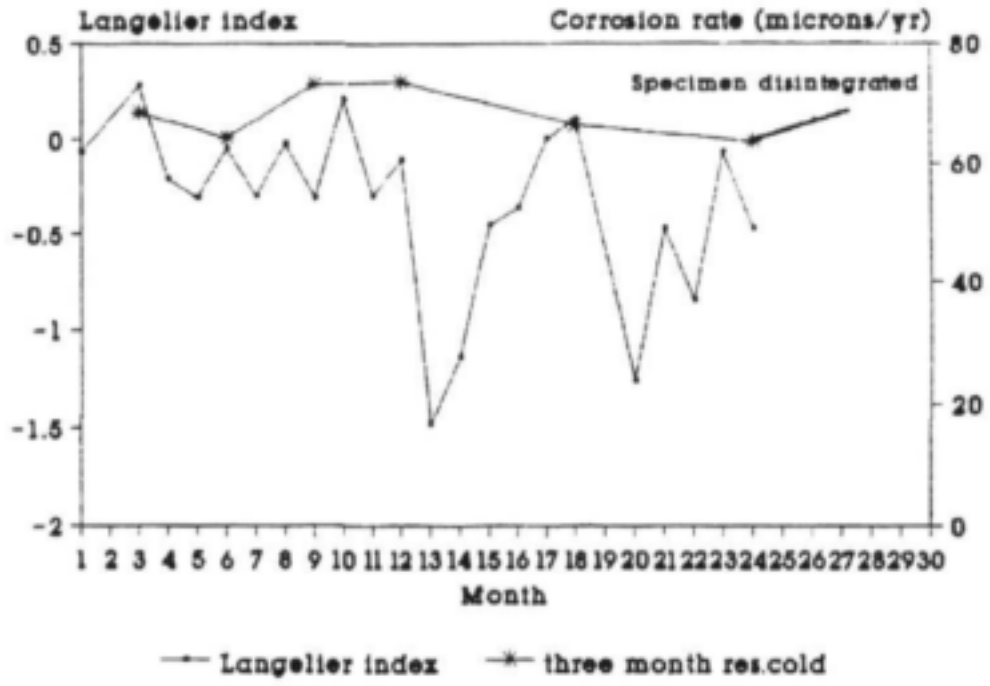

Figure 77. Langelier index versus corrosion rate of mild steel measured by 3-monthly mass loss in cold water (CSIR).

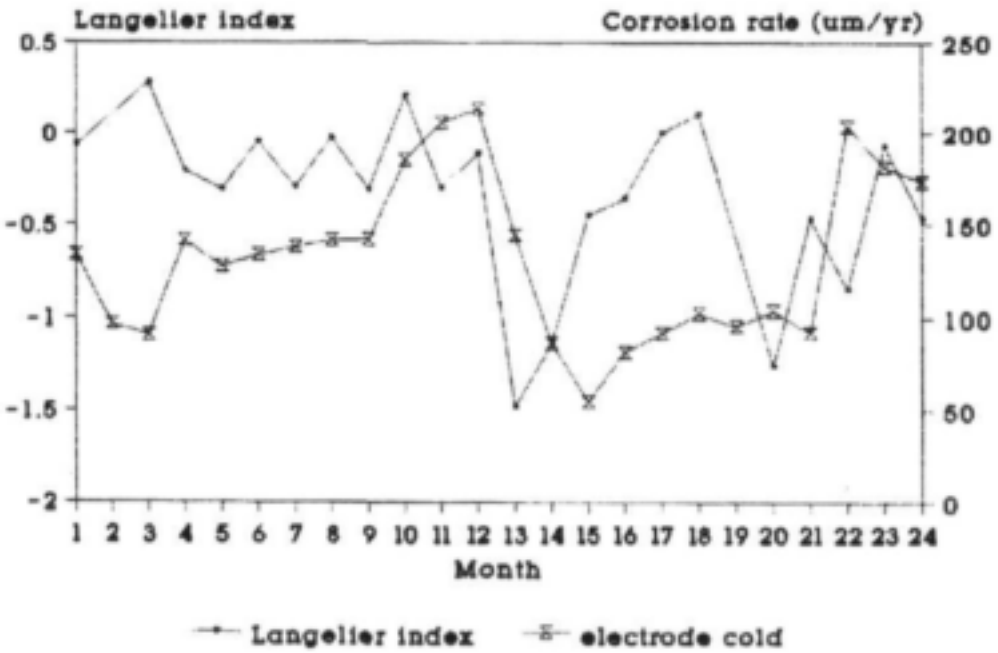

Figure 78. Langelier index versus corrosion rate of mild steel measured by an electrode in cold water (CSIR).

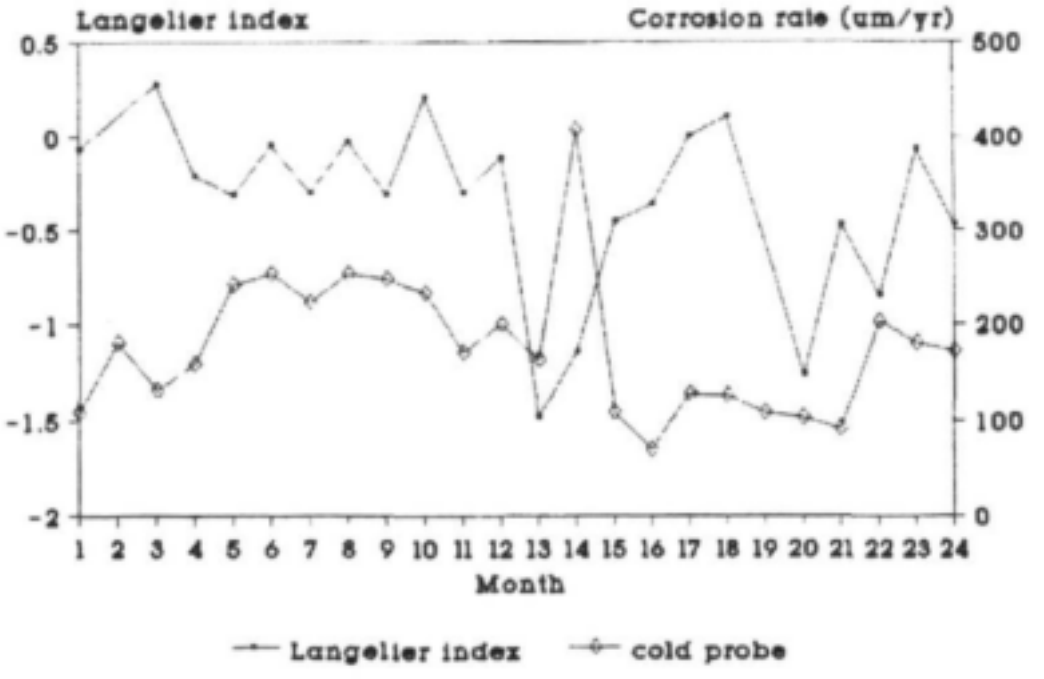

Figure 79. Langelier index versus corrosion rate of mild steel measured by a probe in cold water (CSIR).

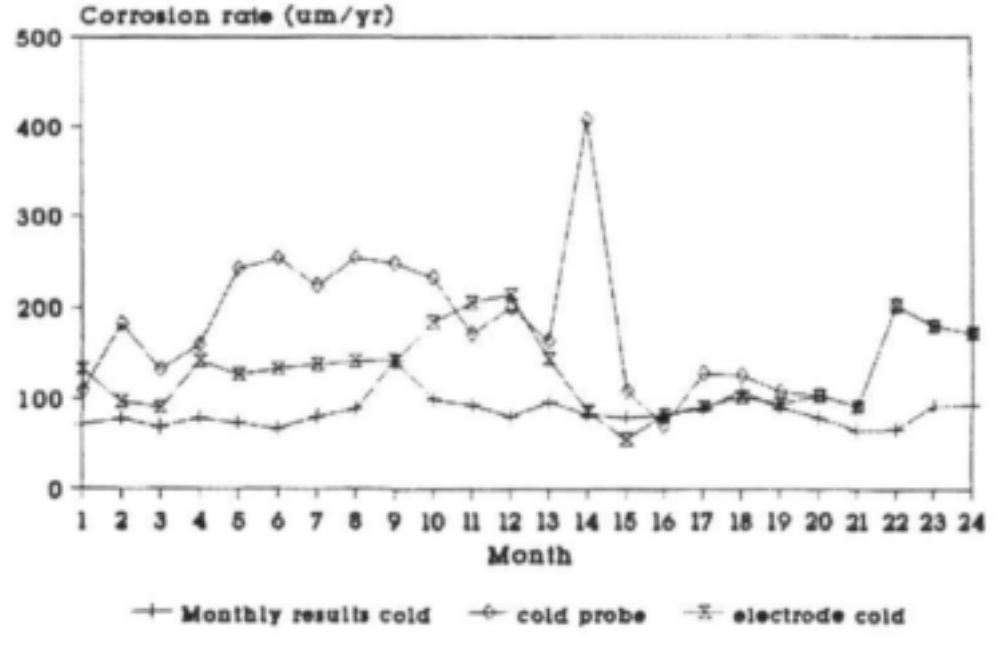

Figure 80. Comparison of the corrosion rates of mild steel obtained by different techniques in cold water (CSIR).

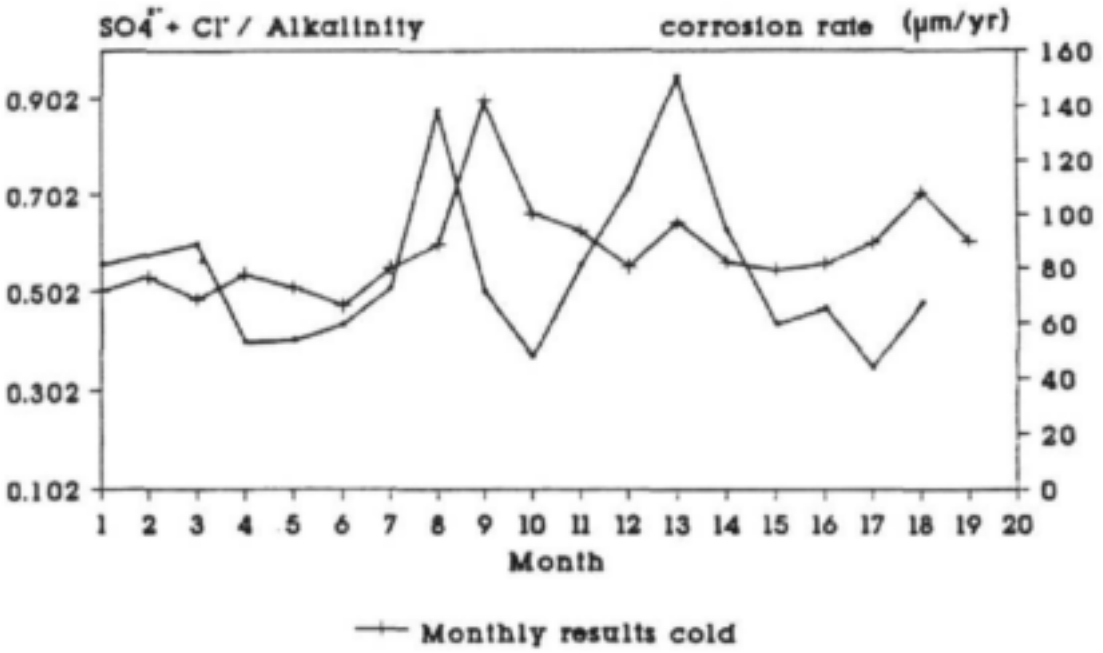

Figure 81. SO_4 + Cl / Alkalinity versus corrosion rate of mild steel in cold water (CSIR).

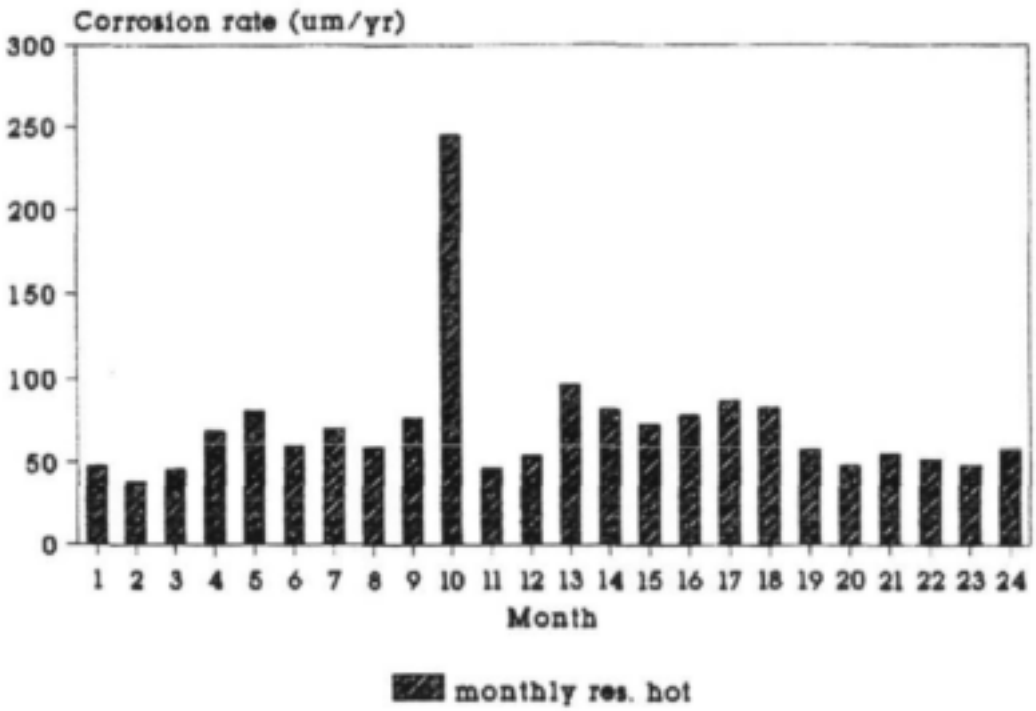

Figure 82. Change in the corrosion rate of mild steel measured by mass loss over 24 months in hot water (CSIR).

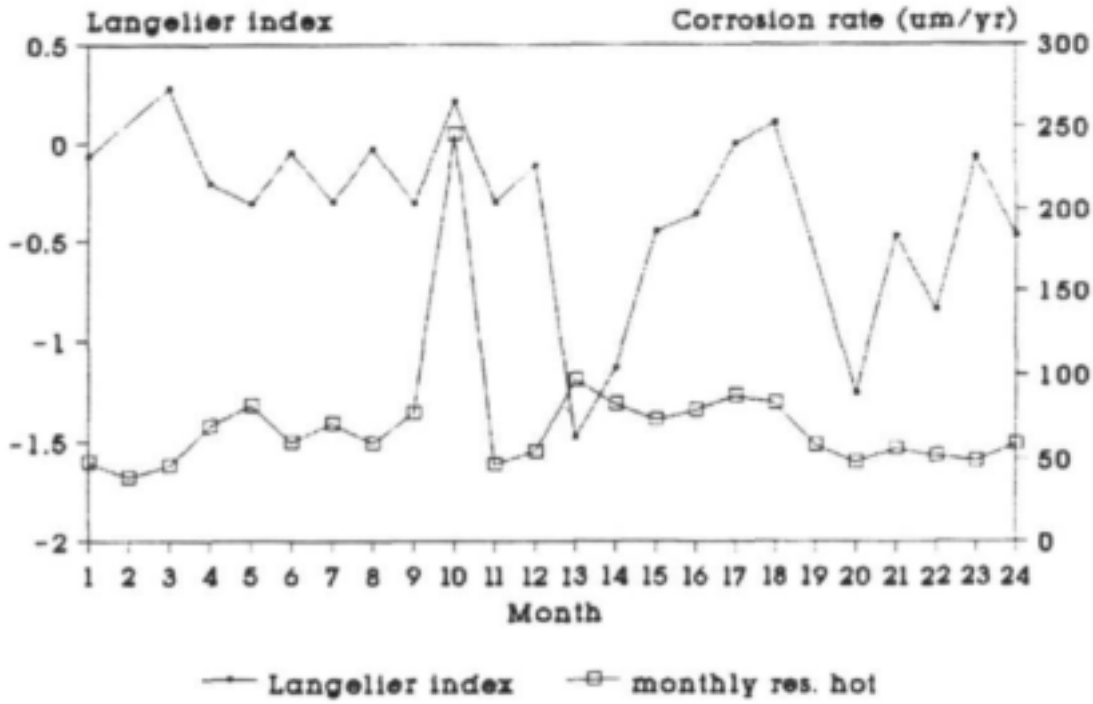

Figure 83. Langelier index versus corrosion rate of mild steel measured by monthly mass loss in hot water (CSIR).

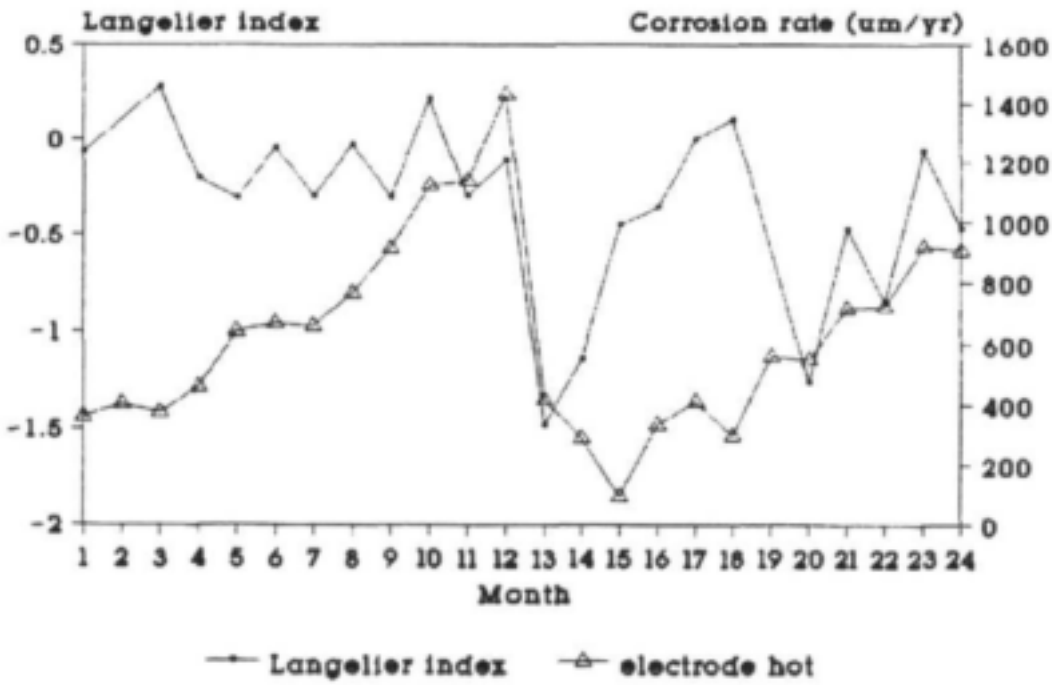

Figure 84. Langelier index versus corrosion rate of mild steel measured by an electrode in hot water (CSIR).

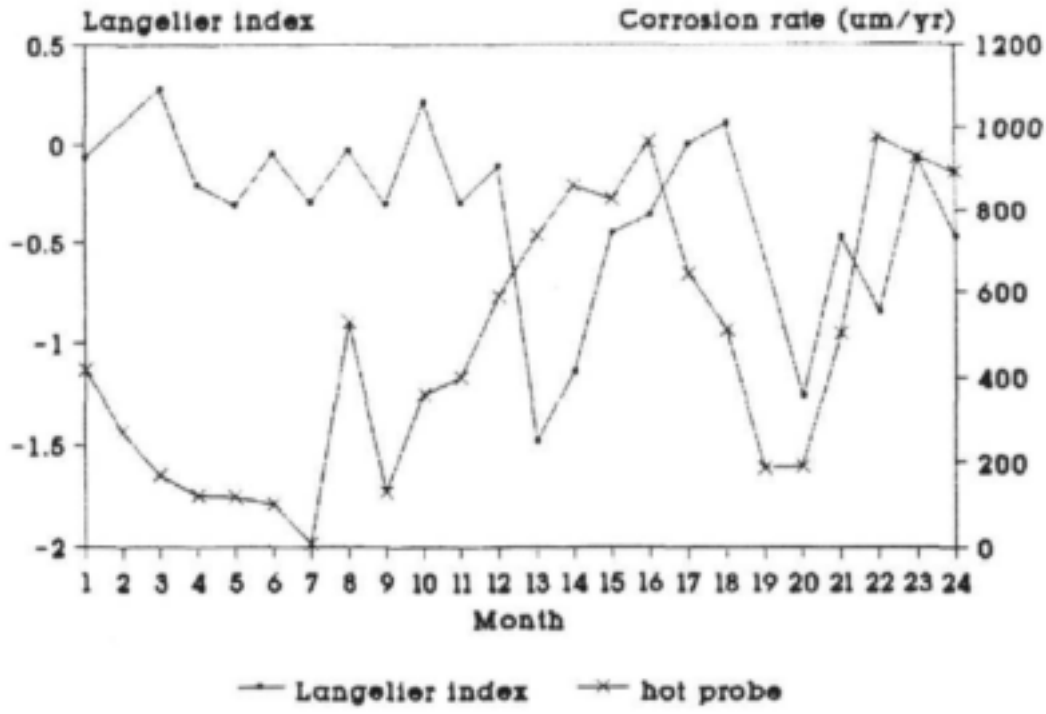

Figure 85. Langelier index versus corrosion rate of mild steel measured by a probe in hot water (CSIR).

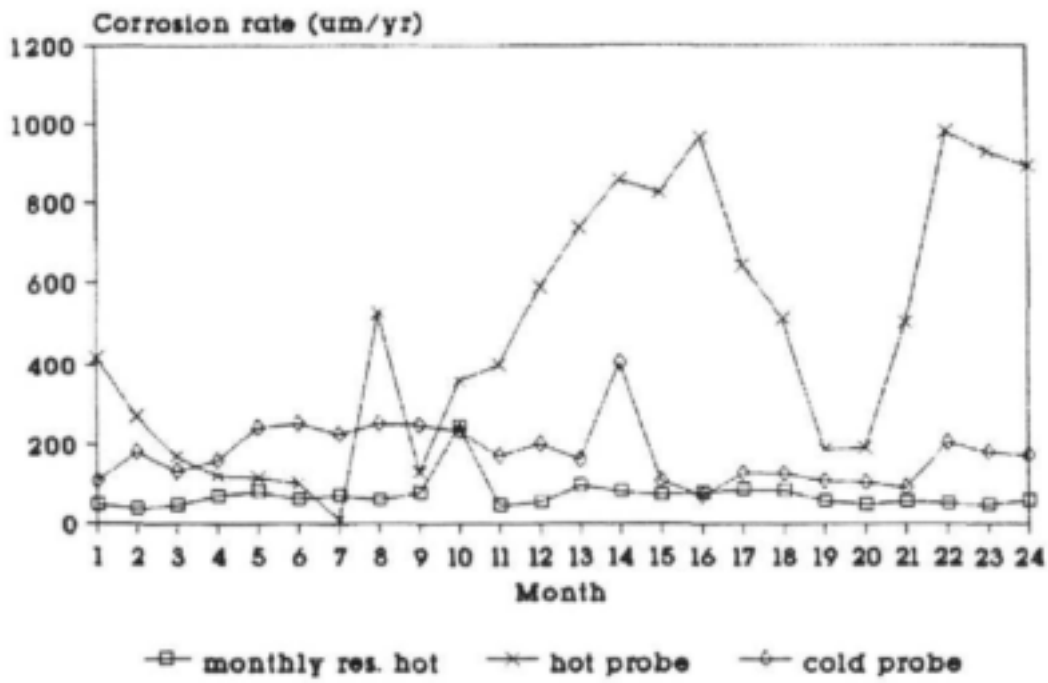

Figure 86. Comparison of the corrosion rates of mild steel obtained by different techniques in hot water (CSIR).

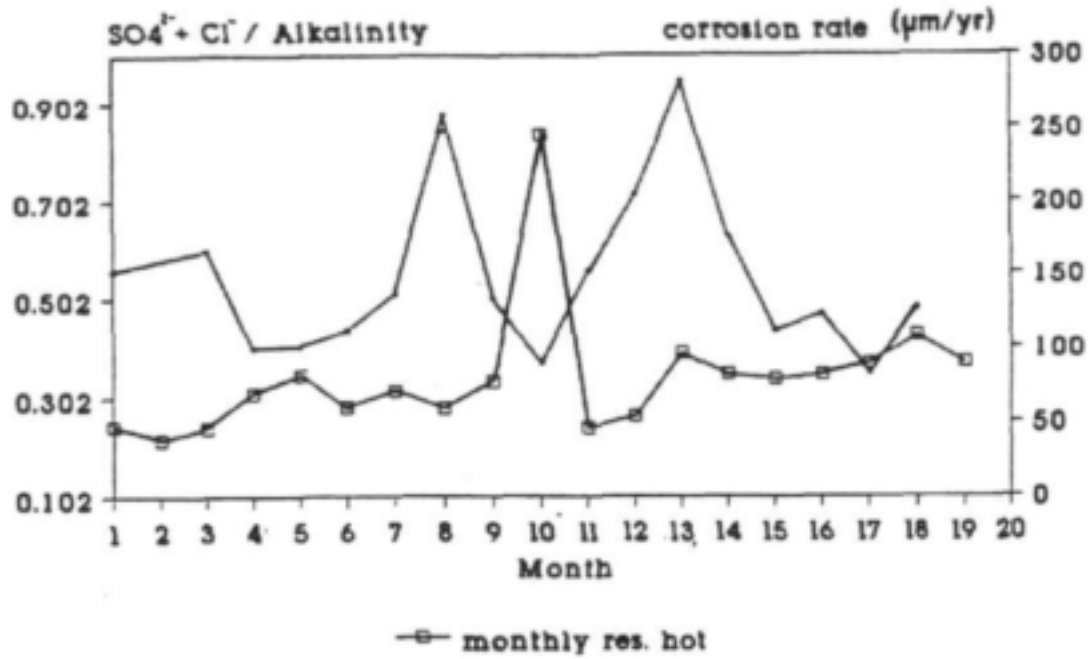

Figure 87. SO_4 + Cl / Alkalinity versus corrosion rate of mild steel in hot water (CSIR).

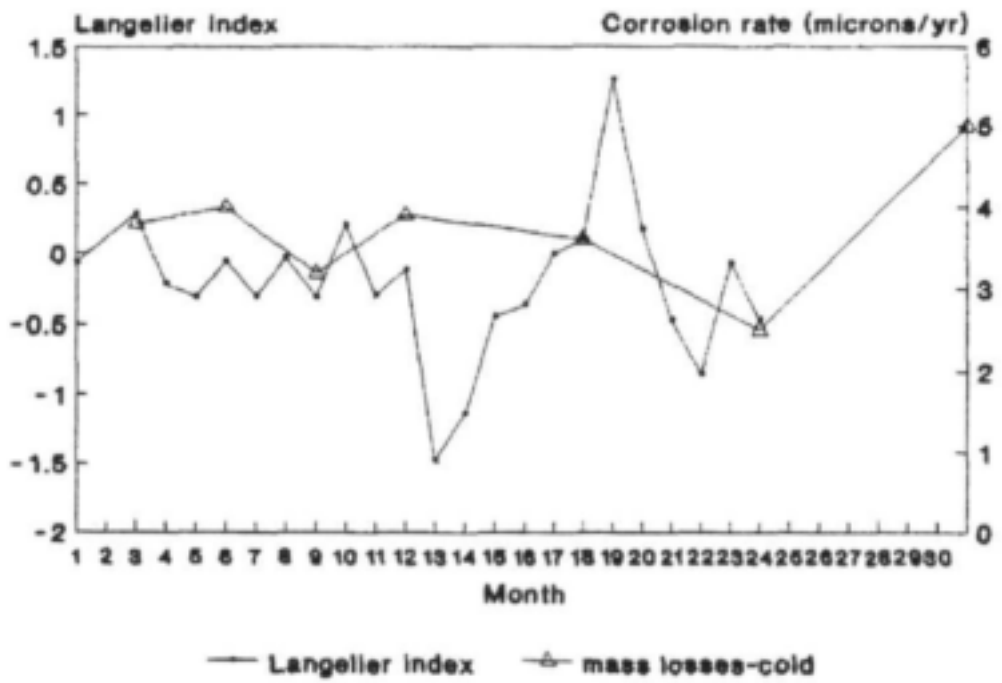

Figure 88. Langelier index versus corrosion rate of zinc measured by 3-monthly mass loss in cold water (CSIR).

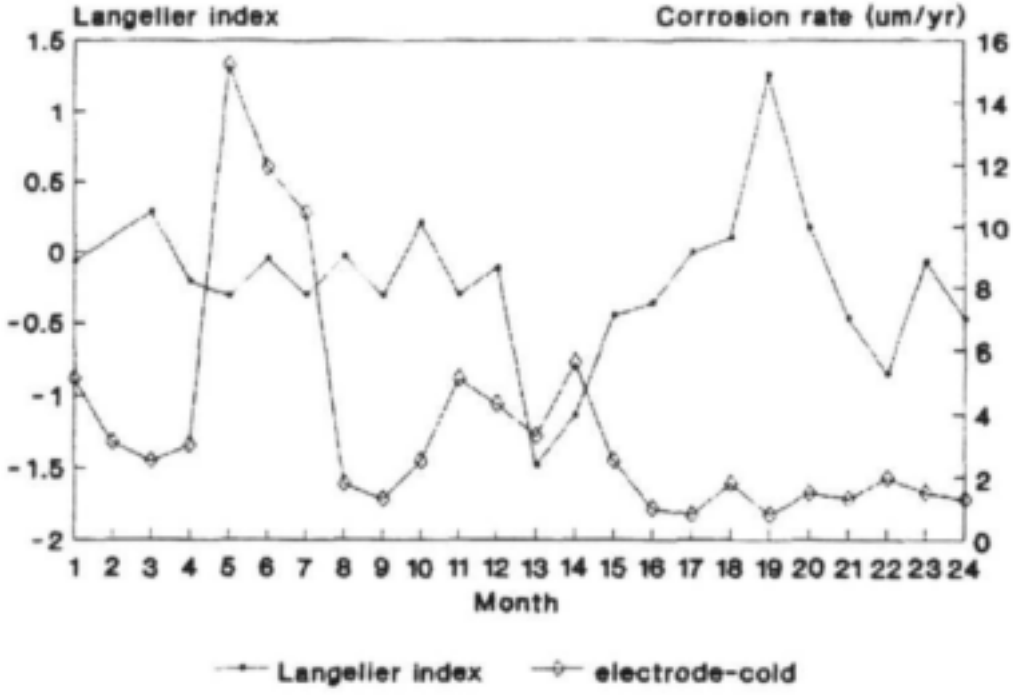

Figure 89. Langelier index versus corrosion rates of zinc measured by an electrode in cold water (CSIR).

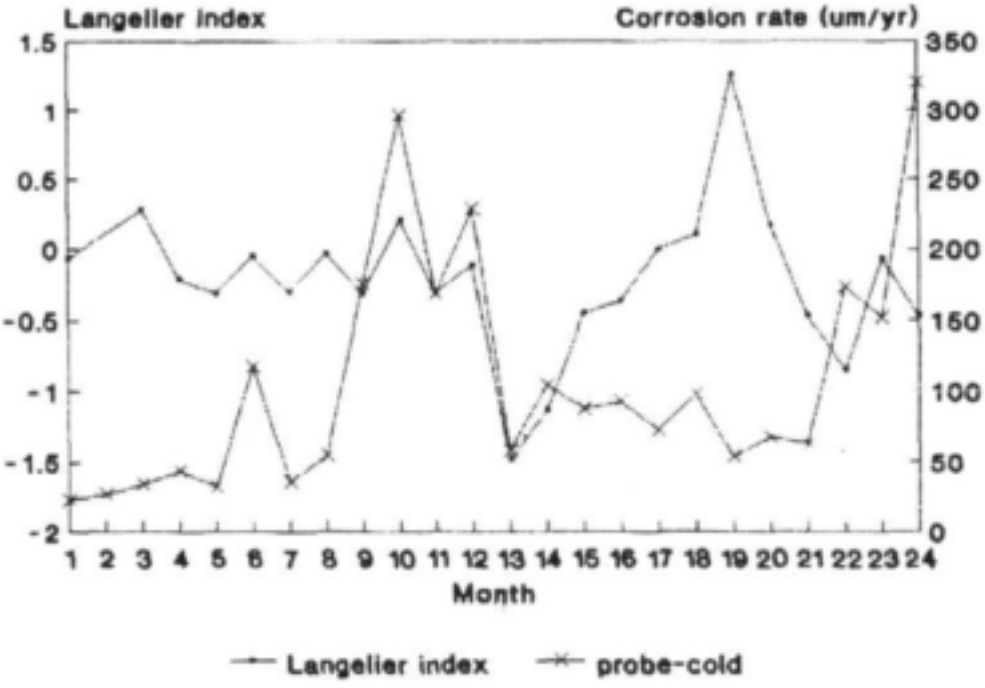

Figure 90. Langelier index versus corrosion rate of zinc measured by a probe in cold water (CSIR).

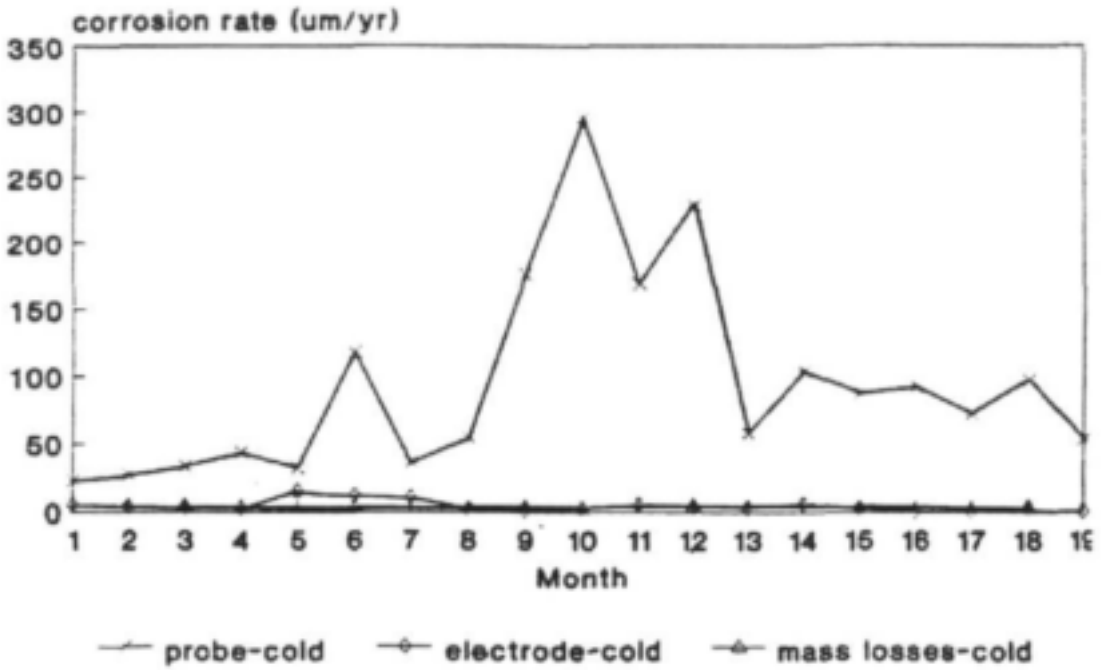

Figure 91. Comparison of the corrosion rates of zinc obtained by different techniques in cold water (CSIR).

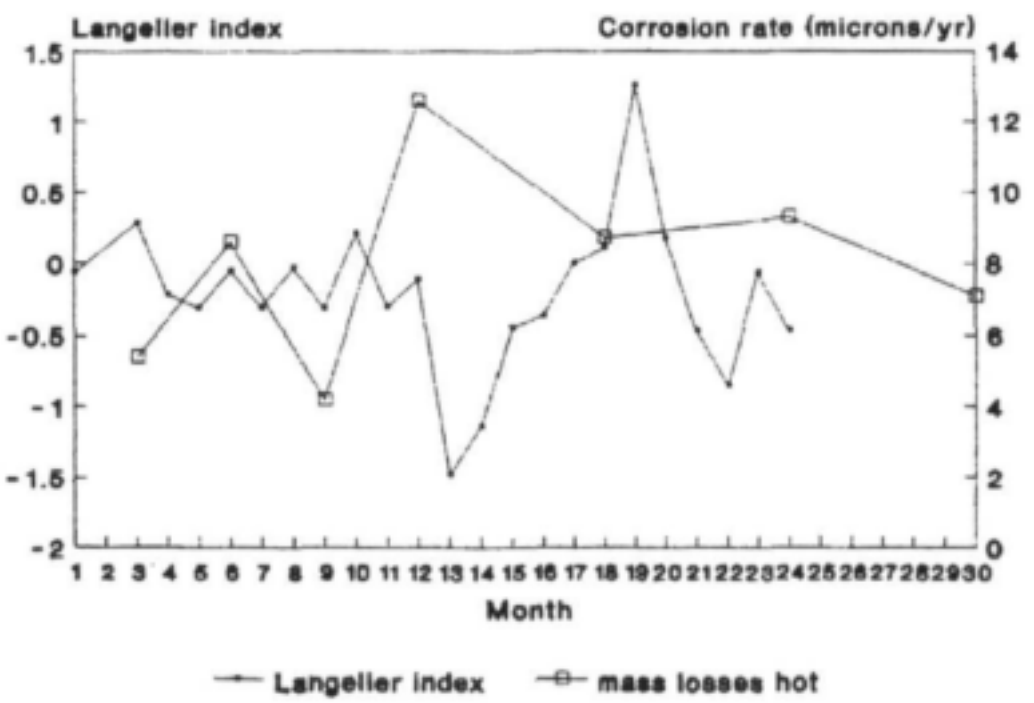

Figure 92. Langelier index versus corrosion rate of zinc measured by 3-monthly mass loss in hot water (CSIR).

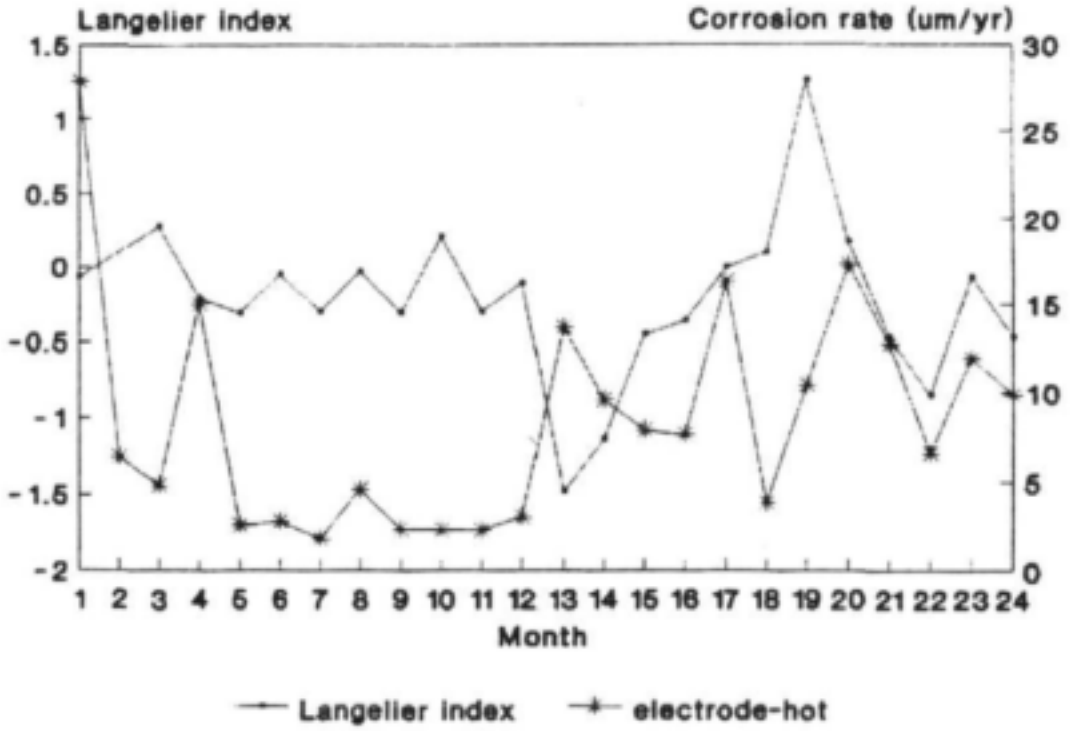

Figure 93. Langelier index versus corrosion rate of zinc measured by an electrode in hot water (CSIR).

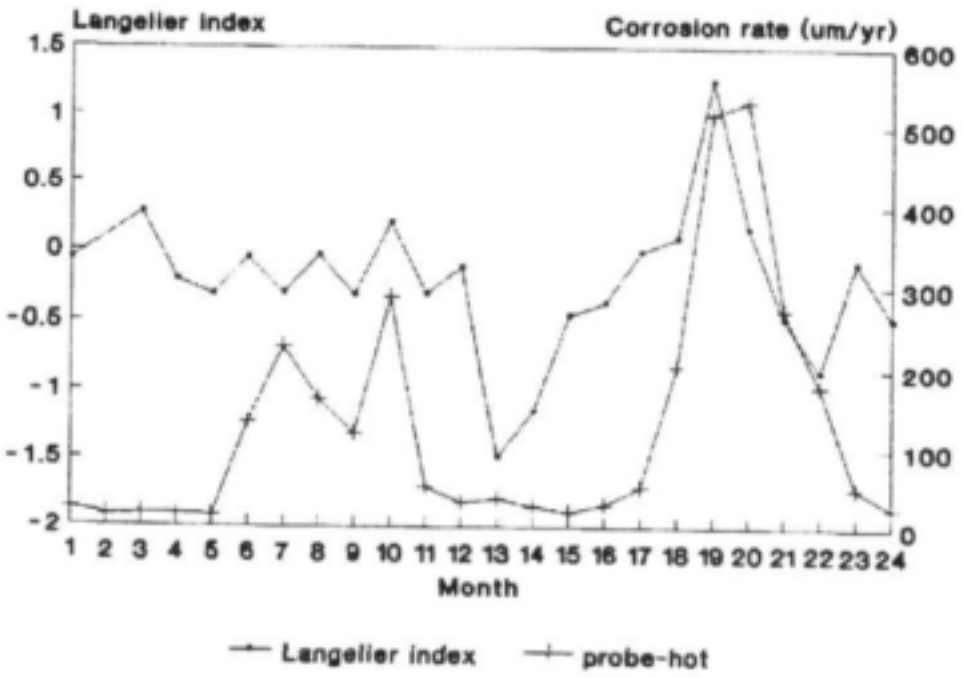

Figure 94. Langelier index versus corrosion rate of zinc measured by a probe in hot water (CSIR).

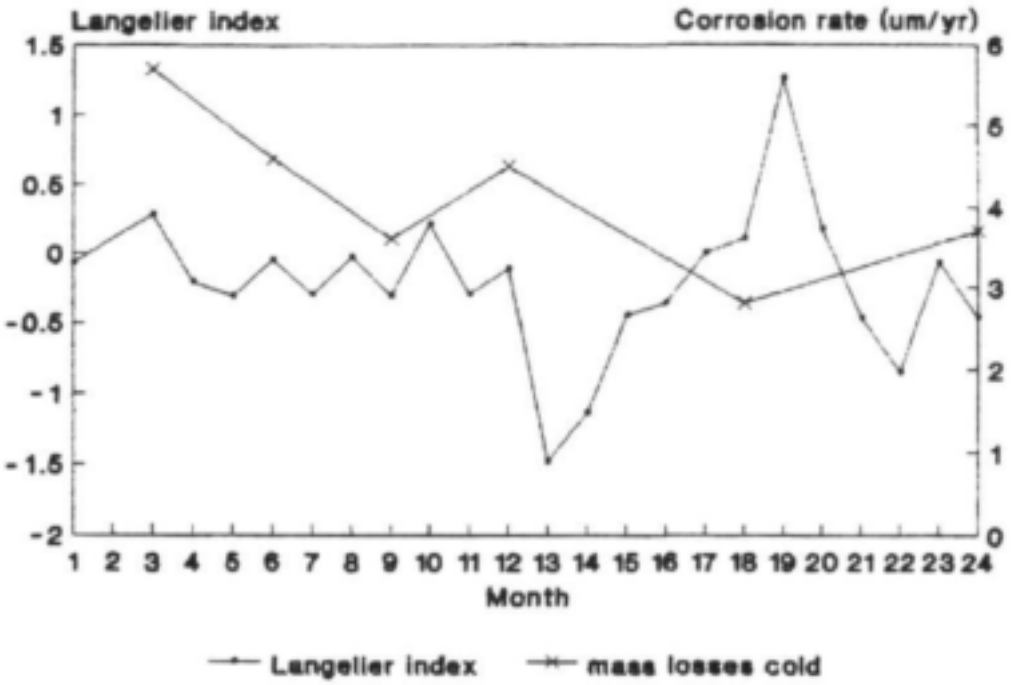

Figure 95. Langelier index versus corrosion rate of brass measured by 3-monthly mass loss in cold water (CSIR).

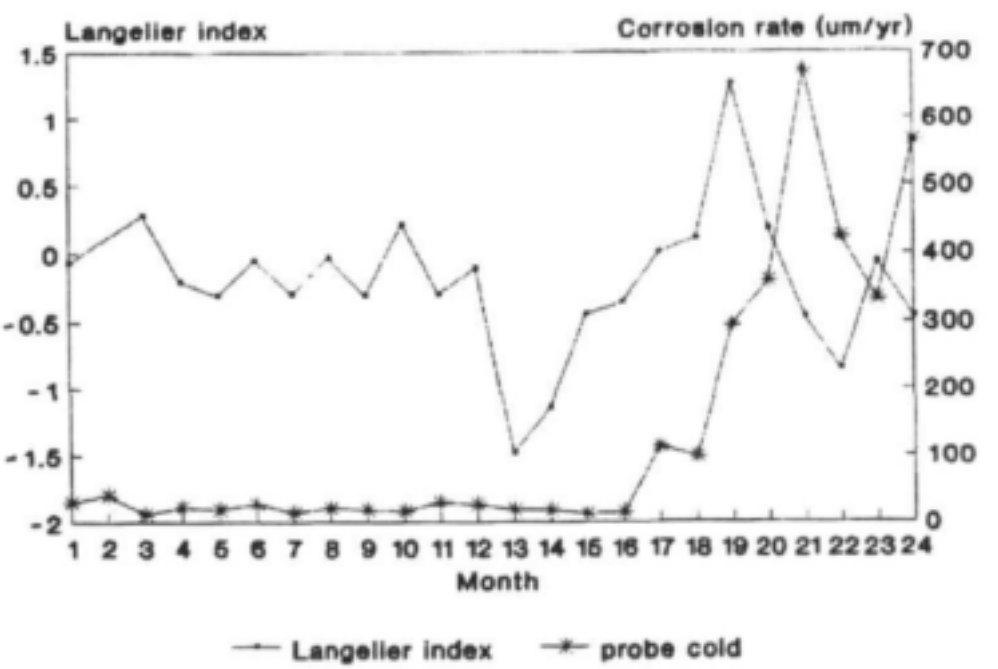

Figure 96. Langelier index versus corrosion rate of brass measured by a probe in cold water (CSIR).

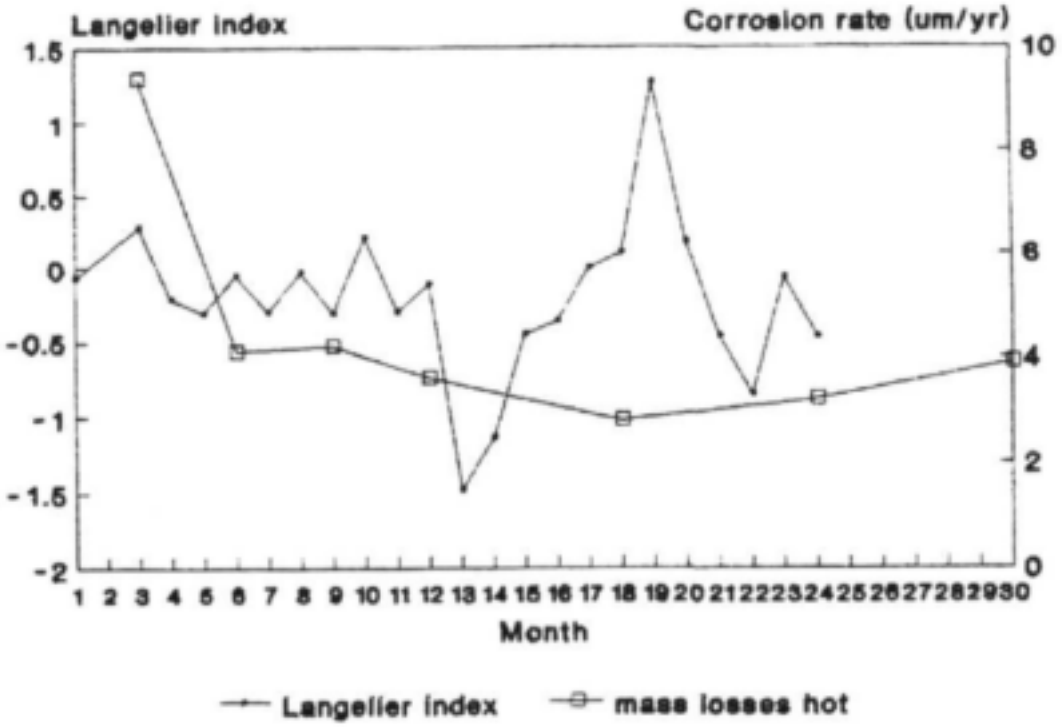

Figure 97. Langelier index versus corrosion rate of brass measured by 3-monthly mass loss in hot water (CSIR).

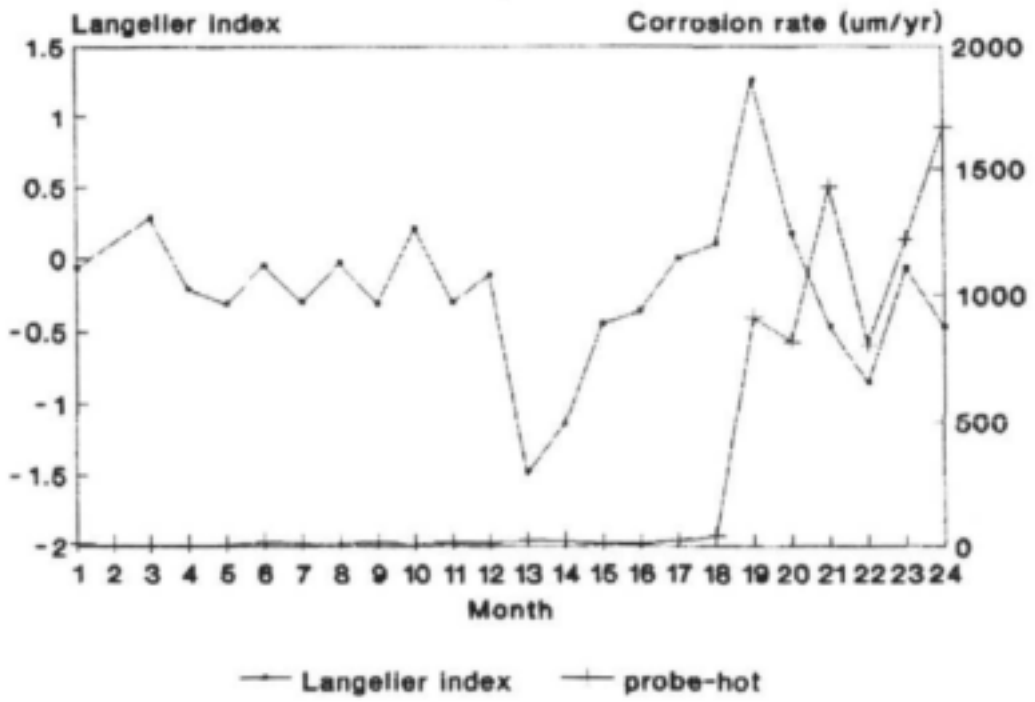

Figure 98. Langelier index versus corrosion rate of brass measured by a probe in hot water (CSIR).

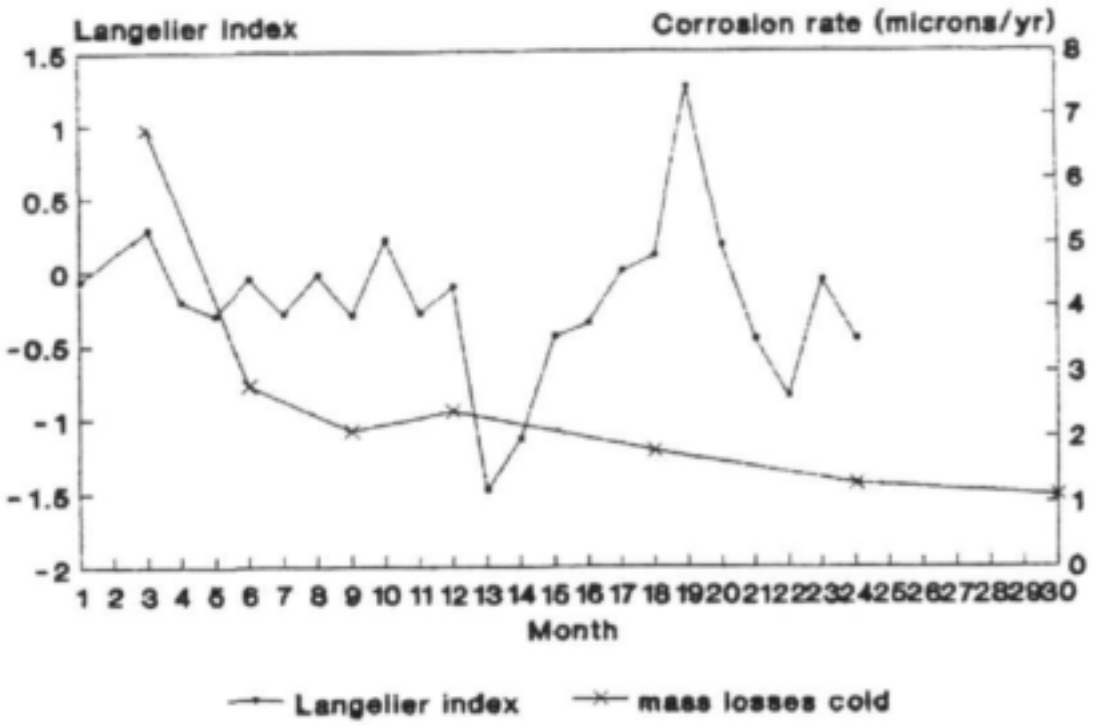

Figure 99. Langelier index versus corrosion rate of copper measured by 3-monthly mass loss in cold water (CSIR).

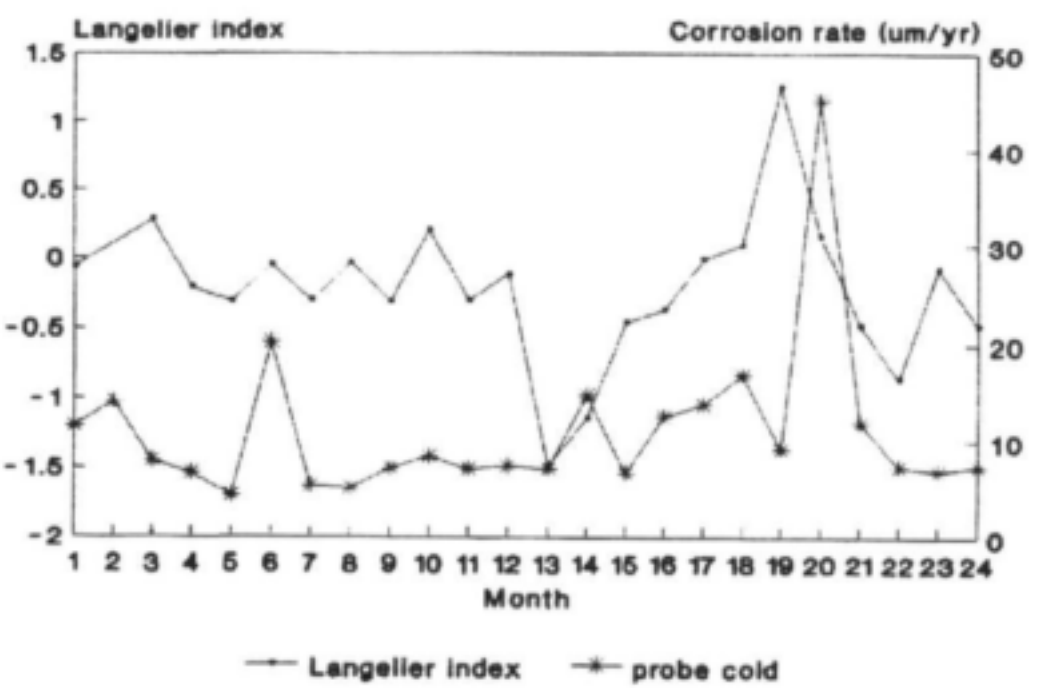

Figure 100. Langelier index versus corrosion rate of copper measured by a probe in cold water (CSIR).

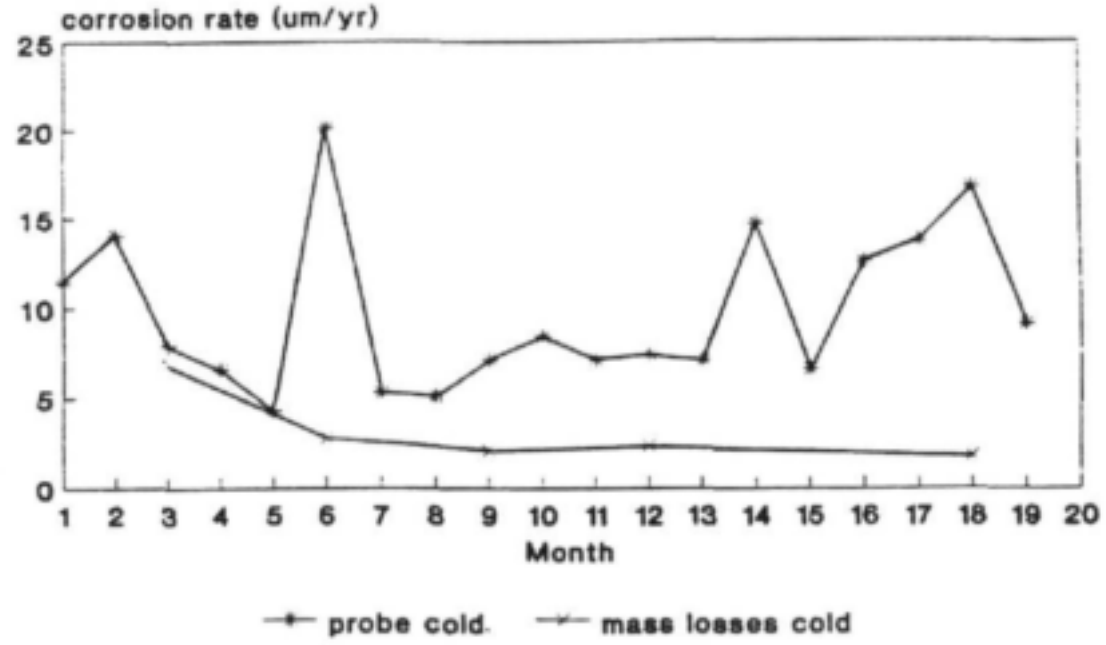

Figure 101. Comparison of the corrosion rates of copper obtained by different techniques in cold water (CSIR).

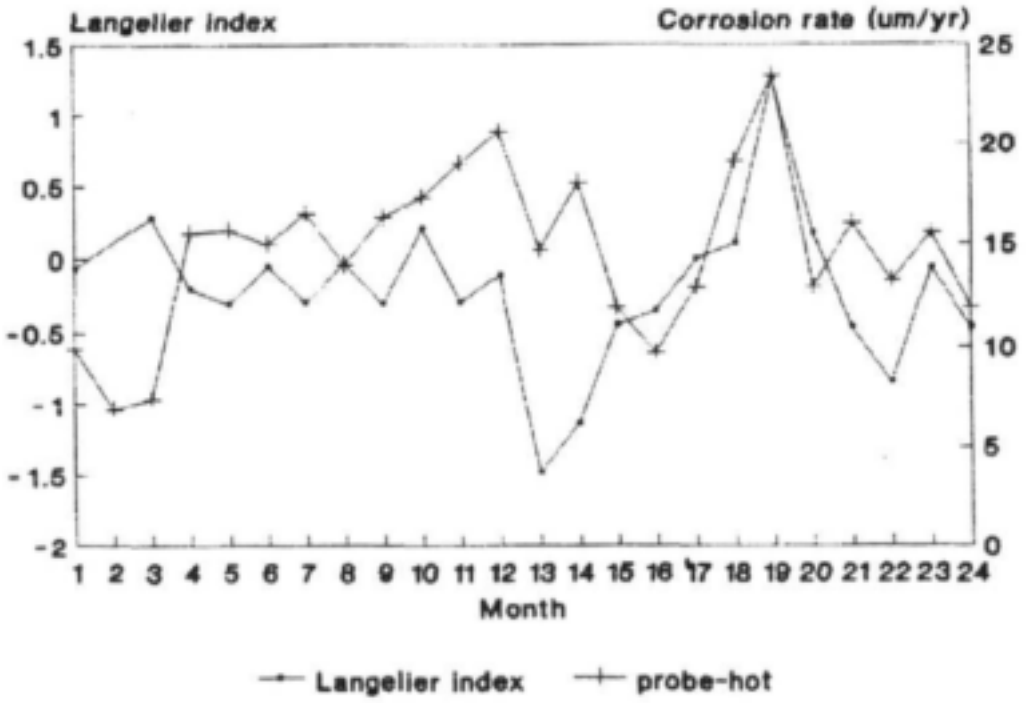

Figure 102. Langelier index versus corrosion rate of copper measured by a probe in hot water (CSIR).

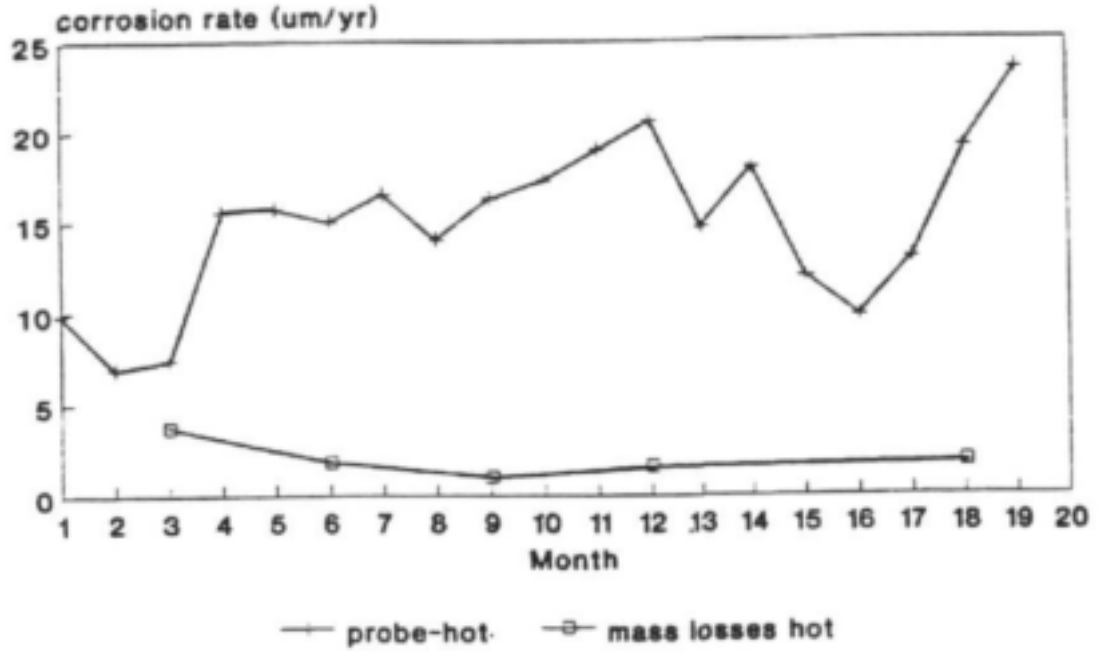

Figure 103. Comparison of corrosion rates of copper obtained by different techniques in hot water (CSIR).

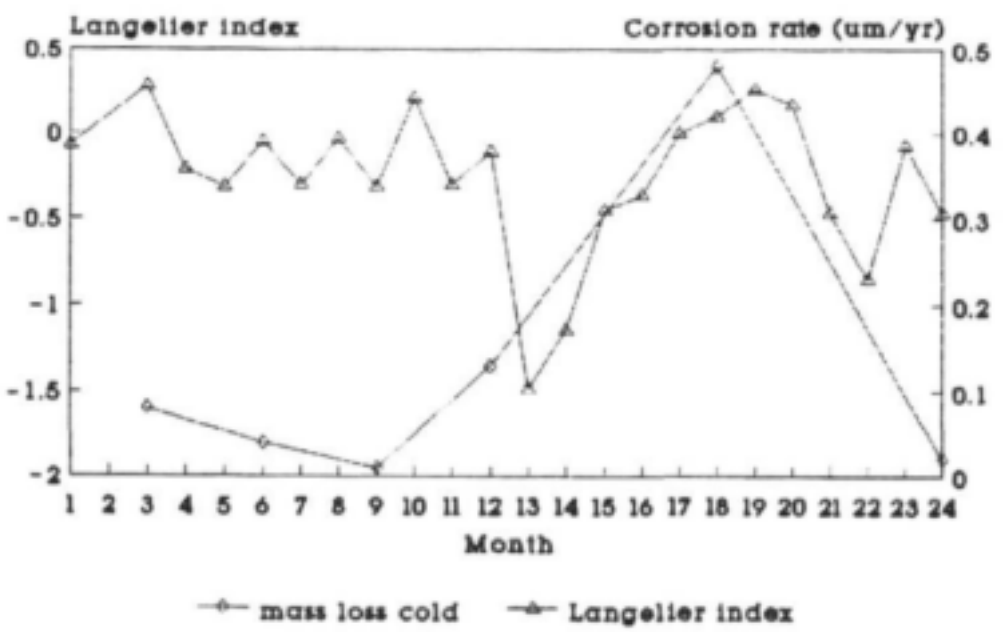

Figure 104. Langelier index versus corrosion rate of 3CR12 measured by 3-monthly mass loss in cold water (CSIR).

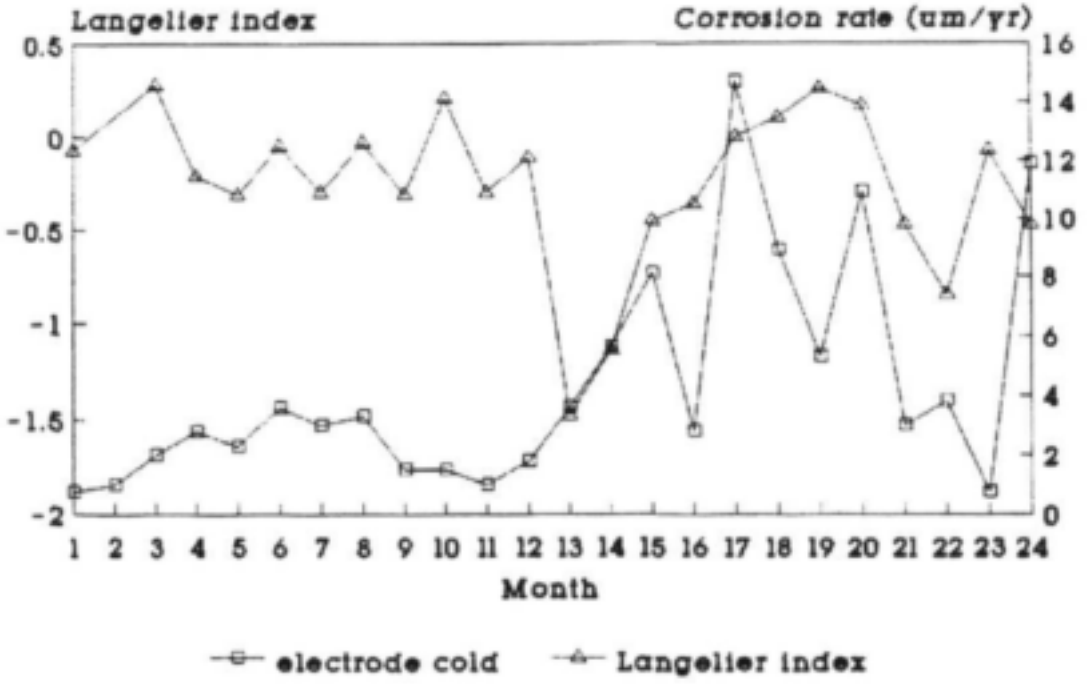

Figure 105. Langelier index versus corrosion rate of 3CR12 measured by an electrode in cold water (CSIR).

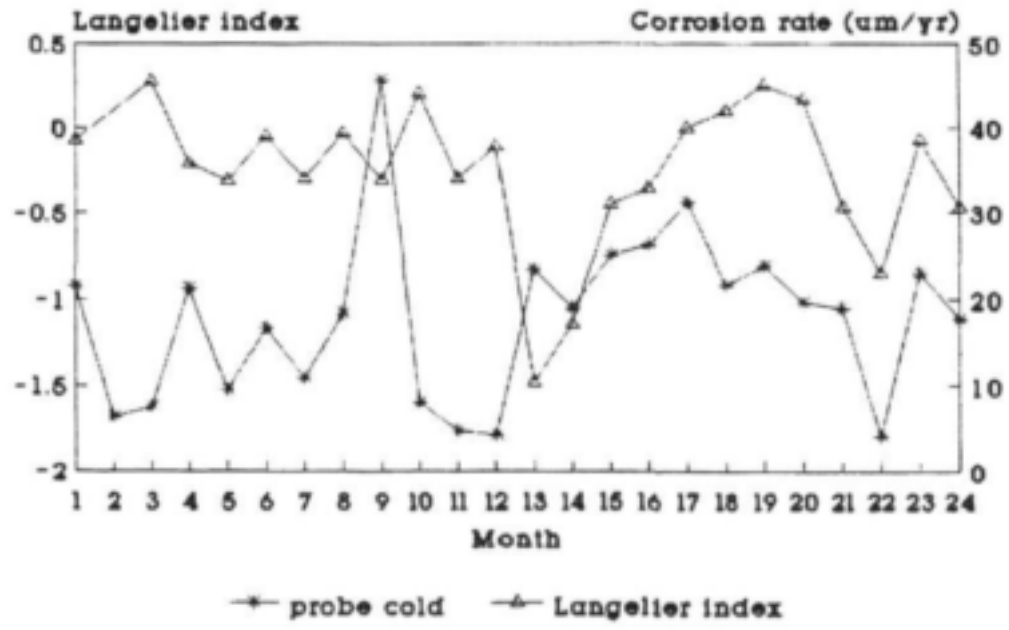

Figure 106. Langelier index versus corrosion rate of 3CR12 measured by a probe in cold water (CSIR).

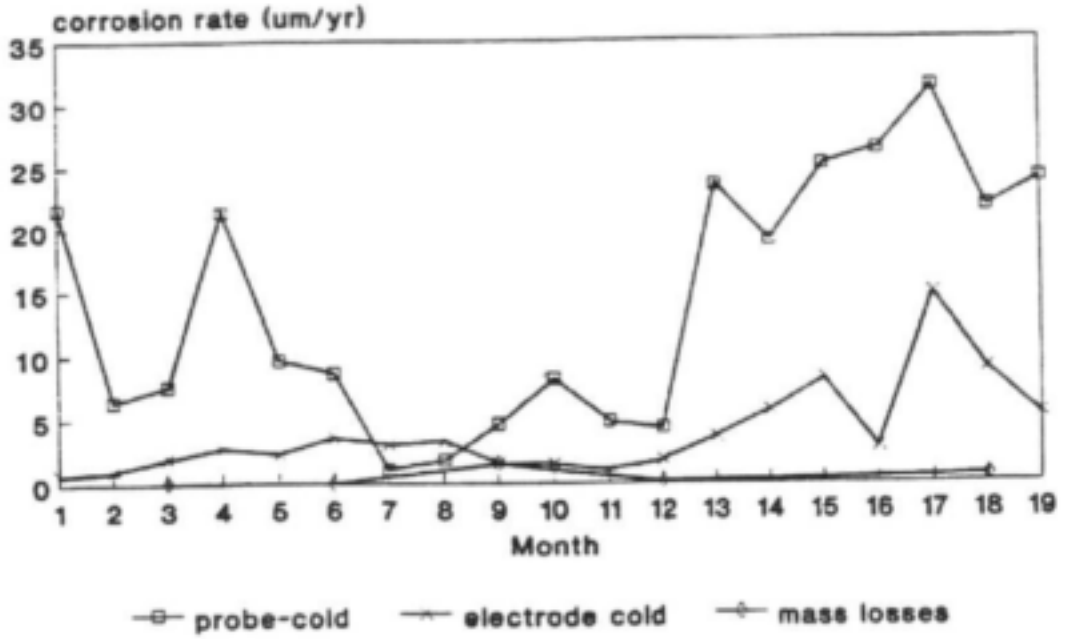

Figure 107. Comparison of the corrosion rates of 3CR12 obtained by different techniques in cold water (CSIR).

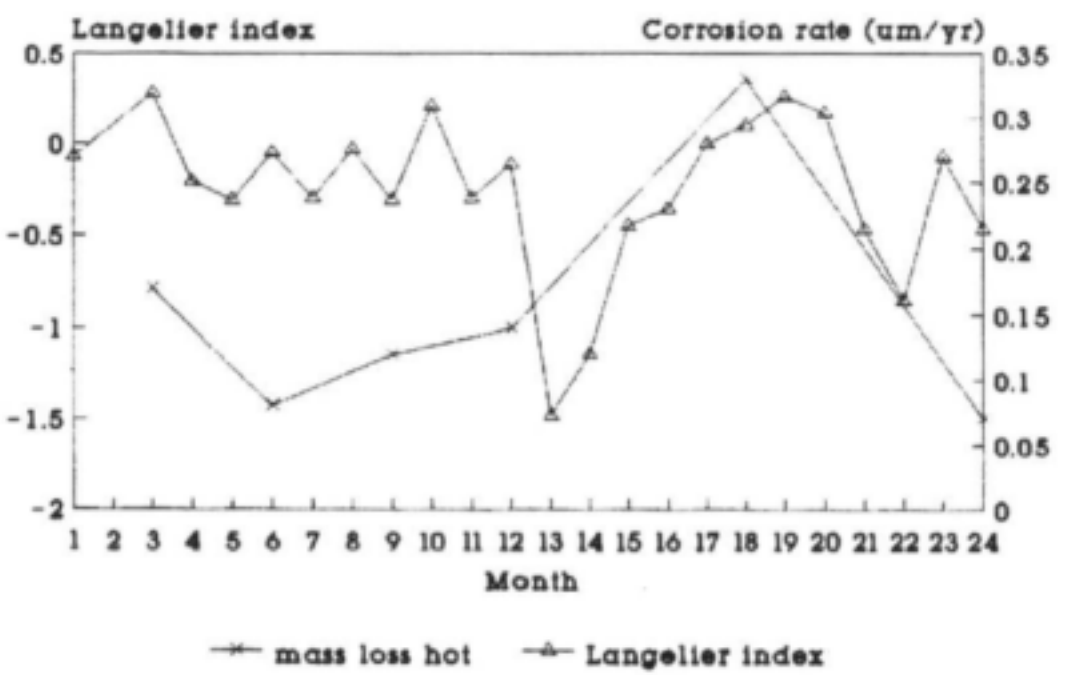

Figure 108. Langelier index versus corrosion rate of 3CR12 measured by 3-monthly mass loss in hot water (CSIR).

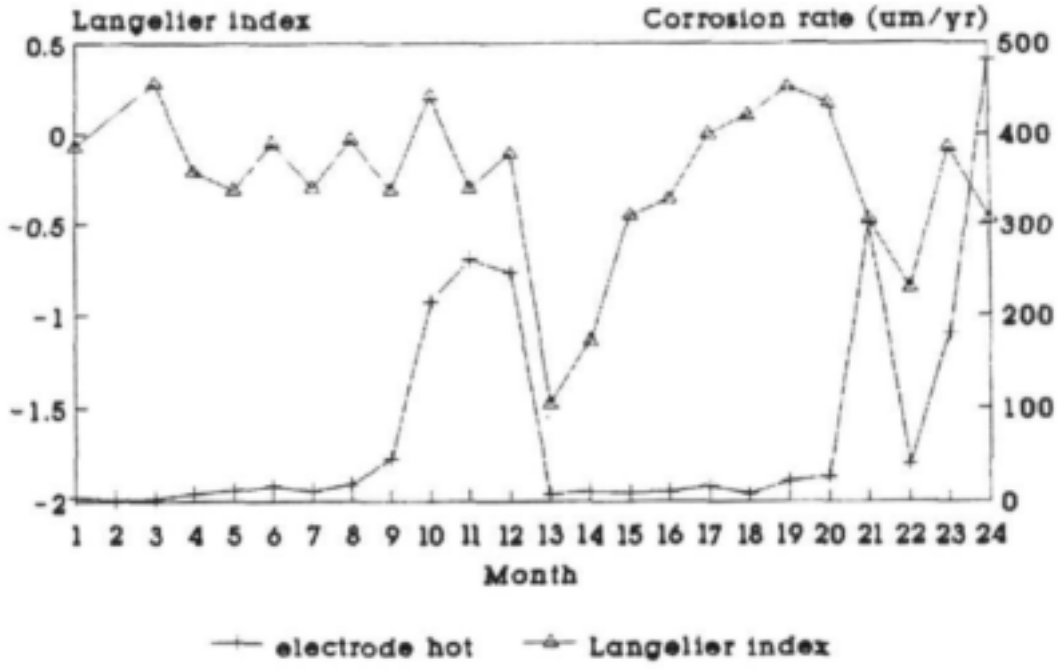

Figure 109. Langelier index versus corrosion rate of 3CR12 measured by an electrode in hot water (CSIR).

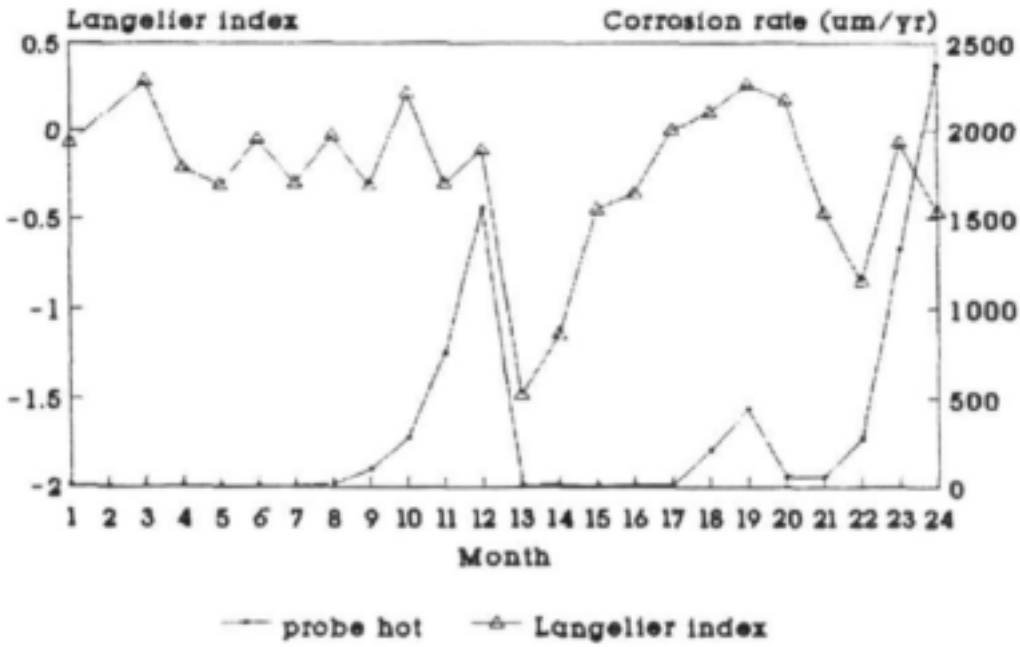

Figure 110. Langelier index versus corrosion rate of 3CR12 measured by a probe in hot water (CSIR).

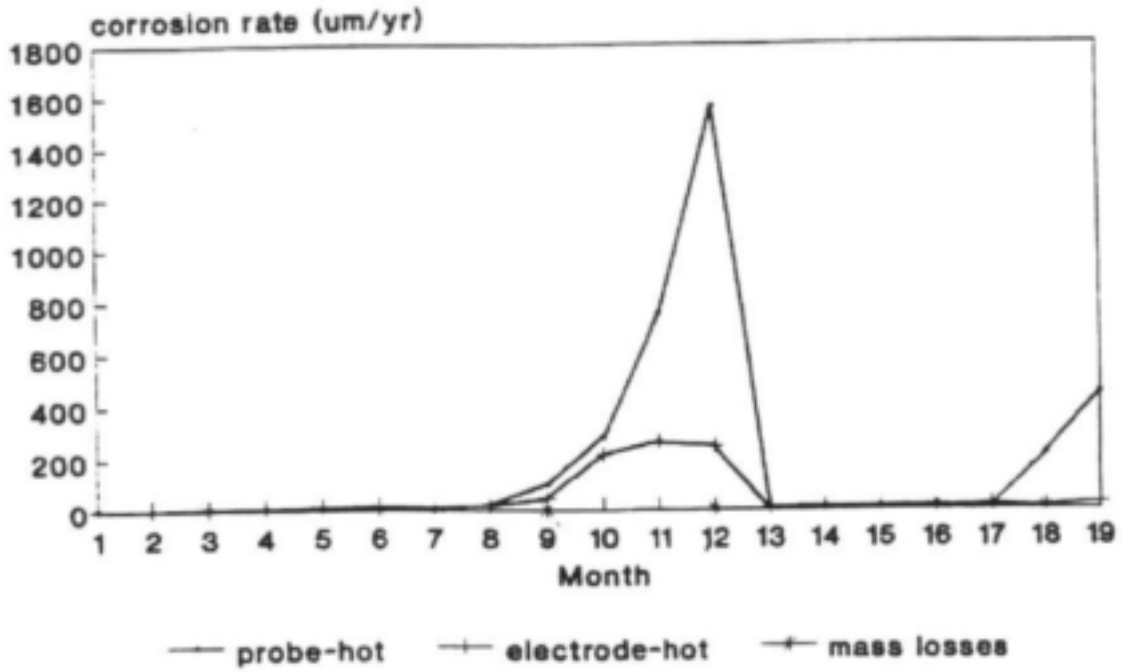

Figure 111. Comparison of the corrosion rates of 3CR12 obtained by different techniques in hot water (CSIR).

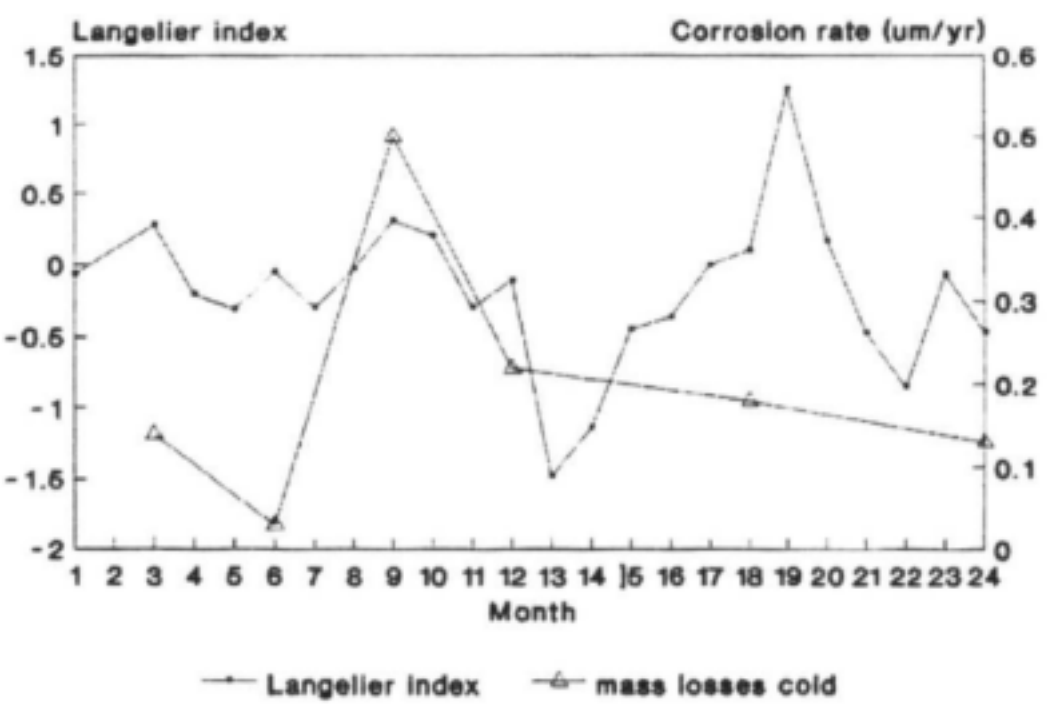

Figure 112. Langelier index versus corrosion rate of 304 measured by 3-monthly mass loss in cold water (CSIR).

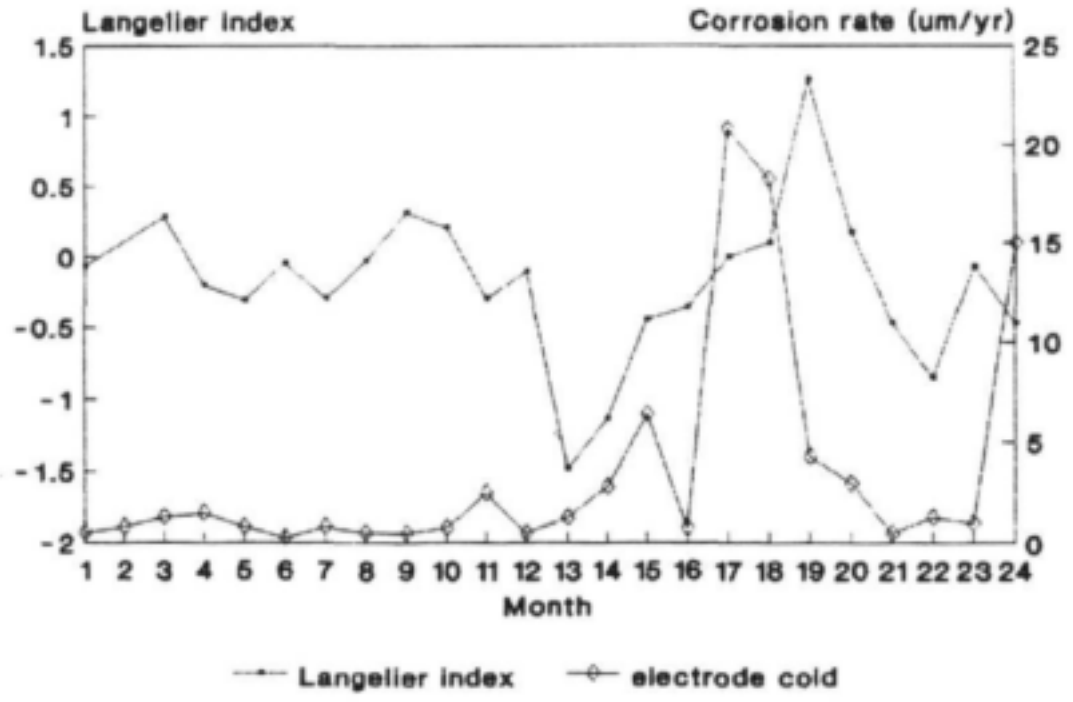

Figure 113. Langelier index versus corrosion rate of 304 measured by an electrode in cold water (CSIR).

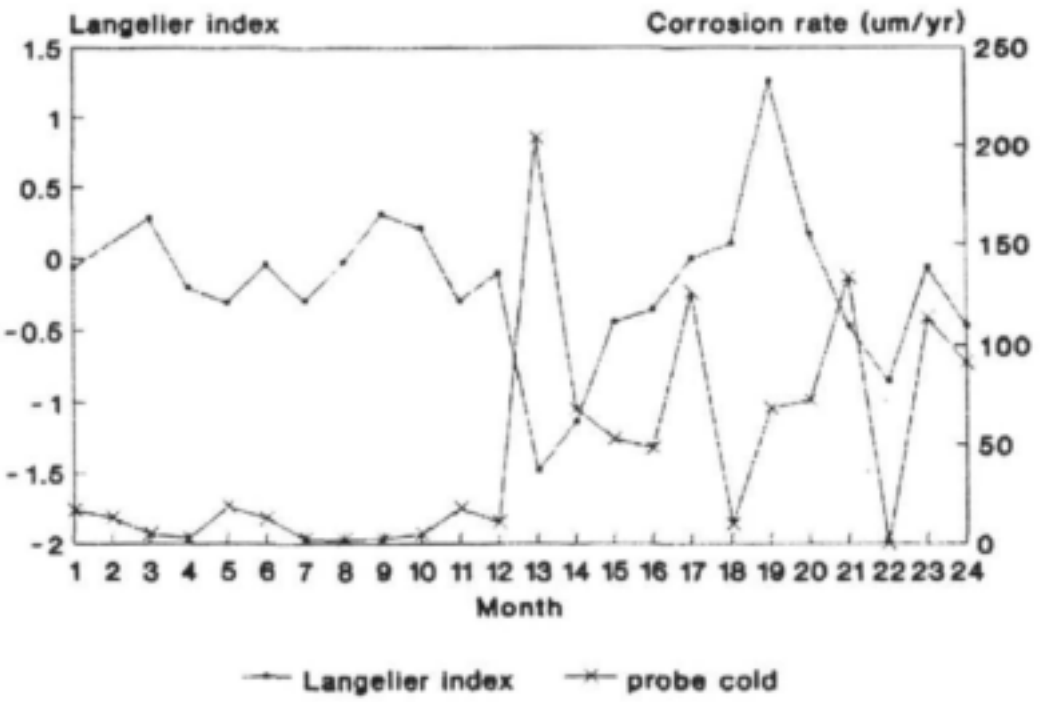

Figure 114. Langelier index versus corrosion rate of 304 measured by a probe in cold water (CSIR).

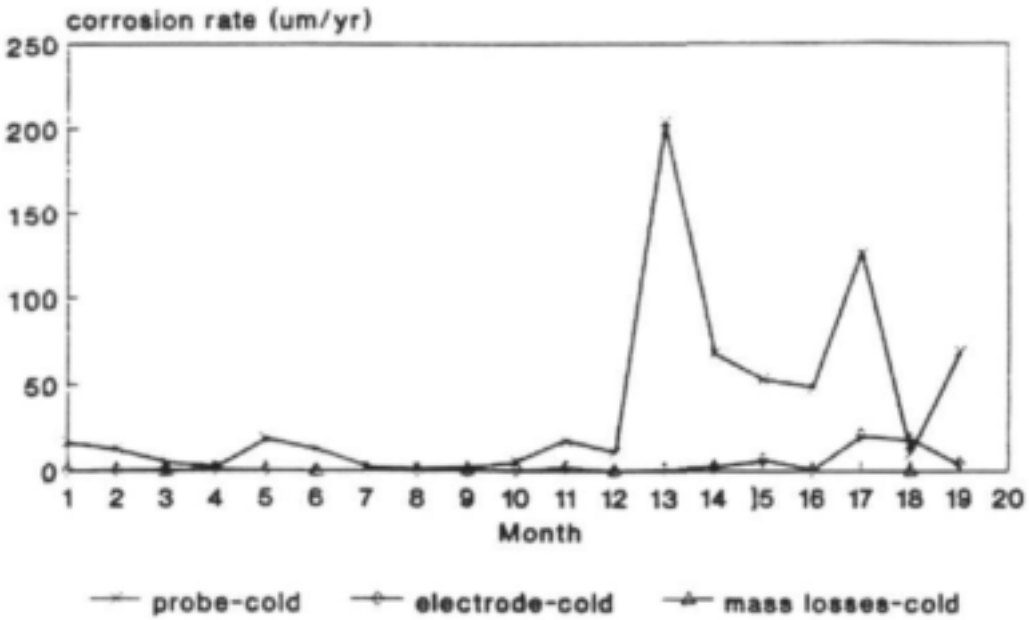

Figure 115. Comparison of the corrosion rates of 304 obtained by different techniques in cold water (CSIR).

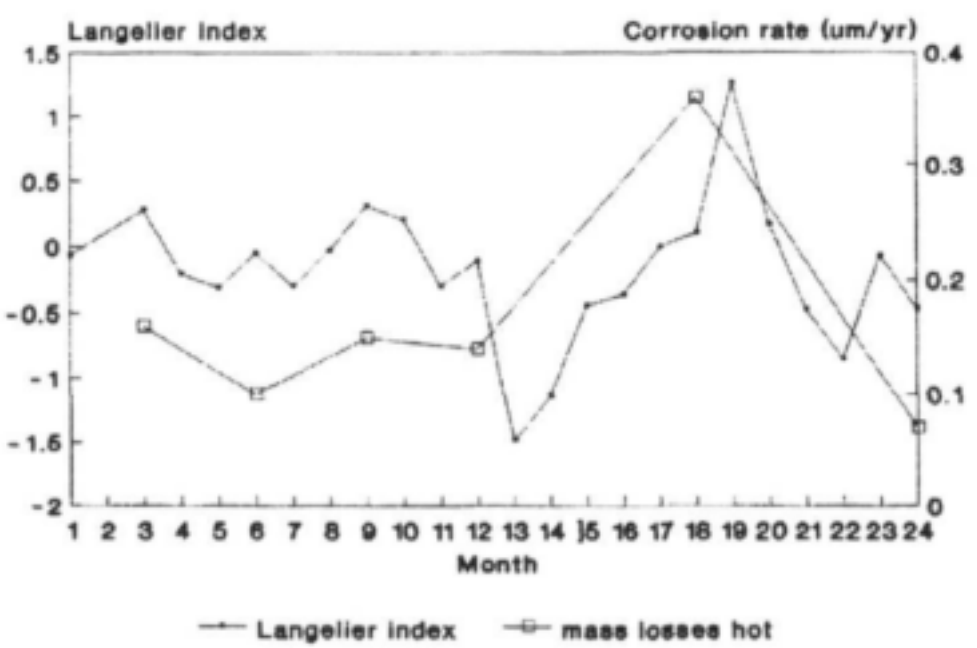

Figure 116. Langelier index versus corrosion rate of 304 measured by 3-monthly mass loss in hot water (CSIR).

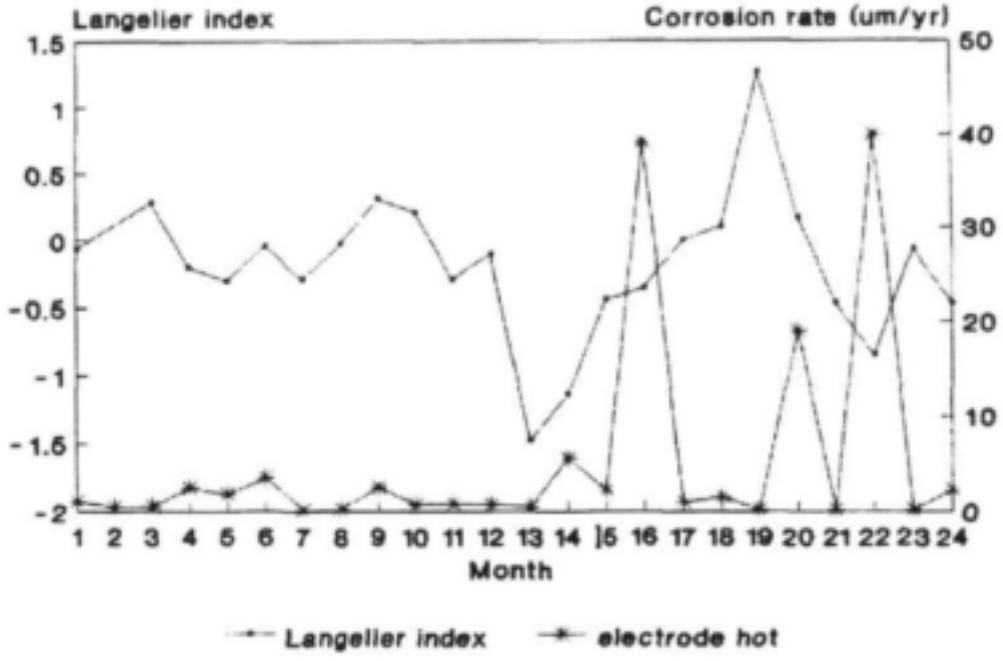

Figure 117. Langelier index versus corrosion rate of 304 measured by an electrode in hot water (CSIR).

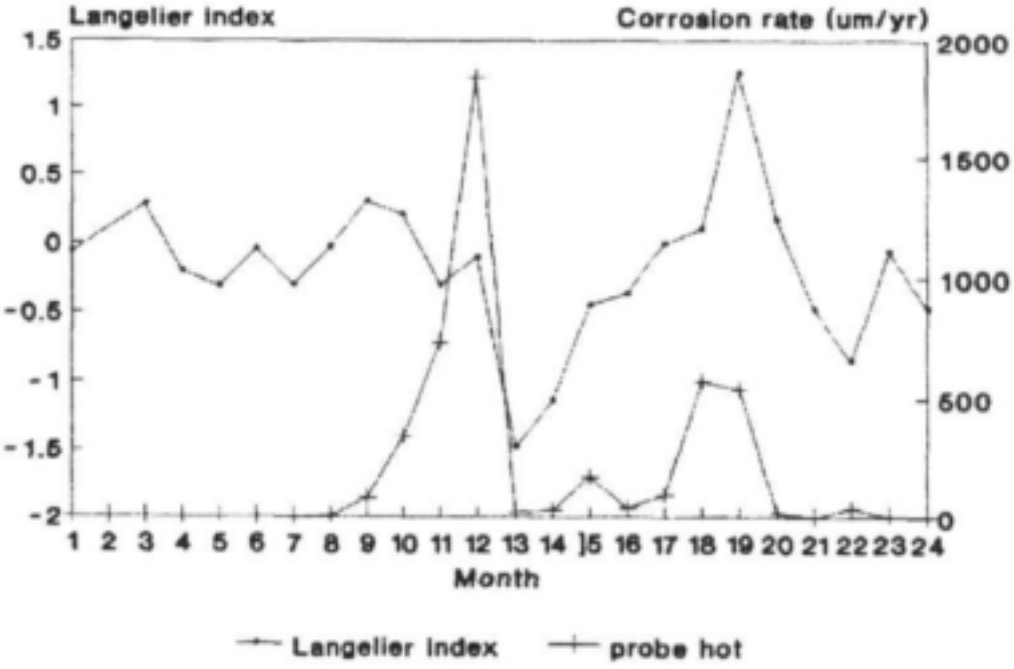

Figure 118. Langelier index versus corrosion rate of 304 measured by a probe in hot water (CSIR).

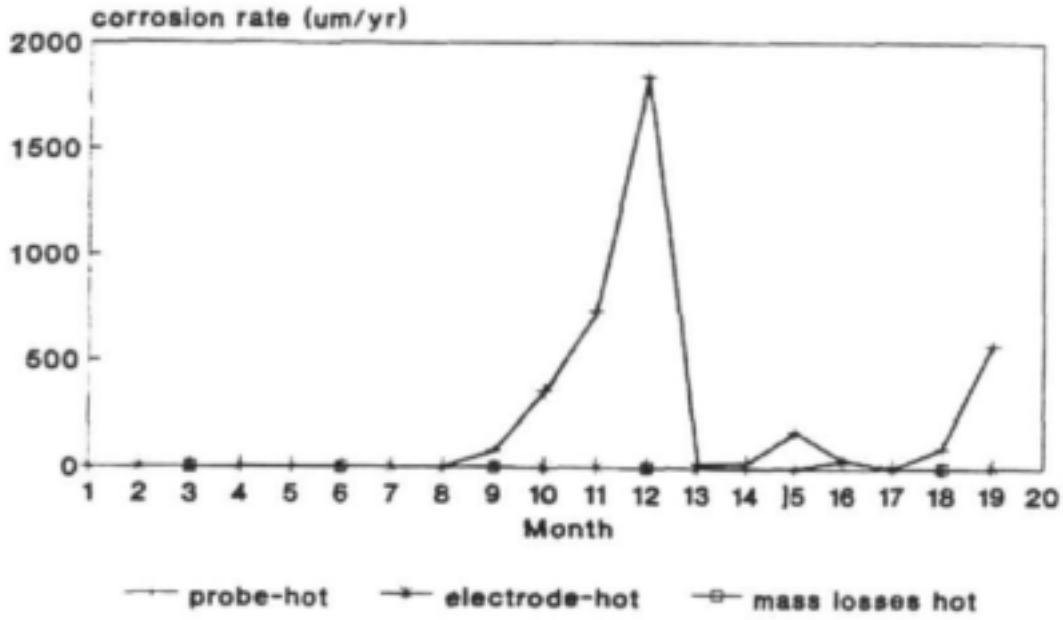

Figure 119. Comparison of the corrosion rates of 304 obtained by different techniques in hot water (CSIR).

Appendix 5. X-Ray diffraction results

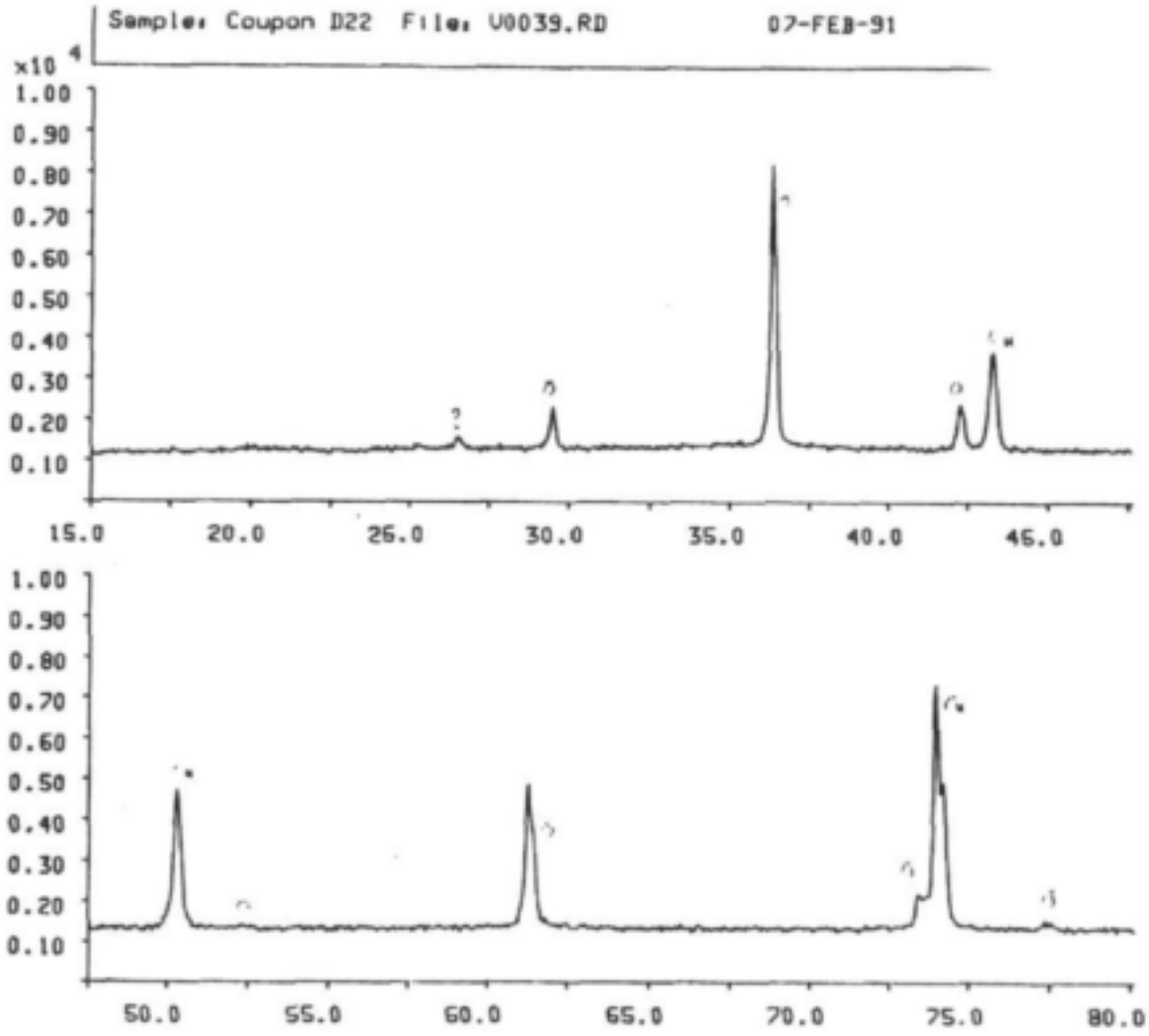

Figure 120. X-Ray diffractogram of copper at Vaal Dam.

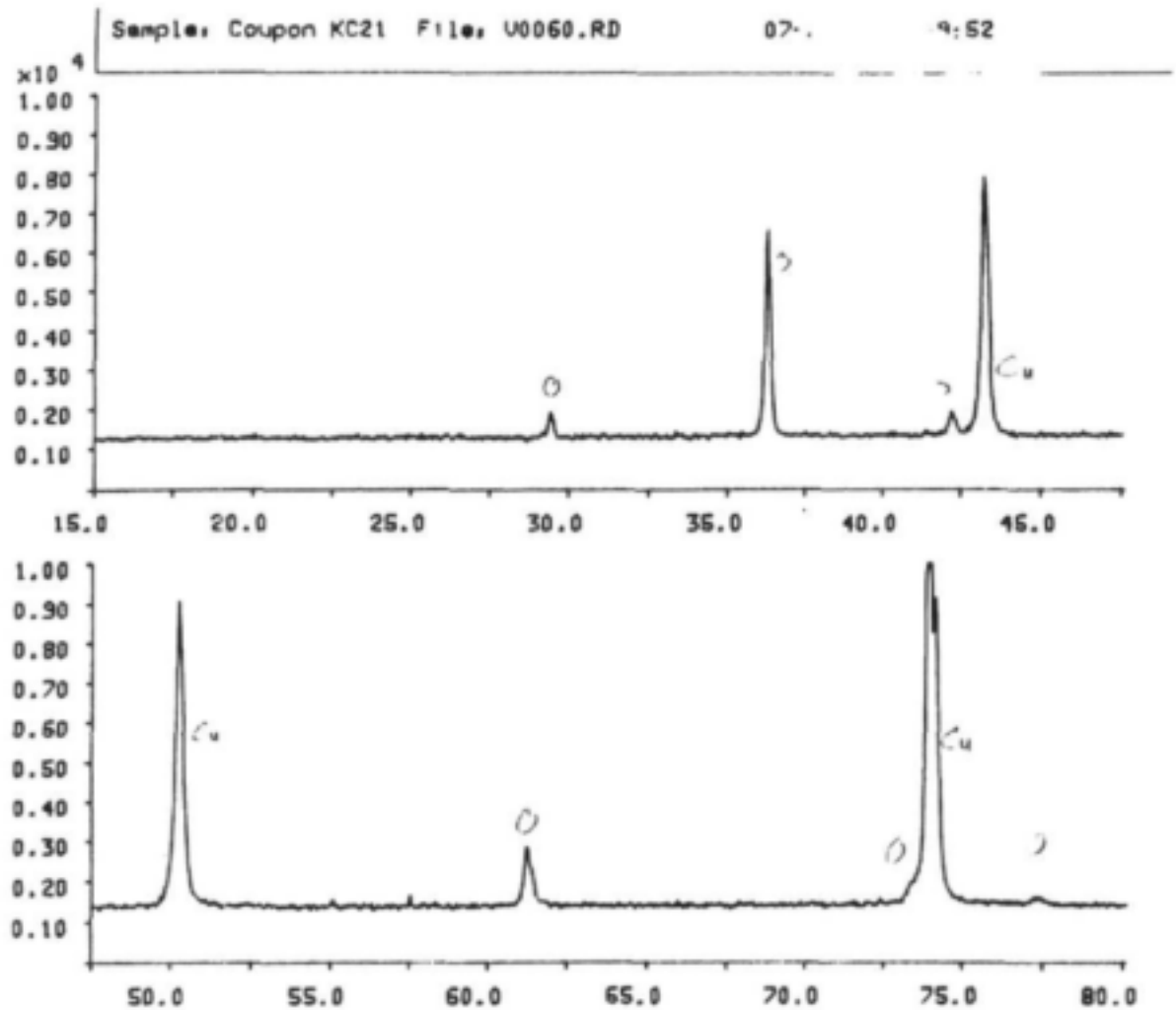

Figure 121. X-Ray diffractogram of copper in cold water at Klerksdorp.

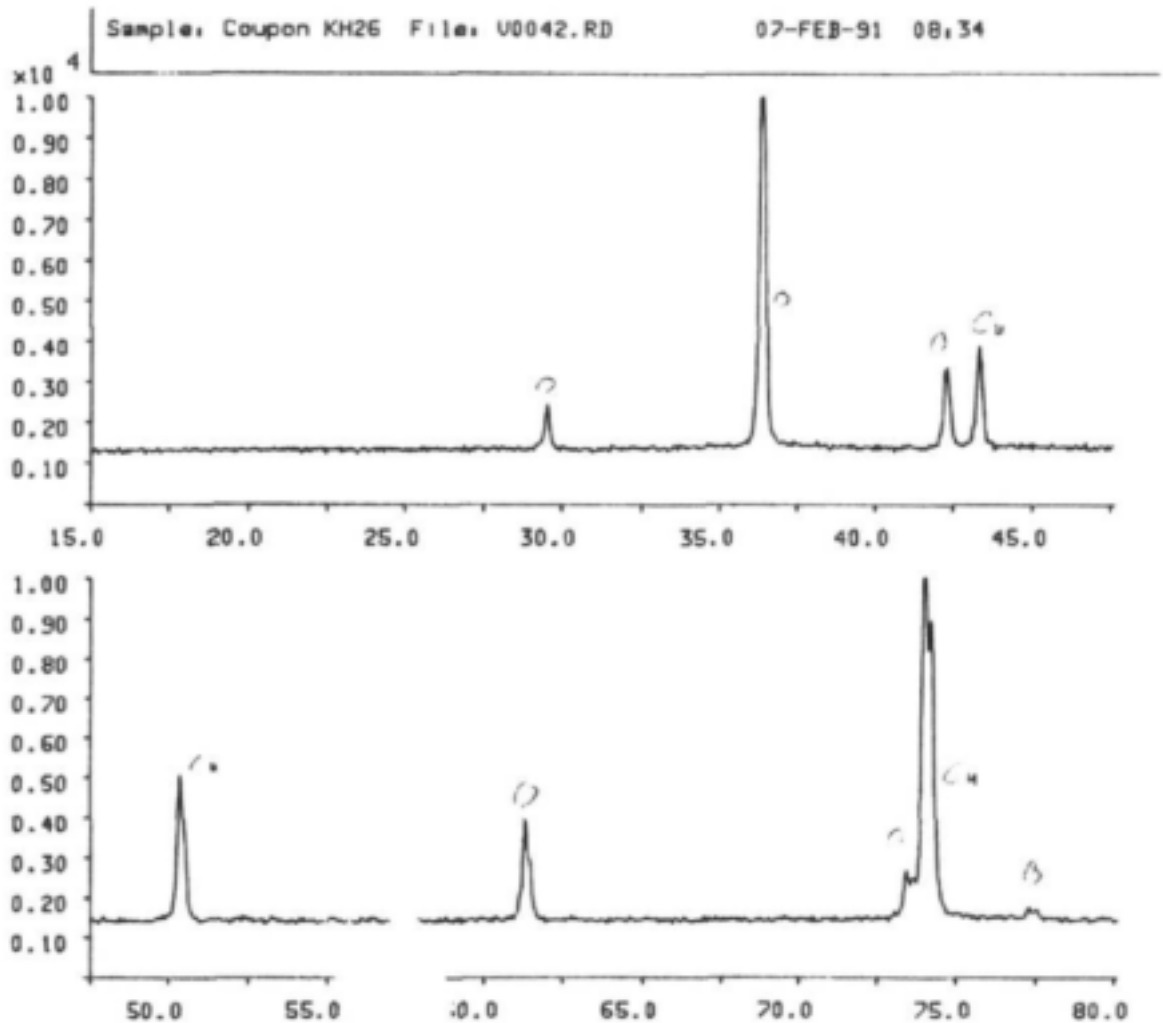

Figure 122. X-Ray diffractogram of copper in hot water at Klerksdorp.

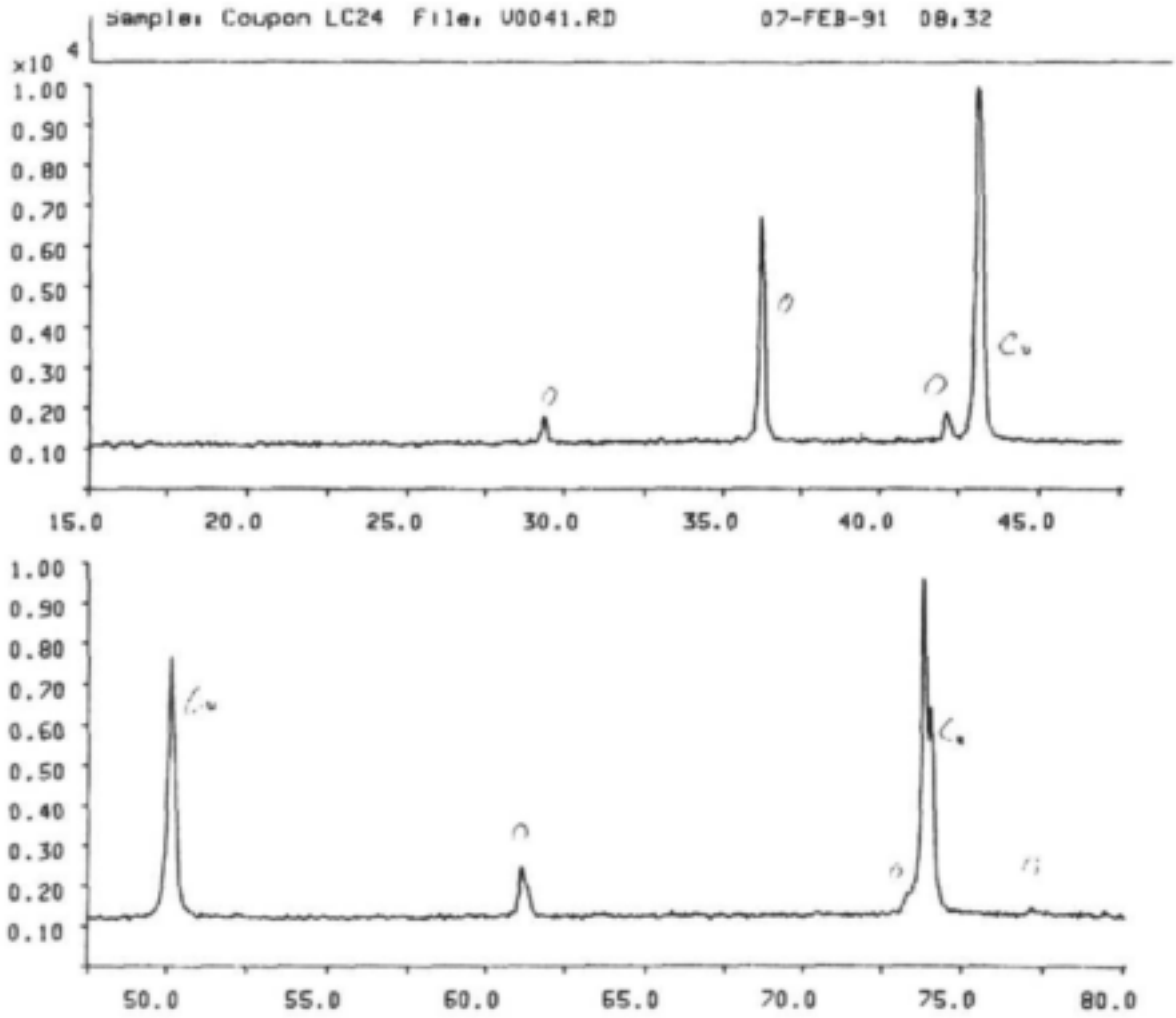

Figure 123. X-Ray diffractogram of copper in cold water at CSIR.

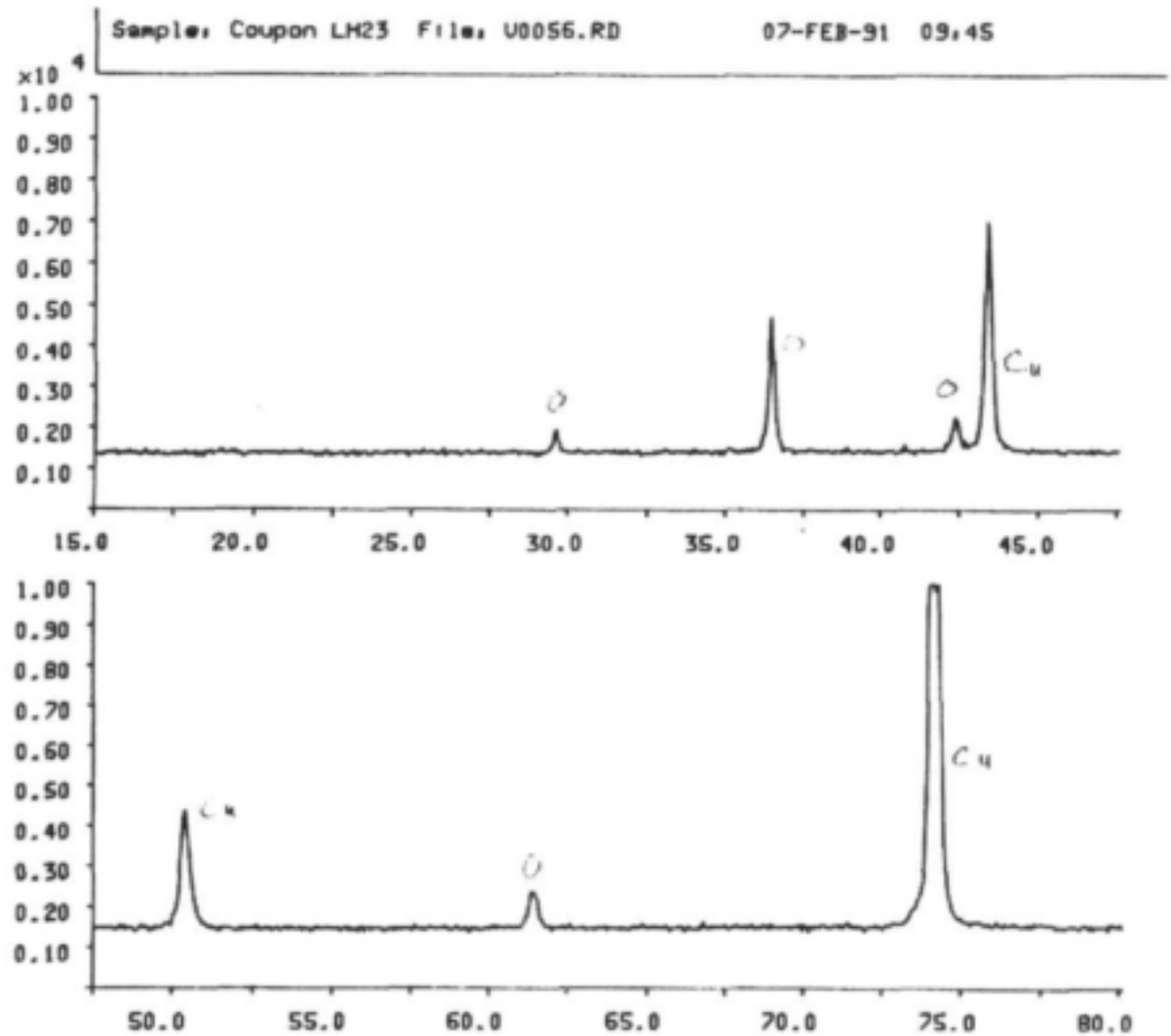

Figure 124. X-Ray diffractogram of copper in hot water at CSIR.

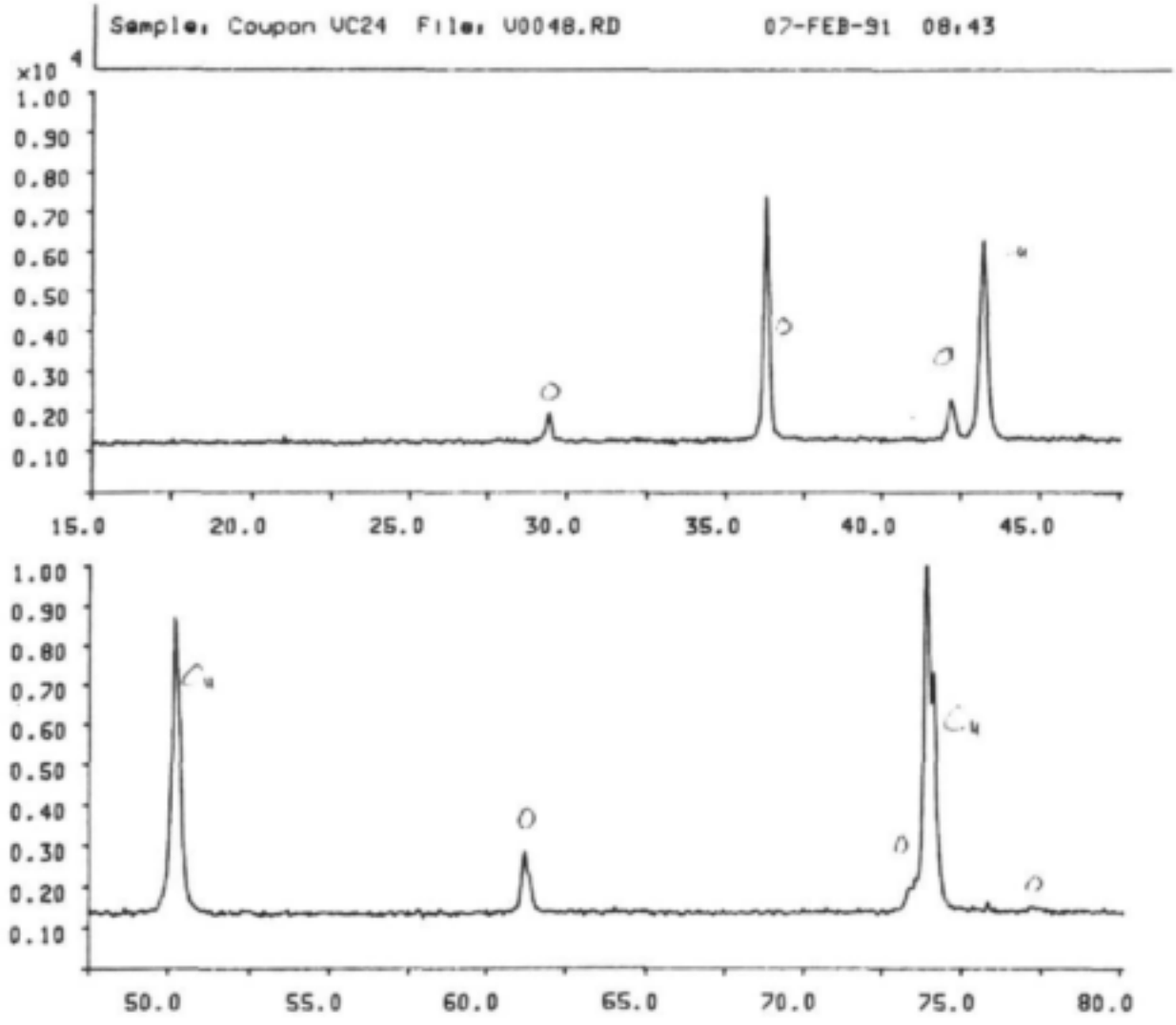

Figure 125. X-Ray diffractogram of copper in cold water at Vereeniging.

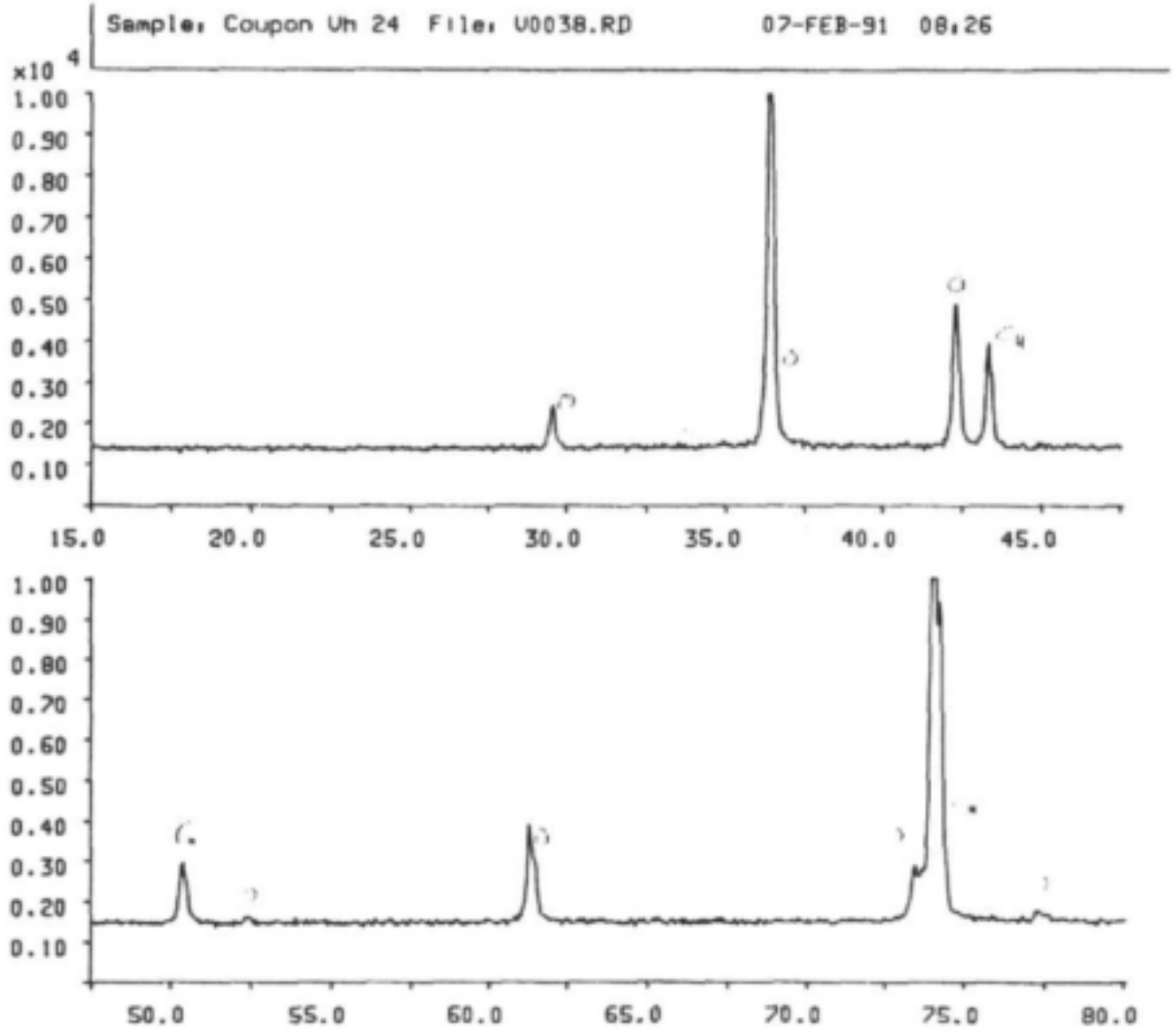

Figure 126. X-Ray diffractogram of copper in hot water at Vereeniging.

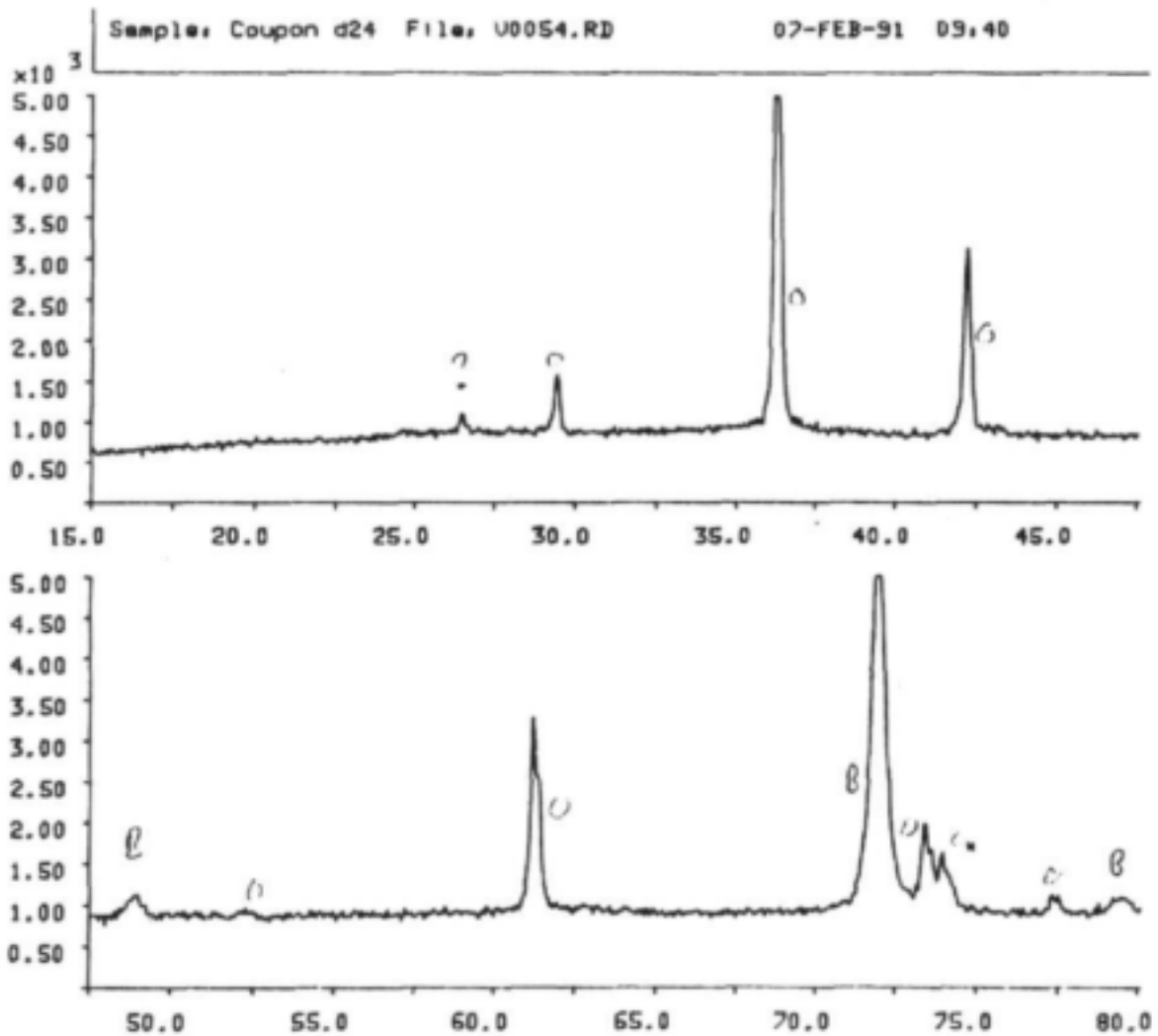

Figure 127. X-Ray diffractogram of brass at Vaal Dam.

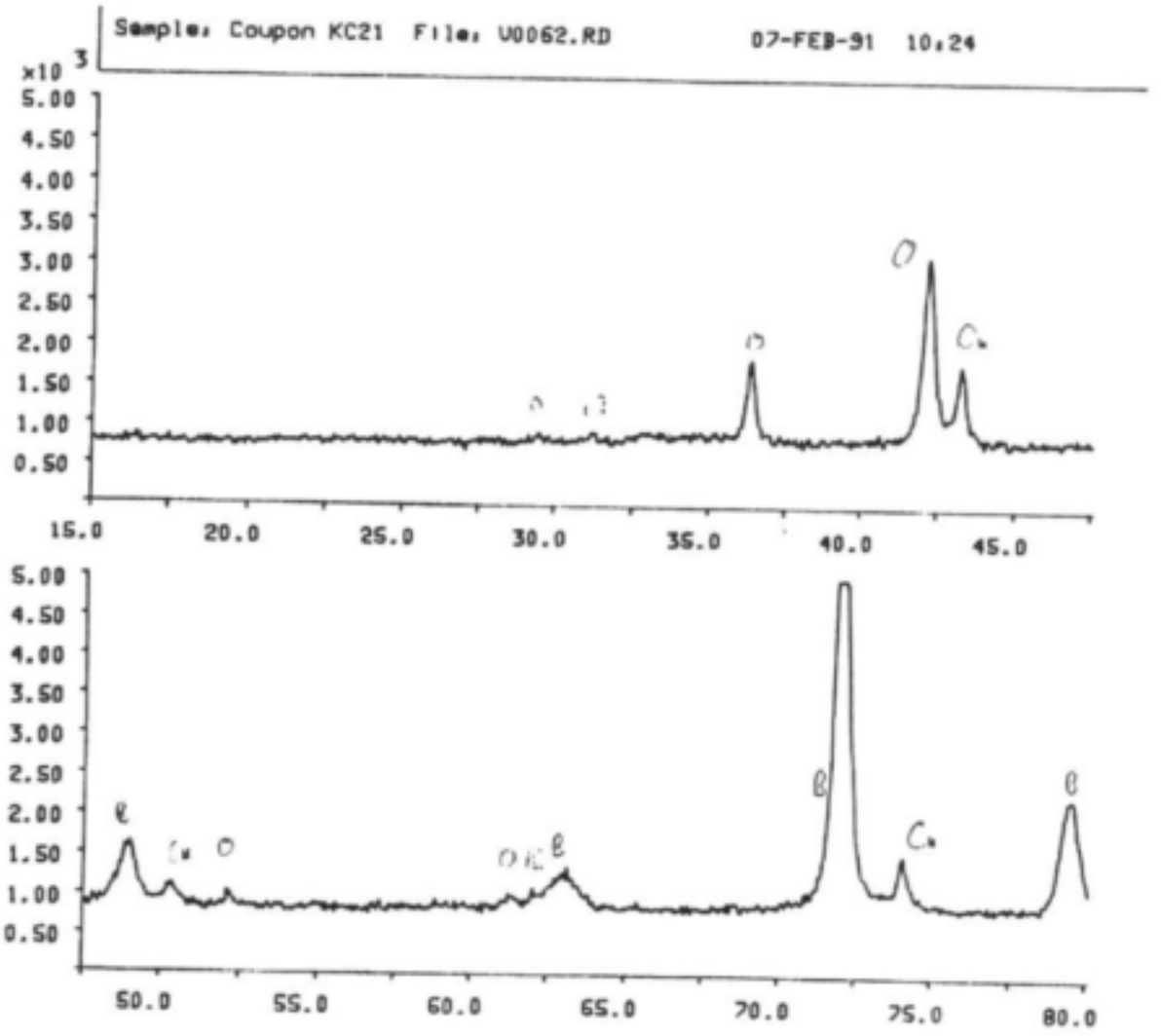

Figure 128. X-Ray diffractogram of brass in cold water at Klerksdorp.

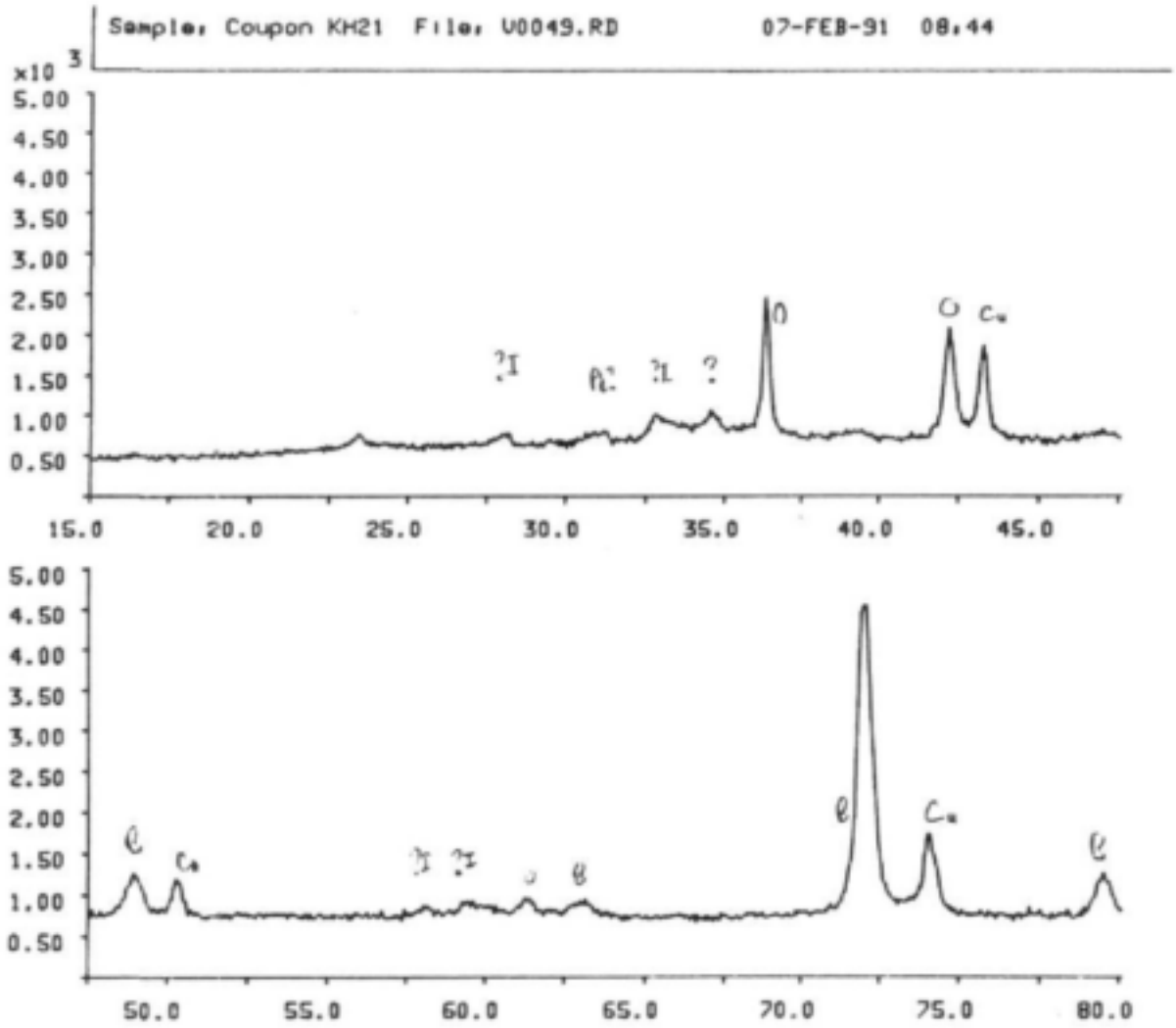

Figure 129. X-Ray diffractogram of brass in hot water at Klerksdorp.

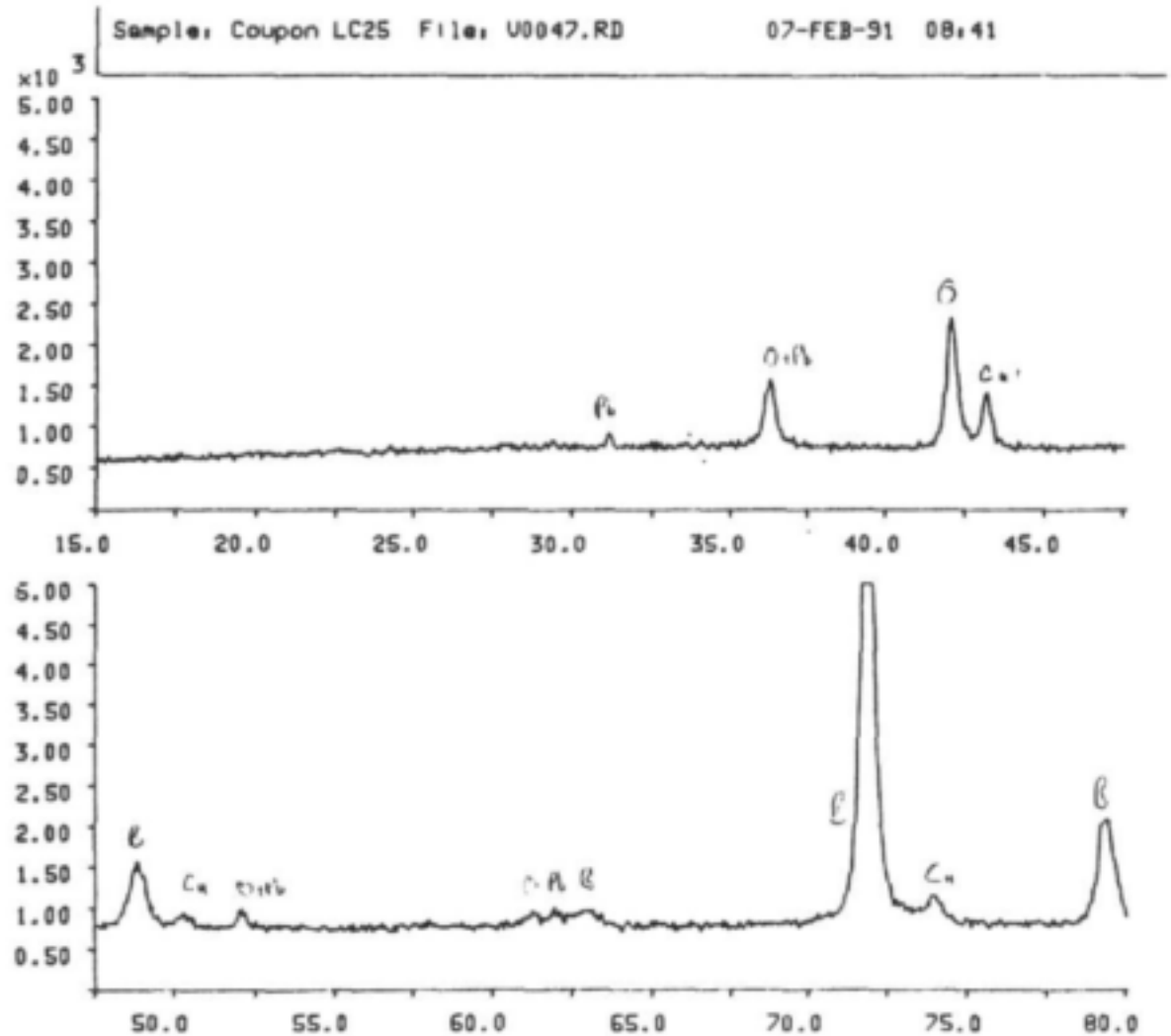

Figure 130. X-Ray diffractogram of brass in cold water at CSIR.

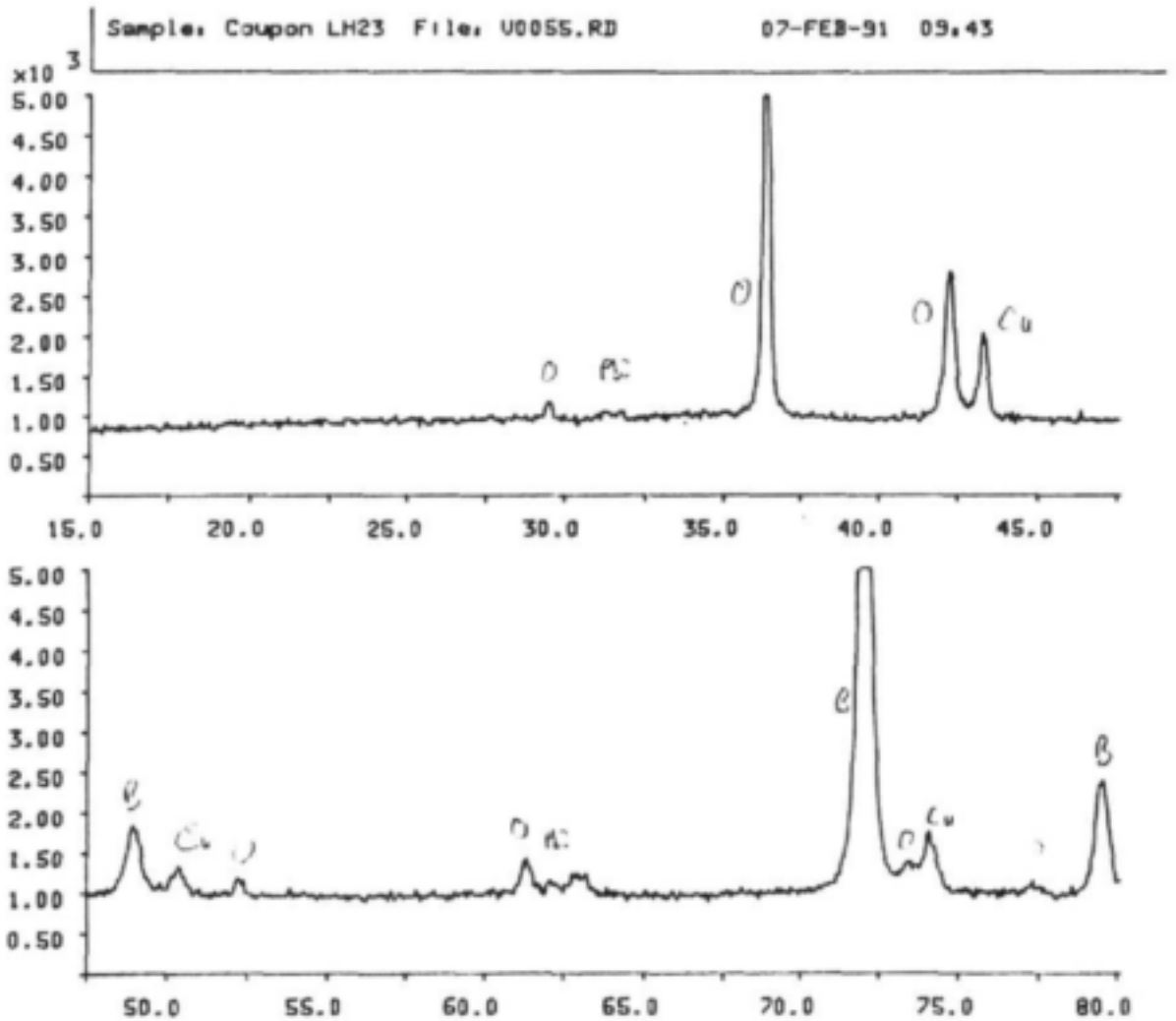

Figure 131. X-Ray diffractogram of brass in hot water at CSIR.

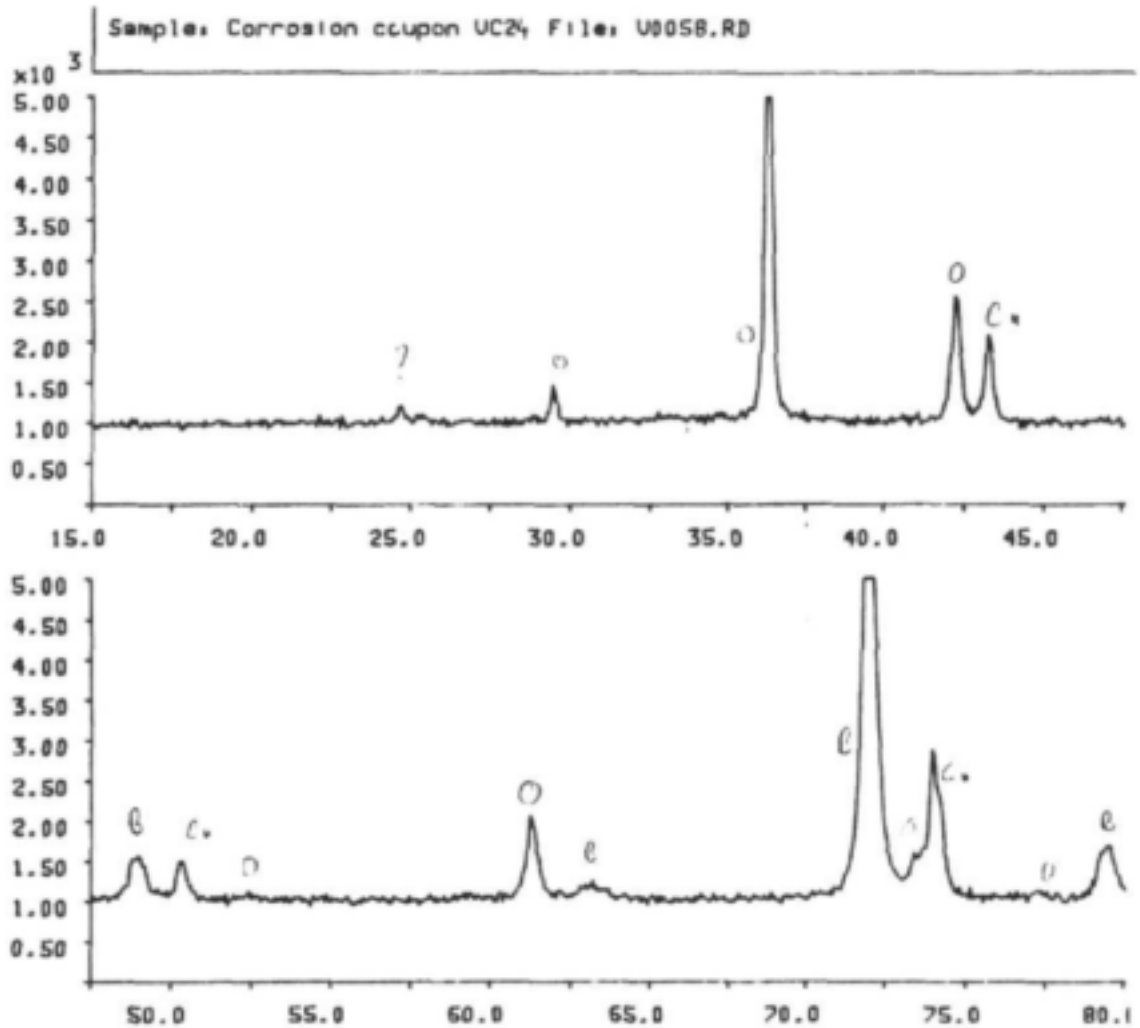

Figure 132. X-Ray diffractogram of brass in cold water at Vereeniging.

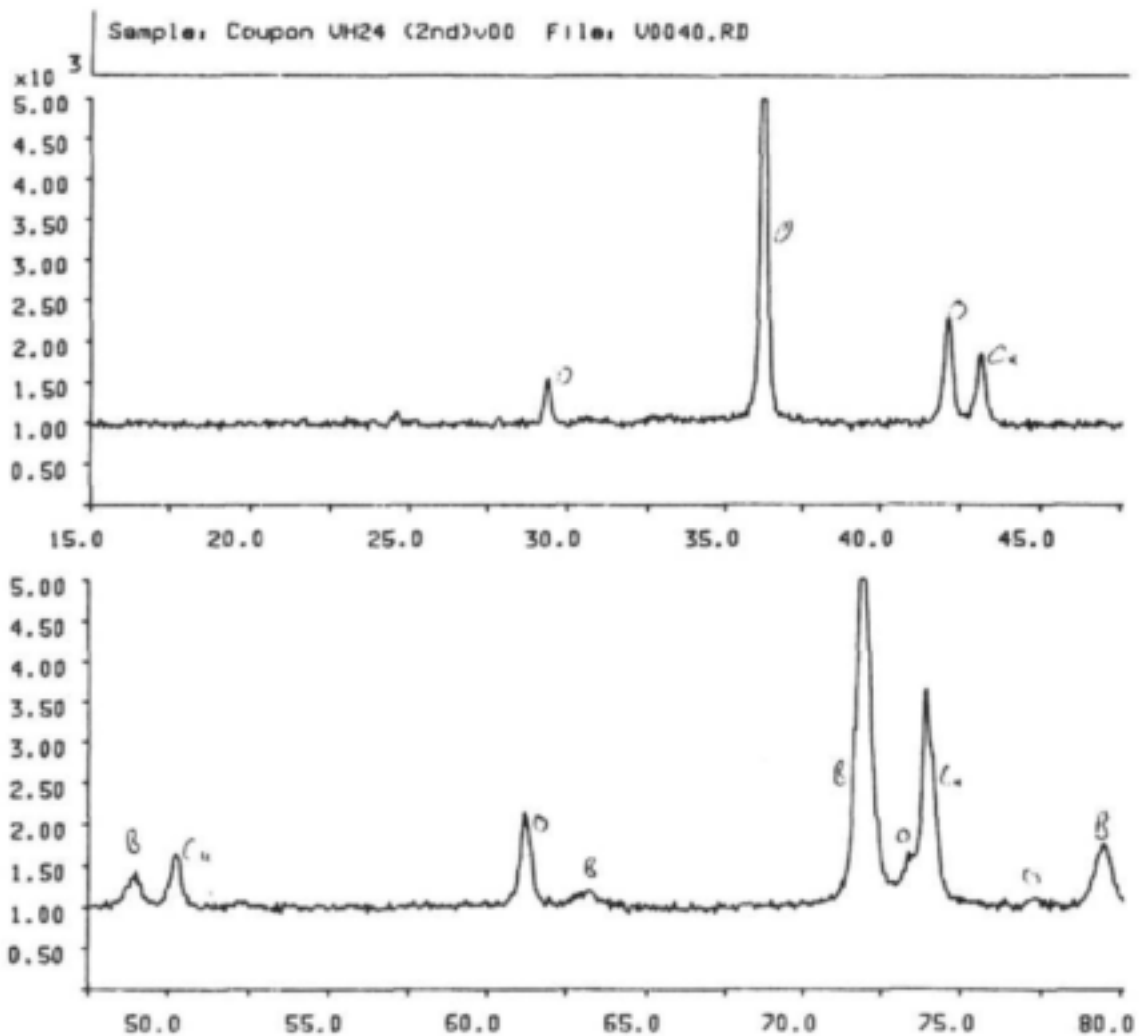

Figure 133. X-Ray diffractogram of brass in hot water at Vereeniging.

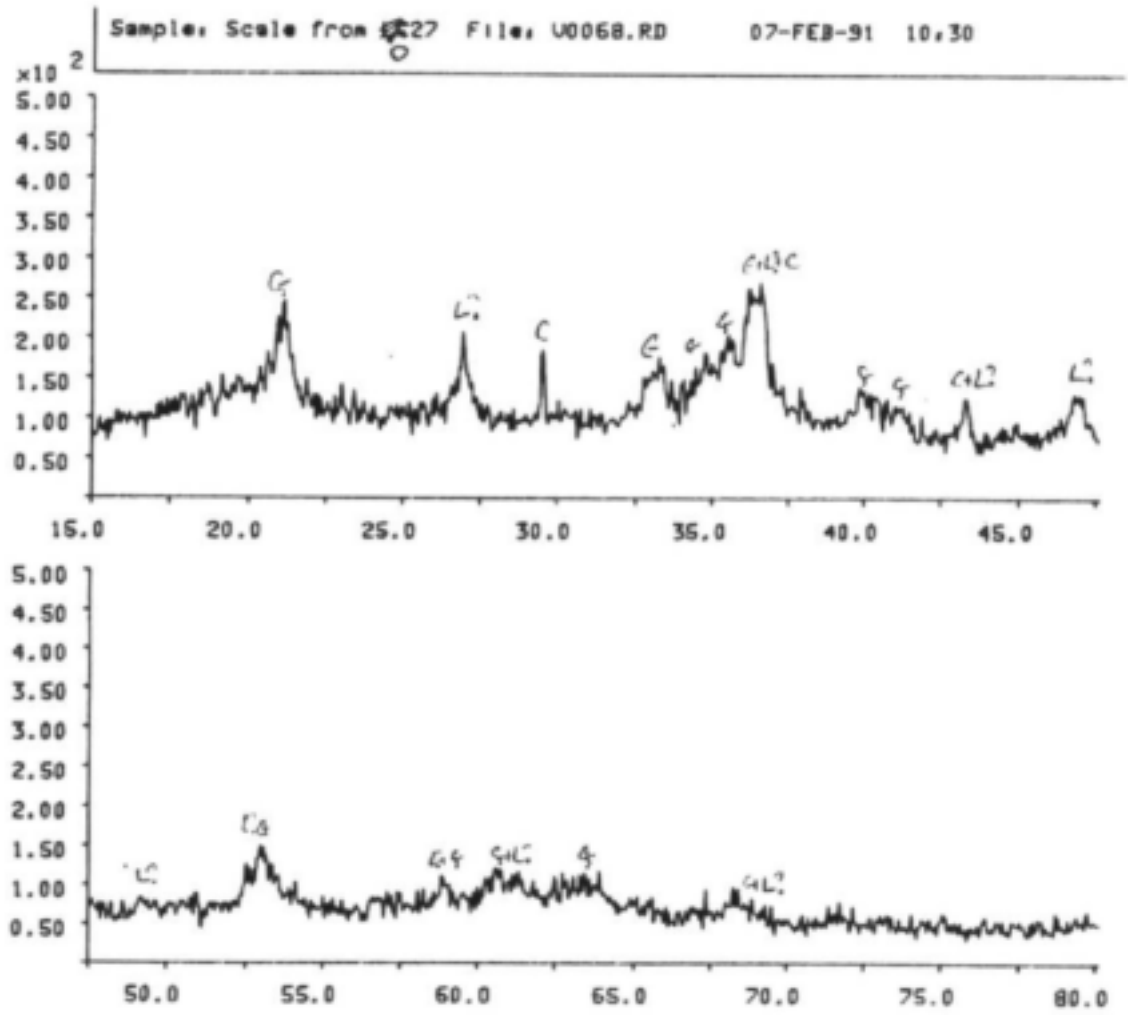

Figure 134. X-Ray diffractogram of mild steel at Vaal Dam.

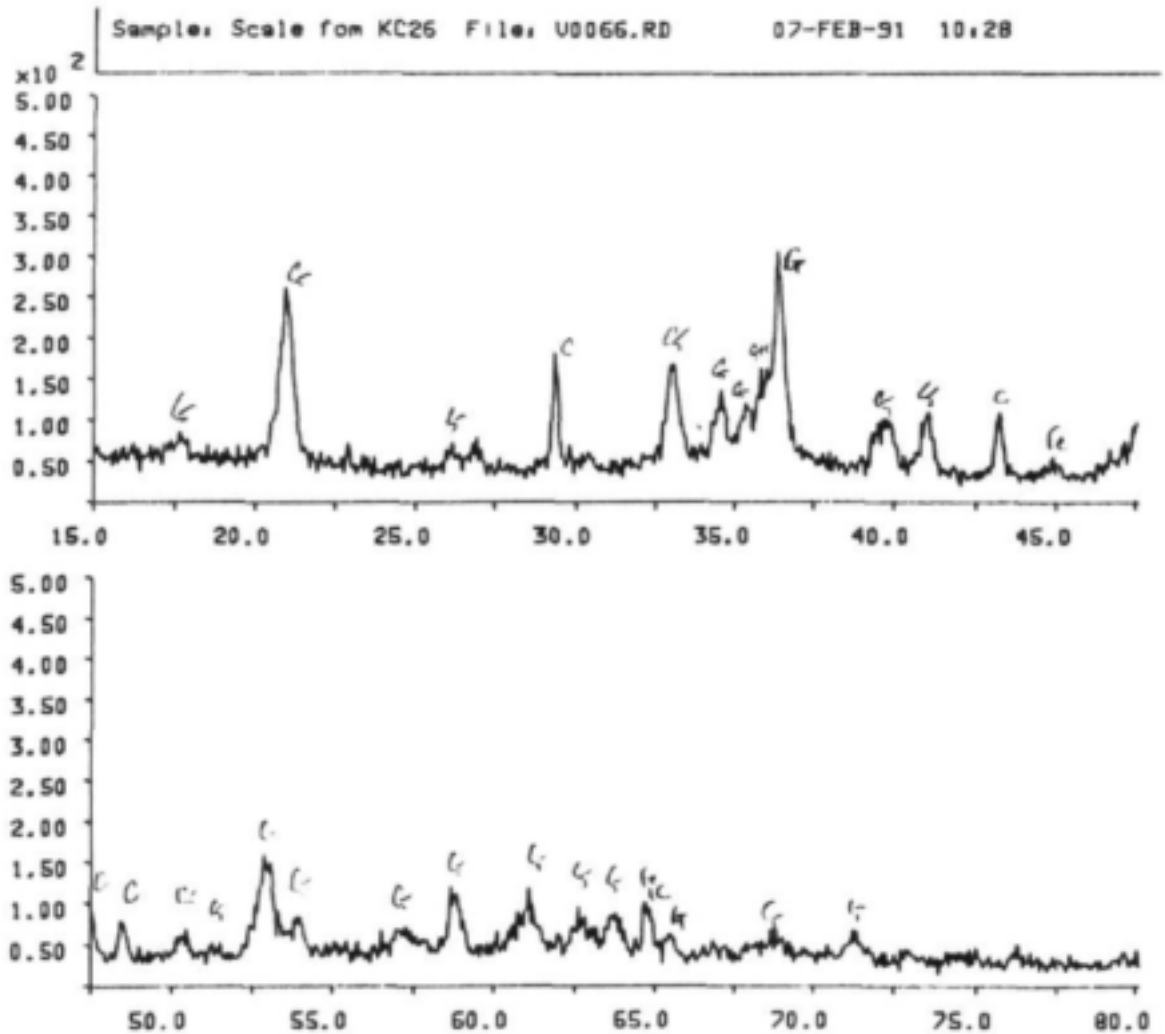

Figure 135. X-Ray diffractogram of mild steel in cold water at Klerksdorp.

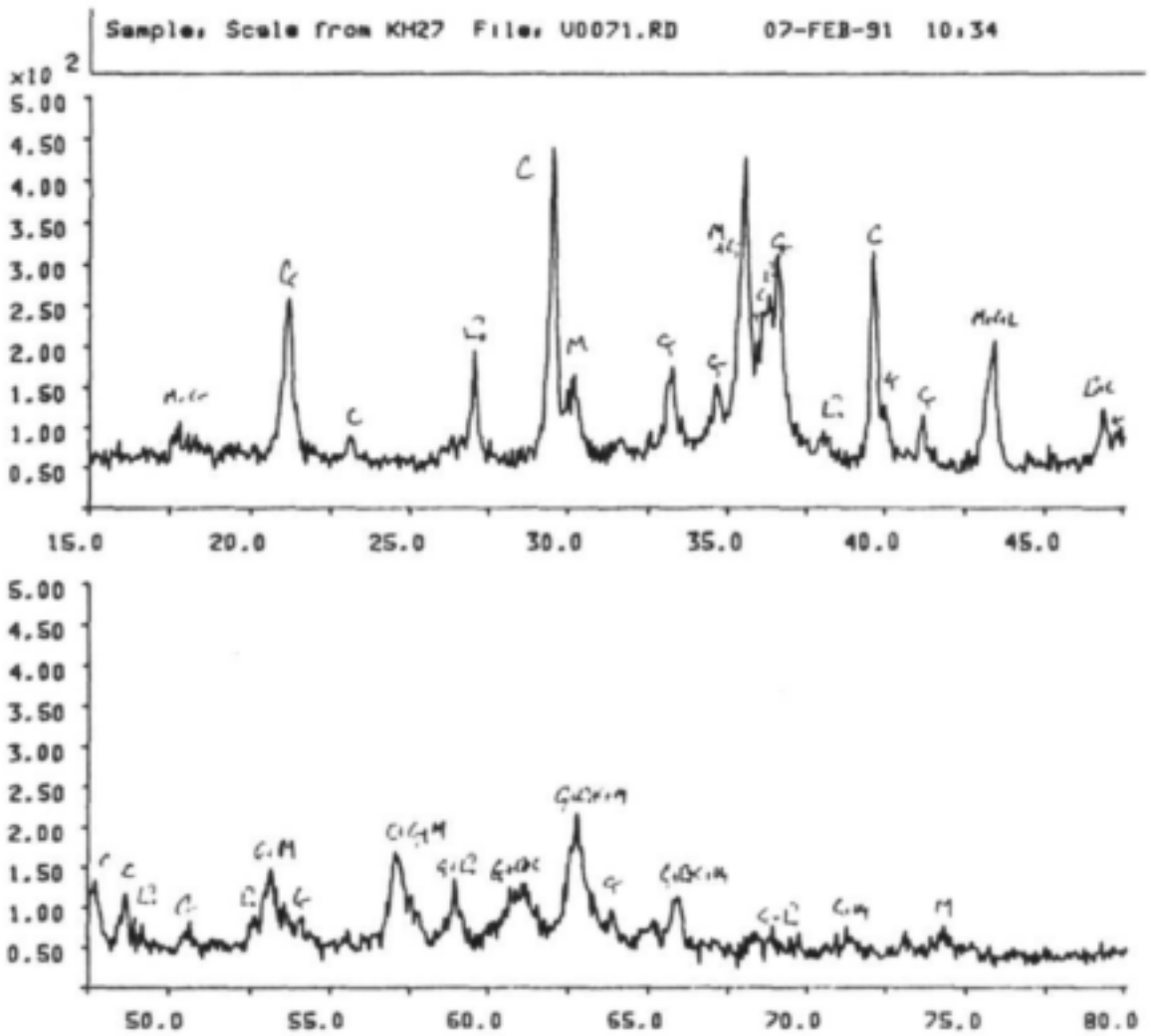

Figure 136. X-Ray diffractogram of mild steel in hot water at Klerksdorp.

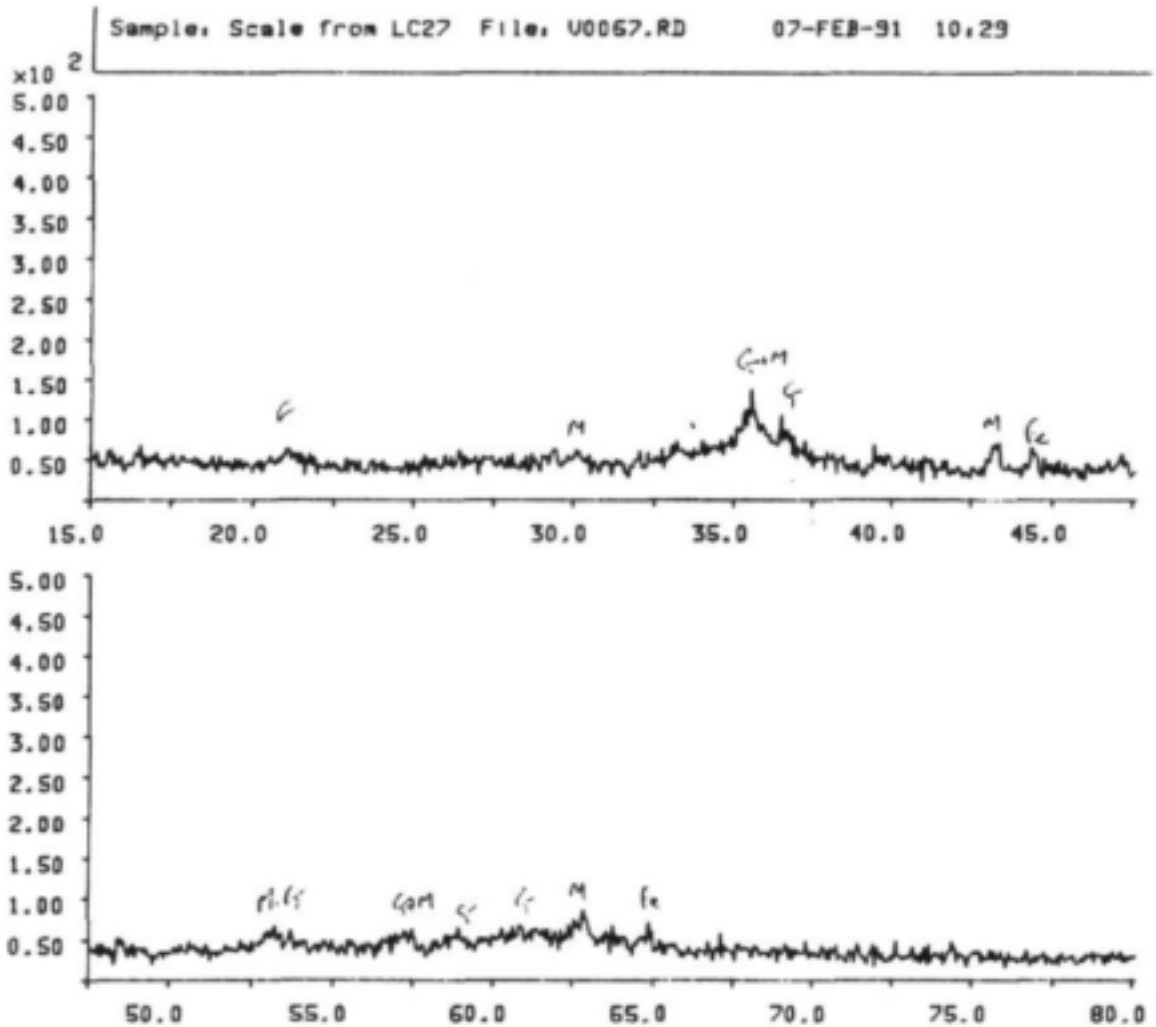

Figure 137. X-Ray diffractogram of mild steel in cold water at CSIR.

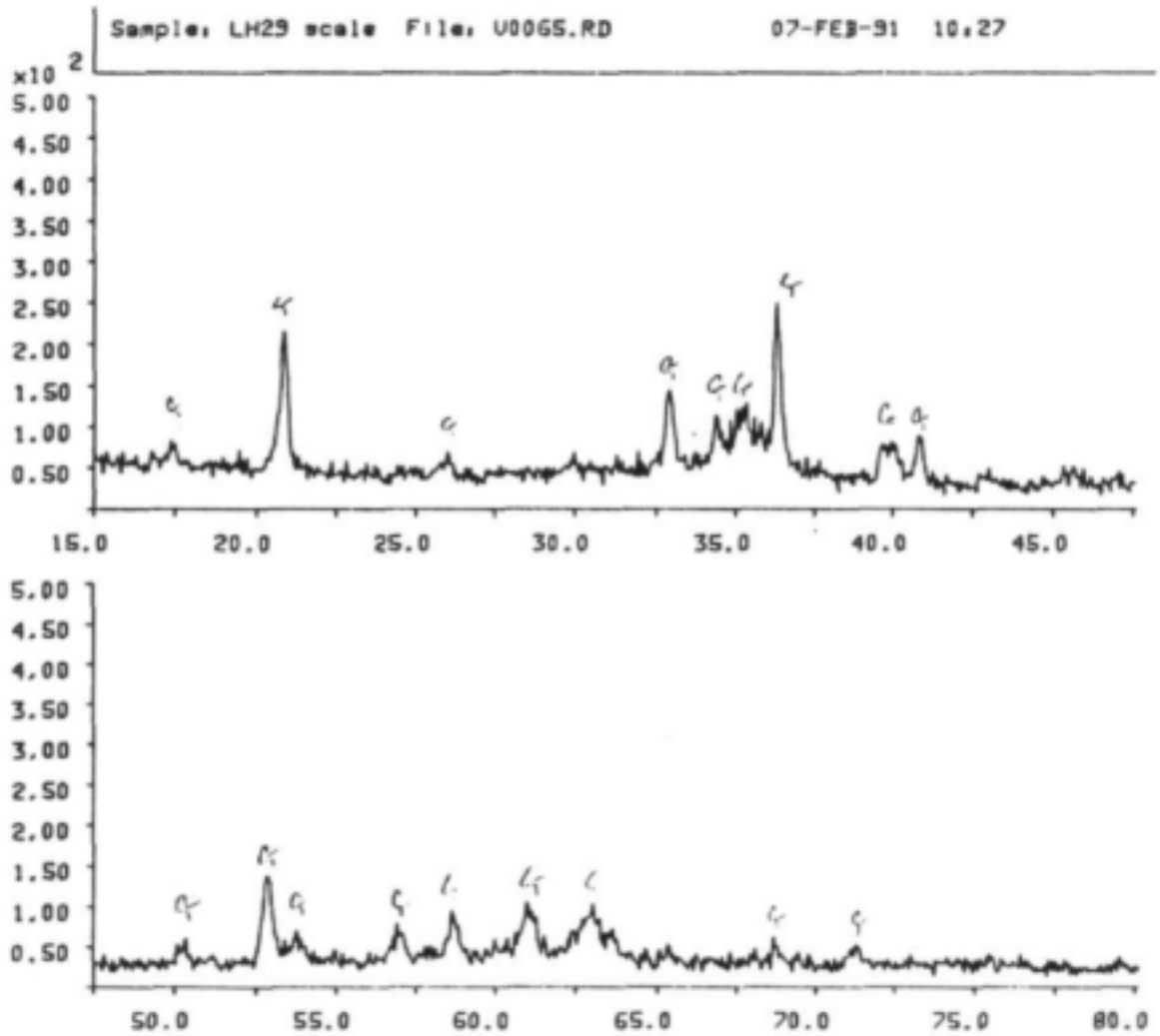

Figure 138. X-Ray diffractogram of mild steel in hot water at CSIR.

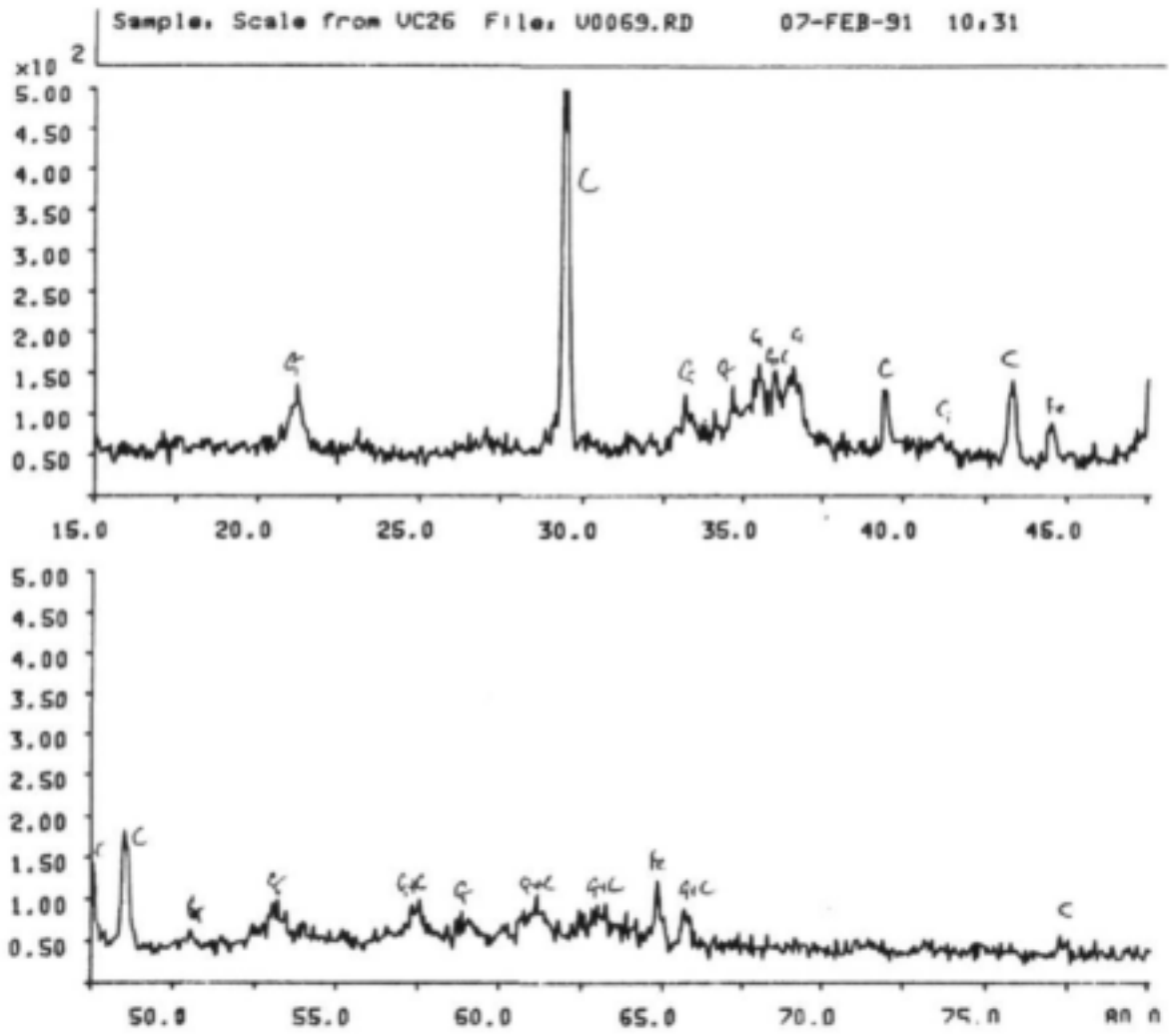

Figure 139. X-Ray diffractogram of mild steel in cold water at Vereeniging.

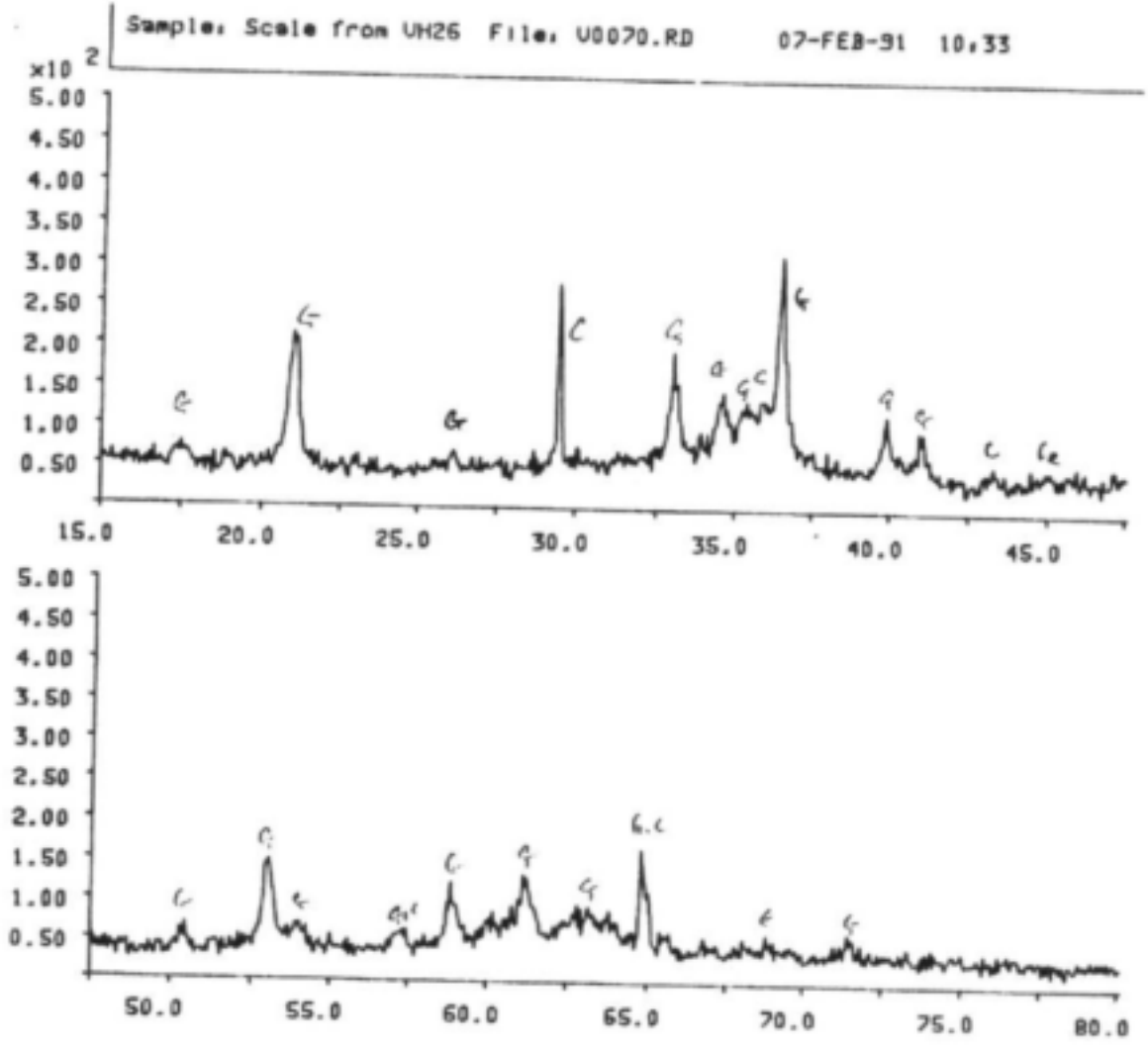

Figure 140. X-Ray diffractogram of mild steel in hot water at Vereeniging.

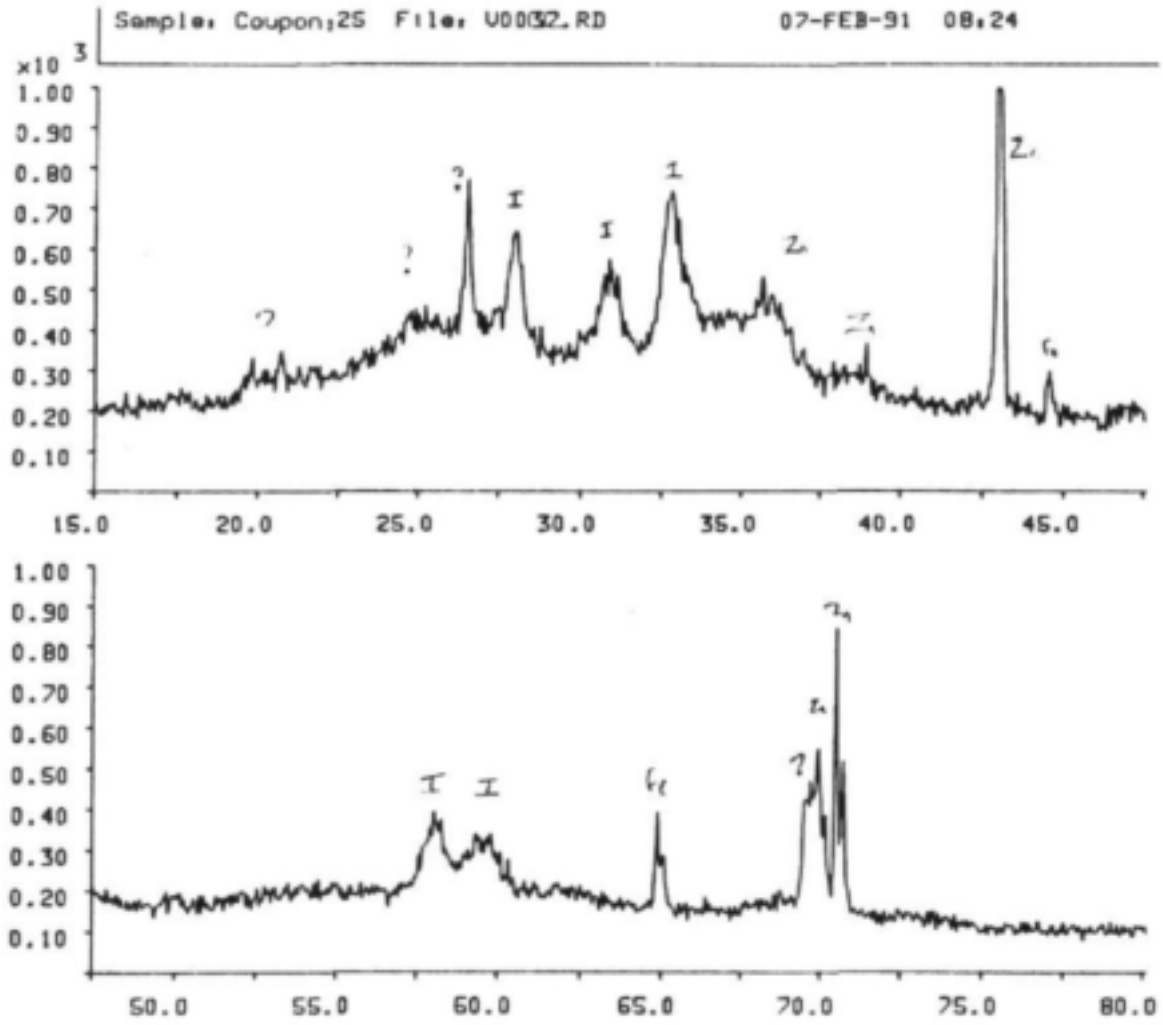

Figure 141. X-Ray diffractogram of galvanised steel at Vaal Dam.

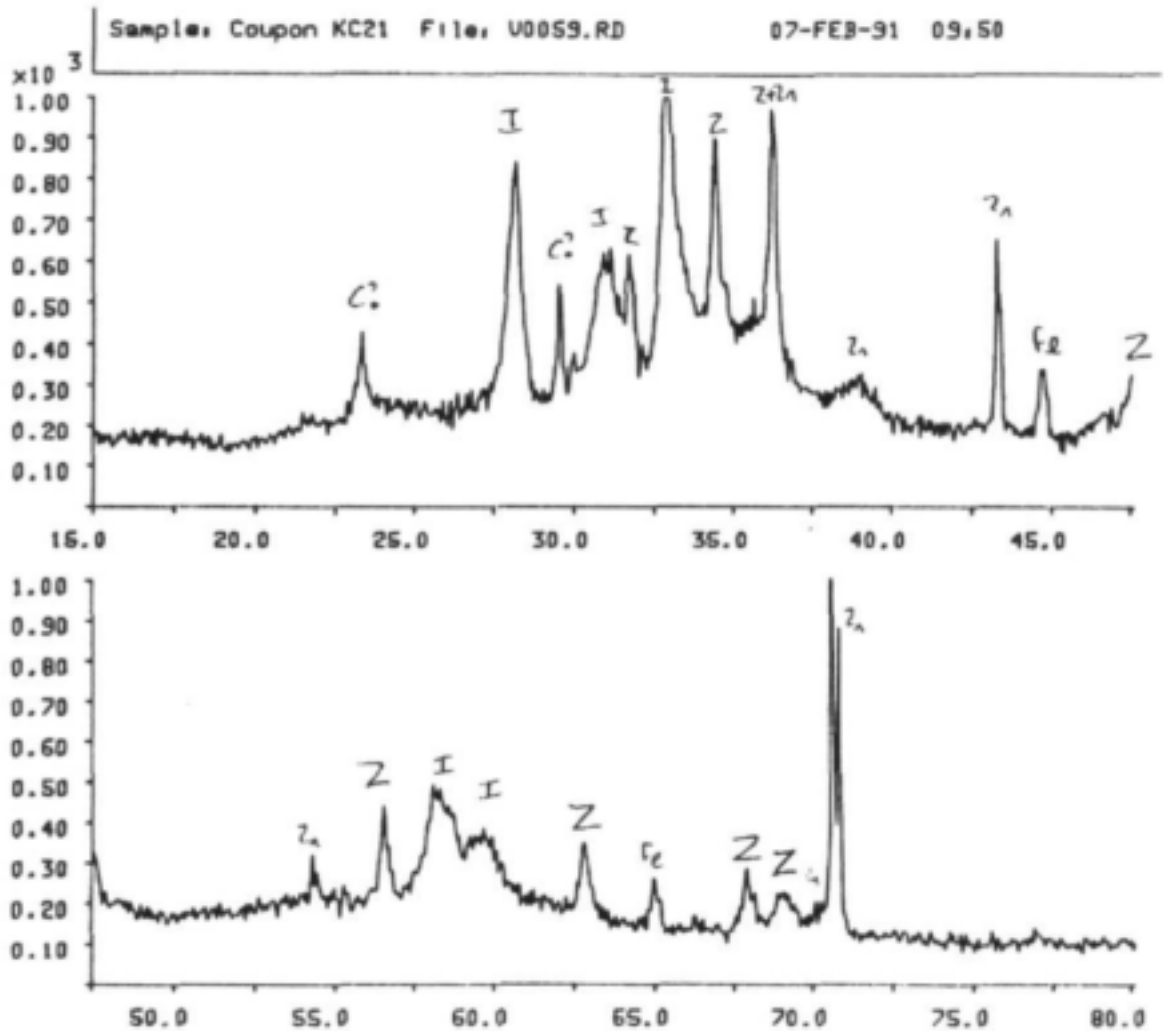

Figure 142. X-Ray diffractogram of galvanised steel in cold water at Klerksdorp.

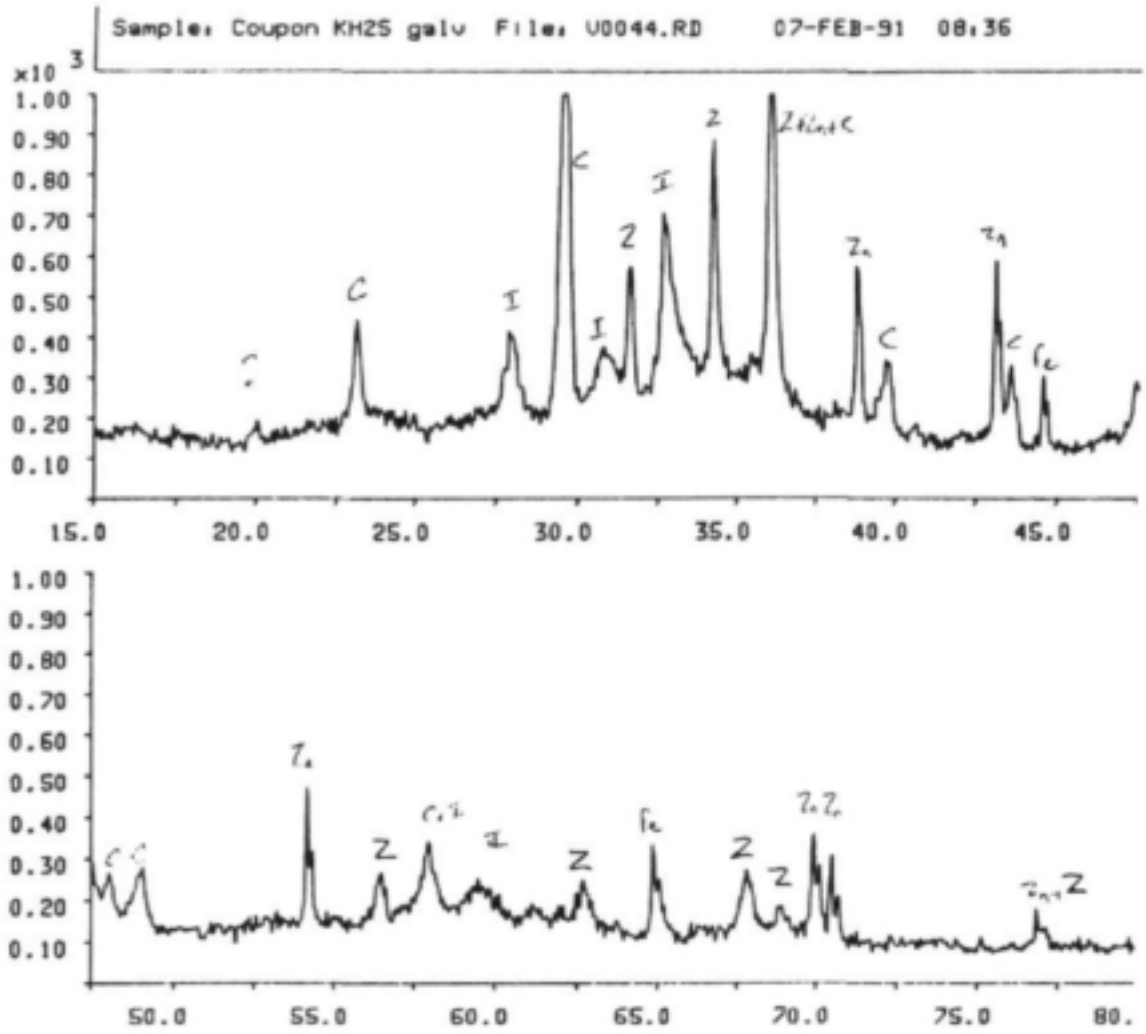

Figure 143. X-Ray diffractogram of galvanised steel in hot water at Klerksdorp.

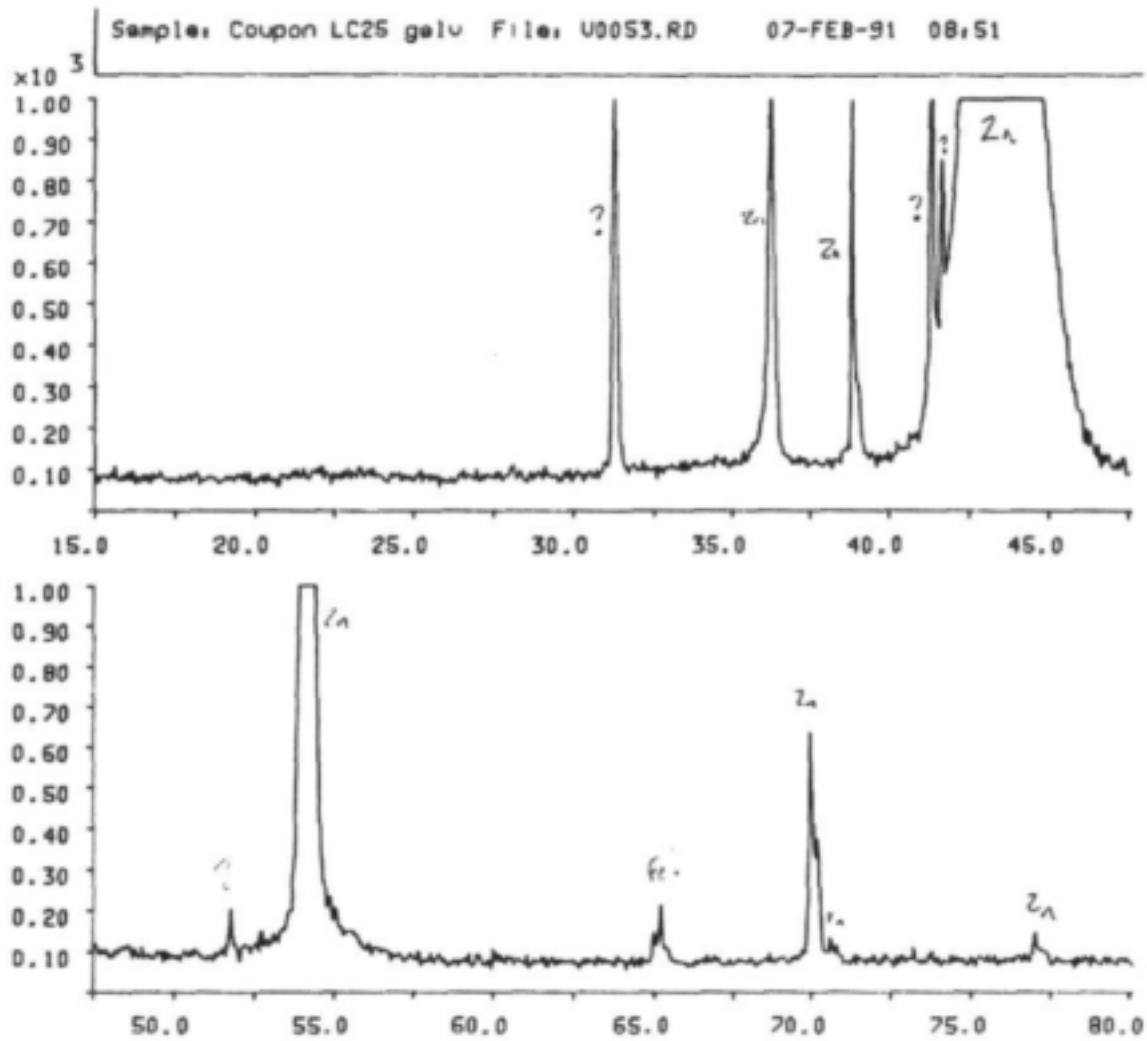

Figure 144. X-Ray diffractogram of galvanised steel in cold water at CSIR.

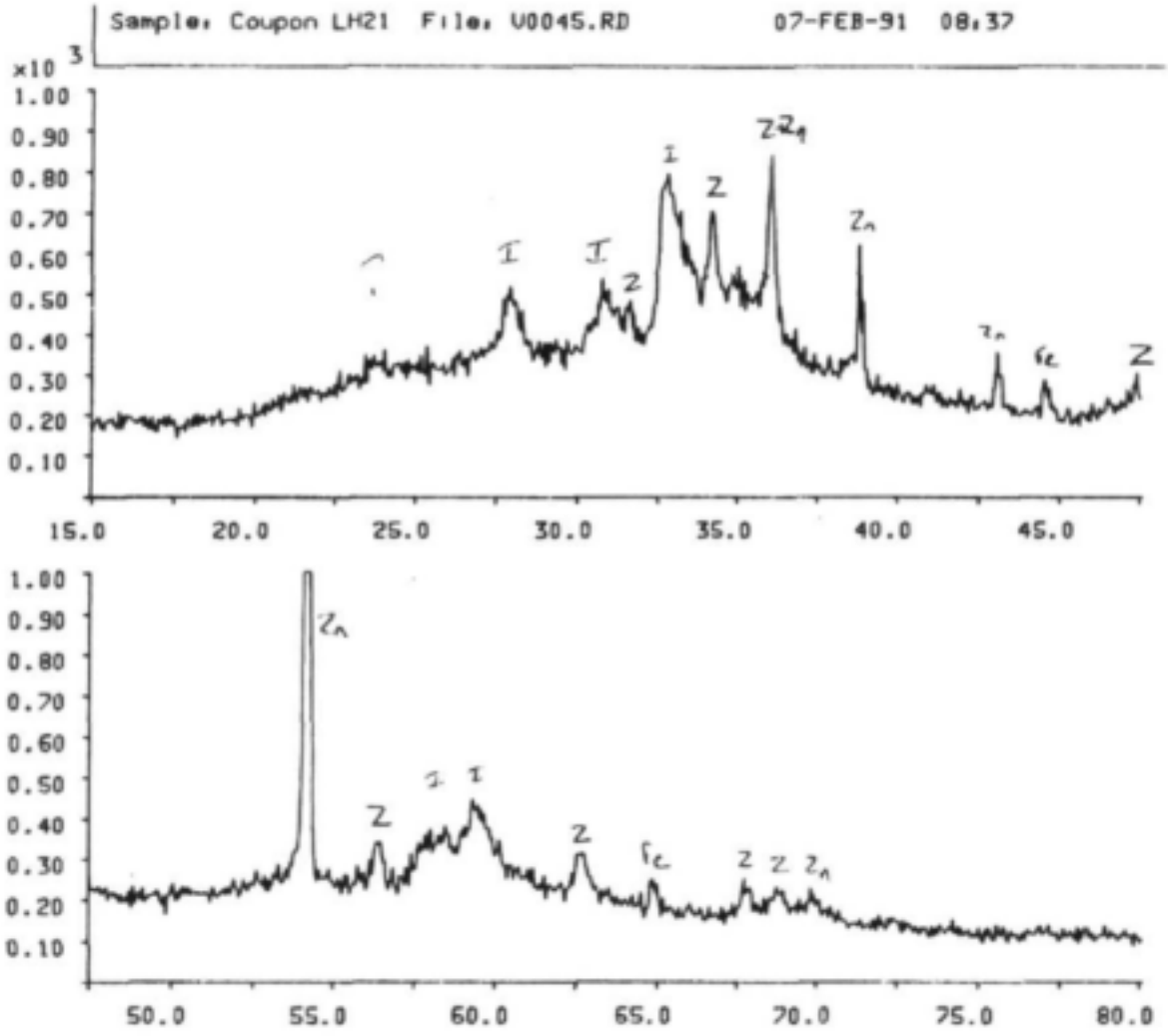

Figure 145. X-Ray diffractogram of galvanised steel in hot water at CSIR.

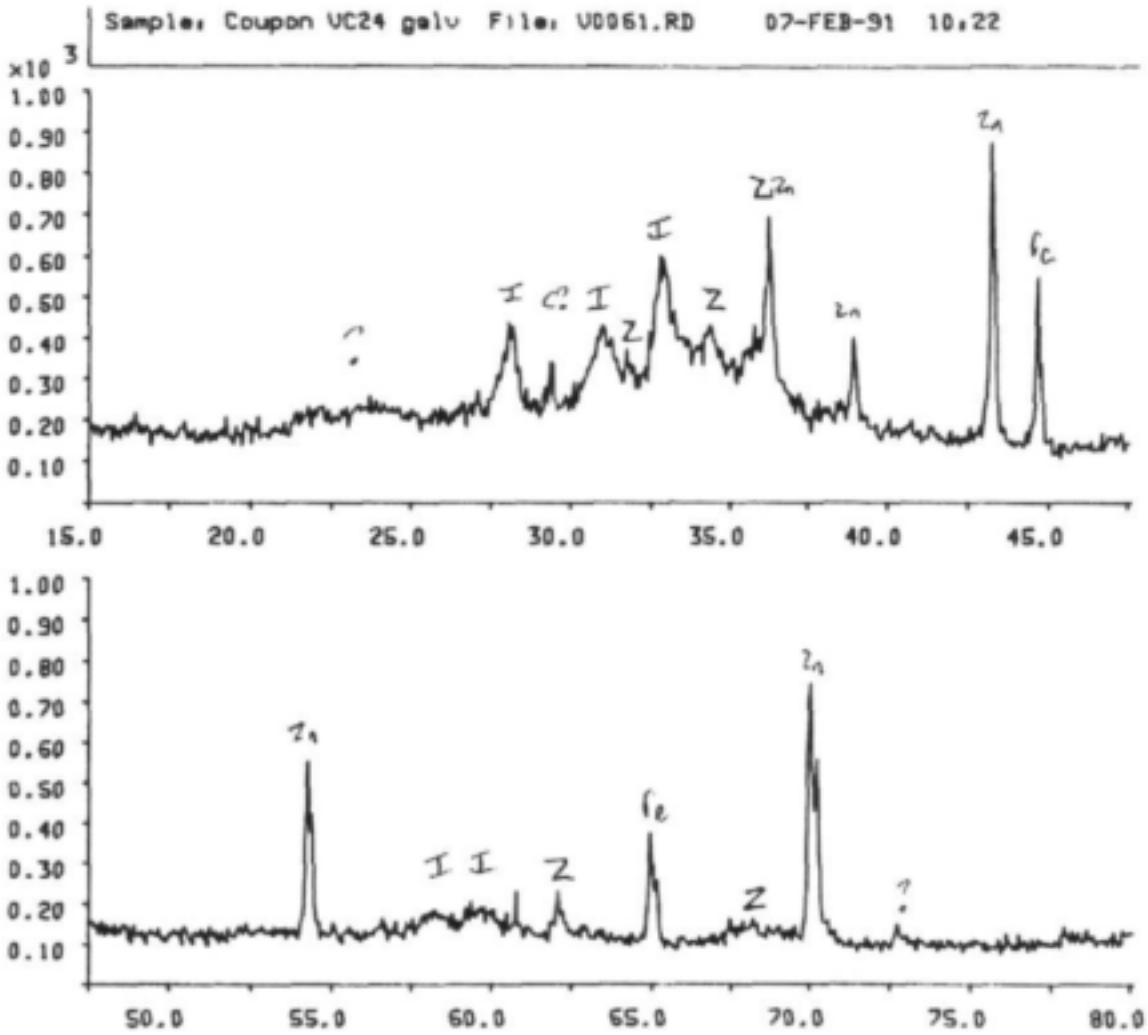

Figure 146. X-Ray diffractogram of galvanised steel in cold water at Vereeniging.

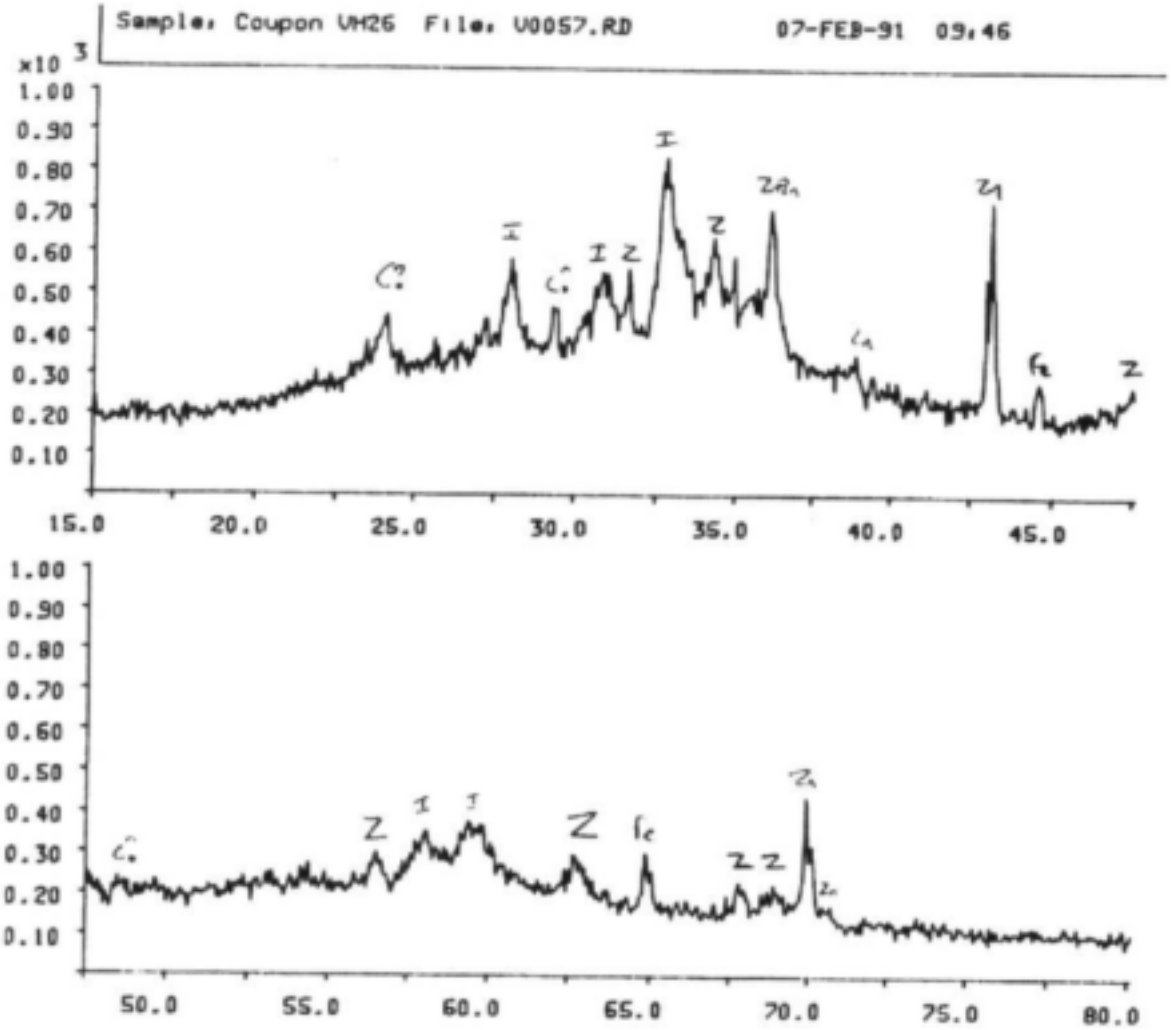

Figure 147. X-Ray diffractogram of galvanised steel in hot water at Vereeniging.

Appendix 6. Corrosion results from various sites

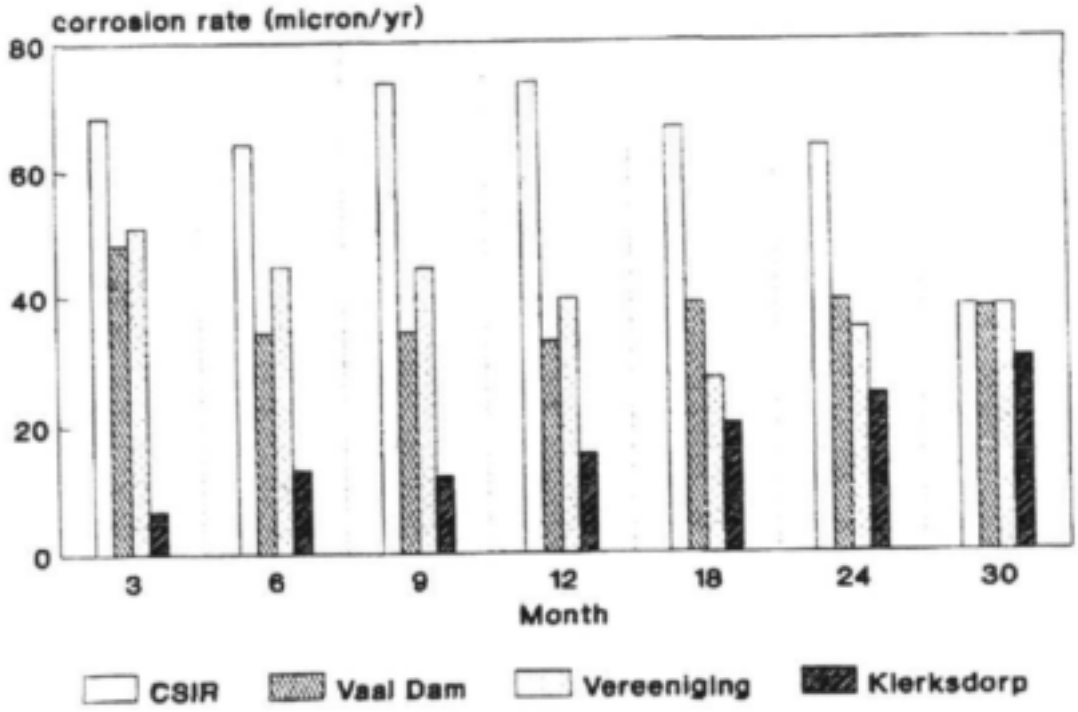

Figure 148. Mass loss of mild steel in cold water determined at three monthly intervals.

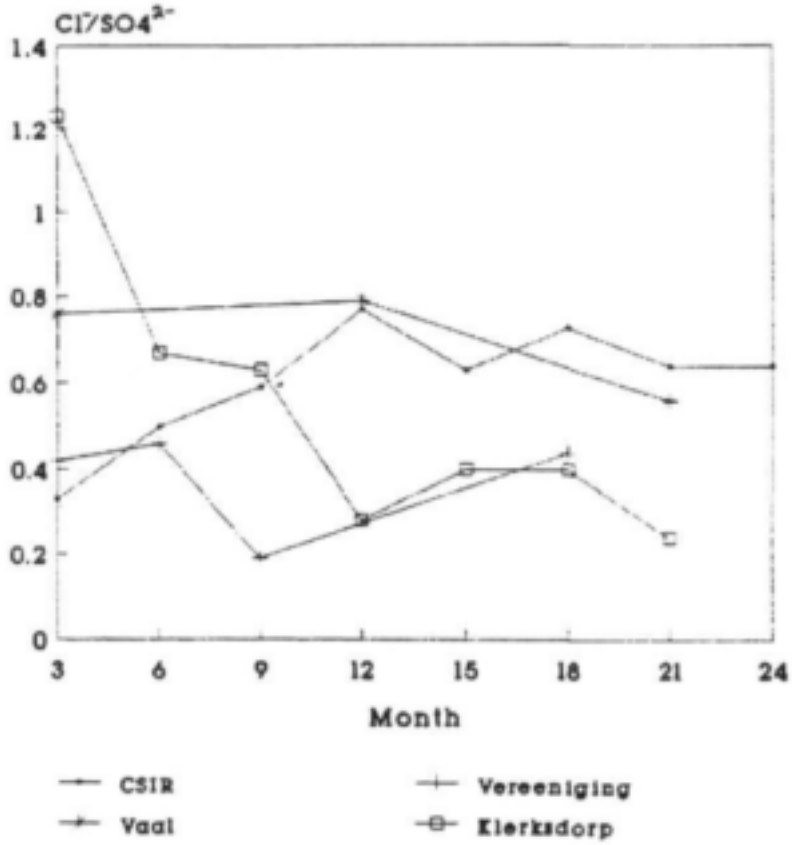

Figure 149. Change in Cl^-/SO_4 ratio over 24 months at different sites.

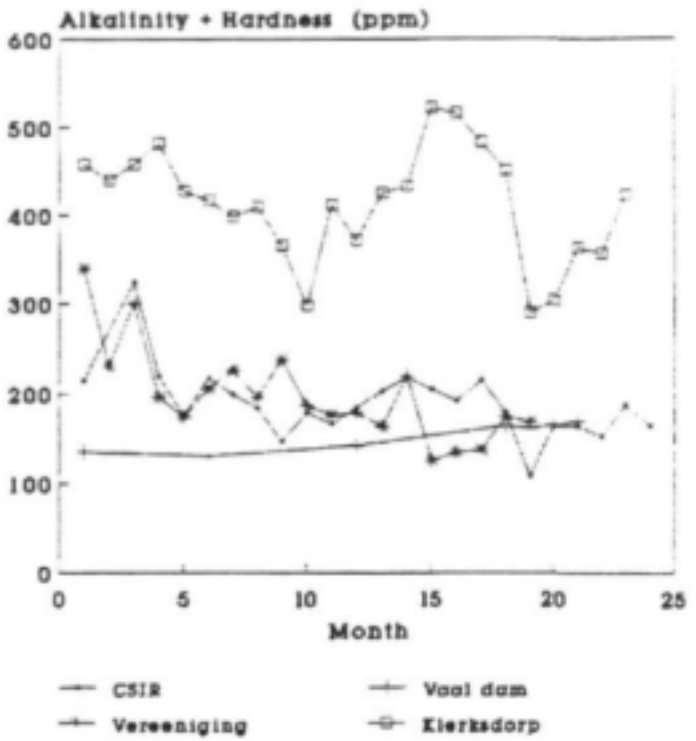

Figure 150. Change in alkalinity + hardness over 24 months at different sites.

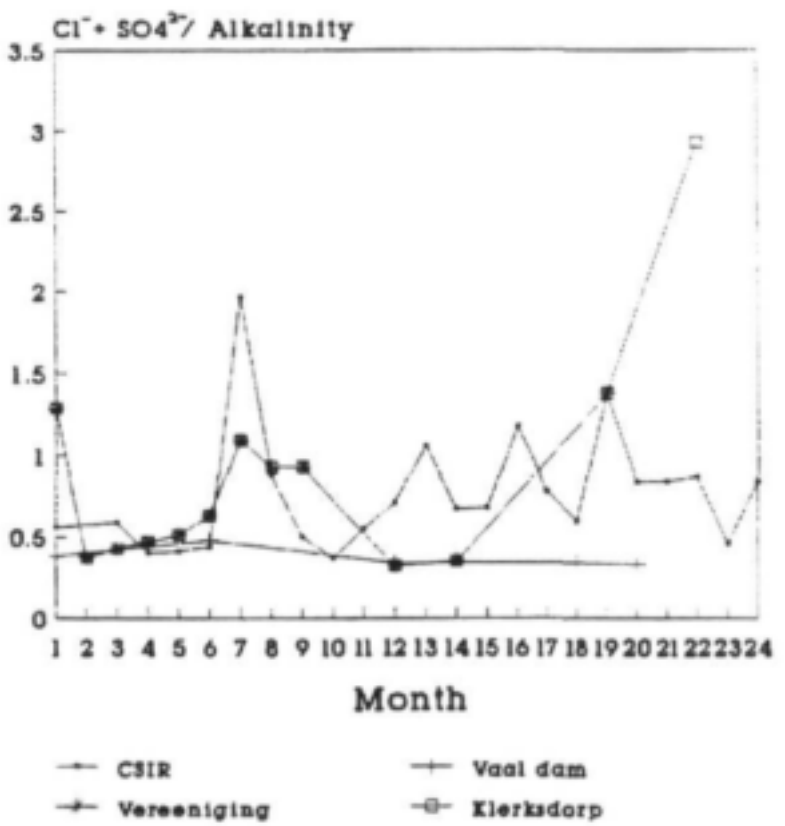

Figure 151. Change in SO_4 + Cl^- / Alkalinity ratio over 24 months at different sites.

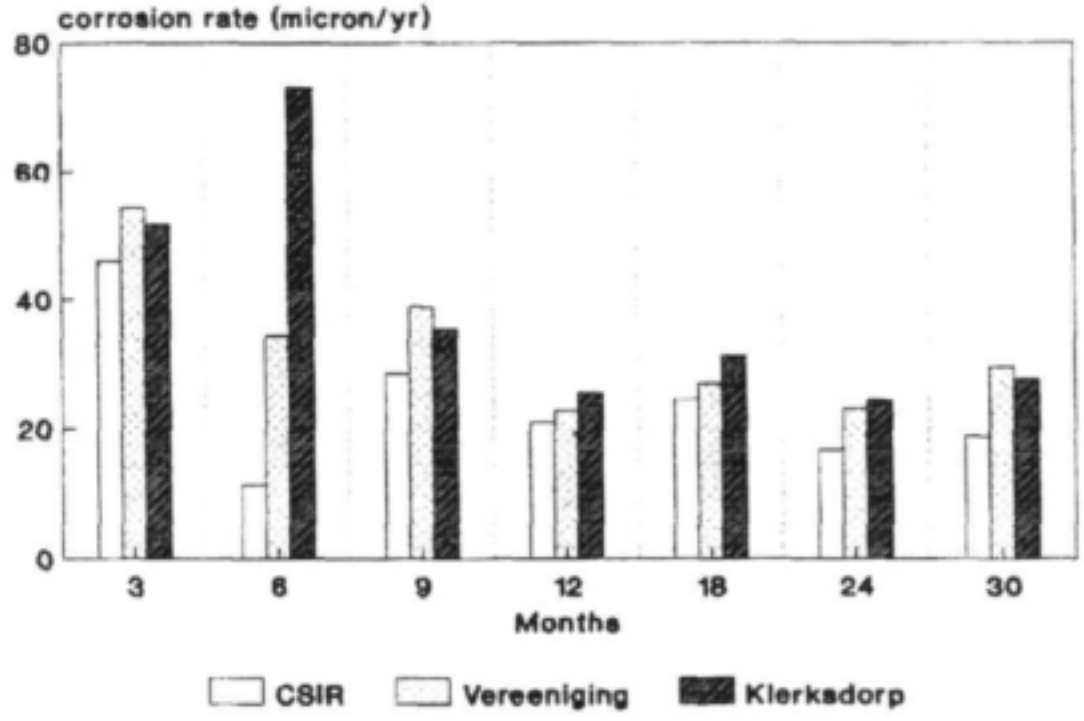

Figure 152. Mass loss of mild steel in hot water determined at three monthly intervals.

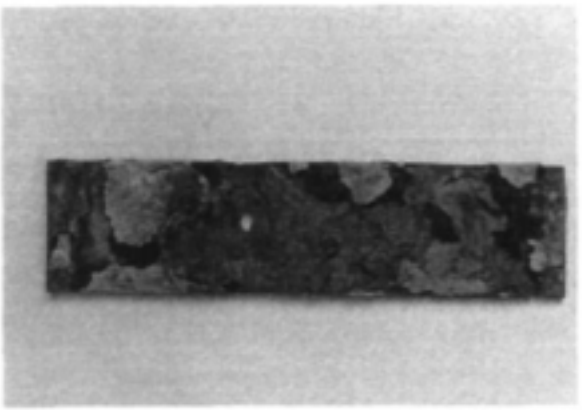

Figure 153. Mild steel coupon exposed in cold water at the CSIR for 18 months.

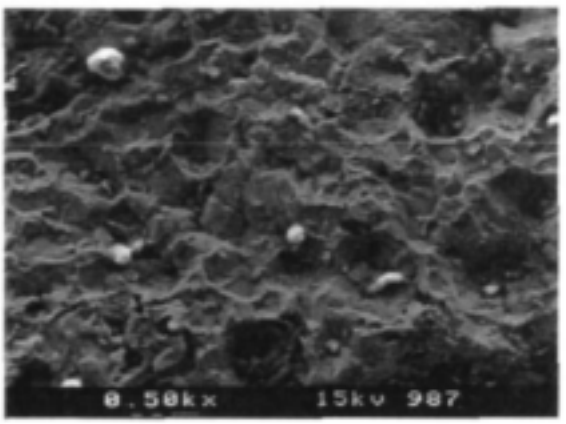

Figure 154. Intergranular attack of mild steel coupon immersed in cold water at Klerksdorp.

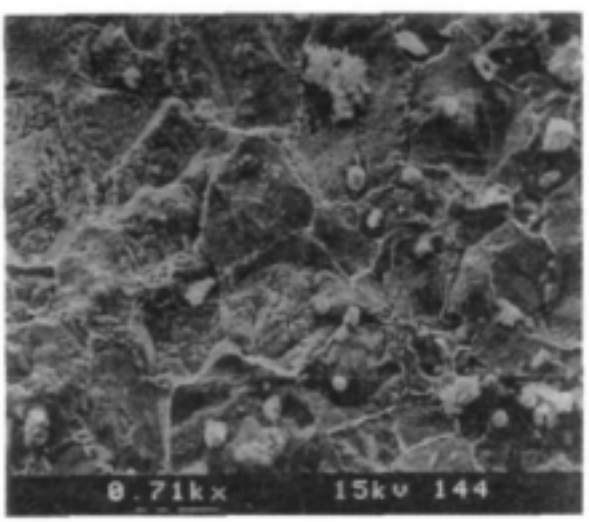

Figure 155. Intergranular attack of mild steel coupon immersed in cold water at Vaal Dam.

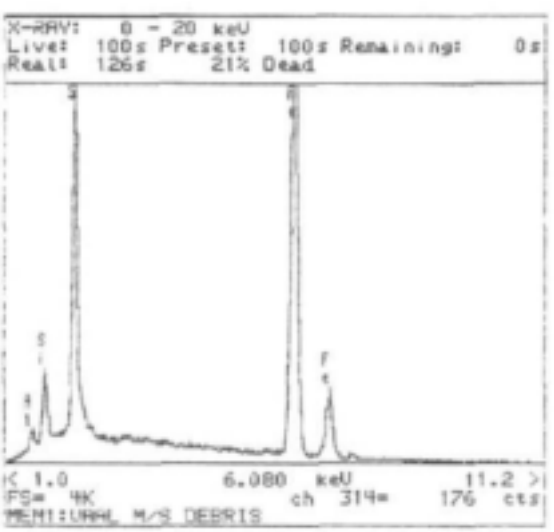

Figure 156. EDS trace of corrosion product on coupon shown in Figure 155.

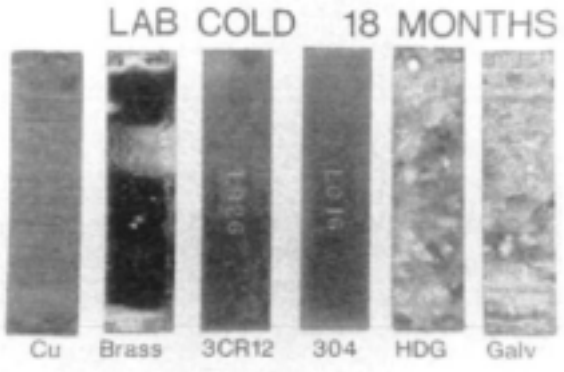

Figure 157. Coupons exposed at CSIR in cold water for 18 months.

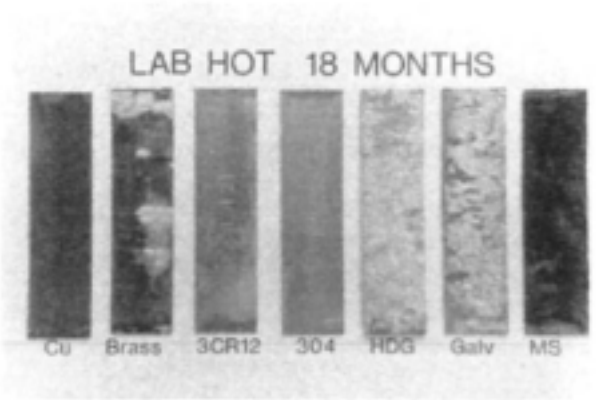

Figure 158. Coupons exposed at CSIR in hot water for 18 months.

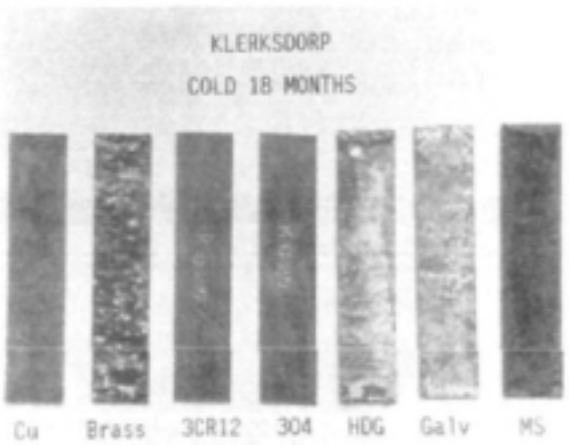

Figure 159. Coupons exposed at Klerksdorp in cold water for 18 months.

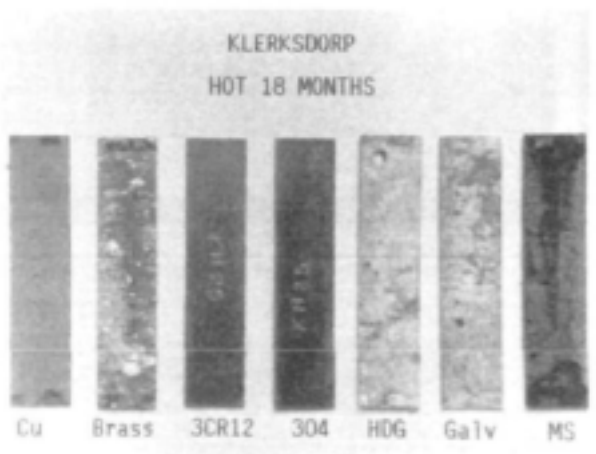

Figure 160. Coupons exposed at Klerksdorp in hot water for 18 months.

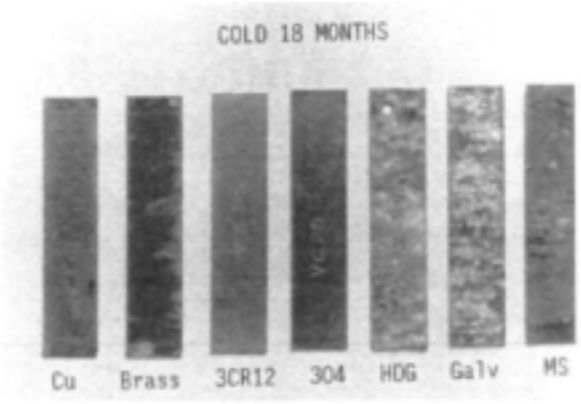

Figure 161. Coupons exposed at Vereeniging in cold water for 18 months.

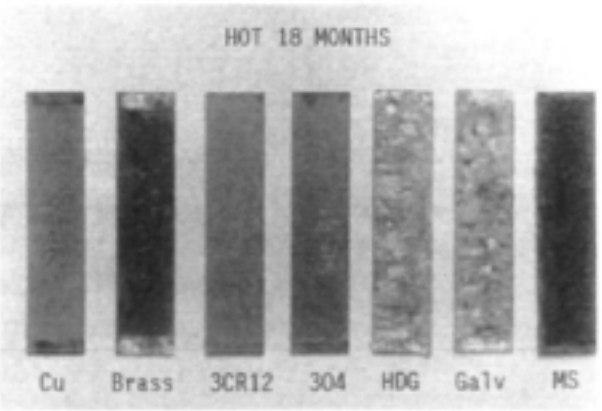

Figure 162. Coupons exposed at Vereeniging in hot water for 18 months.

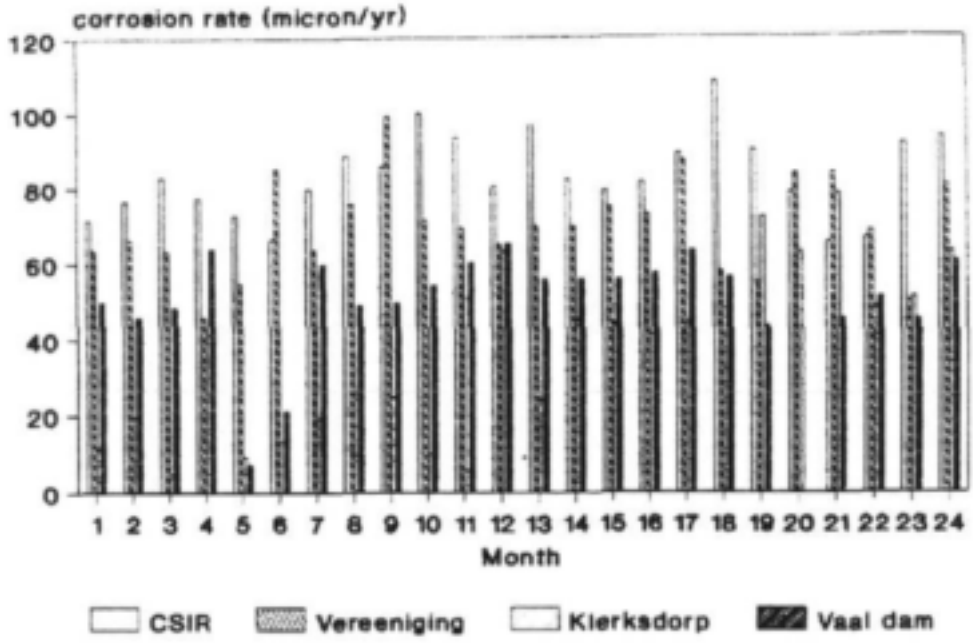

Figure 163. Corrosion rate of mild steel in cold water measured by monthly mass loss at four different sites.

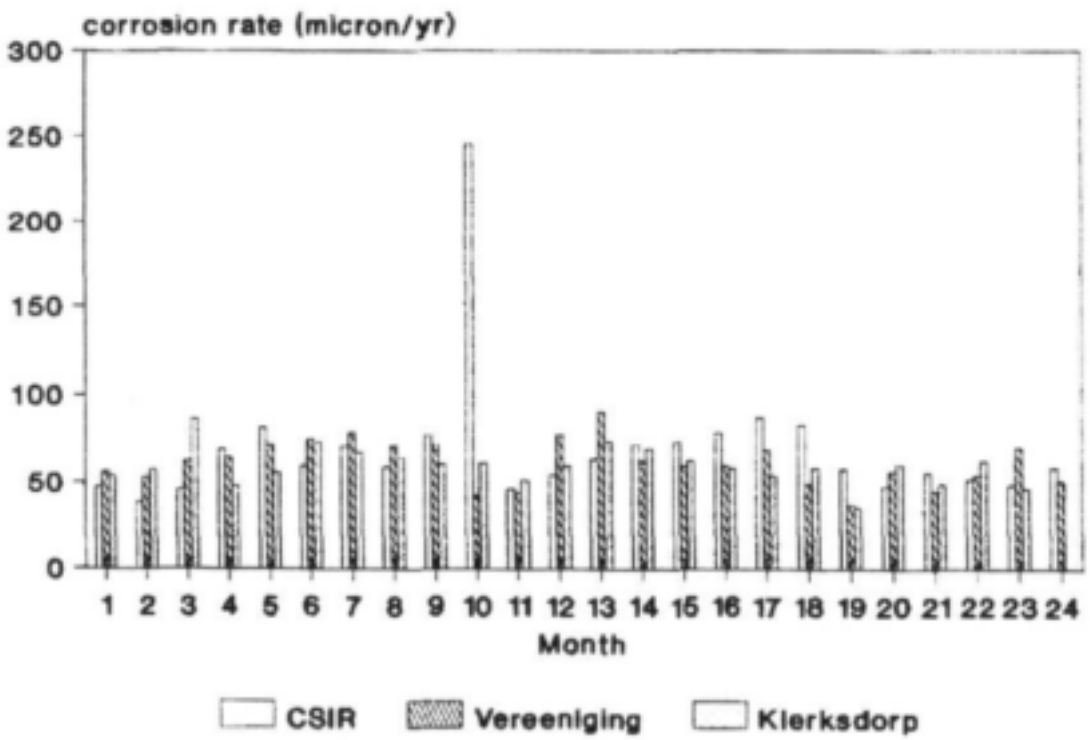

Figures 164. Corrosion rate of mild steel in hot water measured by monthly mass loss at three different sites.

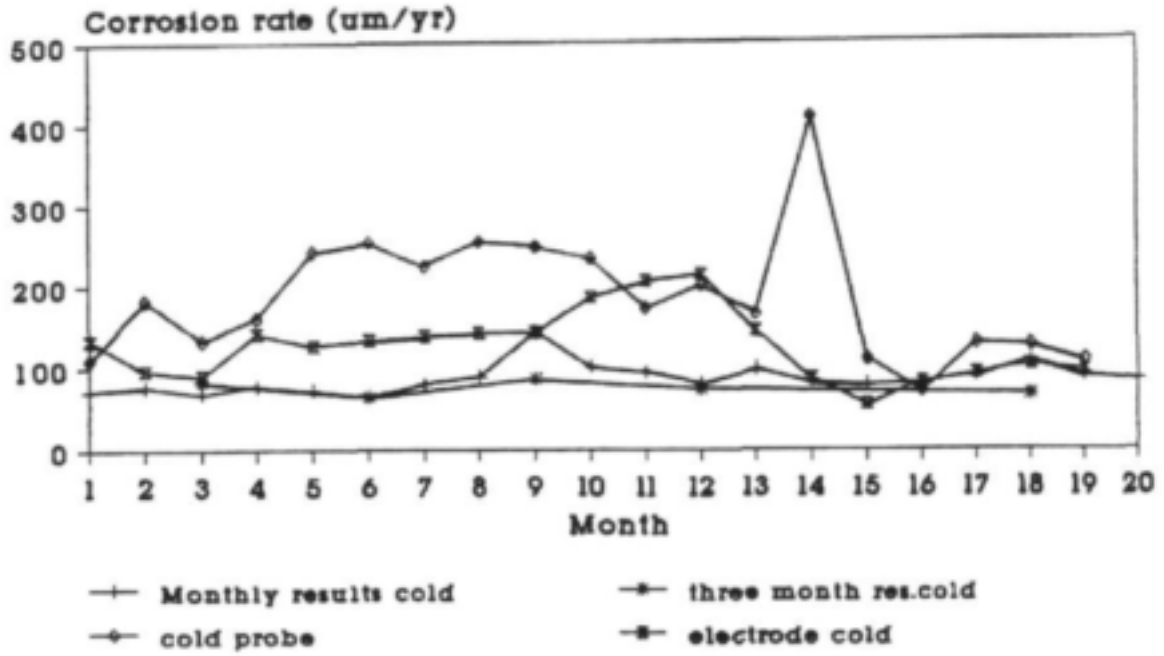

Figure 165. Comparison of the corrosion rates of mild steel in cold water obtained by different techniques (CSIR).

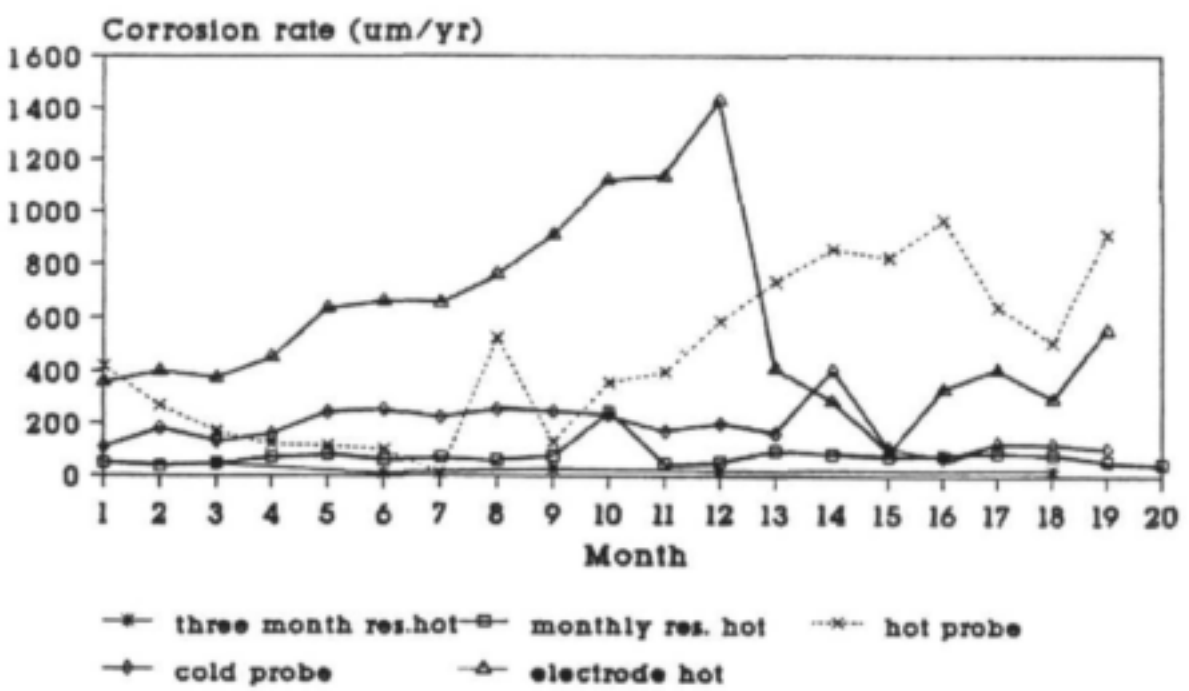

Figure 166. Comparison of the corrosion rates of mild steel in hot water obtained by different techniques (CSIR).

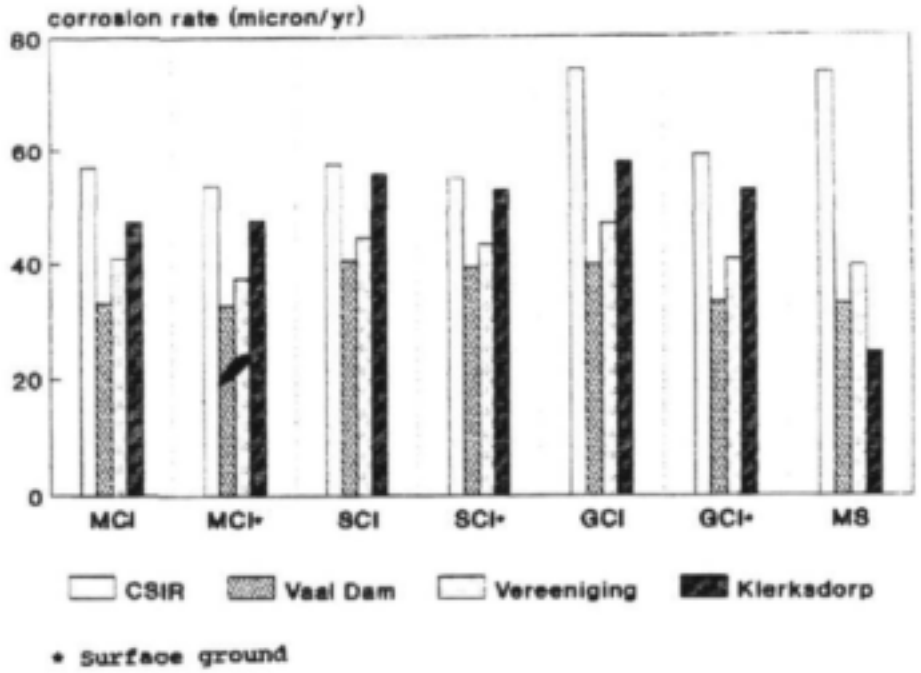

Figure 167. Corrosion rates of different cast irons in cold water after one year at different sites.

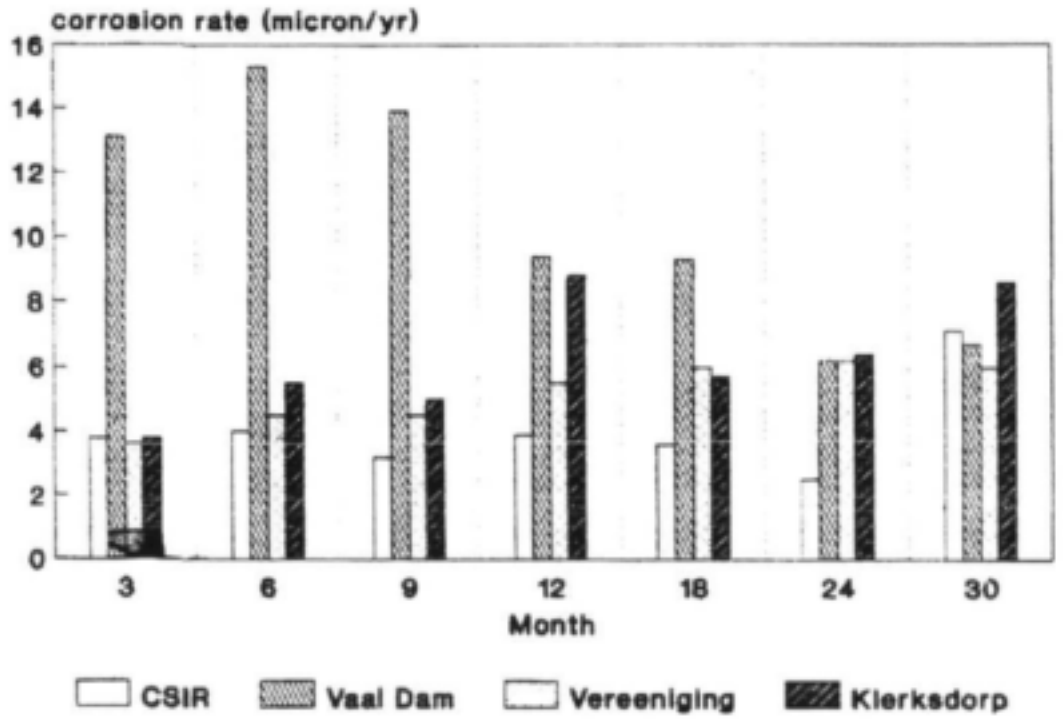

Figure 168. Mass loss of zinc in cold water determined at three monthly intervals.

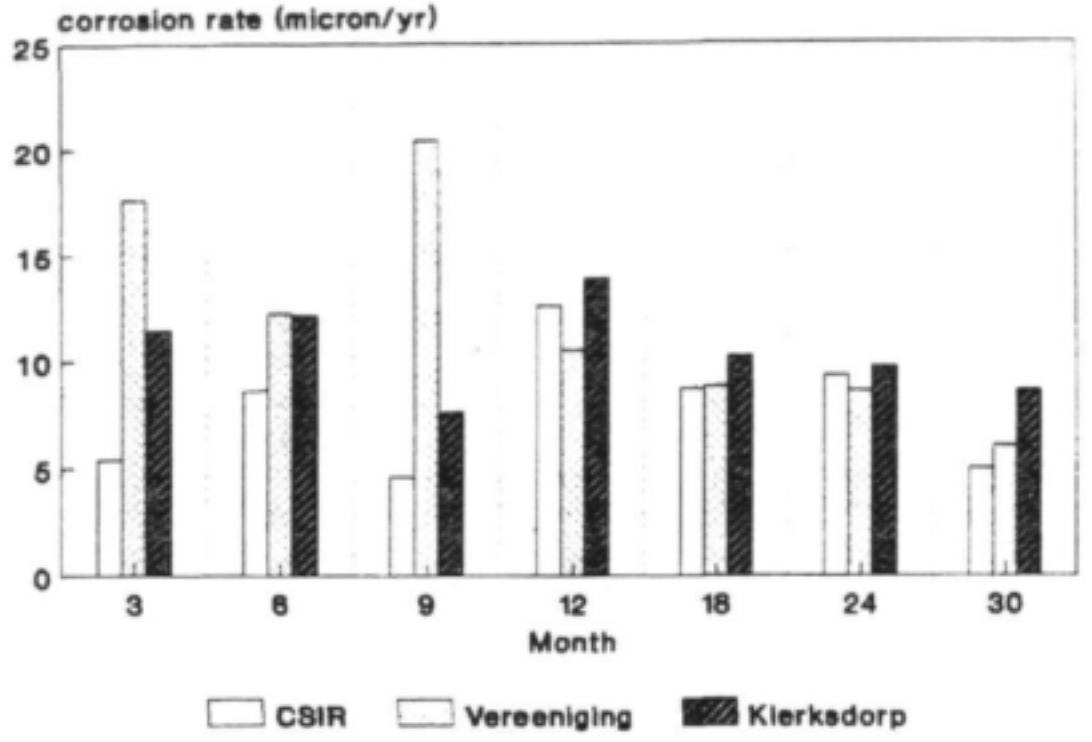

Figure 169. Mass loss of zinc in hot water determined at three monthly intervals.

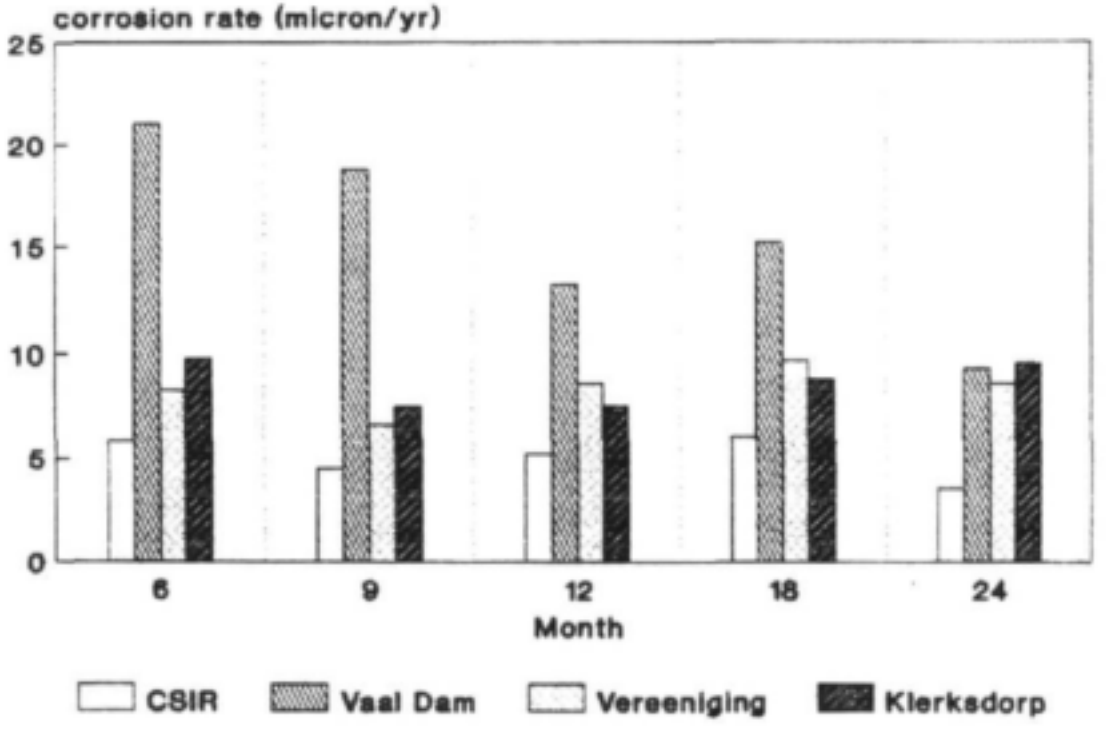

Figure 170. Corrosion rate of hot dipped galvanised zinc in cold water at four different sites.

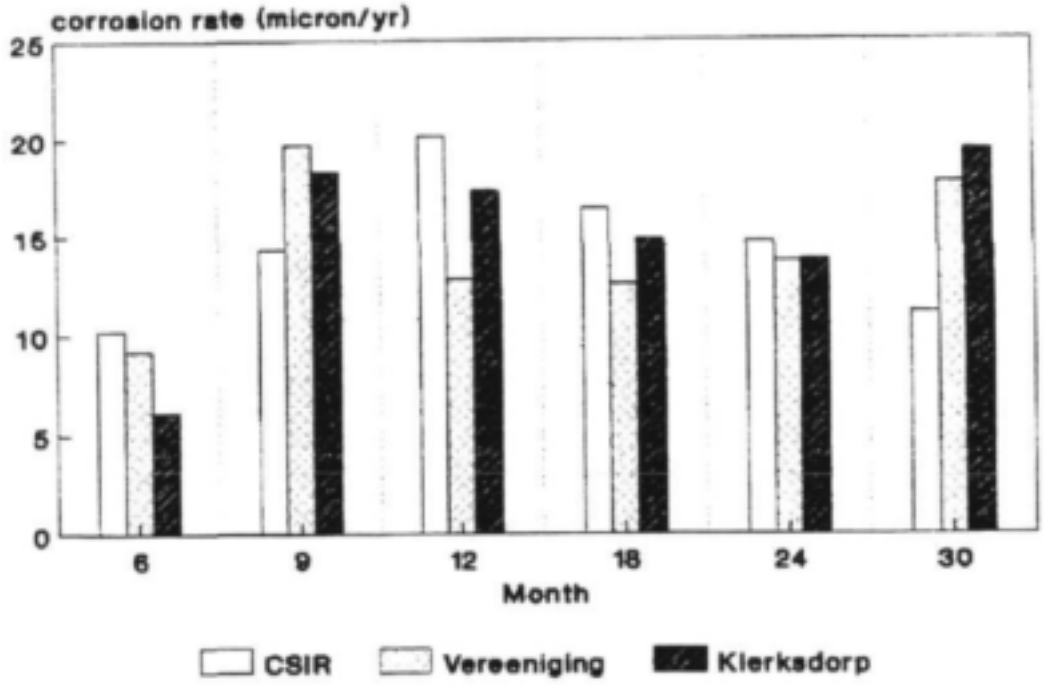

Figure 171. Corrosion rate of hot dipped galvanised zinc in hot water at three different sites.

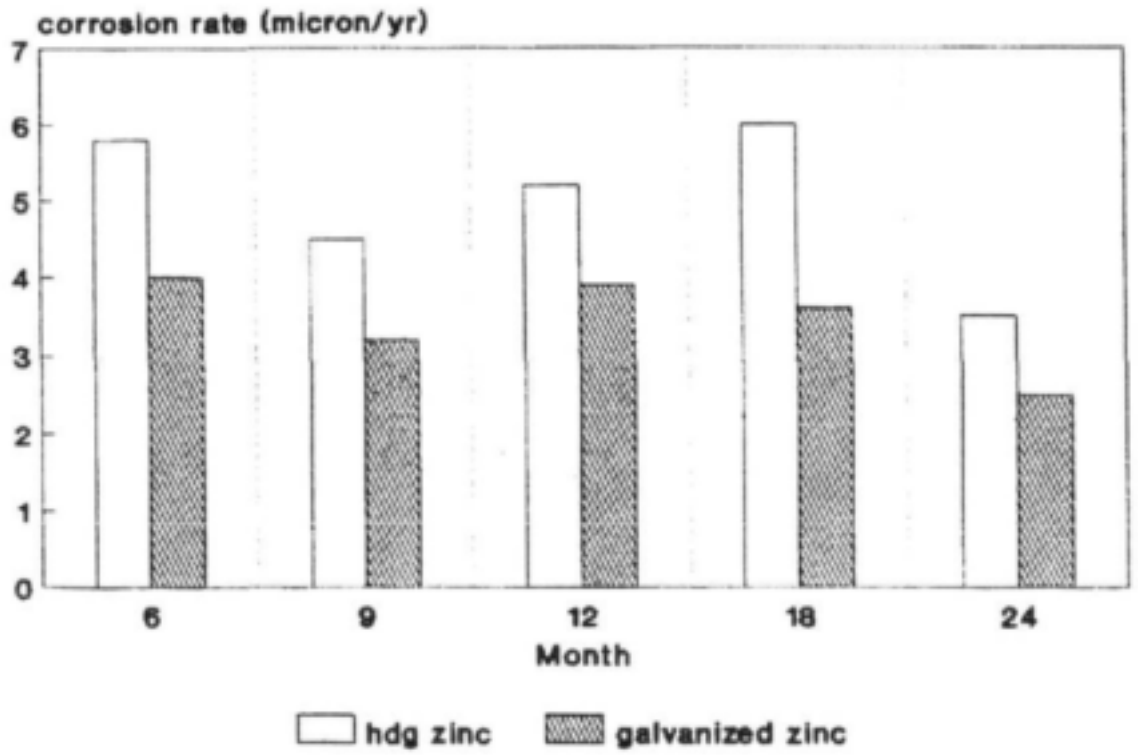

Figure 172. Comparison of the corrosion rates of hot dipped galvanised zinc and galvanised zinc in cold water measured by mass loss (CSIR).

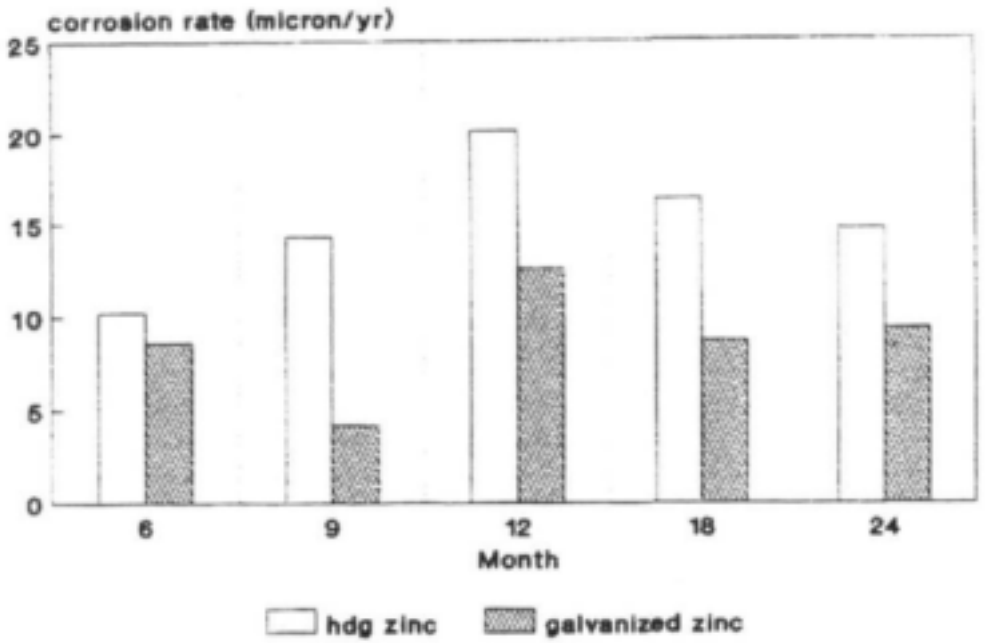

Figure 173. Comparison of the corrosion rates of hot dipped galvanised zinc and galvanised zinc in hot water measured by mass loss (CSIR).

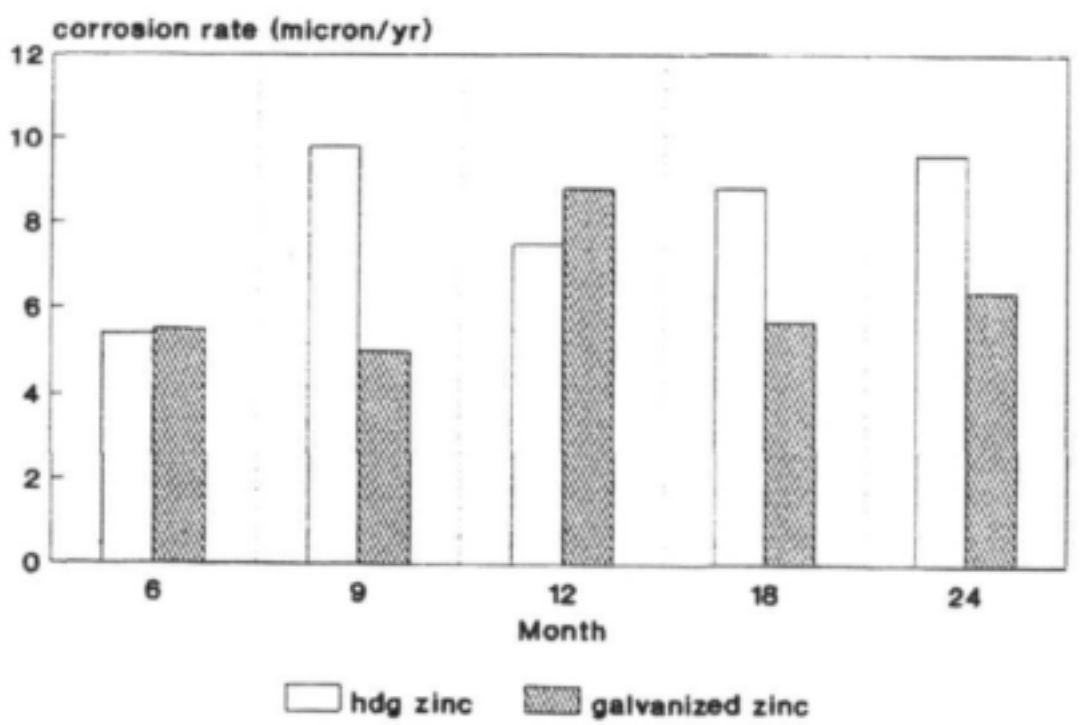

Figure 174. Comparison of the corrosion rates of hot dipped galvanised zinc and galvanised zinc in cold water measured by mass loss (Klerksdorp).

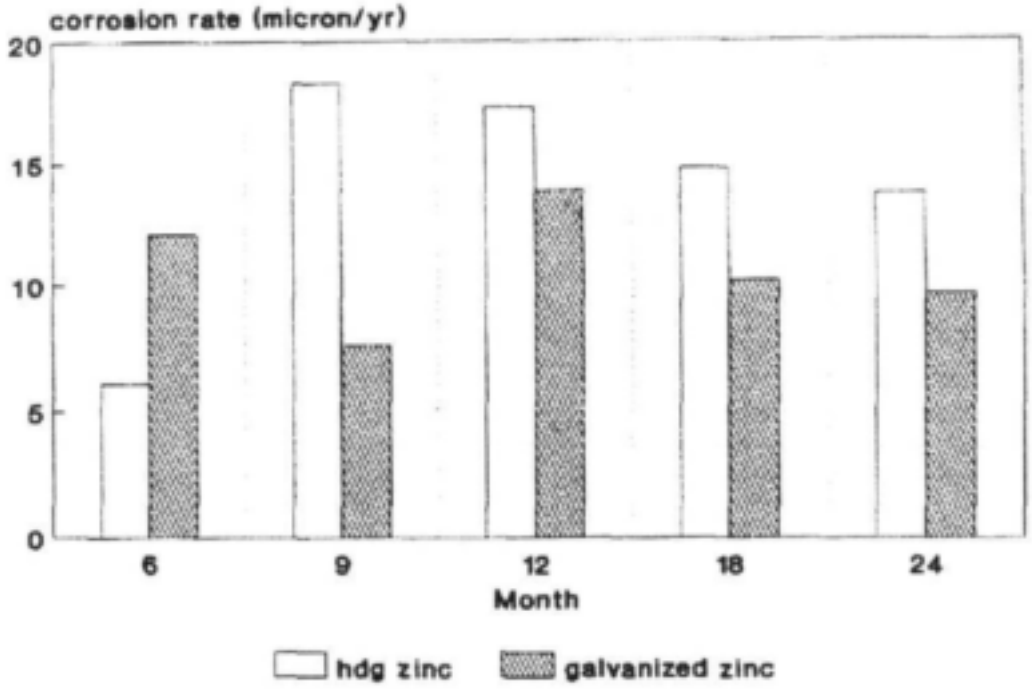

Figure 175. Comparison of the corrosion rates of hot dipped galvanised zinc and galvanised zinc in hot water measured by mass loss (Klerksdorp).

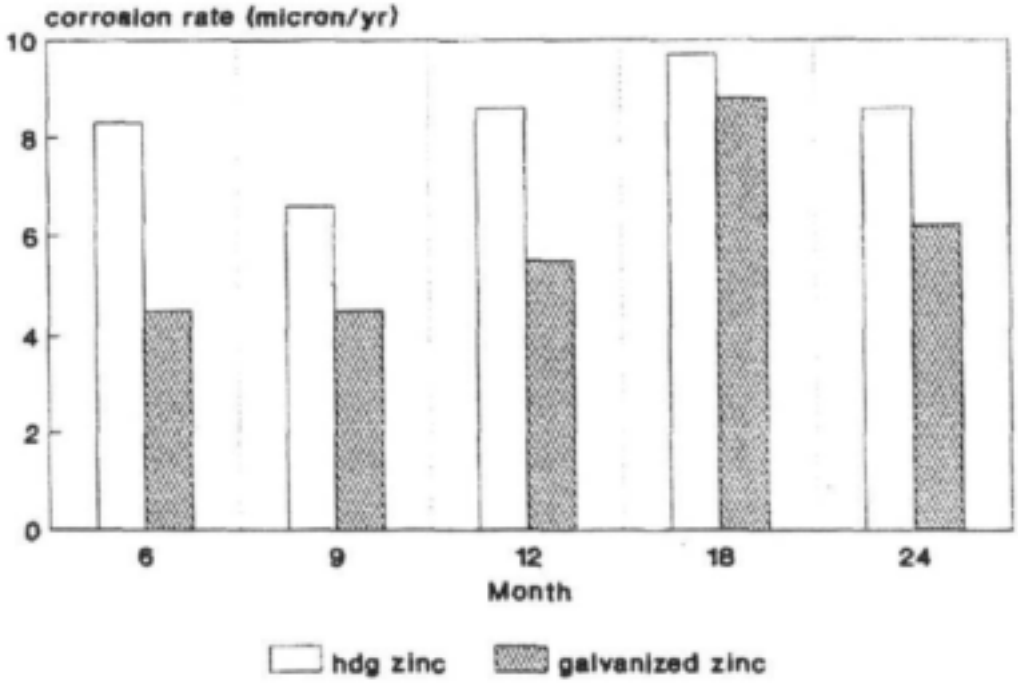

Figure 176. Comparison of the corrosion rates of hot dipped galvanised zinc and galvanised zinc in cold water measured by mass loss (Vereeniging).

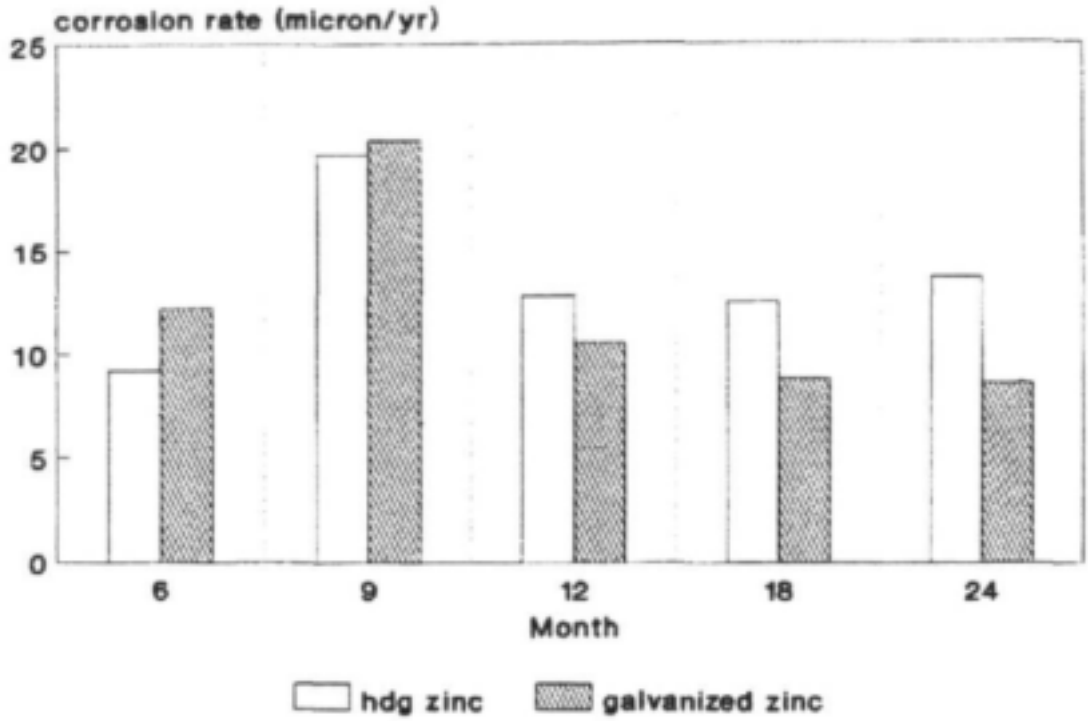

Figure 177. Comparison of the corrosion rates of hot dipped galvanised zinc and galvanised zinc in hot water measured by mass loss (Vereeniging).

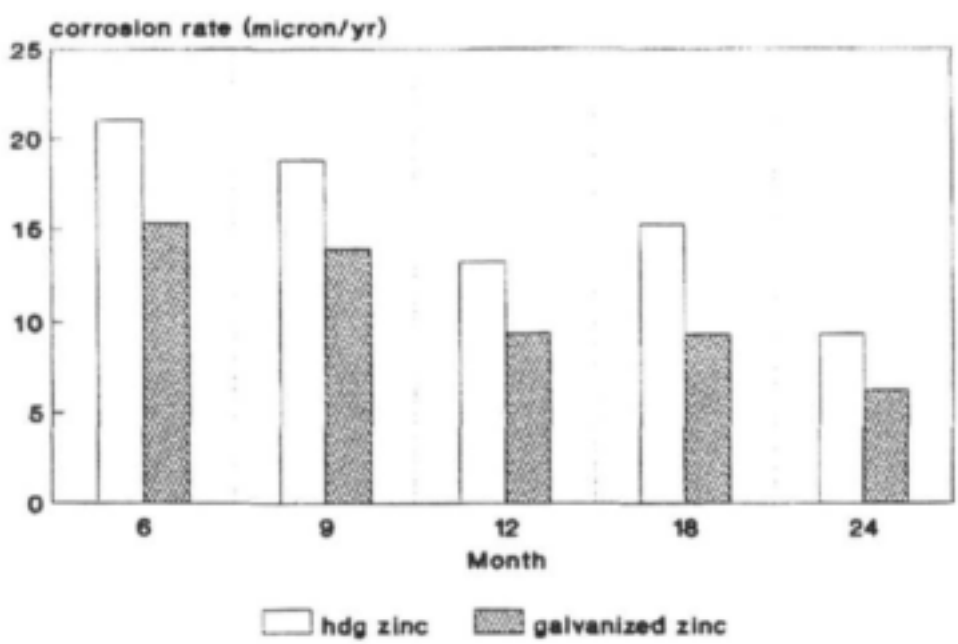

Figure 178. Comparison of the corrosion rates of hot dipped galvanised zinc and galvanised zinc in cold water measured by mass loss (Vaal Dam).

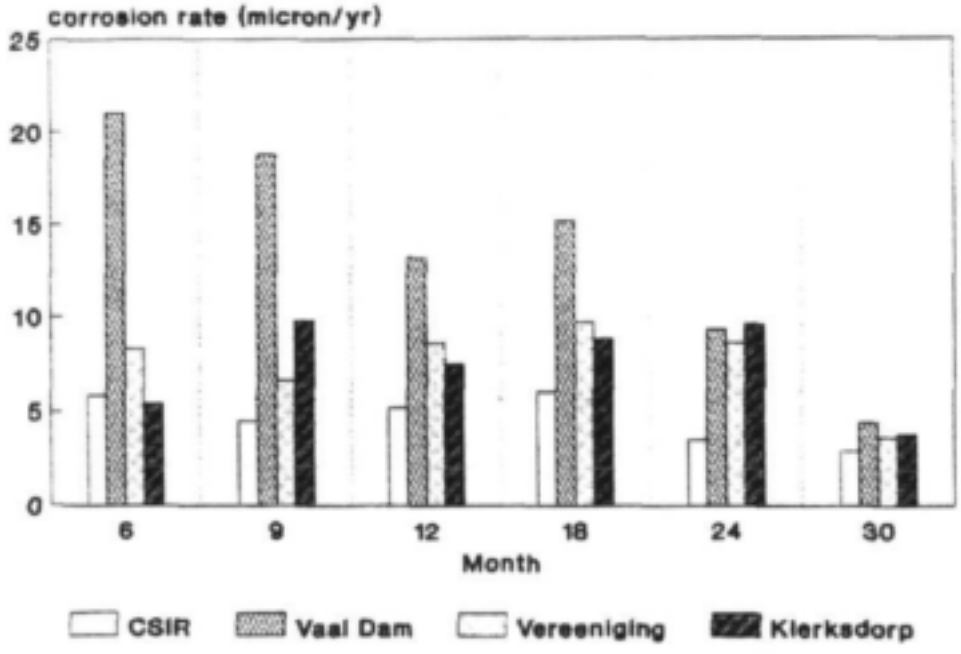

Figure 179. Mass loss of brass in cold water determined at three monthly intervals at different sites.

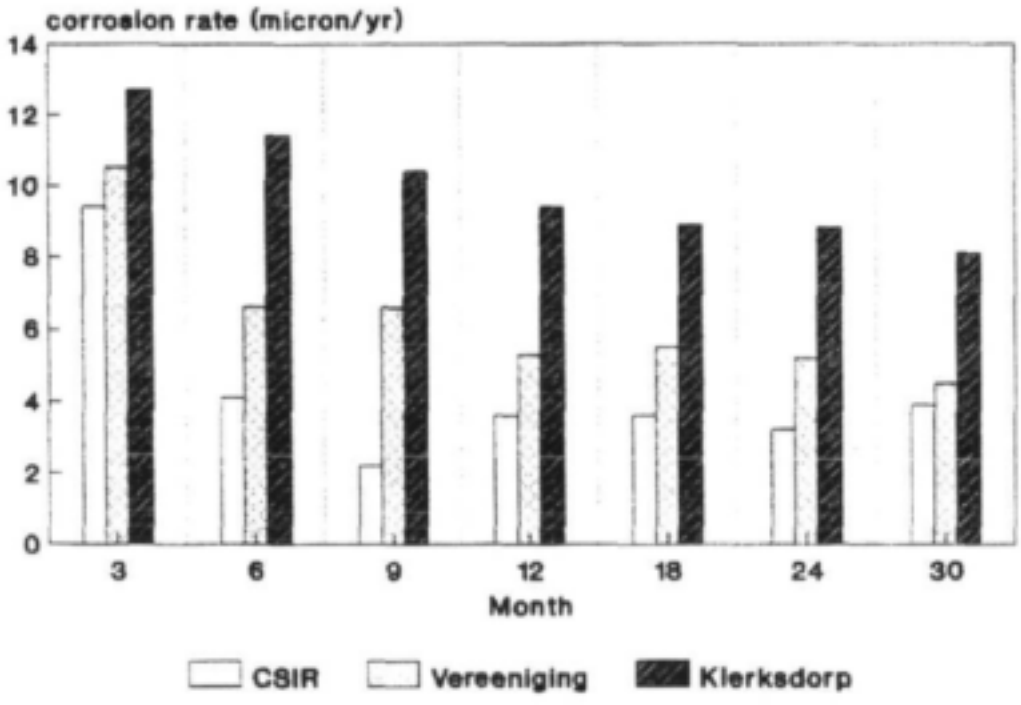

Figure 180. Mass loss of brass in hot water determined at three monthly intervals at different sites.

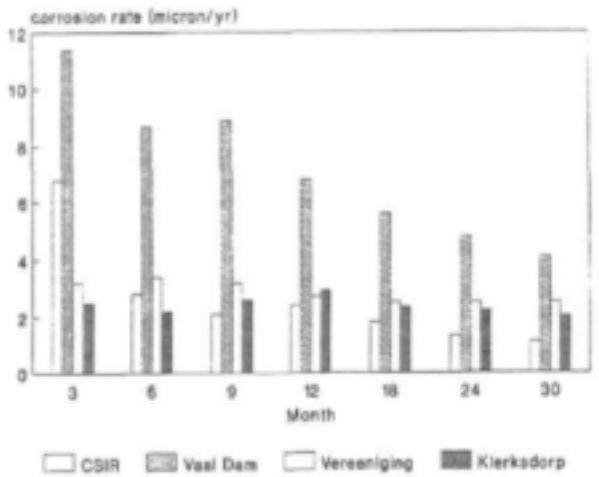

Figure 181. Mass loss of copper in cold water determined at three monthly intervals at different sites.

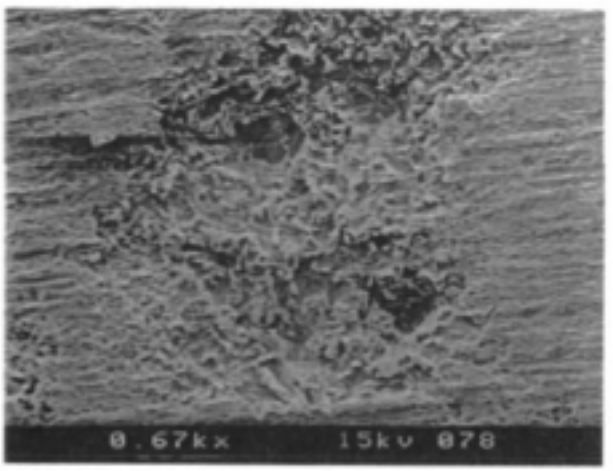

Figure 182. Copper coupon immersed for nine months in cold water at Klerksdorp. Note initiation of pitting.

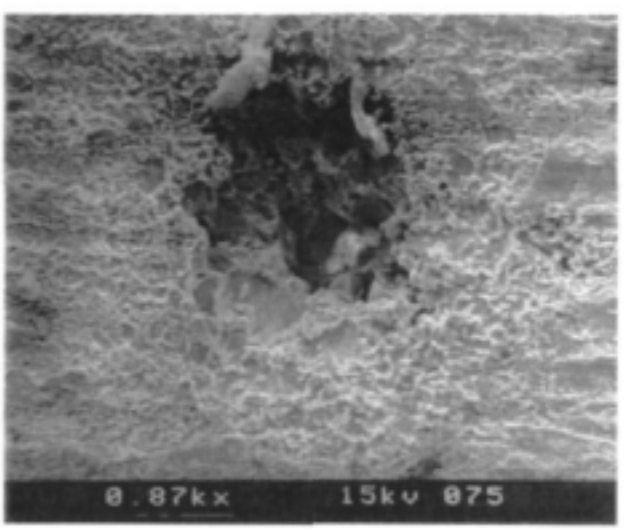

Figure 183. Copper coupon immersed for 12 months in cold water at Klerksdorp. Pitting is more pronounced.

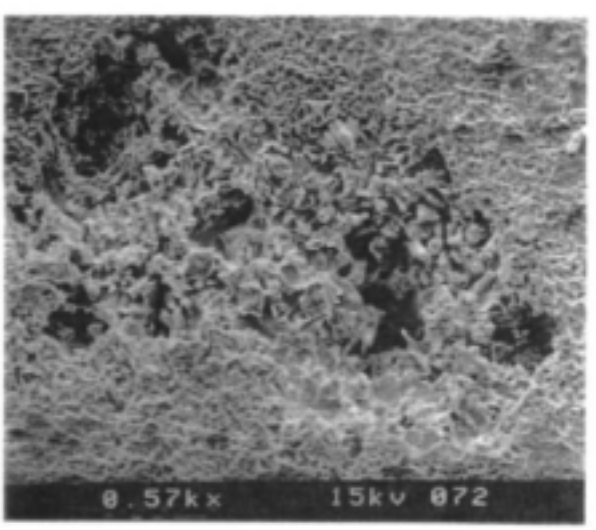

Figure 184. Copper coupon immersed for 18 months in cold water at Klerksdorp.

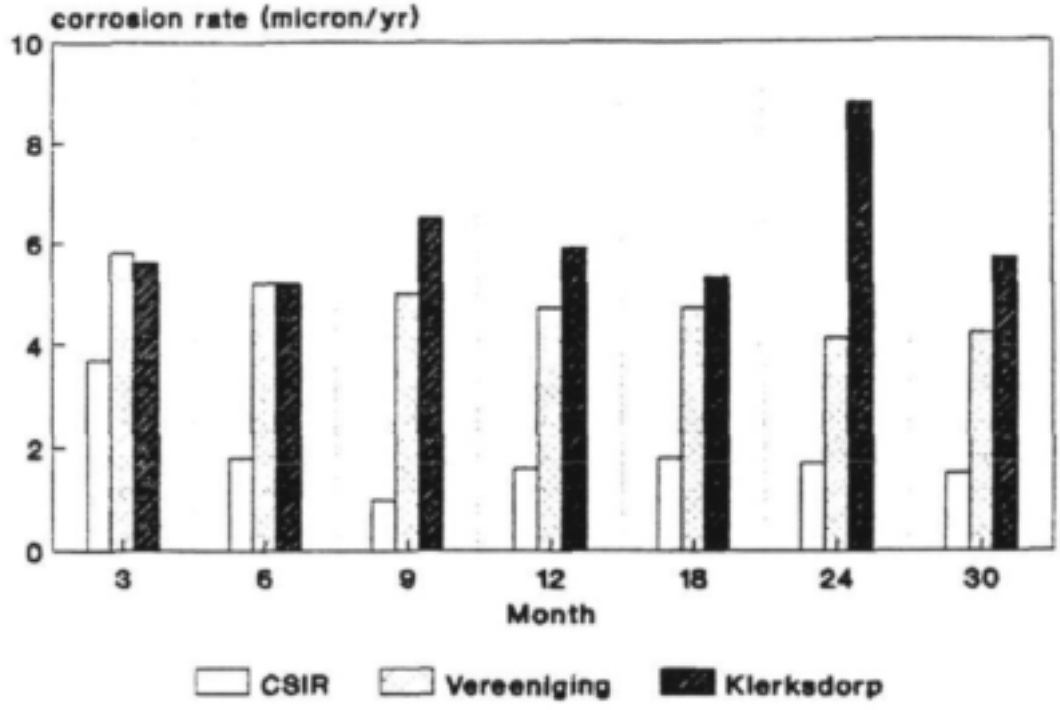

Figure 185. Mass loss of copper in hot water determined at three monthly intervals at different sites.

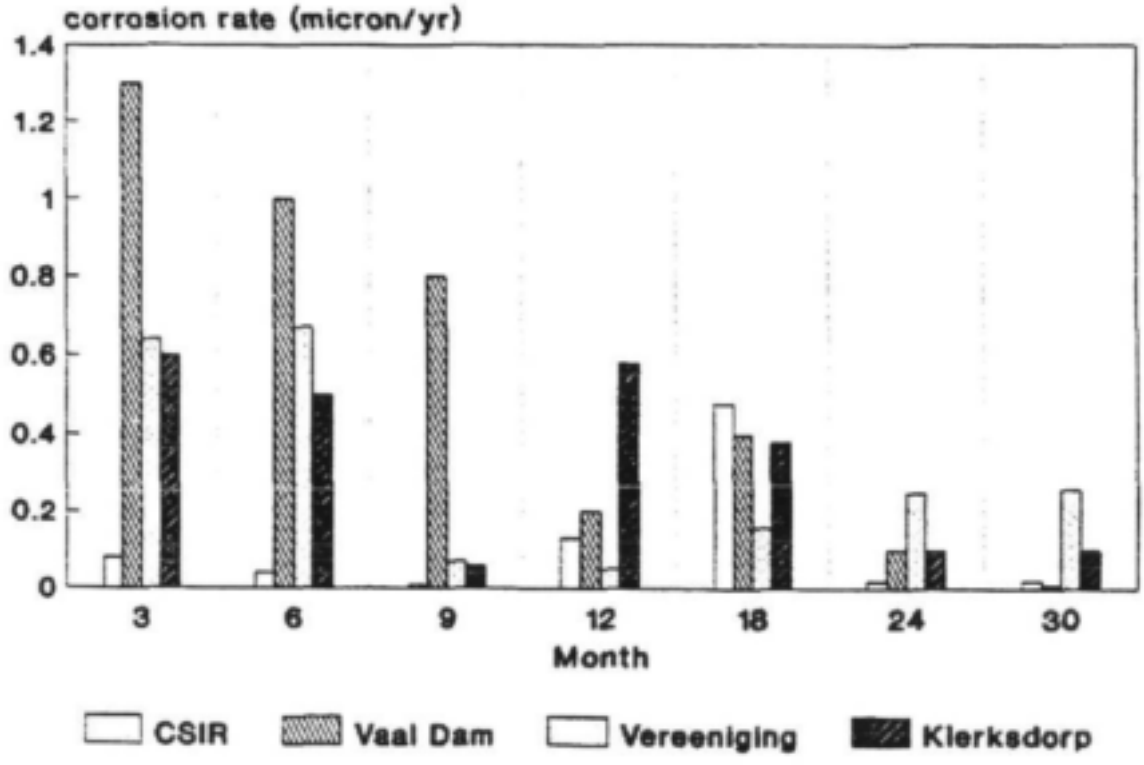

Figure 186. Mass loss of 3CR12 in cold water determined at three monthly intervals at different sites.

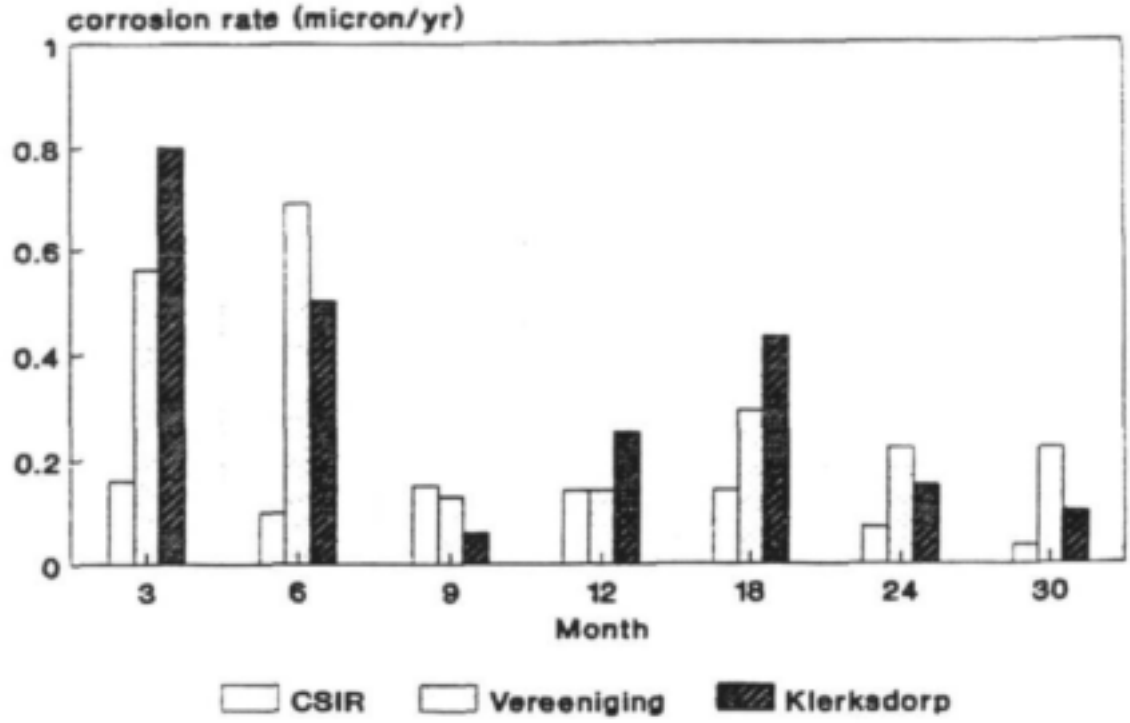

Figure 187. Mass loss of 3CR12 in hot water determined at three monthly intervals at different sites.

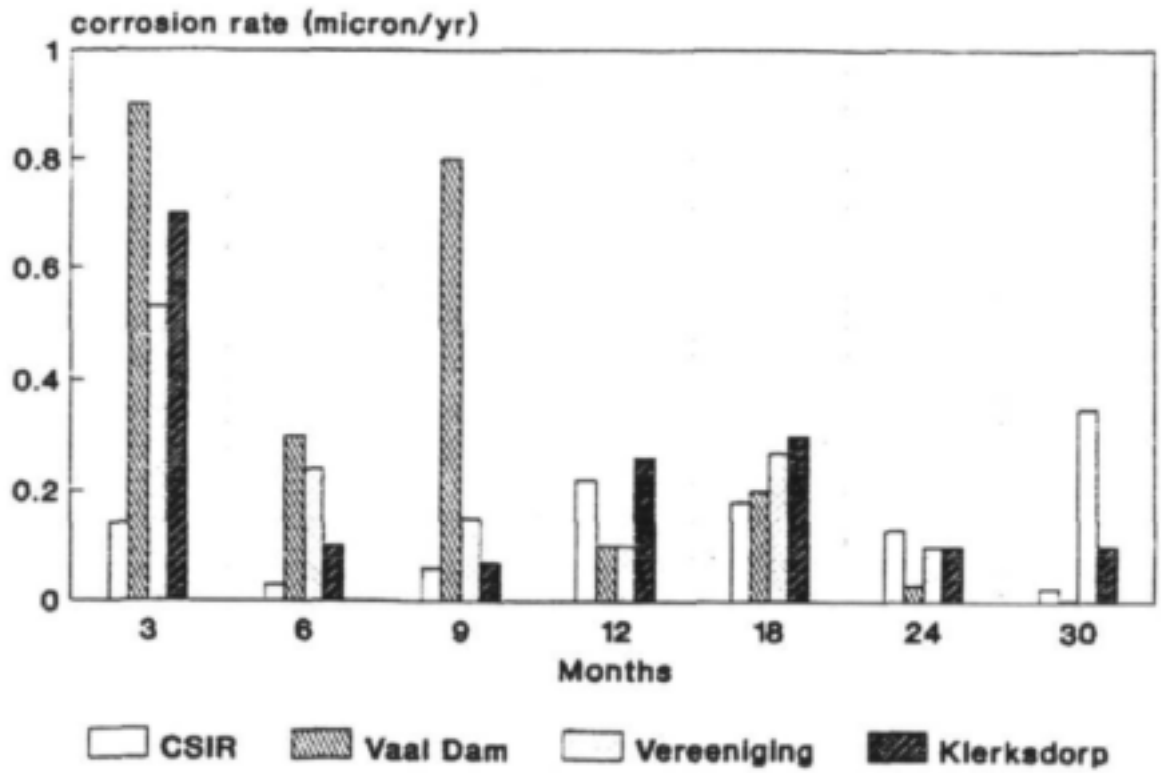

Figure 188. Mass loss of 304 in cold water determined at three monthly intervals at different sites.

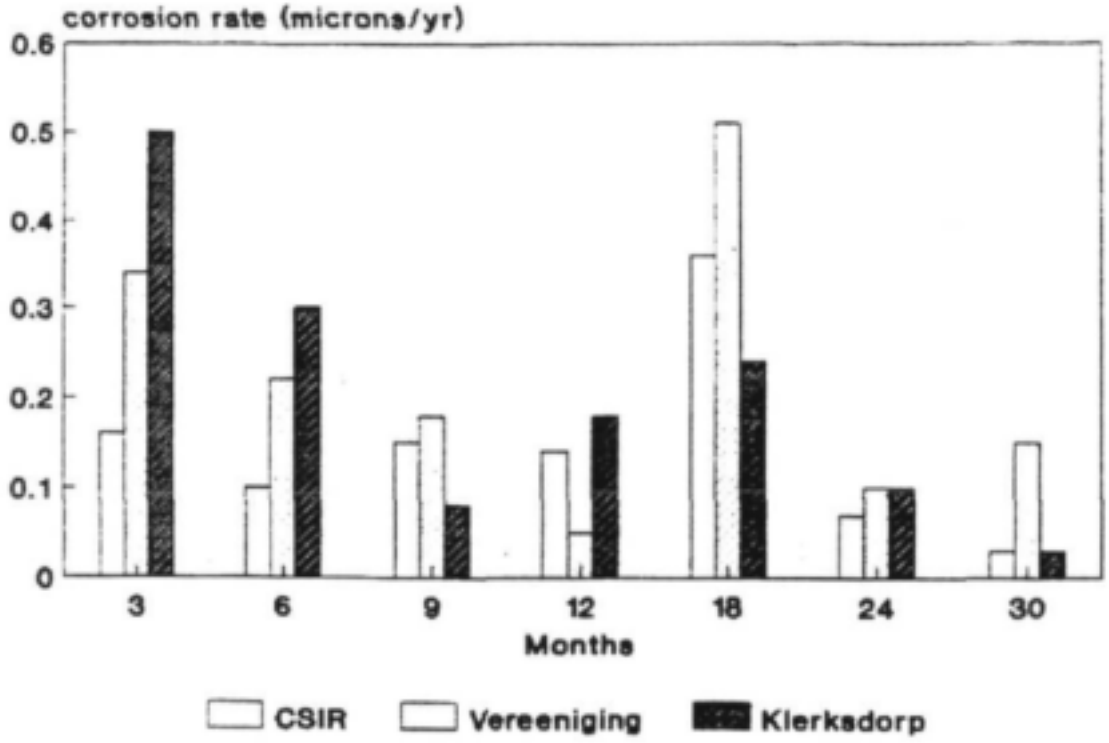

Figure 189. Mass loss of 304 in hot water determined at three monthly intervals at different sites.

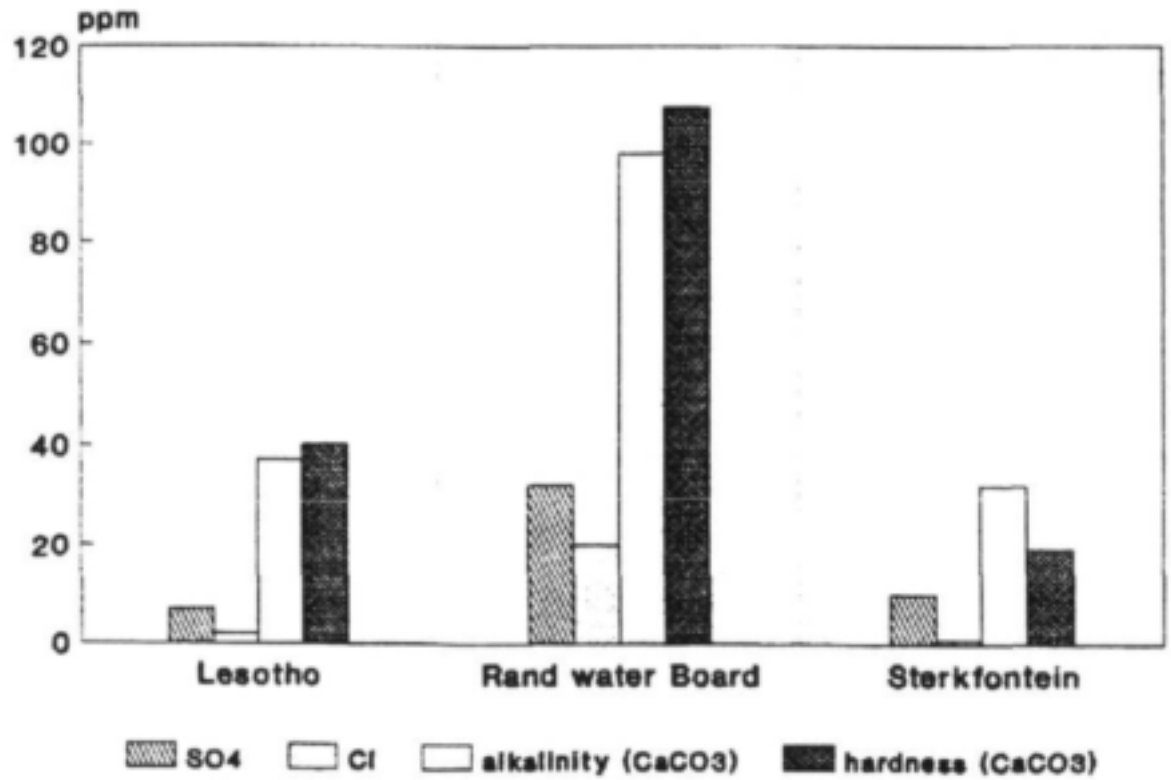

Figure 190. Comparison of water quality between Lesotho, Sterkfontein and Rand Water Board water samples.

Appendix 7. Microbiological examination of coupons

MICROBIAL CORROSION STEP REPORT

Composition of biofilms on various alloys in potable water

by

A Bondonno

MINE HOISTING, METALLURGICAL AND CORROSION SERVICES
Division of Materials Science and Technology
January 1991

ABSTRACT

Bacterial and fungal growth were found on most of the metal coupons tested after one year of exposure to potable water at sites in Pretoria, Klerksdorp and Vereeniging and to raw water at the Vaal Dam. Bacteria of the family *Micrococcaceae* were predominant in the potable waters while the genus *Bacillus* predominated in the raw water. Generally bacterial counts were higher in the cold water systems while fungi predominated in the hot water. Many slime producing cultures ensured a coherent biofilm under which sulphate reducing bacteria could develop. The latter organisms were isolated from most of the mild steel samples.

1. INTRODUCTION

Microbially induced corrosion (MIC) is now accepted as an important contributor to the millions of rands that corrosion costs S A industry annually. The microorganisms which have been associated with corrosion involve many genera and species. The most important bacteria which play a significant role in the corrosion process are those involved in the sulphur cycle. Of these sulphate-reducing bacteria (SRB) are the most significant. These organisms are ubiquitous in nature and are often found infecting industrial aqueous systems. The adhesion of bacteria to surfaces and the subsequent slime production to form biofilms, which harbour SRB, can cause many problems in these systems ranging from affecting the quality and flow of water to corrosion of the metal surface beneath the biofilm layer.

There is strong evidence to suggest that a large proportion of burst steel water pipes in the Johannesburg municipality failed due to MIC. A random survey of 50 damaged pipes removed from the Johannesburg area during 1989 showed that 60% of them most probably failed due to microbial attack. Furthermore, in a study carried out on a recently failed pipe from a Johannesburg water mains, it was found that MIC resulted in its failure. Samples cultured from the corrosion product showed the presence of large numbers of SRB. In addition intergranular attack within the pits and the presence of sulphur species at the base of the pits provided further evidence for the involvement of microorganisms.

Further evidence for the involvement of microorganisms in the corrosion processes in the potable water distribution system was revealed in a recent research programme undertaken by the corrosion group for the WRC. This entailed exposing samples of various metal alloys to potable water, in sites in Pretoria, Klerksdorp and

Vereeniging and to raw Vaal Dam water, in order to determine the effect of water composition on corrosion. After 9 months some samples (particularly the mild steel and cast iron) showed evidence of MIC. These samples were covered by a black corrosion product and tubercles. SRB were isolated and pitting attack beneath the tubercles was found.

Although routine microbiological analysis of potable water takes into account microbes which are human pathogens, those which many bring about corrosion are not routinely tested for. The latter would normally be destroyed by residual chlorine in the water but are protected beneath the tubercles and biofilm on the pipe wall. It is thus important to determine how an adequate treatment can be implemented.

As a first step it is necessary to determine the extent to which bacteria are involved in the corrosion process. Before adequate treatment can be implemented, however, it is important to determine the types and numbers of microorganisms involved, their succession patterns in these environments and the time period required for corrosion to be initiated.

This is a preliminary study to determine the types of organisms which have colonized the various coupons which have been exposed to both hot and cold water for one year at the Pretoria, Klerksdorp, Vereeniging and Vaal Dam sites. This will give some indication of the composition of the biofilm before time interval studies and succession pattern studies are undertaken.

2. EXPERIMENTAL PROCEDURE

Samples of all metal types viz. mild steel (MS), hot-dipped galvanized steel (HDG), copper (Cu), brass (B), galvanized steel (G), 3CR12, 304 stainless steel and zinc (Zn) were collected from all four sites after one year of exposure. At the potable water sites samples were exposed to both hot and cold water.

The samples were placed in bottles containing sterile distilled water and transported to the laboratory.The biofilm was removed from the coupons by gentle scraping and finally by sonication in the transport medium for 15 minutes. The medium was then serially diluted in sterile distilled water. All dilutions were carried out in duplicate.

Diluted samples were spread onto Pseudomonas agar, Nutrient Agar, (general purpose) and Sabouraud Dextrose Agar (selective for fungi). The method for isolation of SRB involved sampling $1cm^2$ of the biofilm on the coupon before scraping and ultrasonication. The sample was cultured anaerobically in SRB medium.

Total viable counts for the aerobic microbial population were determined by the plate count method. SRB were not enumerated but a simple present/absent test was performed.

Colonies representing the predominant microbial populations in the samples were isolated from plates of highest dilution which still showed microbial growth. Pure cultures of the isolates were obtained by repeated transfer of the bacterial isolates onto the relevant media. These cultures were used in the identification tests.

Identification of bacteria to family (and in some cases

genus) level was carried out by means of morphological characteristics and biochemical reactions. Fungi and yeasts were not identified and were enumerated as one group.

3. RESULTS AND DISCUSSION

Culture and isolation tests carried out on the samples exposed at the four sites gave an indication of the variety of microorganisms present in the biofilm on the metal surfaces. Unfortunately the viable plate count method does not give accurate quantitive results. Another drawback is that in utilizing a limited range of culture media, not all organisms present can be isolated. For example, besides testing for SRB, no other anaerobic organisms were tested for.

Figures 1-7 indicate the predominant organisms isolated at each site. Bacteria belonging to the family *Micrococcaceae* which includes the genera *Micrococcus, Staphylococcus* and *Planococcus*, were the predominant organisms in both hot and cold potable waters. Bacteria of the genus *Micrococcus* are obligate aerobes which are common in soil and water. Bacteria of the genus *Bacillus* predominated in the Vaal Dam water. These are G^+ endospore forming bacteria and were found to be amongst the predominant genera in a study carried out on potable waters in the Pretoria area by the Watertek Group (Augostinos, 1990). The greatest variety of microorganisms were isolated from this site as expected since this water was untreated. Other organisms which were isolated relatively frequently from all four sites were bacteria belonging to the genera *Pseudomonas*, *Aeromonas* and *Flavobacterium* and a large variety of fungi and yeasts. In general it was found that bacterial counts were higher in cold waters while the fungi predominated in the hot water systems.

Figures 8-11 show the total count of organisms/mm^2 for each sample at the different sites. As expected, there was a greater proliferation of organisms in the cold water systems compared to the hot waters. Except for the Pretoria site, MS generally supported the most microbial growth. This is in agreement with results obtained by Augostinos et al (1990), although the variety of alloys tested in their programme was not as great. At the Klerksdorp and Vereeniging sites the MS and Zn generally exhibited the most colonization while the Cu and B showed the least. This was expected since copper ions are toxic to many microorganisms. In contrast, the Cu and B coupons at the Pretoria site supported the most microbial growth suggesting that either a copper-tolerant organism was present or contamination of the plates had occurred during experimentation. In the case of the coupons from the Vaal Dam site, MS showed the most colonization with Cu having the next largest amount. At all sites colonization of the stainless steels (304 and 3CR12) was low. The galvanized steel showed the least support of microbial growth with only one site recording growth on this type of coupon.

Many cultures, both bacterial and fungal, were found to be slime producing. This slime has the function of binding the organisms together to form a complex biofilm on the metal surface. It is beneath these layers that anaerobic regions develop allowing SRB to proliferate. SRB were isolated from MS samples from the cold water systems in Pretoria and Klerksdorp, from both the hot and cold systems in Vereeniging and from the Vaal Dam. In addition, SRB were isolated from the surfaces of some electrochemical probes and electrodes. These included a copper probe from the hot water system in Vereeniging and 3CR12 probes from both hot and cold water systems at the same site. It thus seems that Vereeniging has the highest incidence of SRB.

4. CONCLUSIONS

Bacterial and fungal growths were found on most of the samples tested. These form biofilms which harbour SRB. Generally, SRB were detected on those samples with the greatest amount of biofilm. The process of biofilm formation on the metal surface is a dynamic one with the periodic sloughing off of mature biofilm and reforming of a new biofilm. We could thus expect variations in the types and numbers of microorganisms present at any one time.

5. RECOMMENDATIONS

The presence of SRB beneath biofilms poses a potentially serious corrosion problem. These organisms are in a protected environment where they can flourish and bring about MIC of the metal surface they colonize. Sampling the flowing water does not give an accurate indication of the number of SRB present beneath the biofilm or of whether they are inducing corrosion. It is recommended that a programme be set up to determine how soon after colonization SRB initiate MIC in conjunction with a corrosion monitoring system which would detect the onset of MIC. This would ensure that corrective action could be taken before a serious corrosion problem manifested itself.

6. REFERENCES

Augostinos, M., Kfir, R. and Venter. S.N. (1990). Assessment of water quality problems due to microbial growth in drinking water distribution systems. Progress report (1989-1990) submitted to the Water Research Commission. Project No. 670 27243.

PRETORIA
HOT WATER

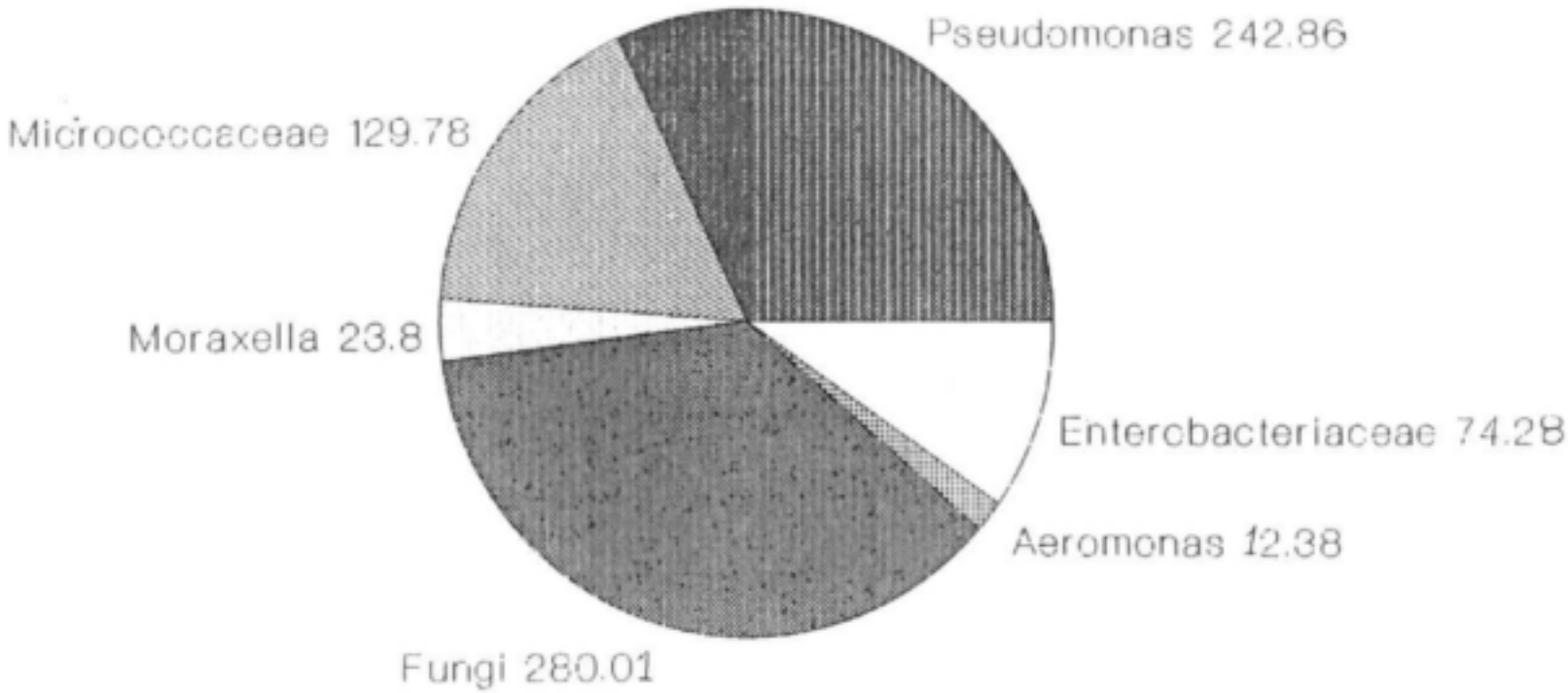

Figure 1
Proportion of microorganisms

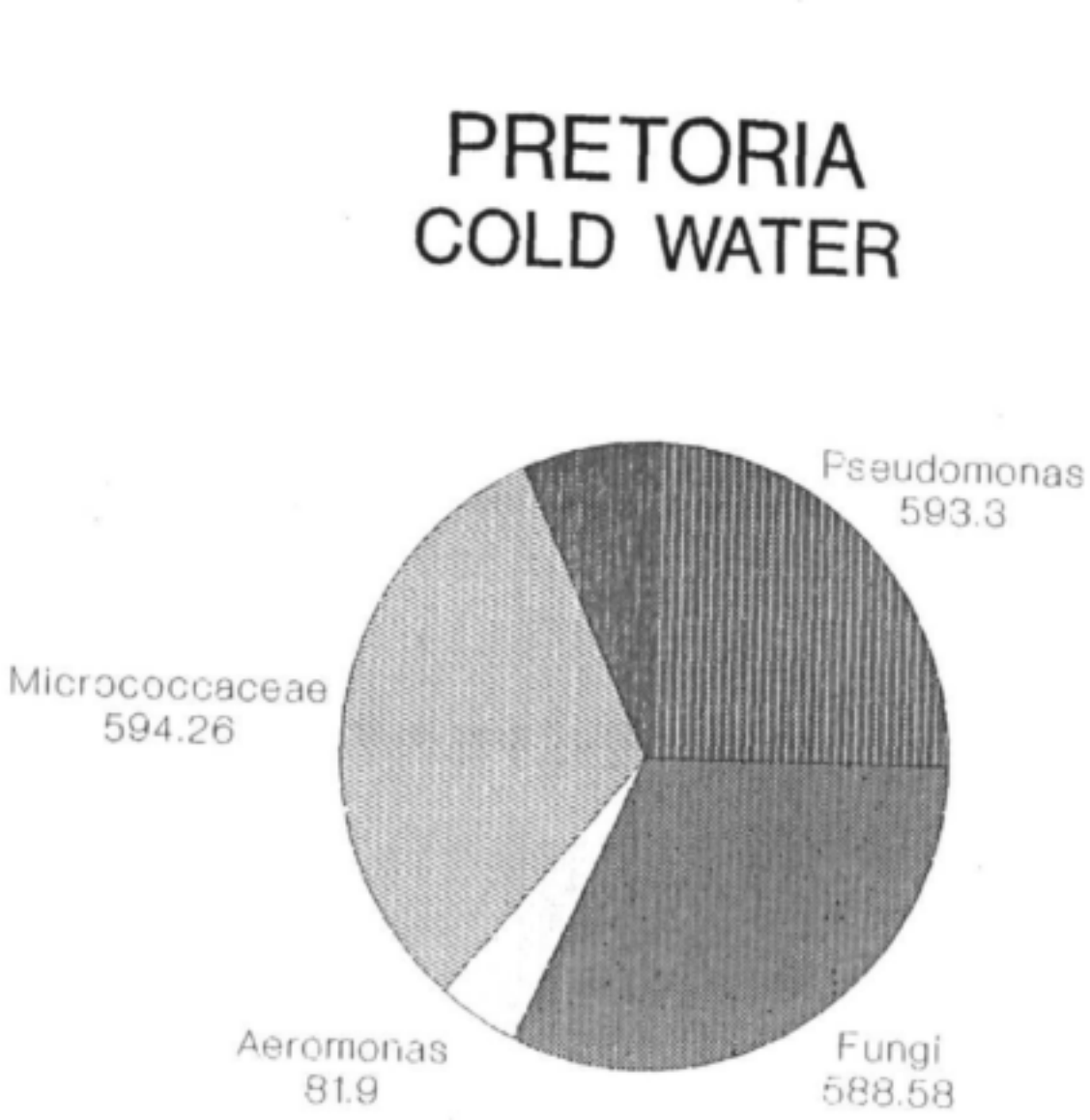

Figure 2
Proportion of microorganisms

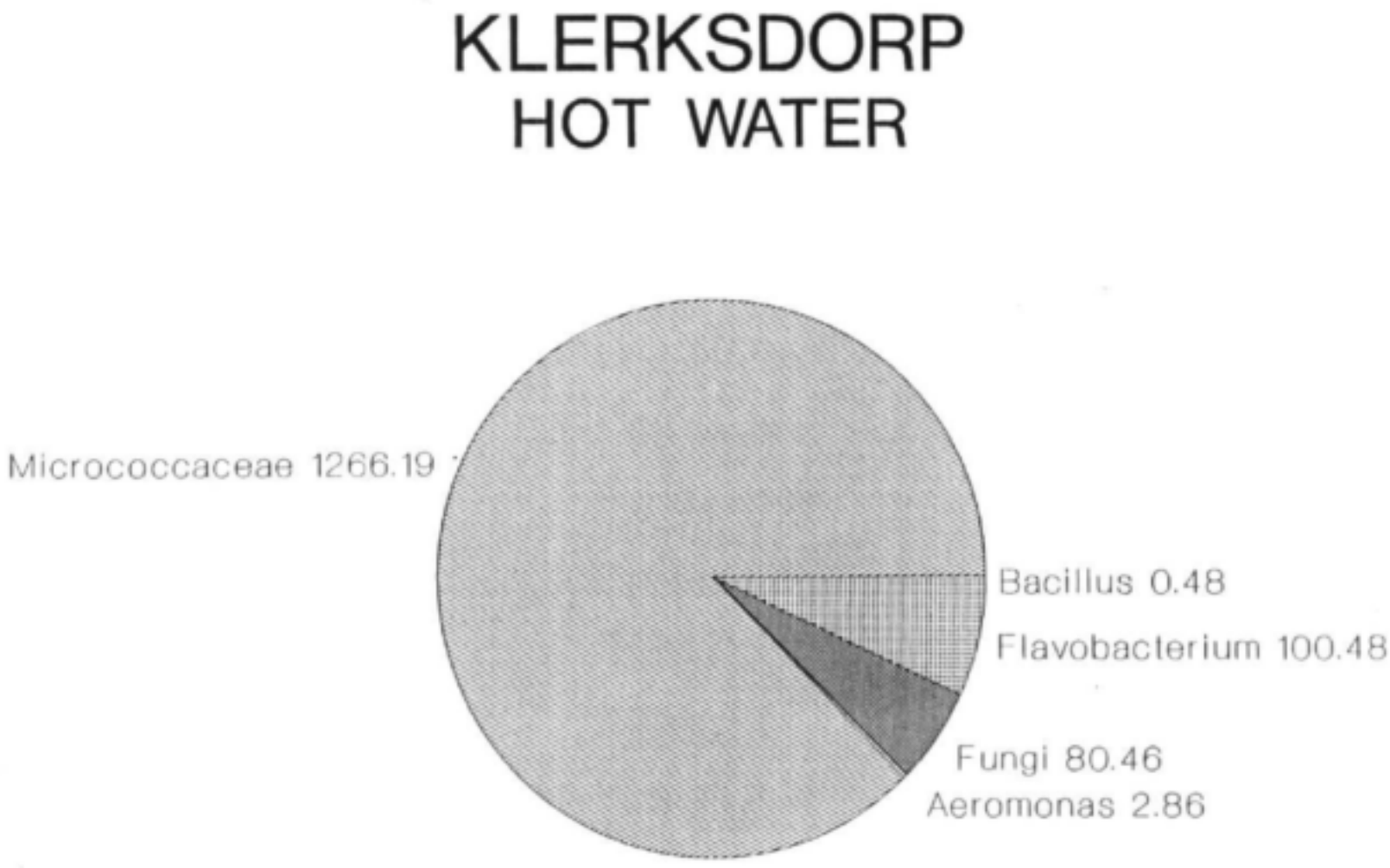

Figure 3
Proportion of microorganisms

KLERKSDORP
COLD WATER

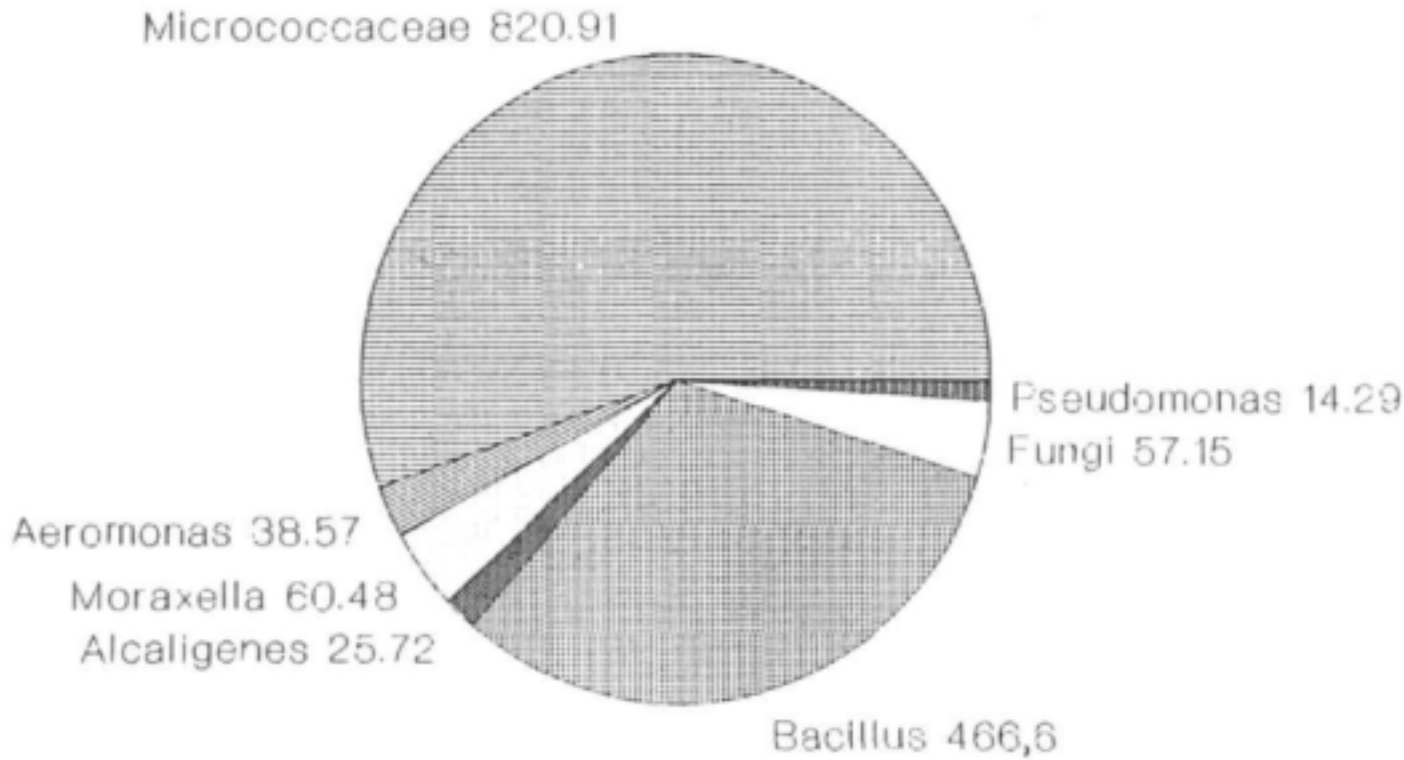

Figure 4
Proportion of microorganisms

VEREENIGING
HOT WATER

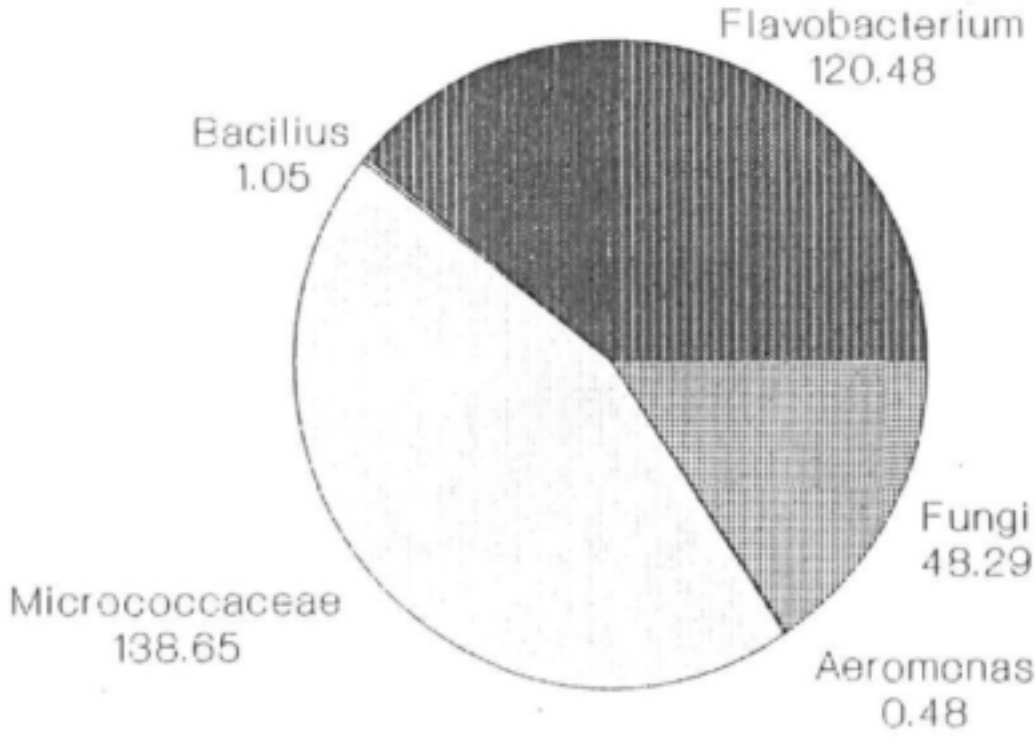

Figure 5
Proportion of microorganisms

VEREENIGING
COLD WATER

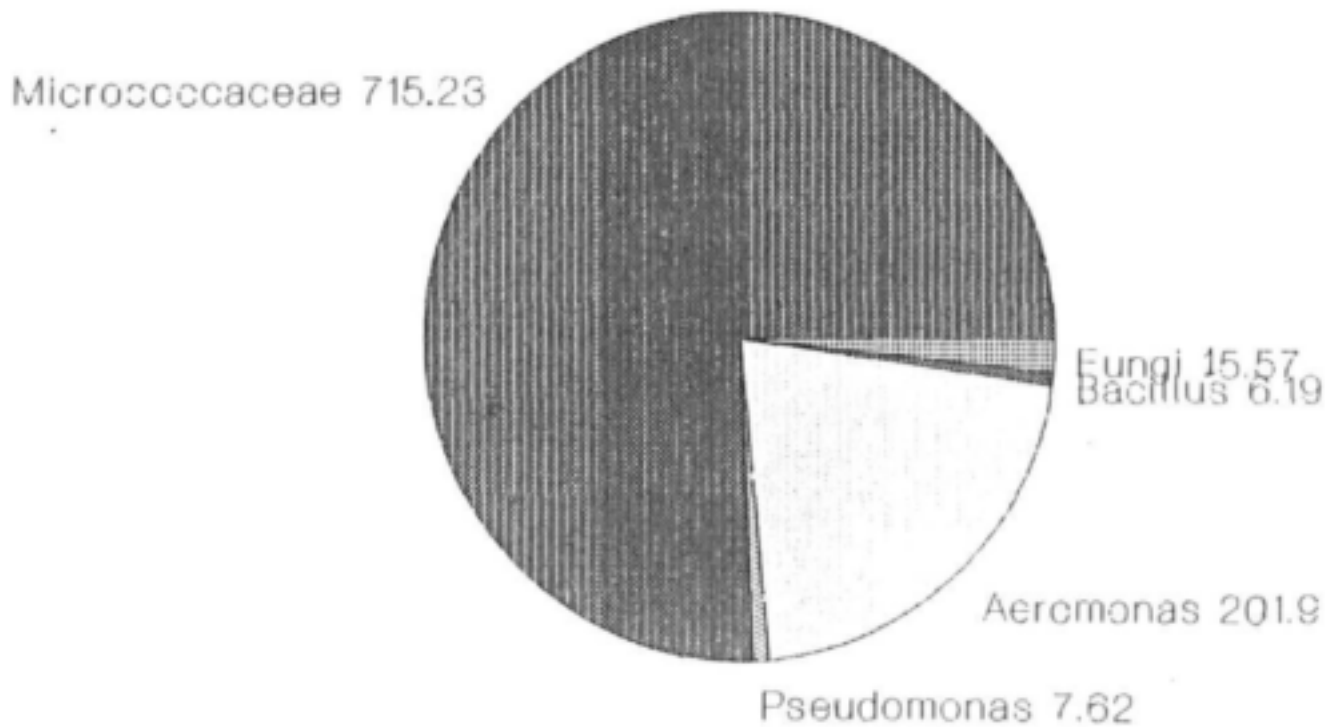

Figure 6
Proportion of microorganisms

VAAL DAM

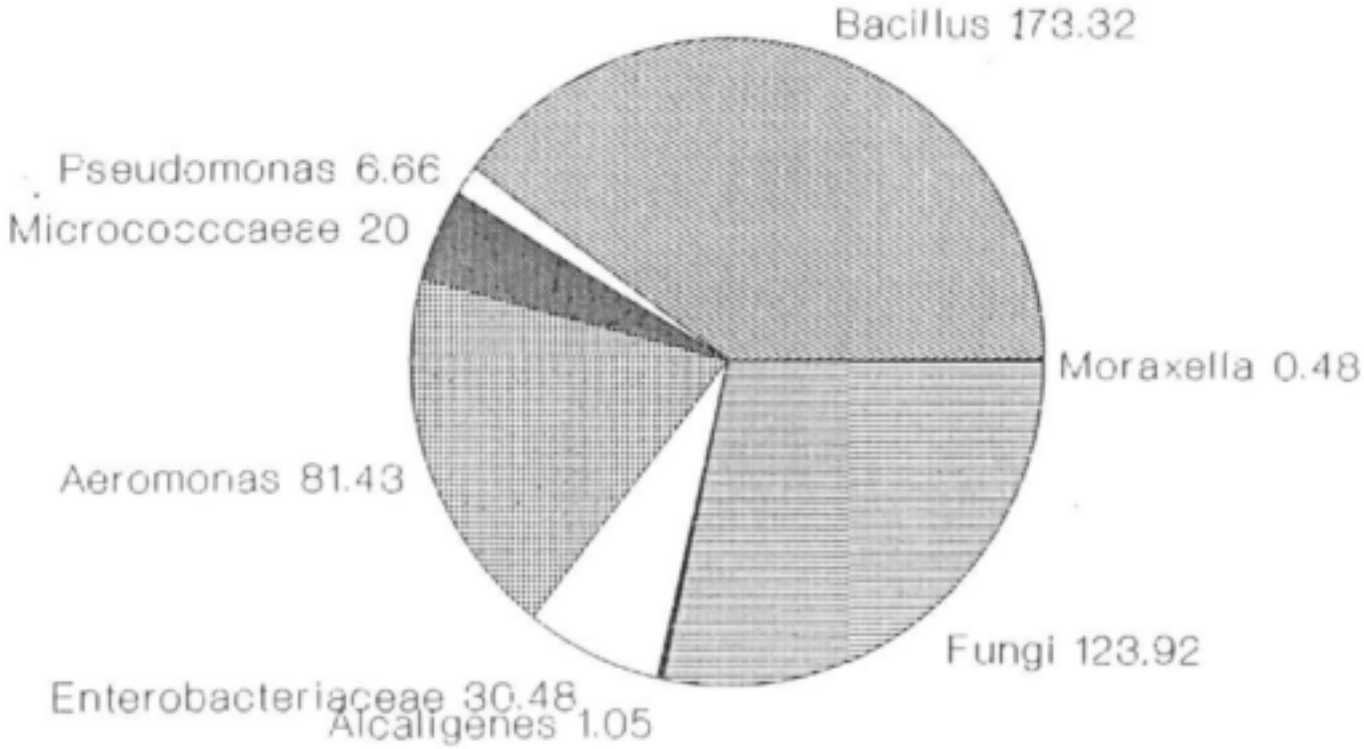

Figure 7
Proportion of microorganisms

PRETORIA

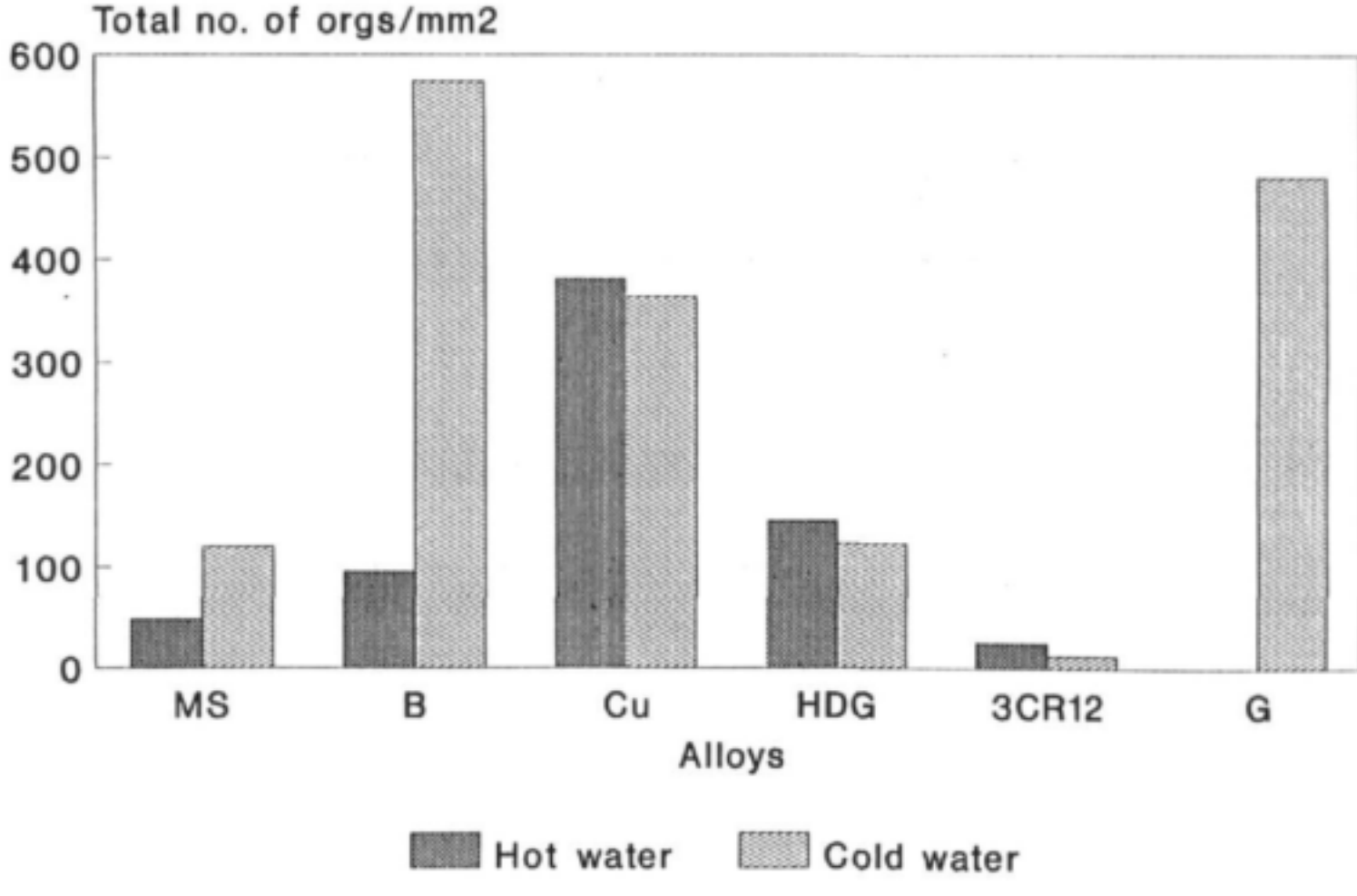

Figure 8
Total microbial count

KLERKSDORP

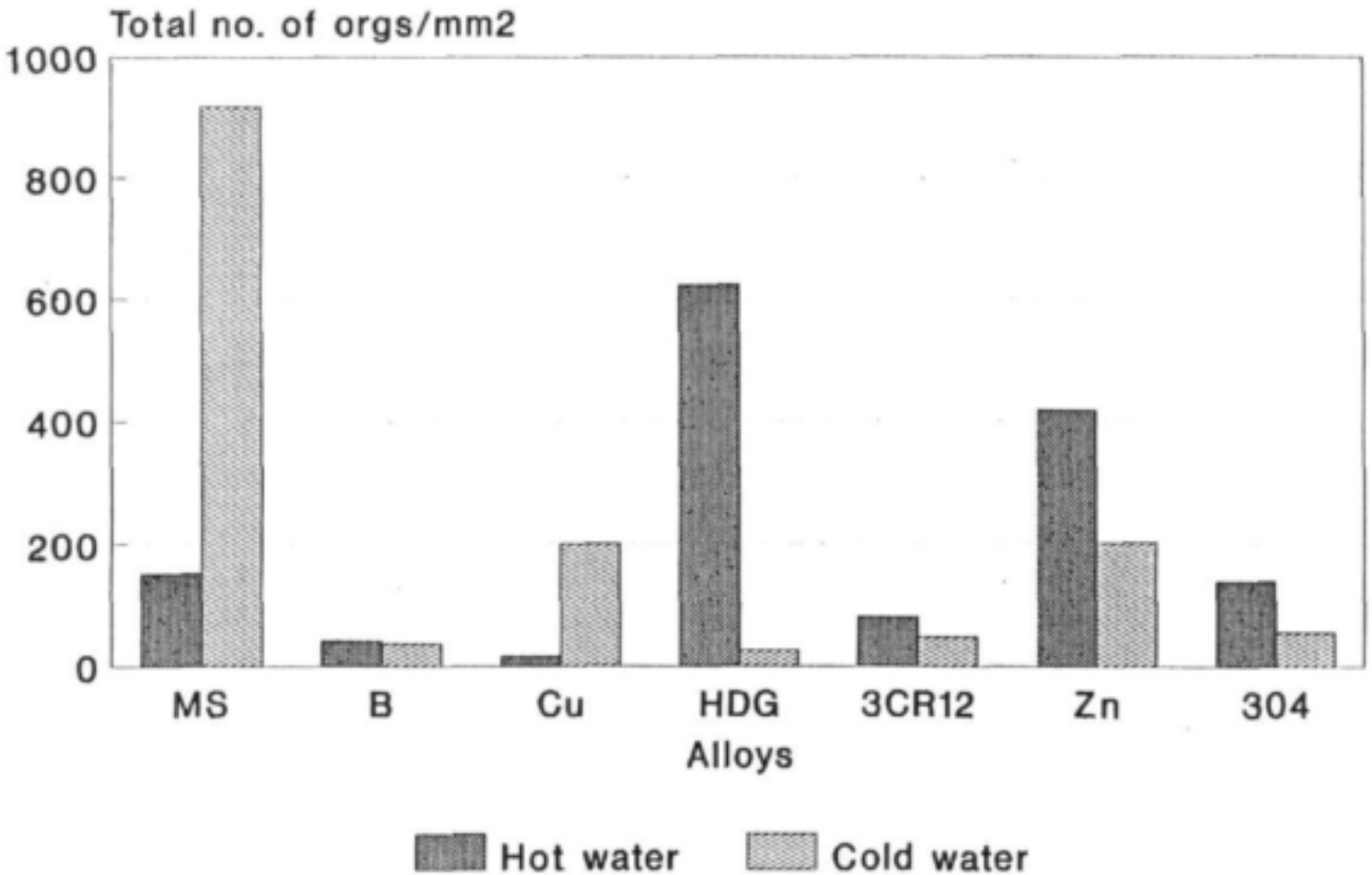

Figure 9
Total microbial count

VEREENIGING

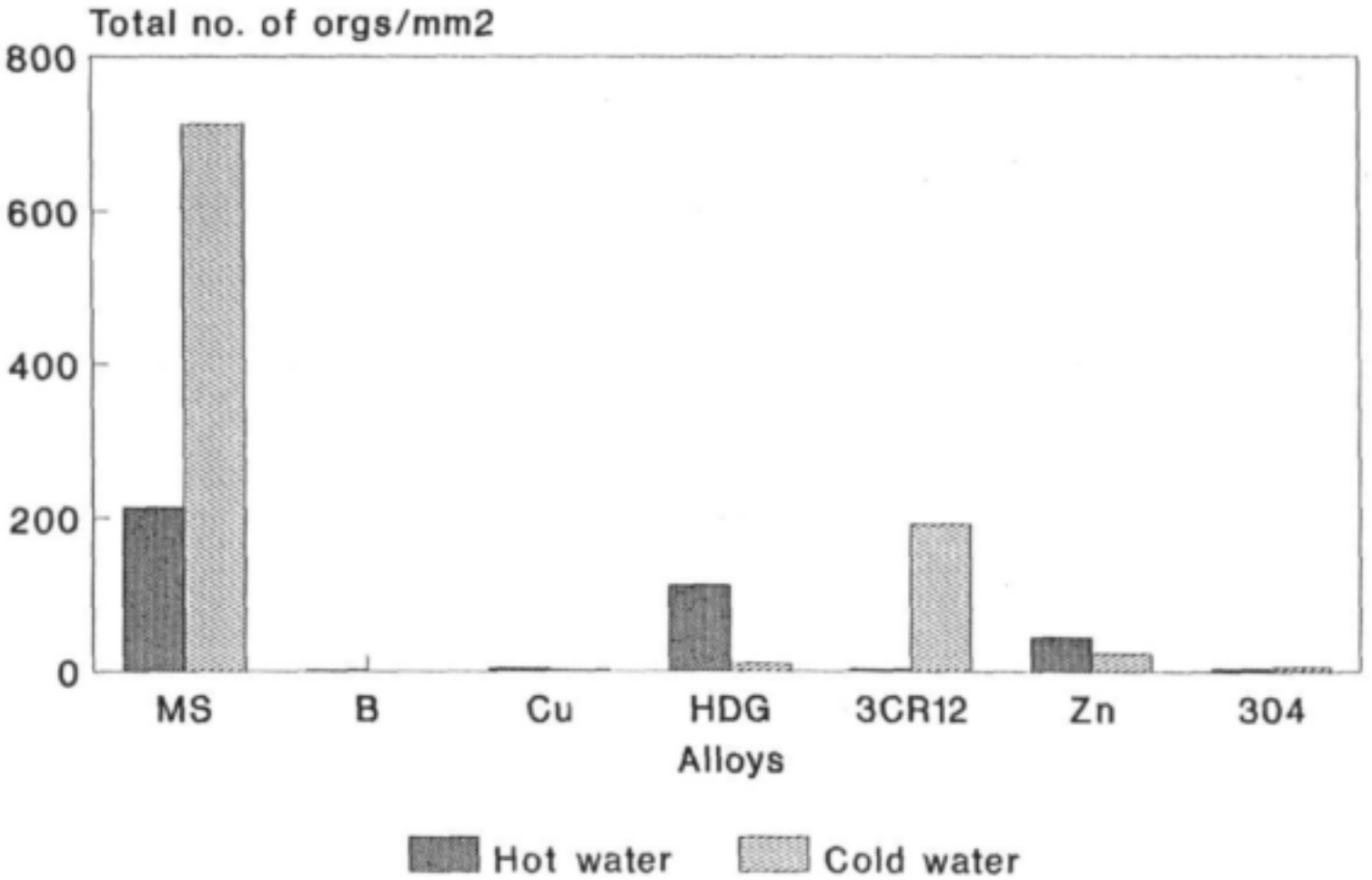

Figure 10
Total microbial count

VAAL DAM

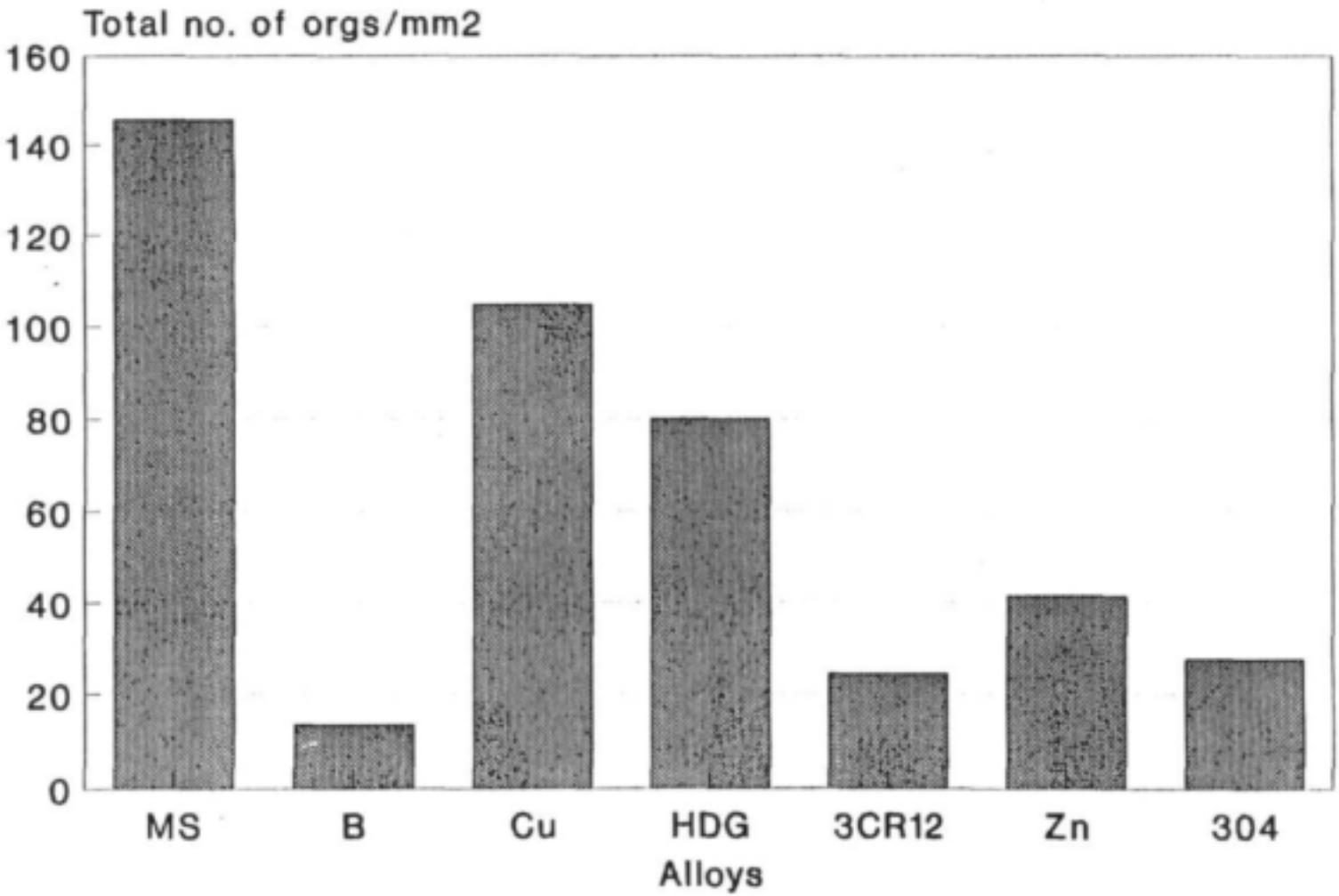

Figure 11
Total microbial count